Integrated Distribution of Wireless and Wired Services Using a Passive Optical Fibre Network

Arsalan Saljoghei

B.Eng., M.Eng.

A Dissertation submitted in fulfilment of the
requirements for the award of
Doctor of Philosophy (Ph.D.)
to the

Dublin City University

Faculty of Engineering and Computing
School of Electronic Engineering

Supervisor: Prof. Liam P. Barry

May 2016

Declaration

I hereby certify that this material, which I now submit for assessment on the programme of study leading to the award of Doctor of Philosophy is entirely my own work, and that I have exercised reasonable care to ensure that the work is original, and does not to the best of my knowledge breach any law of copyright, and has not been taken from the work of others save and to the extent that such work has been cited and acknowledged within the text of my work.

Signed: _____

ID No.:_____

Date:_____

Table of Contents

Acknowledgments

Firstly, I would like to thank my family for their continuous support and encouragement throughout my entire education.

I would like to thank my supervisor Prof. Liam Barry for given me the opportunity to be his student and undertake this project. Without his patience, support and guidance the completion of this work would have been impossible.

I would also thank my friends Asmma and Wil whom provided a fun time for me during my PhD, the same goes to all the other good people from various departments in the engineering department whom I had the pleasure of meeting and spending time with. Lastly, I would also like to thank all my colleagues at the optics-lab; Fernando, Jingyan, Sepideh, Desi, Eamonn, Colm, Vidak, Prince, Sean, Aravind, Anthony and Kevin, these people not only helped me in times of need for my studies but also helped me to relax outside the work hours.

Arsalan Saljoghei

May 2016

List of Acronyms

ADC - Analog-to-Digital Converter

ADSL - Asymmetric Digital Subscriber Loop

AoF – Analogue over Fibre

APD - Avalanche Photodetector

ASE - Amplified Spontaneous Emission

ATM - Asynchronous Transfer Mode

AWG - Arrayed Waveguide Grating

B2B - Back-to-Back

BBU – Base Band Unit

BER - Bit-Error Rate

BERT - Bit-Error Rate Tester

CAPEX - Capital Expenditure

CATV – Cable Television

CD - Chromatic Dispersion

CO - Central Office

Coax - Coaxial

Co-WDM - Coherent WDM

CP - Cyclic Prefix

CPRI – Common Public Radio Interface

CW - Continuous Wave

CWDM - Coarse Wavelength Division Multiplexing

DAB - Digital Audio Broadcast

DAC - Digital-to-Analog Conversion

DCF - Dispersion Compensating Fibre

DD - Direct Detection

DD-MZM - Dual-Drive Mach Zehnder Modulator

DFB - Distributed Feedback

DFT - Discrete Fourier Transform

DM – Discrete Mode

DI - Delay Interferometer

DoF – Digital over Fibre

DPSK - Differential Phase Shift Keying

DQPSK - Differential Quadrature Phase Shift Keying

DS - Downstream

DSB - Double Sideband

DSL - Digital Subscriber Loop

DSP - Digital Signal Processing

DVB - Digital Video Broadcast

DWDM - Dense Wavelength Division Multiplexing

EAM - Electro-Absorption Modulator

ECL - External Cavity Laser

EDFA - Erbium Doped Fibre Amplifier

EML - Externally Modulated Laser

EPD - Evolved Packet System

ESA - Electrical Spectrum Analyser

EVM - Error Vector Magnitude

ETDM – Electrical Time Division Multiplexing

FBMC - Filter Bank Multi Carrier

FDM - Frequency Division Multiplexing

FEC - Forward Error Correction

FIR - Finite Impulse Response

FP - Fabry-Perot

FSAN - Full Service Access Networks

FTTB - Fibre to the Block

FTTC - Fibre to the Curb

FTTH - Fibre to the Home

FTTN - Fibre to the Node

FTTx - Fibre to the x

G – Generation

GSM - Global System for Mobile Communications

HFC - Hybrid Fibre-Coaxial

HNLF - Highly Non-Linear Fibre

HRPD - High Rate Packet Data

HSPA - high speed packet access

ICI - Inter-Carrier Interference

IDFT - Inverse Discrete Fourier Transform

IFWM - Intra Four Wave Mixing

IM/DD - Intensity Modulation with Direct Detection

IMD – Intermodulation Distortion

IMI – Imaginary Interference

IMP –Intermodulation Products

IFoF – IF over Fibre

IP - Internet Protocol

ISI - Inter-Symbol Interference

ISDN -Integrated Service Digital Network

ITU - International Telecommunication Union

LO - Local Oscillator

LTE - Long Term Evolution

MAI – Multi Access Interferences

MAN - Metropolitan (metro) Area Network

MC – Multicarrier

MCM - Multi-Carrier Modulation

MLL - Mode-Locked Laser

MMF - Multi-Mode Fibre

MZM - Mach-Zehnder Modulator

NF - Noise Figure

NRZ - Non-Return-to-Zero

Nyquist Tx - Nyquist Transmitter

OBPF - Optical Band Pass Filter

ODN – Optical Distribution Node

ODSB –Optical Double Side Band

O-E-O - Optical-Electrical-Optical

OFDM - Orthogonal Frequency Division Multiplexing

OFDMA – Orthogonal Frequency Division Multiple Access

OLT- Optical Line Terminal

ONU - Optical Network Unit

OOK - On-Off Keying

OQAM- Offset Quadrature Amplitude Modulation

OTDM – Optical Division Multiplexing

PAM - Pulse Amplitude Modulation

PAPR - Pear-to-Average Power Ratio

PC - Polarisation Controller

PDM - Polarisation Division Multiplexing

PMD - Polarisation Mode Dispersion

PON - Passive Optical Network

POTS – Plain Old Telephone Services

PPG - Pulse Pattern Generator

PRBS - Pseudo-Random Bit Sequence

PSK - Phase Shift Keying

p2p – Point to Point

QAM - Quadrature Amplitude Modulation

QPSK - Quadrature Phase-Shift Keying

Q-Well - Quantum Well

RIN - Relative Intensity Noise

ROADM - Reconfigurable Optical Add/Drop Multiplexer

RoF – Radio over Fibre

RTS - Real-Time Scope

RZ - Return-to-Zero

RN – Remote Node

RSOA – Reflective Semiconductor Amplifier

SDM - Space Division Multiplexing

SMS - Short Message Service

SNR - Signal-to-Noise Ratio

SOA - Semiconductor Optical Amplifier

SSB - Single Sideband

SMT – Staggered Multi Tone

SSMF - Standard Single Mode Fibre

TDM - Time Division Multiplexing

TIA - Trans-Impedance Amplifier

UDWDM - Ultra Dense Wavelength Division Multiplexing

US – Upstream

UMTS - Universal Mobile Telecommunication Systems

VCSEL - Vertical Cavity Surface Emitting Laser

VOA - Variable Optical Attenuator

VoIP - Voice over IP

WDM - Wavelength Division Multiplexing

WiFi - Wireless Fidelity

WiMax - Worldwide Interoperability for Microwave Access

WLAN - Wireless Local Area Networks

WWAN - Wireless Wide Area Networks

XPM - Cross Phase Modulation

CDM – Code Division Multiplexing

UWB – Ultra Wide Band

List of Tables

List of Figures

Abstract

Integrated Distribution of Wireless and Wired Services Using a Passive Optical Fibre Network.

Written by Arsalan Saljoghei

The desire for high bandwidth multi-media reach content and the exponential growth of Internet traffic has led to the penetration of optical technologies into the access segment in the form of Fibre-To-The-x (FFT-x) topologies. Due to its cost effectiveness and low energy consumption, most FFT-x models have been based on Passive Optical Networks (PONs) where the employment of in-line active components has been discouraged. Next generation optical access networks are required to provide higher bandwidth-distance product and support wireless services in a cost effective manner.

Through experimental and simulation work, this thesis examines the use of multicarrier modulation formats such as Orthogonal Frequency Division multiplexing (OFDM) and Filter Bank Multi Carrier (FBMC) as mans of helping to meet the bandwidth-distance requirements set for next generation optical access networks. OFDM and FBMC both exhibit high spectral efficiency and a tolerance to chromatic dispersion making them excellent candidates for use in next generation optical access networks.

In order to promote cost efficiency these systems are also studied in conjunction with Direct Modulation of novel laser devices and direct detection. In this work, the accommodation of Long Term Evolution (LTE) services in hybrid wired/wireless optical access networks is also demonstrated using spectral notching either by deactivation of subcarriers in OFDM or line-coding techniques in OOK based wired services. The use of FBMC and OFDM is also studied in light of uplink transmission in optical access networks without the employment of spectral guard bands that is commonly used for the reduction of Multiple Access Interference (MAI).

Introduction

The continuing growth in demand for high-speed communications and media-rich content such as on-demand video streaming, VoIP and online gaming, has led to a corresponding need for high speed communication links. To meet such demands, service providers have continually aimed at reducing the physical distance between the end-user and the closest optical communication link. The emergence of optical technologies close to the vicinity of the end-user's premises as a means for communicating with the wider networks can solve the so called "last-mile bottleneck" which had been formed as result of technological discrepancies between the core/metropolitan and access networks. The topologies under which optical technologies can be employed in access networks have been termed Fibre-To-The-X (FTTX), amongst these; FTT-Home (FTTH) is seen as a long term solution for meeting the growing bandwidth demands. However unlike core and metropolitan networks, where the associated costs are shared amongst a wide array of users, in FTTH topologies costs can escalate with the rising number of users. Thus optical based access networks must be constructed in a cost effective manner such that Capital Expenditure (CAPEX) and Operational Costs (OPEX) can justify profitability. In fulfilling this vision, Passive Optical Networks (PONs) have been heralded as an appropriate candidate for FTTX network architectures, coalescing reduced CAPEX and OPEX by promoting equipment sharing and energy efficiency through the elimination of in line active equipment. In past two decades, PON systems have been standardized and deployed worldwide, with the earliest technologies such as Asynchronous Transfer Mode PON (ATM- or A- PON) operating at sub Gb/s link rates. In response to growing end user's bandwidth demands a series of post A-PON standards have appeared within these past two decades, each with upgraded capabilities and higher supportable date rates. The successor to A-PON which has been termed Broadband-PON (B-PON) achieved a superior downstream rate of 1.25 Gb/s and sub Gb/s rates in the upstream, these figures were further increased in the later standards such as Gigabit PON (GPON) and Gigabit Ethernet PON (GE-PON) with data rates achieving up to 2.5 Gb/s in the downstream and 1.25 Gb/s in the upstream. These two standards had been the most popular and prevalent means for PON based FTTX architecture, however this trend is changing with carriers switching to 10 G capable PON systems, and a new set of new standards, namely 10 GE-PON and XG-PON, both with the capability of reaching 10 Gb/s in downstream/upstream have been proposed. The most recent standardized PON technology is known as Time Wavelength Division Multiplexing PON (TWDM-PON), this standard exploits Wavelength Division Multiplexing (WDM)

and is built upon the 10G PON technologies which allows for backward compatibility with some of the key device architectures used in 10 GE-PON and XG-PON systems. TWDM can reach link rates up to 80 Gb/s both in downstream and upstream directions however this technology is still at its deployment infancy.

The high cost associated with high bandwidth electrical amplifiers, optical modulators, directly modulated lasers, and receivers, as well as the impact of the dispersive channel on high bandwidth signals, places a hurdle on the practical realization of low cost PONs operating at 10+ Gb/s per optical channel, using On Off Keying (OOK). This in turn has led to a series of studies into the employment of new modulation and multiplexing schemes in PONs which benefit from better spectral efficiencies and higher resilience to impairments inherent to optical fibre. Some of the proposed schemes are Subcarrier Multiplexing (SCM), Pulse amplitude Modulation (PAM), single carrier phase modulated schemes and multi carrier optical phase or intensity formats such as Orthogonal Frequency Division Multiplexing (OFDM) and Filter Bank Multi Carrier (FBMC). These latter two schemes also exploit the concept of orthogonality which consequently allows for high levels of spectral efficiency. These two multicarrier modulation schemes are also of interest in optical access given their high tolerance to chromatic dispersion allowing long propagation lengths. Furthermore, FBMC and OFDM can also offer the means for the implementation of dynamic bandwidth allocation, which is crucial in multi user access scenarios; this factor is provided by the high granularity created following the subdivision of the available bandwidth into finite subcarriers.

At the same time, the wide availability of high bandwidth services for cellular application has led to a dramatic increase of traffic over cellular access network. Concurrently, cellular service providers are required to adhere to growing demands of traffic by increasing the available capacity over their access networks. Such capacity extensions are envisioned to be fulfilled by increasing spectral efficiency, deployment of more cells and migrating to higher operational frequencies. In contemporary cellular 4G technologies, increases in spectral efficiency are achieved by the employment of highly spectrally efficient modulation formats such as OFDM and spatial diversity schemes, with Heterogeneous Network (HetNet) architectures being another proposed strategy for the enhancement of the available capacity. Furthermore, the exploitation of larger bandwidths available at higher operational RF bands is currently being discussed for 5G technologies.

The split of conventional Base station (BS) functionalities into a Remote Radio Head (RRH) and a Base Band Unit (BBU) has been a common approach taken towards the simplification of a BS. This methodology allows for the positioning of the BBU in a

location far from the radio antenna. The BBU, which is responsible for the management and control of the radio resources accounts for a significant portion of the overall energy consumptions of the BS, and its relocation, saves possible costs associated with site rental and electrical cabling. The RRH, which is responsible for the wireless transmission and reception is usually placed on top of the radio tower and it commonly communicates with the BBU via a (Common Public Radio Interface) CPRI protocol. CPRI is an OOK modulated continuous stream signal generated by the digitalization of the uplink and downlink wireless signals at the BBU and RRH respectively. A significant draw back from such fronthauling schemes which are based on Digital over Fibre (DoF) transmission, is the resultant high data rates as a consequence of the digitalization process, which hinders the use of high bandwidth optical technologies. This data rates over the CPRI interfaces are also expected to dramatically increase in response to the capacity extensions in the next generation cellular access systems.

A new cellular access architecture that has been attracting attention amongst service providers is called the Cloud Radio Access Network (C-RAN). This topology still employs the split BS concept with the difference being that the BBUs responsible for many RRH are localized in a common centralized location. With an aim to converge the functionality of multiple BBUs in one unified block, C-RAN topologies can achieve a significant level of cost saving and network functionality enhancement. The cost savings arise by resource sharing and impose complexities to the part of the subsection of the BS, which is responsible for the wireless radiation. However, such complexities can be reduced by using Analogue over Fibber (AoF) techniques for fronthauling. AoF simplifies the BS by removing the need for subsystems needed previously for providing an interface between the analogue and digital subsystems in DoF type architectures, and this simplification in turn leads to a significant reduction of data rates over the fronthaul link experienced in DoF protocols such as CPRI. The use of AoF techniques for the optical transmission of cellular services at various operational frequencies have been studied extensively in conjunction with external and direct modulation as well as intensity and phase modulation schemes. These AoF techniques can be categorized into Radio Frequency over Fibre (RFoF) and Intermediate Frequency over Fibre (IFoF). RFoF allows efficient traffic management whereas enhanced functionalities will stem from the reduction of delays experienced by inter BBU communication. This reduced latency allows for the implementation of efficient interference management algorithm for the eradication of interference between neighbouring cell sites in high capacity HetNets or densified cell architectures deployed to provide higher cellular capacity.

The typical fronthauling links operating based on the CPRI interface or other Digital over Fibre (DoF) schemes can for a simple BS, since the only functional blocks required at radio station are electrical amplifiers, optical transceivers and passive RF equipment. To provide font hauling for cellular systems requiring MIMO or using a common fibre for providing fronthauling to multiple antennas operating at similar frequencies, the IFoF schemes may be adopted. Compared to RFoF this technique will require extra local oscillators, filters and transceivers for the required translation of the operating RF frequencies. AoF techniques are known to be more susceptible to device nonlinearities and dispersion compared to DoF means of transmission; however, various approaches can be taking to limit these shortcomings, thus AoF techniques can also play a key role in next generation cellular access systems.

The increased interest in FTTX architectures exploiting PON architectures and their deployment for the provision of high capacity wired access networks has been increasing the availability of fibre rich services in a given geographical region. This presence of fibre in turn sets the scene for a unified wired/wireless access network whereby the high bandwidth fronthauling or backhauling needs of next generation high capacity cellular access systems can be provided by high capacity PON systems. Such unification can potentially allow for a better utilization of network resources and lead to lower OPEX and CAPEX.

The use of PON for the accommodation of CPRI like protocols has been discussed in recent years; however certain difficulties exist. First, the high data rates experienced by CPRI in certain scenarios will require the use of high capacity Point to Point (p2p) links in contrast to architecture such as PON. Secondly the integration of CPRI protocols in PON will also require a major variation in the bandwidth assignment mechanisms used in PON protocols. In contrast, AoF can overcome these shortcoming attributed to DoF systems. The reduced bandwidths incurred by AoF transmission can allow for a wired and multiple wireless signals to co-exist over one optical channel in PON systems. However such hybrid wired/wireless systems using AoF techniques for the transmission of wireless signals will require a certain means for the reduction of interference between various services sharing a common optical channel. Two common means proposed for such interference management has been the use of distinct wavelengths for individual services or the introduction of large frequency guard bands between various services.

The work carried out in this thesis is mainly aimed at the study of two aspects regarding next generation PONs. These are concerned with the exploitation of highly spectrally efficient modulation format in downlink and uplink channels in PON, and techniques for

interference management which can give rise to an efficient hybrid wired/wireless PON system. At first, the thesis looks at the exploitation of highly spectrally efficient modulation formats such as OFDM and FBMC in the downstream of intensity modulated PONs using direct laser modulation for cost efficiency. The work initially studies the impact of device nonlinearities and laser Relative Intensity Noise (RIN) on quality of multicarrier OFDM signals through experimental and simulation evaluations. The exploitation of OFDM and FBMC systems are also studied in uplink PON where user synchronization plays an important role. The second set of studies presented in this thesis aim at solving some of the issues proposed by hybrid wired/wireless PONs employing AoF schemes for fronthauling. In these studies of hybrid PONs various possible means of interference management are studied and deployed in order to avoid significant bandwidth extensions. The two particular interference management schemes employed were involved with the manipulation of individual subcarriers in multicarrier modulation formats and in other cases, integration of custom made line coders for single carrier modulation formats.

Main Contributions

The main contributions of this work are:

Performance improvement by optical injection in a directly modulated OFDM based hybrid wired/wireless PON – In prior work carried out on hybrid PONs, which accommodate multiple AoF signals carrying cellular services, substantial frequency guard bands were used between distinct services (wired / wireless) operating over one optical channel in order to avoid interference [1-3]. In certain cases the operational frequency of the cellular bands were also intentionally shifted to further accommodate for interference management [4]. In this work by de-activating a set number of pre-defined subcarriers in the wired OFDM band operating at 12.5 Gb/s, it was possible to accommodate for multiple in-band wireless RF AoF signals carrying LTE services on one optical channel without the need for further up/down frequency conversion of the AoF signal for the alleviation of interference. In addition, the majority of previous work in the area of intensity modulated OFDM systems using direct modulation neglected a detailed investigation into the impact of RIN and nonlinearity on performance [5-8]. In this work through experimental work and numerical simulations an insight is provided into the distinct impact of laser RIN and nonlinearity on performance of directly modulated OFDM system. The advantages of optical injection in AoF systems (reduction of nonlinearity, RIN and chirping) has been long established in the Microwave Photonics (MWP) field [9, 10], however it's realization can be impractical in terms of cost effective PON systems owing to its complex

architecture. In a move to alleviate these complexities it is possible to integrate the optical injection process in one device, and in this work we make use of a novel integrated device comprising of two Discrete Mode (DM) lasers with optical injection. This has been the first demonstration of directly modulated hybrid PON using an integrated transmitter with optical injection. The simple fabrication process of DM lasers along with their integrated structure can aid the system to achieve cost effectiveness and better performance [11]. By using this monolithically integrated device in experimental evaluations, the impact of laser nonlinearity and RIN was shown to decrease as result of optical injection, and these results were further validated by using numerical simulations.

Hybrid wired/wireless TDM-PON and line-coding **–** The employment of OOK type modulation formats for wired signal in hybrid wired/wireless PON employing AoF techniques has been previously demonstrated, however in most cases due to the limited electro-optical bandwidth, the data rates chosen for the wired signal were below the rates currently available for commercial PONs [4]. Nevertheless in all cases in order to reduce the interference between the wired and wireless entities the AoF signal was upconverted to high frequencies to avoid interference with the wired baseband signals [12]. The elimination of high frequency local oscillators for the up/down conversion of AoF signals can reduce system costs. Thus, in this work to make possible the integration of wireless services on the same wavelength without the employment of high frequency local oscillators for up/down frequency conversion, binary line coding methods are used to spectrally shape the wired OOK signal by creating multiple spectral notches in the signals spectrum [13-18] which can subsequently be used to accommodate for the in-band AoF signals. In this work for the first time, the in-band transmission of AoF signals carrying LTE services in an OOK band operating at 10 Gb/s is demonstrated. The generated in-band spectral notches employed for interference management were obtained based on various structures of interleaved 8B10B and MB810 line encoders.

FBMC in downlink and uplink channels in PONs **–** Despite the advantages of OFDM for optical communications it also has some shortcoming [19]. To combat dispersion, OFDM employs a Cyclic Prefix (CP) which can potentially reduce the overall spectral efficiency of the system [20]. Furthermore the inherent structure of the prototype functions used in OFDM [21] makes it sensitive to synchronization issues in the link [22, 23]. FBMC is known to be capable of alleviating the shortcomings of OFDM, thus this work employs and evaluates the role of FBMC in both downlink and uplink channels of PON [23]. The previous work carried out on FBMC based PON systems has been limited, and the work that has been carried involved the employment of external modulators [24-28]. In this work for the first time, the performance of FBMC in conjunction with direct modulation of low

cost lasers was studied for data rates up to 14.8 Gb/s and fibre propagation distances up to 75 km, demonstrating the role that FBMC can play in long reach intensity modulated PONs.

The difficulties associated with modulation formats such as FBMC and OFDM in multiple access schemes such as uplink communications has been widely studied in the wireless domain [23, 29]. Certain approaches had been introduced to overcome the Multi Access Interface (MAI) resulting from a de-synchronization of carriers amongst operating users [22, 30]. In all previous works carried out on FBMC/OFDM-PON, with one exception with regards to OFDM-PON, the resilience of these systems to MAI was enhanced by the intentional introduction of frequency guard bands. The presented work in this thesis for the first time looks at guard band less FBMC multiple access systems in uplink PON where comparisons are drawn to similar OFDM based architectures.

Thesis Structure

This thesis is structured as follows:

Chapter 1 describes the evolution of optical communication networks as well as the drivers behind their continued growth in capacity. Various multiplexing techniques that can be used to increase the optical link's capacity are outlined. The optical network topologies are introduced with a particular interest given to both current and possible future variants of optical access networks.

Chapter 2 provides a brief introduction to the evolution of cellular technologies in the past decades. Key subsystems responsible for enabling wireless transmission over optical links are presented and their properties discussed. Subsequently, the advantages of using optical access networks for the accommodation of wireless backhaul are examined. Various system architectures employable for the optical transmission of wireless bands in the optical access network along with their advantages and disadvantages are also outlined, with past examples presented from the literature.

Chapter 3 focuses on creating an efficient means for the co-existence of wired and wireless services in OFDM based PON structures, without the need for frequency up and down conversion or WDM. This is achieved by the de-activation of numerous subcarriers in the wired band, which results in the creation of a spectral notch, within which the wireless LTE services are operated with reduced level of inter-band interference. This work also focuses on the impact of nonlinearity and RIN in direct modulation OFDM systems. Through

experimental and simulation studies, performance deterioration as result of laser nonlinearity and RIN is evaluated. The role of optical injection in the reduction of nonlinearity and RIN is discussed. The optical injection is experimentally achieved by using a novel monolithically integrated device.

Chapter 4 describes a method in which spectral notches were created in the spectrum of optical channels in PONs which were modulated by serial OOK modulation formats. These notches were then used to accommodate for wireless signals without needing high frequency local oscillators for their up/down conversion. These spectral notches in the spectrum were created by the employment of a system of binary line encoders. The motivation behind this work emerges due to the technological state of currently standardized PON topologies, in which the key modulation format used is OOK. The feasibility of this scheme is demonstrated both experimentally and through simulation models by using two different line encoders and LTE wireless signals.

Chapter 5 explores the employment of FBMC based modulation formats in intensity modulated PONs both in downlink and uplink communication channels. In downlink the impact of such a system is evaluated experimentally with respect to varying data-rates and various lengths of fibre. In the uplink the impact of Multi Access interference which arises from the loss of orthogonality between the subcarriers of neighboring ONUs is studied and compared to OFDM PON. Through experimental and simulation models the impact of MAI at uplink channels in this FBMC based PON architecture is studied.

Chapter 6 gives a concise summary of the conclusion that can be drawn from the results and discussions presented in this thesis. The potential for future work in the areas discussed throughout this thesis is also outlined.

Chapter 1

Optical Access Networks

This chapter provides a general overview on optical communications. Different key architectures making up an optical network are defined and the technological progress in each is presented. The ever-increasing demand for greater network speeds is outlined and the challenges posing next generation optical networks are discussed.

1.1 Introduction

The advent of the internet and the fast growth in bandwidth requirements, has forced telecommunication networks to employ optical technologies. The major shift from copper cabling can be attributed to the properties of fibre, which are its low loss, high bandwidth and immunity to Electromagnetic Interference (EMI).

There are number of breakthroughs that revolutionised optics and kick started the employment of this technology in telecommunications. The very first step was the demonstration of the first working laser in 1960 [31], followed by the realization of a transport medium for the lightwave information. The first major step for the identification of a suitable waveguide for optical frequencies was taken by Kao and Hockham [32], where required specifications for an adequate waveguide were laid out. Following Kao's specifications researchers at Corning were able to achieve a loss profile equivalent to 17 dB/km in 1970 [33], and this figure was later reduced to 4 dB/km in 1972. This progress

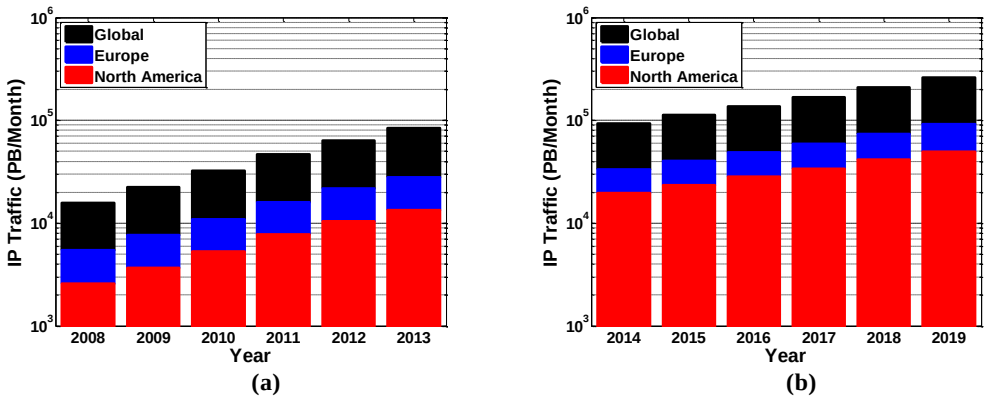

Figure 1.1. Forecasted growth in IP traffic, from (a) 2008, and (b) 2014.

made way for the introduction of the earliest optical fibre communications systems in late 1970's with capacities reaching 45 Mbps [34]. With the objective of reducing costs per information bit, the capacity per optical fibre and its reach has increased rapidly, leading to links capable of transmitting at many Tb/s and reaching thousands of km of fibre in recent years [35]. A key player responsible for the rapid increase in transmission capacity in optical fibre was the introduction of Erbium-doped Fibre Amplifier (EDFA) in the late 1980's [36]. EDFAs made possible the amplification of optical channels without the need for a mid-line electro-optical conversion for the re-generation processes. EDFA's also provided the basis for simultaneous amplification of multiple wavelength channel's accommodated by one optical fibre in Wave Division Multiplexing (WDM) architectures [37]. Other factors responsible for the notable increase in capacity of optical fibre have been the exploitation of advanced modulation formats, Digital Signal Processing (DSP) techniques, and Forward Error Correction (FEC) coding [38].

Figure 1.1 points to the estimated growth in global Internet Protocol (IP) traffic [39, 40] between the years 2008 to 2019. Given the introduction of bandwidth-intensive applications both in wired and wireless communications, the global internet traffic in 2008 was more than 10 exabytes per month, this number then increased by more than fivefold in the year 2013. The IP traffic in North America and Europe in 2008 accounted for 25% and 28% of global traffic respectively. These two figures each experienced an increase of 19% and 20% accordingly by the year 2013. Mobile data traffic in 2008 accounted for 0.3% of global IP traffic, this figure saw an unprecedented growth of 131% in the five year time frame from 2008.

By 2014 the global IP traffic reached 59.9 exabytes per month and it's estimated to increase by 23 % by 2019 and reach 167.9 exabytes per month in 2019. The global mobile traffic in 2014 accounts for 2.5 exabytes which is estimated to increase to 29.5 exabytes by 2019. In 2014 wired devices accounted for 54% of the IP traffic, and this figure is set to

change by 2019, where the contribution of wired devices reduces to 33 % while Wi-Fi and mobile devices will account for the other 66% of the traffic.

The forecasted growth in IP traffic clearly highlights the increase of demand from the end-user for on-demand multimedia services and bandwidth hungry applications. In light of these demands, the current telecommunication industries are expected to be under pressure for providing solutions by developing the next generation technologies required in every segment of the optical network.

In order to meet the forecasted growth in telecommunication traffic, operators are actively moving towards a paradigm shift in their networks by introduction of advanced technologies. In the access portion, this paradigm shift is achieved by substituting the existing copper based system such as Asymmetric Digital Subscriber Line (ADSL), Plain Old Telephone Services (POTS) or Cable Television (CATV) with optical fibre [41]. In many parts of the world Fibre–To-The-X (FTTx) technologies are actively being employed in order to future proof against the forecasted bandwidth demands. Most model of FTTx are based on the Passive Optical Network (PON) [42], due to its cost effectiveness and low energy consumption per bit.

1.2 Multiplexing Techniques

In optical links in order to overcome the bandwidth limitations imposed by serial channels, and increase capacities, several serial links can be multiplexed together. The simplest technique involves the overlaying of various serial channels onto distinct fibre cables; such method is called Spatial Division Multiplexing (SDM) and leads to higher cost if the required numbers of fibres are not already installed between the service provider and the end-user. However with the introduction of multi-core fibres, SDM is becoming an attractive multiplexing technique for expansion of the transmission capacity [43]. The majority of today's fibre installations are single core, for this reason, multiplexing techniques are adopted in which additional channels can be transmitted by changing the terminating equipment. Some examples of such methods are Electrical Time Division Multiplexing (ETDM), Wavelength Division Multiplexing (WDM) and Orthogonal Frequency Division Multiplexing (OFDM).

1.2.1 Electrical Time Division Multiplexing

In high capacity fibre optic communication systems, the introduction of Electronic Time-Division Multiplexing (ETDM) or TDM reduces the cost for per bit of transmission. This reduction in cost is dominated by factors such as low power consumptions, small footprint, reduced management effort and complexity in the system [44]. ETDM operates by adapting the majority of signal processing techniques in the electrical domain, and thus using optical techniques only for transmission of data using low loss optical links.

Figure 1.2 represents a typical ETDM transmission system. At the transmitter side a number of electrical data tributaries running at low data rates are aggregated to a higher temporal line rate using an electrical multiplexer. Subsequently an external optical modulator such as a Mach-Zehnder Modulator (MZM) or a directly modulated laser diode is used for the electro-optical conversion of the high speed ETDM signals [45]. An electrical amplifier stage is usually required between the electrical multiplexer and the circuitry driving the external modulators, in order to compensate for the high voltage swings required by the optical modulators [46]. An optical link is then used as a communication channel for transmission of the generated optical ETDM signal. At the receiver end, the optical signal is converted back to the electrical domain by a high-speed photodiode, and at this point, a synchronous electrical clock signal is recovered from the incoming data signal and is further used for the identification of an electronic decision point and de-multiplexing.

The standard for 100 GbE systems was approved in 2010, which specified the transmission of 100 Gb/s using four separate optical channels each carrying 25 Gb/s. Nevertheless, a solution based on a 100 Gb/s single wavelength channel using ETDM is capable of significant cost reduction [47]. On the contrary, ETDM systems approaching 100 Gb/s using a single wavelength channel suffer from the so-called “electrical bottleneck” which

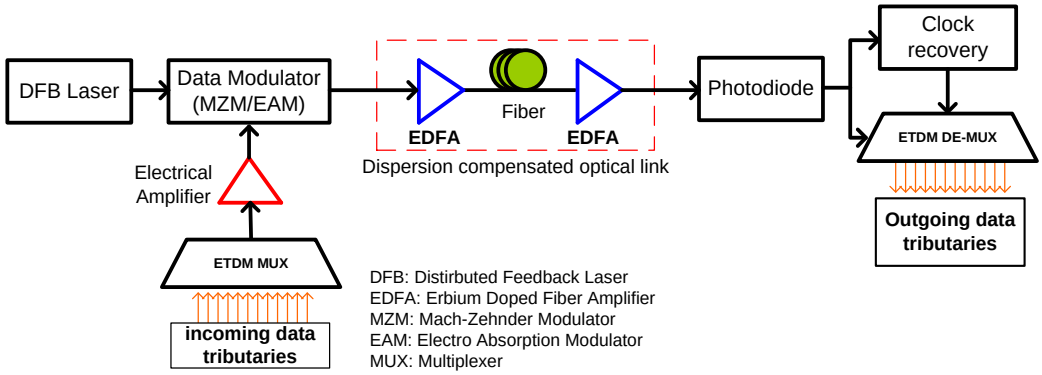

Figure 1.2. Typical setup of an ETDM system

limits the performance of the system due to shortcomings inherent to the driver amplifier and the optical modulator. Based on past evolution of classical core transport hierarchies (e.g. SONET/SDH) the stepwise upgrade of bitrate by a factor of four for each generation based on previous standards (2.5 G, 10 G, 40 G) placed an expectation for the next generation ETDM bitrates to be at 160 Gbit/s. However, such high bitrate is far beyond the operation speed of current electronic and opto-electronic components [48]. The limitations preventing viable realization of high capacity ETDM systems are associated with the bandwidth and output power of available driver amplifier along with bandwidth and required V_{pi} of the commercially available optical modulators [49], which can result in significant system penalties.

In order to reach the 100 G capacity point with reduced levels of performance penalty in a single channel transmission system based on ETDM, electrical multiplexing techniques can be combined with advanced modulation formats such as differential-quaternary-phase-shift-keying (DQPSK) and/or various multiplexing schemes such as Polarization Division Multiplexing (PDM) [49]. The highest reported serial channel data rate based on ETDM is 107 GBaud/s. In this work PDM and quadrature phase-shift keying (QPSK) [50] as-well-as 16-ary Quadrature Amplitude Modulation (16 QAM) were used [51]. However, these high capacity ETDM realizations suffer from considerable penalties, which can be attributed to the optical modulator's bandwidth and the quality of the electrical signals driving the optical modulator [52].

1.2.2 Optical Time Division Multiplexing

To alleviate the so called electrical bottleneck, encountered with ETDM systems due to performance limitations induced by the electronic devices [49] for data rates approaching

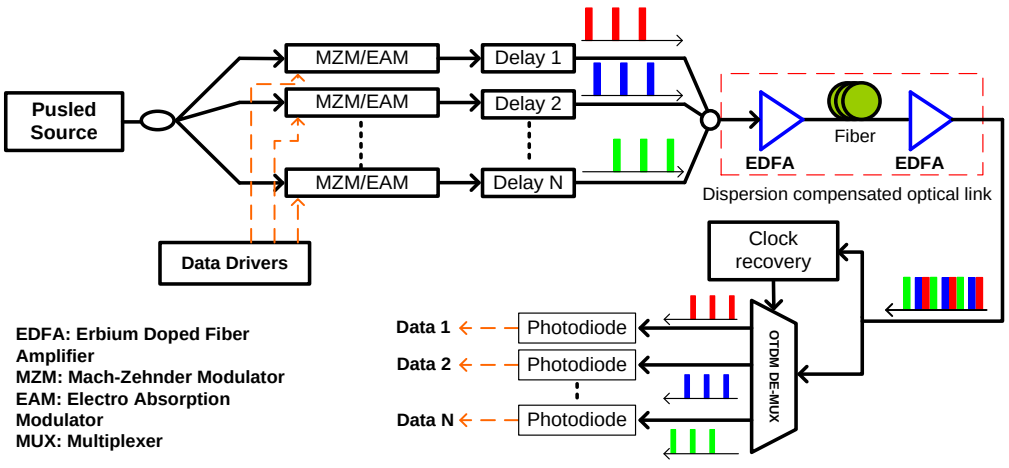

Figure 1.3. Typical setup of an OTDM system

100 Gb/s and above, Optical Time Division multiplexing (OTDM) technique is seen as an alternative candidate. In OTDM high serial interface rates can be achieved by the utilization of optical devices and leveraging efforts on optical techniques. The idea behind OTDM is based on parallelization of an optical RZ pulse train produced by an optical pulse source into multiple paths. Each path is subsequently equipped with an optical modulator that is driven by an electrical data driver. The modulated optical pulses from each tributary are then time delayed with respect to each other and are optically combined to generate a high-speed optical serial link. Finally, at the receiver-end some means of optical de-multiplexing is then employed to separate the serialized optical pulses into their correct tributaries [53].

Figure 1.3 presents a typical system architecture required for forming a full OTDM system. The pulsed source at the transmitter-end is a key device in such systems, and it is realizable by pulse carving methods using EAM's or MZM's, gain switching of laser diodes, and Mode Locking techniques. To minimize errors, the generated pulse train must have low levels of jitter for synchronization issues, and low amplitude noise as well as high extinction ratios [53] to provide higher resilience to noise present in the channel.

The reported data rates achieved in OTDM are typically higher than those achieved in ETDM systems [54], with data rates of 1.28 Tb/s initially demonstrated by employing polarization multiplexing techniques [55]. To further increase data rates advanced modulation schemes were also employed, where 3.56 Tb/s had been realized using 8PSK in conjunction with coherent detection [56].

1.2.3 Wavelength Division Multiplexing

In order to exploit the large inherent bandwidth in optical fibres, optical carriers at evenly spaced optical frequencies can be multiplexed together and subsequently transmitted through a single optical fibre. Each distinct optical carrier can then be modulated individually by various electrical modulation schemes. This multiplexing technique is called Wavelength Division Multiplexing (WDM). WDM is analogous to FDM in radio communications that is constituted of multiple modulated RF carriers operating at a close proximity in frequency, whilst using the same communication medium. WDM has allowed for the exploitation of the vast bandwidth available to fibre, e.g. 10s of 100G signals can now be multiplexed and transmitted over a common fibre link. The concept of WDM was pursued since the very early commercial optical communication systems in the 1980s, where after 15 years of research, commercial systems with capacities between 20-40 Gb/s appeared in 1995. With the increase of global demand on bandwidth, created by the widespread use of the internet, WDM capacities in order of terabits per second were

reached by the year 2000 experimentally [35]. To meet the forecasted bandwidth demands in upcoming years [57], both the commercial and research communities are seeking ways to surpass the existing capacity limits in fibre. Experimental work has demonstrated transmission capacities over 100 Tb/s and transmission through over 200 km of fibre [58]. Capacities up to 1 Petabyte/s have also been demonstrated for transmission over 10s of km of fibre [59].

The popularity of WDM in high capacity optical links was driven by the advent of Ebrium doped fibre amplifiers, which ensured simultaneous amplification of multiple wavelengths without the need of in-line re-generation processes [35]. WDM is a widely deployed scheme in core and metro networks, and the high link capacities as-well-as the bandwidth flexibility provided by WDM, also makes it a viable solution for access topologies [60].

According to the International Telecommunication Union (ITU), the channel spacing or the frequency spacing between each operation optical carrier in a deployed WDM system in core and metro networks is either 100 GHz for Coarse WDM (CWDM) or 50 GHz for Dense WDM (DWDM) [61]. To increase the spectral efficiency defined as bits/second/hertz, the spacing can be decreased even further to 12.5/25 GHz spacing forming Ultra Dense WDM (UDWDM).

WDM systems take on architecture similar to that presented in Figure 1.4. At the transmitter and receiver-ends instead of using optical filters and splitters for multiplexing and de-multiplexing they use more advance technologies, such as Arrayed Waveguide Gratings (AWG's) [62] for multiplixing and de-multiplixing multile wavelenghts (λ) to/from the optical fibre. At the receiver, each wavelength is sent to a specific receiver for O/E conversion.

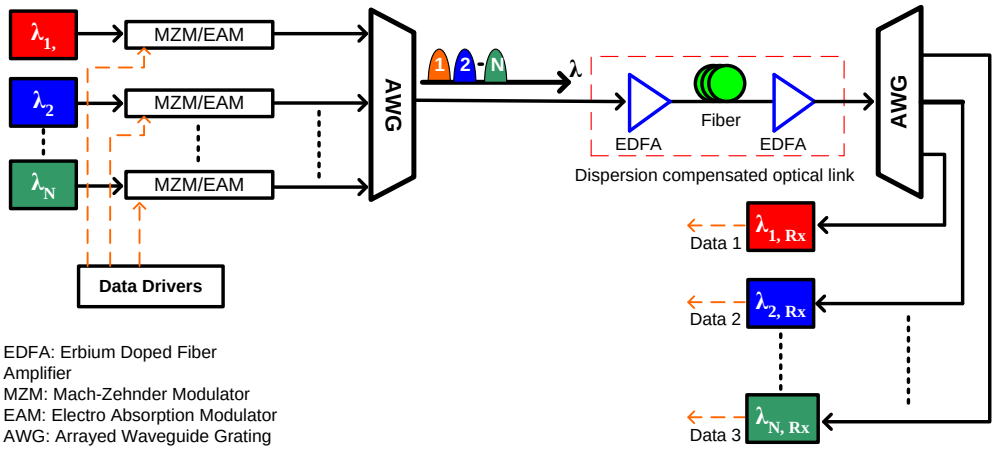

Figure 1.4. Typical setup of a WDM system

1.2.4 Orthogonal Frequency Division Multiplexing

Initially considered for RF applications in the mid-1980s [63], Orthogonal Frequency Division Multiplexing (OFDM) is now being used to form the basis of many practical wireless standards [64], such as WiFi, WiMAX, LTE and UWB. OFDM also has created the basis of many Digital Subscriber Line (DSL) standards as well as TV and radio broadcasting protocols in most of the world [65].

Similar to FDM, OFDM is a Multi Carrier (MC) system composed of multiple harmonically related tones, each carrying a different data load modulated by QAM symbols. The premise behind MC systems is that a high capacity serial stream can be split into multiple lower data rate tributaries, elongating the symbol period per each subcarrier. The novelty in OFDM in contrast to FDM comes through the elimination of the guard bands between subcarriers, which in FDM is used to minimize inter carrier interference (ICI). The elimination of guard bands is achieved by forming an orthogonal relationship between the operational subcarriers; and this relationship eliminates the need for guard bands and also allows the modulated subcarriers to overlap one-another in the frequency domain. The possibility of overlapping orthogonal subcarriers provides increased spectral efficiency by making it possible to transmit more data in a compact spectrum. Figure 1.5 presents the overlapping of three orthogonal subcarriers in the frequency domain.

The resilience of OFDM to inter symbol interference (ISI) caused by the dispersive channel, in contrast to a serial transmission system is identified as one of its main advantages [66]. The second advantage of OFDM is the transformation of complexity in transmitters and receivers from analogue to the digital domain, where linear channel impairments can be simply accounted for accordingly [66].

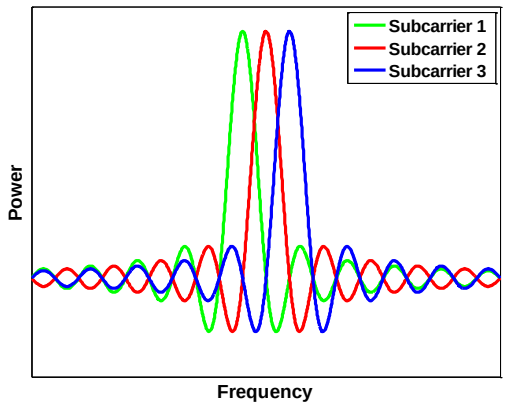

Figure 1.5. Spectral content of three orthogonal subcarriers in OFDM

The demand for higher data rates across dispersive optical channels and the advancements in DSP has resulted in tremendous amounts of work on the application of OFDM in optical communications [66]. The implementation of OFDM in an intensity modulation and direct detection (IM-DD) scenario in optical communication systems, requires the output of the electrical OFDM Transmitter to either directly modulate a laser diode [5], or drive an external optical modulator such as a MZM biased at the quadrature point [3]. Otherwise, Coherent OFDM can be employed, where direct detection techniques are replaced with coherent detection [67], at the expense of complex receivers, that enhances receiver sensitivity.

1.3 Optical Networks

Today's optical networks constitute a number of interconnected sub-networks. These are access (connecting the end user to wider networks which are the core and metro networks), metropolitan (interconnection of the access to the core network) and core networks (which transport information over very long distances) [68]. Each of these distinct network topologies have an array of distinct architectural properties that adhere to specific issues regarding to its position in the wider network. For example, many users rely on core networks thus equipment and energy costs are subdivided amongst a large population. Whereas in access networks the related costs are higher as every user will account for distinct equipment and energy consumption. Due to increased and bursty demands on bandwidth, optical networks are required to become more reconfigurable and dynamic in order to adapt to changing traffic patterns in the network [69], created by applications and devices requiring on-demand services.

1.3.1 Core Networks

Metro and access networks rely on the core for information transactions over distances between hundreds to thousands of kilometres. These networks constitute many nodes and amplified links, and at each node the aggregated data carried on various tributaries is either routed to other nodes or metro networks. Core networks use WDM and amplification through EDFAs to exploit the bandwidth of optical fibre. Earlier core networks operating at line rates of 2.5 or 10 Gbps and 20 optical channels were able to provide capacities of 50-200 Gbps [70]. Such data rates marked a significant increase in fibre capacity compared to the earliest commercial systems in the late 1970's which provided capacities of around 40 Mbps [34]. The increase in demand for bandwidth and capacity from access networks, and advances in the field, has led to increases in the line rates and number of optical channels

per optical fibres currently employed. Such advancements in the field of optical communications have provided the possibility for core networks to have capacity extensions from hundreds of Gbps to tens of Tbps in recent years [38]. And such progress in core networks has pushed the bandwidth bottleneck towards metro and access networks.

A significant breakthrough for deployed core networks today has been the advent of optical bypass. In legacy core networks, all wavelengths traversing a node were subjected to optical-electrical-optical (O-E-O) regeneration, regardless of the final destination of that wavelength. This scheme increased the number of required per-wavelength transponders in a given node which in-turn also increased power consumption and costs. Optical bypass technology has made it possible to limit the O-E-O regeneration process only to traffic being added or dropped from a node, with the transiting traffic remaining in the optical domain.

Other factors that are contributing to the progress in core networks are the employment of dispersion compensating entities such as Dispersion Compensating Fibre (DCF), Electronic Dispersion Compensation Techniques and FEC coding [70].

1.3.2 Metropolitan Area Networks

Metropolitan (metro) Area Networks, or MANs, extend over 100s of kilometres and act as an interface between core and access networks as shown in Figure 1.6. Unlike core

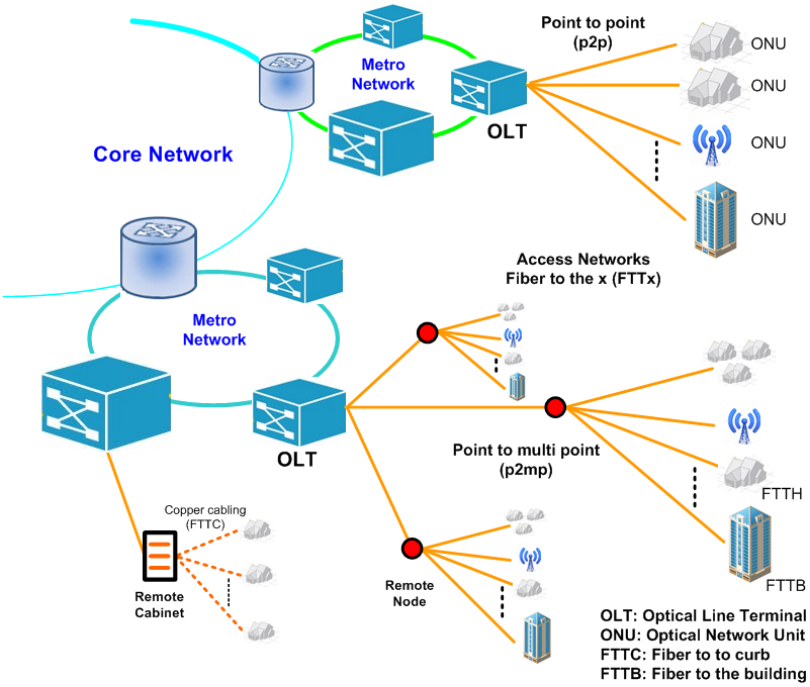

Figure 1.6. Optical network topology

networks, in which traffic is mostly point to point (p2p) with many optical amplifiers and only a few reconfigurable optical add/drop multiplexers (ROADMs), metro networks are highly meshed, where every node is a wavelength switching point [71]. At the nodes which provide an interface to access networks, wavelengths carrying data to/from access networks can be either dropped or added accordingly.

The increasing bandwidth demand emerging from the access network has driven metro networks to be dominated by channel capacities of 10 Gbps on dispersion managed fibre plant, with the transition towards 100 G systems now being considered [71].

Similar to the core the reduction in O-E-O regenerators in metro networks has led to lower energy consumption and costs in metro. The replacement of fixed OADMs to ROADMs is allowing the network to evolve towards meeting the changing traffic patterns. The increase in spectral efficiency and capacity per channel, provided by the employment of advanced modulation schemes and DWDM will also help to facilitate forthcoming bandwidth demands.

1.3.3 Access Networks

Access networks are usually referred to as the last mile, as this is the segment of network, which connects the end user (residential or business) to the metro, and core networks (Figure 1.6). Given the fast growth in internet traffic, mostly dominated by video services such as video conferencing, a high demand is being placed on access topologies to fulfil end user's needs. These demands are being effectively meet by employing optical technologies in the access networks.

In order to push optical technologies closer to the end user, Fibre To The x (FFTx) networks have been deployed widely worldwide. The various models of FTTx, which namely are FFTH (home), FTTC (curb), FTTN (node) and FTTB (building), define architectures within which the end user can be connected to the wider optical network. The connections in FTTx can involve a dedicated optical fibre link as is the case for FTTH or a combination of fibre and copper cable as implemented in case of FTTC scenario.

The FTTx models are based on two main physical architectures; these are mainly P2P or point to multipoint (P2mP). The P2P links connect the end user to the central office or OLT by a dedicated fibre link, and such a connection is provided to a user that requires higher data rates. In P2mP as the name suggests, the bandwidth available in a single link is shared between multiple end users.

Currently deployed optical systems in access networks have capacities of around 2.5 Gbps, and these systems are being upgraded to 10 Gbps links. To further increase these capacities future optical access networks are envisioned to use WDM or other advanced single carrier or multi carrier's modulation and multiplexing schemes such as QPSK, QAM, OFDM or FBMC.

1.4 Optical Access Technologies

Technological upgrades which led to capacity extensions in both core and metro, has pushed the "bandwidth bottleneck" towards access networks, due to the existence of legacy, low bandwidth equipment in the access. From the early days, the significance of fibre optics in access was identified by operators such as Bellcore where they predicted that FTTC and FTTH solutions could be at economical parity with copper based solutions before the late 1990s [68]. Initially, the integration of optical solutions in access networks was proposed in the 1980s by large carriers [72]. However, these proposals did not proceed to commercialization, given the lack of demand and high costs at the time. The commercial introduction of fibre in a closer proximity to the user initially started by carriers deploying Subscriber Loop Carrier (SLC) systems, which replaced copper lines with optical fibre for the first few km between the central office and the serving office. In the late 1990s the Cable TV (CATV) operators started to enhance their broadcast quality by integrating fibre in their infrastructure in the form of Hybrid Fibre Coaxial (HFC) [41] systems which brought fibre within 150 m of the end user. In 1998, BellSouth began to use FTTC for new installations or refurbishments that brought fibre within 100's of meter of the end-user, which like HFC used electrical cabling for the drop connection. FTTC is also a hybrid structure as it uses DSL type transmission over the drop portion of the fibre [73].

FTTC systems usually employ OFDM based DSL from the cabinet which can be either positioned at the street corner or basement of a building to the user's premises over electrical copper cabling. Early DSL systems used 1.1 MHz of bandwidth and a bit rate of 364kb/s, these bandwidths subsequently increased to 2.2 MHz for VDSL and 30 MHz for VDSL2 [68]. FTTC schemes can also simultaneously support POTS and Integrated Service Digital Network (ISDN), by multiplexing these low frequency services at either the central office or the Optical Network Unit (ONU). A significant limitation of FTTC is the employment of copper cabling which compared to optical fibre has higher attenuation and no immunity to EMI. These factors reduce the allowable bandwidth-distance product in the drop link connecting cabinet and the end users. DSL lines with 1.1 MHz bandwidth are

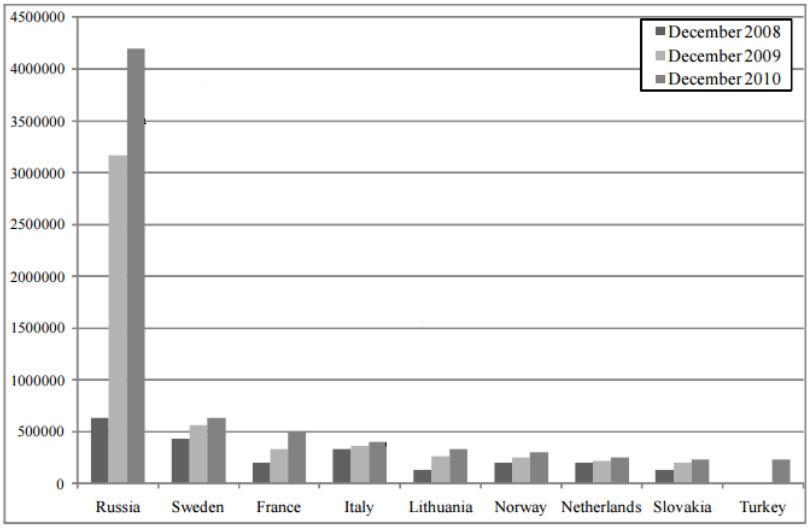

Figure 1.7. FTTH/FTTB connected homes in Russia and Europe 2008-2010 [75].

capable of supporting 2.5 km, VDSL lines operating at 15 Mb/s can have reaches up to 1.7 km and at 52 Mb/s their distance are reduced to only 300 m or less [74]. From the early days since fibre was introduced into access networks, the replacement of the drop link by optical fibre and the realization of all optical access topology were seen as a means for providing higher bandwidth signals over longer distance.

With the growing per-user demands for higher bandwidth in wired access networks, a definite progression towards all optical access topologies such as FTTH was envisioned. Looking at IP traffic in 2009 (Figure 1.1) it was estimated that in Asia-Pacific and North America, the total traffic reached 5.5 and 3.3 exabytes per month, and this clearly can be seen as a driver for worldwide deployment of FTTH/B technologies. In December 2009 it was estimated that 38.8 and 7.6 million houses in Asia-Pacific and North America respectively were connected to FTTH technologies [9, 46],

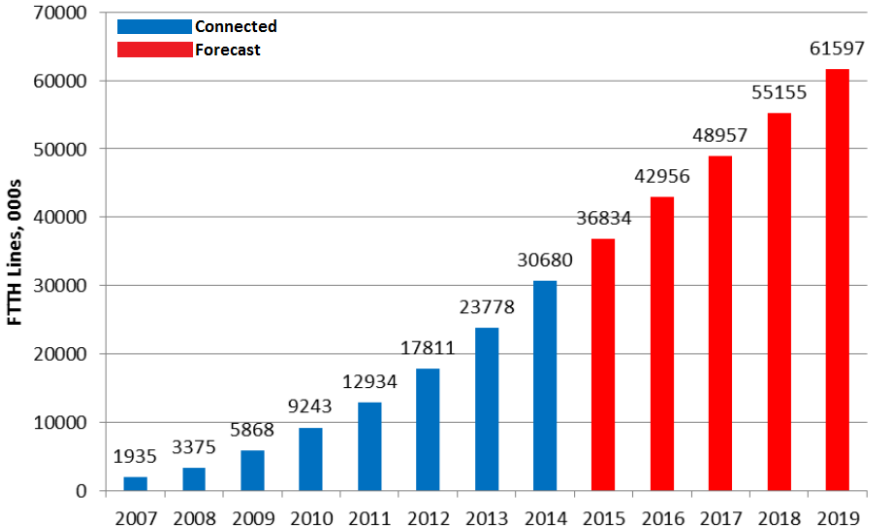

Figure 1.8. FTTH/FTTB connected homes in Russia and Europe and forecast 2007-2019 [76]

As it can be seen in Figure 1.7, in December 2010 approximately 3.9 million subscribers were identified to have access to FTTH/B technologies throughout Europe and 4.2 million in Russia. Europe ranks lowest in FTTH/B installations compared to North America and Asia-Pacific but it was anticipated in 2010 for operators to have the capacity to support 22.3 million premises by FTTH/B [75].

As shown in Figure 1.8 the total number of connected premises by FTTH/FTTB in both Europe and Russia had reached 30.6 million by 2014, which compared to 2010 accounts for a 231% increase. The figures in 2014 are forecast to increase by nearly 100% by 2019 where it's anticipated that European IP traffic will reach 41.5 exabytes per month, at this point 61.6 million households will be connected to FTTH/B services [76].

1.4.1 Passive Optical Networks

Most FTTx topologies are based on Passive Optical Networks (PON's), due to their cost effectiveness and low energy consumptions per bit [42]. These topologies achieve cost reductions by eliminating all active equipment within the link, leaving the active equipment at the extreme ends of the communication link. The active equipment in the central office is called the Optical Line Terminal (OLT) and it is responsible for transmitting and receiving the multiplexed data tributaries from/to N number of users. At the receiver, the active equipment, which is also a transceiver, is positioned in the user's premises (Optical Network Terminal) or in close vicinity of the user (Optical Network Unit) and the drop from this point to the user is usually done with electrical cabling. As shown in Figure 1.9, in PON an optical fibre connects the central office or OLT to a remote node via an optical fibre. In todays deployed PONs the Remote Node (RN) is equipped with a 1:N passive splitter, which creates N copies of the incoming optical signal from the OLT, each copy is then sent to different users sharing the same feeder fibre, via separate fibre connections

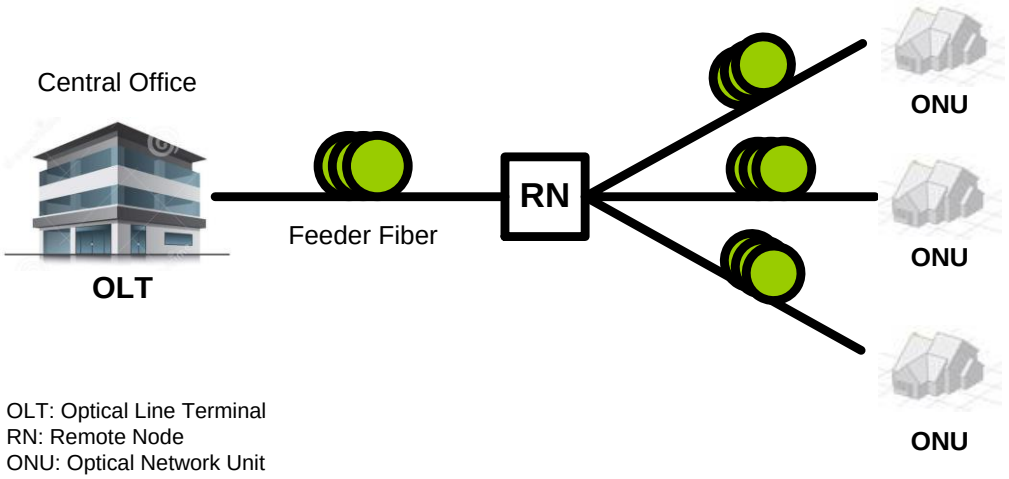

Figure 1.9. Simplified PON architecture

(Distributing/drop Fibre). The RN is positioned closer to the serving users, in order to minimize the required length of N distributing fibres and reduce the costs associated with the installation of fibre. By using a common feeder fibre, passive splitter and OLT, network resources are shared effectively

Some of the requirements of future PON deployments are higher supportable bandwidths per user, higher user count, dynamic bandwidth assignment, extended reach compared to legacy systems and lower costs [42]. A key to reaching a highly scalable PON with a very high splitting ratio, apart from the optical or electrical equipment, is the high multiplexing level required to handle all individual data flows that travel along the fibre. All of the contemporary standardized and deployed PON topologies operate based on On Off Keying (OOK) modulation format in conjunction with Time Division Multiplexing, where the need for increased data rates necessitates the need for the intervention of high cost and high bandwidth electro-optical devices, rendering the system more susceptible to dispersive effects in fibre which in turn can also limit the maximum possible reach of the system. To address such issues with single carrier OOK, a shift in the employed modulation and multiplexing format has been envisioned for next generation PONs [42, 67]. The proposed modulation formats in these systems are based both on coherent and direct means of reception. PONs exploiting the use of a coherent receiver such as phase modulated single carrier systems have the potential to provide higher spectral efficiencies, higher resilience to noise, higher split ratios and a remarkable path towards Dense-WDM (DWDM) with dynamic wavelength allocation. The subsequent use of high speed Digital Signal Processing (DSP) algorithms in association with coherent reception in these architectures can further aid to combat dispersive effects in fibre and allow further system reach. However all these affinities towards coherent reception in PONs are repelled by the immense level of optical and electrical complexity in the receiver front-end [42]. On the other hand, direct detection methods as used in contemporary PON systems has the attractiveness of reduced costs as a result of eliminating the complexities that are introduced by coherent systems. To increase spectral efficiency in direct detection system, modulation formats such as Subcarrier Multiplexing (SCM) [77, 78], Pulse Amplitude Modulation (PAM) [79, 80] and orthogonal multicarrier modulation formats are employed [67]. In SCM electrical RF subcarriers each modulated with Quadrate Amplitude Modulated (QAM) symbols are combined and used to intensity modulate an optical signal. PAM operates on the same basis as OOK (2 level PAM) with the difference being that number of signal levels are increased. Adapting orthogonal multicarrier modulation formats can provide a high level of spectral efficiency in contrast to SCM, since the frequency guard bands used are eliminated by overlapping neighboring subcarriers and avoiding Inter

Carrier Interference (ICI) by introducing orthogonality between these subcarriers. Two examples of multicarrier modulation formats employing orthogonal subcarriers are OFDM and Filter Bank Multi Carrier (FBMC).

Equipping each user in PON with a distinct wavelength in a move to realize of a true WDM-PON architecture has always been envisioned to provide the most functional access network [41]. However the requirement and the management of wavelength specific transmitters/ receivers can force the architecture to suffer from high Capital Expenditure costs (CAPEX) and operational expenditure costs (OPEX) [42]. Nevertheless, to compensate for the possible high costs associated with single carrier optical channel operating at 10+ Gb/s, recent PON standards have aimed at introducing finite number of fixed wavelengths in a PON link each operating at maximum rate of 10 Gb/s. To increase the split ratios or to provide extra flexibility in the bandwidth available to the end users, different multiplexing and modulation formats can be combined to form hybrid multiplexing. The possible multiplexing techniques are discussed in the following sections.

1.4.1.1 Time Division Multiplexed PON (TDM-PON)

The requirement for optical technologies in access networks in order to fulfil growing bandwidth demands, created the basis for the establishment of the Full Service Access Networks (FSAN) organisation in 1995. FSAN aimed at accelerating the commercialization of optical access technologies. Since the establishment of FSAN, numerous standardizations were put forth, specifying requirements for PON deployments. All commercial PON deployments as a result of these standardizations employed Time Division Multiplexed Access (TDMA) for multiplexing the bandwidth shared by N users. Figure 1.10 shows the typical structure of a TDM-PON, where the OLT here assigns a time slot to each end user, which contains the downlink data for that user. The optical signal containing the multiplexed data after traversing the optical feeder line, is split into N

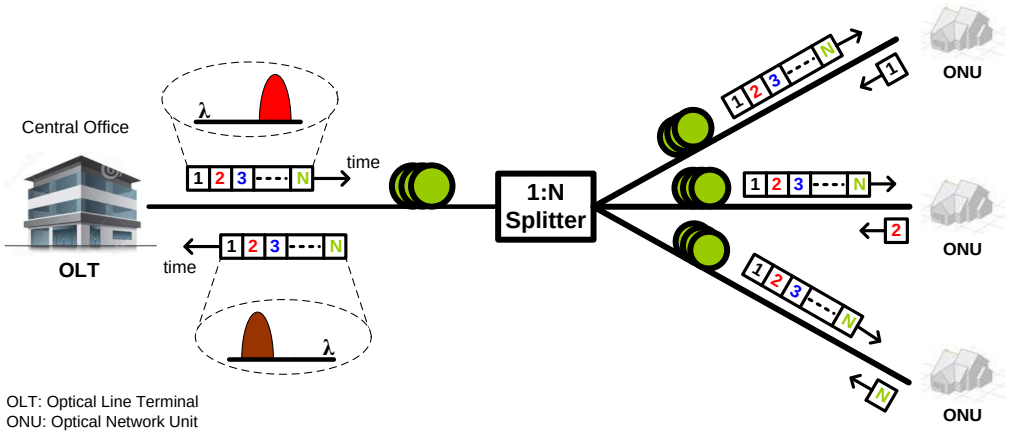

Figure 1.10. Typical TDM-PON Architecture

identical copies at the RN by a 1:N optical splitter, and subsequently each ONU extracts it's data load from the time slot assigned to it. In the uplink, each user is also assigned a time slot at which the ONU transmits its data on. Each ONU operates at a common wavelength and subsequently the optical information from each ONU is coupled at the power splitter at the RN. As the uplink and downlink streams are deployed on the same optical feeder fibre, it is crucial to avoid interference between the two. In currently standardized TDM-PON this interference avoidance is achieved by using separate wavelengths for the downlink and uplink streams.

One of the earliest propositions for TDM-PON appeared in 1987 under the name "telephony on passive optical network (TPON)" where bi-directional telephone services were carried by a passive optical distribution network [81]. Proposals for all optical structures did not reach commercialization due to low demand and high costs. FSAN recommended the first TDM-PON, which was based on Asynchronous Transfer Mode (ATM) protocol, this technology was called ATM-PON or (APON) which operated at downlink rates of 155/622Mb/s and 155 Mb/s for uplink. APON was ratified by the ITU in 1998 and later redefined in 2005 with extra functionalities [82]. The new set standards were called Broadband PON (BPON) (ITU-T G.983.1) which has a nominal line rate of 1.25 Gb/s in the downstream and a line rate up to 622 Mb/s in the uplink.

The successor technologies to APON/BPON were ITU-T G.984 Gigabit PON (GPON) [83] and IEEE 802.3ah Gigabit Ethernet PON (GE-PON) [84]. In these scenarios downlink data rates of 2.5 Gb/s and 1 Gb/s were achieved for GPON and GE-PON respectively and 1.25 Gb/s in the uplink direction. Currently GE-PON and GPON have become the most popular choice for FTTx deployments worldwide [42]. The next step after standardizing gigabit capable PON systems for meeting bandwidth demands, became the standardization of technologies capable of operating at 10 Gb/s. FSAN along with ITU-T and IEEE had defined their prospective for 10 Gb/s PON systems in IEEE Std. 802.3av 10 GE-PON [85] and ITU-T XG-PON [34]. 10 GE-PON supports symmetric upstream/downstream line rates of 10.3/10.3 Gb/s and asymmetric line rate of 10.3/1.25 Gb/s. XG-PON on the other hand is devised to support two data stream variants of 10/2.5 Gb/s and 10/10 Gb/s for downstream/upstream. A major requirement that was set by IEEE and ITU during the compiling of standards for 10G capable systems was the re-usability of already deployed feeder fibre and optical splitters. This factor allows the 10G standards to co-exist with legacy technologies; this decision was driven in respond to carriers requiring an easy and cost effective migration path from legacy technologies such as GPON and GEPON. Field trials have been already carried on both XG-PON and 10 GE-PON by numerous

organizations such Verizon [86] and the first commercial tests and deployment of XG-PON have been carried by BT and ZTE [87] .

1.4.1.2 Wavelength Division Multiplexing PON (WDM-PON)

Currently deployed PON topologies technically operate on a WDM basis, whereby two wavelengths are used per channel, one for the uplink and another for the downlink [42], and with both shared by N users. On the contrary, a true WDM-PON system would require multiple wavelengths both for the downlink and for uplink. Following the standardization of 10 Gb/s TDMA based systems by ITU and IEEE, it was realized that TDMA-PON is incapable of keeping up with requirements of future access deployments [88], thus in light of that matter WDM technology was considered as a promising candidate [89] for the realization of high capacity optical access links.

A typical WDM-PON realization would have an architecture shown in Figure 1.11, where multiple optical transceivers are housed at the OLT each operating at a distinct wavelength. Each transceiver at the OLT has the capability to employ various modulation techniques such as simple OOK schemes or more advanced modulation formats requiring coherent receivers. The resulting wavelengths are subsequently multiplexed at the transmitter using a WDM splitter such as an Arrayed Waveguide Grating (AWG) and then propagated through a feeder fibre. The multi-wavelength link is then de-multiplexed at the Remote Node (RN) by another de-multiplexer such as an AWG, where the isolated wavelength is routed towards its assigned ONU by a distributing fibre.

In recent years, WDM technologies have been vastly exploited in core and metro networks, although this adaptation has not been commercially possible in access networks yet. Adaptation of WDM technologies is seen as a viable solution for the exploitation of the large bandwidth in optical fibre, which allows an easy route for future upgrades and extensions for new bandwidth hungry technologies and applications.

WDM-PON also requires each ONU also to operate at distinct optical frequencies in order to avoid interference at the uplink. Employing wavelength specific sources both at the

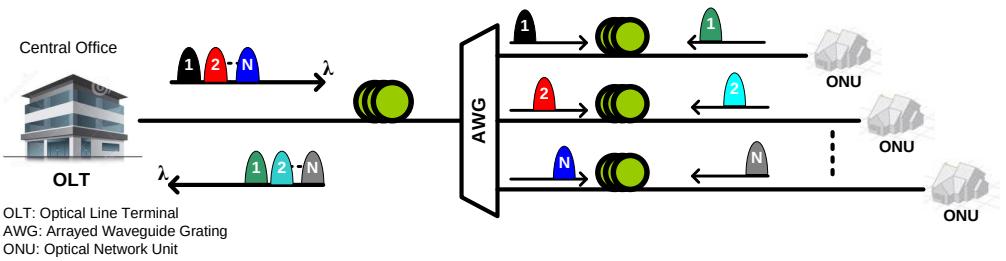

Figure 1.11. Typical WDM-PON architecture

ONU and OLT leads to large inventory of transmitters [90] which significantly raises costs and management efforts. To tackle the management issue, Tuneable Laser (TL) diodes such as tuneable Distributed Feedback Laser (DFB) lasers [91] have been considered, but adaptation of such lasers would involve high costs and requirements such as prior knowledge of operating wavelengths at each ONU, wavelength alignment with the AWG, frequency control for interference avoidance and low switching times [92].

To optimize costs, schemes such as wavelength reuse have been proposed [93]. In these schemes, the inclusion of optical sources in the ONU is eliminated by using the downlink optical signal in conjunction with a Reflective Semiconductor Optical Amplifier (RSOA) for transmission of the uplink data. RSOA's in wavelength reuse schemes are intentionally operated at the gain saturation region, in order to remove the downlink data, and subsequently direct modulation of the ROSA can be used to convey uplink data on the same wavelength used for downlink. A draw back from this scheme is related to the degradation in upstream data at the OLT, as result of it interfering with the downlink signal [42].

Other methods considered to address the large inventory of optical sources in WDM PON's had been based on the integration of colourless sources in the ONU. One form of colourless source is based on the employment of broad-spectrum optical transmitters such as directly modulated Light Emitting Diodes (LEDs) at the ONU. In these systems, the light from the LED after passing through an AWG in the uplink direction, has its spectral content is accordingly sliced. Due to the additional noise in such a system it has a short uplink reach, and FEC methods are needed to compensate for the drawbacks [94]. Other colourless sources can be formed by seeding optical light to ONU's from a Central Light Source housed at the OLT. In these architectures the seeded light is then either used to injection lock a Fabry Perot (FP) lasers [95] or seed ROSA's [96] at the ONU. Self-seeding of RSOA at ONU's has been also investigated in [97], and in such a scheme the uplink wavelengths are chosen by the AWG, as it slices the ASE spectrum from the ROSA originating from each ONU. In order to self-seed the RSOA's, the spectrally sliced ASE bands after passing the AWG in the uplink direction are fed back to the ONU through a passive reflective path made up of an optical circulator and a bandpass filter [42] in the remote node (RN).

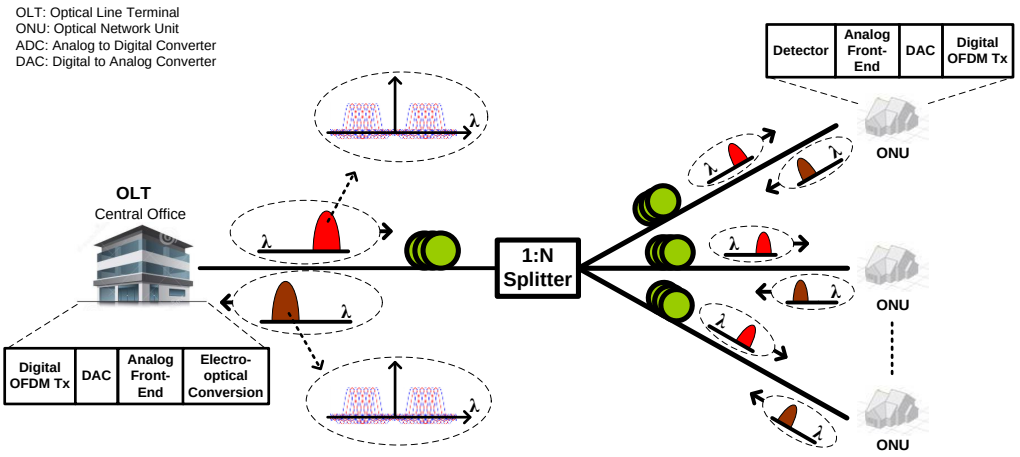

Figure 1.12. Typical OFDM-PON Architecture

1.4.1.3 Orthogonal Frequency Division Multiplexed PON (OFDM–PON)

In OFDM-PON, typical TDM technologies used for transmission and reception are replaced by OFDM capable transceivers. Typical system architecture for OFDM-PON is illustrated in Figure 1.12. At the OLT the user data is modulated onto multiple orthogonal subcarriers in DSP using the Inverse Fast Fourier Transform (IFFT) operation, the resulting digital samples are then converted into analogue by high speed DAC's. Subsequent to the analogue conversion, necessary filtering and up-conversion is carried out in the analogue front-end. The resulting electrical signal is then conveyed on an optical carrier either by directly modulating the laser diode or the employment of external modulators. The optical carrier containing the OFDM channel is replicated into N copies at the Optical Distribution Network (ODN) by an 1:N splitter, where a complete copy of the transmitted OFDM band is sent to each ONU. In the case of intensity modulation with direct detection (IM-DD) OFDM-PON, a simple photodetector is sufficient for the optical to electrical conversion at the receiver. Following the electrical conversion and application of analogue front-end, the signal is digitalized by ADC's and sent to an OFDM receiver equipped with a single tap to recover the transmitted symbols.

Flexible bandwidth allocation is a compelling present day reality for PON's [67] because of multi user nature of such technology requiring efficient bandwidth utilization. The multiple subcarriers that make up the OFDM band can efficiently address the issue of flexible bandwidth allocation by employing OFDM-Access (OFDMA). OFDMA technology currently is being widely exploited in wireless communication standards such as Long Term Evolution (LTE). OFDMA can similarly be implemented in PON's by dynamically assigning different number of subcarriers to various ONU's based on traffic

demands. For achieving higher flexibility, the bandwidth available to each subcarrier can further be subdivided between different ONU's in time by employing TDMA. Bandwidth flexibility can be furthered enhanced by converging OFDMA scenarios with WDM in PON systems, where wavelengths can be static or dynamic as transceivers are equipped with tuneable sources and receivers.

The overlapping orthogonal subcarriers in OFDM account for its spectral efficiency. The resulting compact bandwidth from OFDM transmitter makes its adaptation in PON's attractive, giving its capability to reach data rates required in a bandwidth efficient manner. The spectral efficient nature of OFDM can alleviate the need for high bandwidth electro-optical equipment used [98]. Apart from its spectral efficiency, the resilience of OFDM to dispersion also makes it a great candidate for PON. Where by introduction of additional overhead in the form of a cyclic prefix (CP), effects of Chromatic Dispersion (CD) can be corrected [67]. This performance against dispersion factor makes OFDM a great candidate for next generation PON is as it fulfils the extended reach requirement.

The main challenge for OFDM-PON systems operating with a power splitter arises from the architectural assignment of uplink wavelength from each ONU, which are set to operate at a nominal wavelength. During the photo-detection process at the OLT, the N de-correlated carriers from N uplink transmitters will mix with each other creating an optical beat noise that reduces the received signal's SNR. This issue can be solved by either deploying a WDM architecture where each ONU is assigned a fixed wavelength on the transmission grid or the optical carrier is supressed at each ONU and the OLT is equipped by a coherent receiver [67].

1.4.1.4 Next Generation Optical Access Technologies

As the demand for bandwidth has increased over the past number of years, legacy PON technologies such as G-PON and E-PON are being seen as incapable of meeting the end user's upcoming service requirements. This issue has forced IEEE and ITU along with FSAN to conduct studies for possible smooth migration from Gigabit capable systems. The studies conducted, resulted in system architectures termed Next Generation PON (NG-PON). The first realization of NG-PON1 was viewed as a mid-term upgrade with capability to coexist with legacy PON infrastructure. Subsequent to NG-PON1, system requirements for a longer-term solution were specified as NG-PON2 [75].

NG-PON1 created the basis for standardised system such as ITU-T XG-PON and IEEE 10G-EPON as were discussed in previous sections. These standards are in the process of deployment and having their purpose-built equipment commercialized by numerous

vendors. Requirements set forth by the ITU-T outlined specifications for NG-PON2, such as minimum data rates of 40 Gb/s [76], and 40 km optional propagation spans that are required to be achieved passively. Initially, candidates chosen to meet these requirements were based on Time-shared WDM (T-WDM), OFDM-PON, and DWDM in conjunction with coherent detection (co-DWM) [99]. As NG-PON2 was devised as a successor to G-PON and XG-PON and in order to avoid high data-rates per wavelength [42] due to cost of electronics, TWDM was considered by ITU-T for use in NG-PON2 [83].

TWDM systems are capable of supporting a maximum of eight wavelength pairs in downlink as-well-as uplink [60], with four wavelengths being the nominal number of bands. These systems are operated by stacking multiple XG-PON transceivers, running either at a symmetric rate of 10/10 Gb/s or 10/2.5 Gb/s for downlink and uplink respectively, resulting in overall aggregate data rates of 40/40 or 40/10 Gb/s in a 4 wavelength scenario. Although TWDM can be extended to reach a maximum ratio of 80/80 Gb/s in an eight wavelength channel.

Figure 1.13 presents a typical TWDM system, at the transmitter multiple XG-PON transmitters operating at various optical frequencies are multiplexed using a WDM multiplexer. At the receiver-end, each ONU is capable of receiving all WDM channels, and thus each ONU is equipped with a variable optical filter in order to select one downlink channel. For uplink, each ONU makes use of tuneable lasers capable of transmitting at any predefined wavelength channel designated for uplink transmission. The extra equipment at

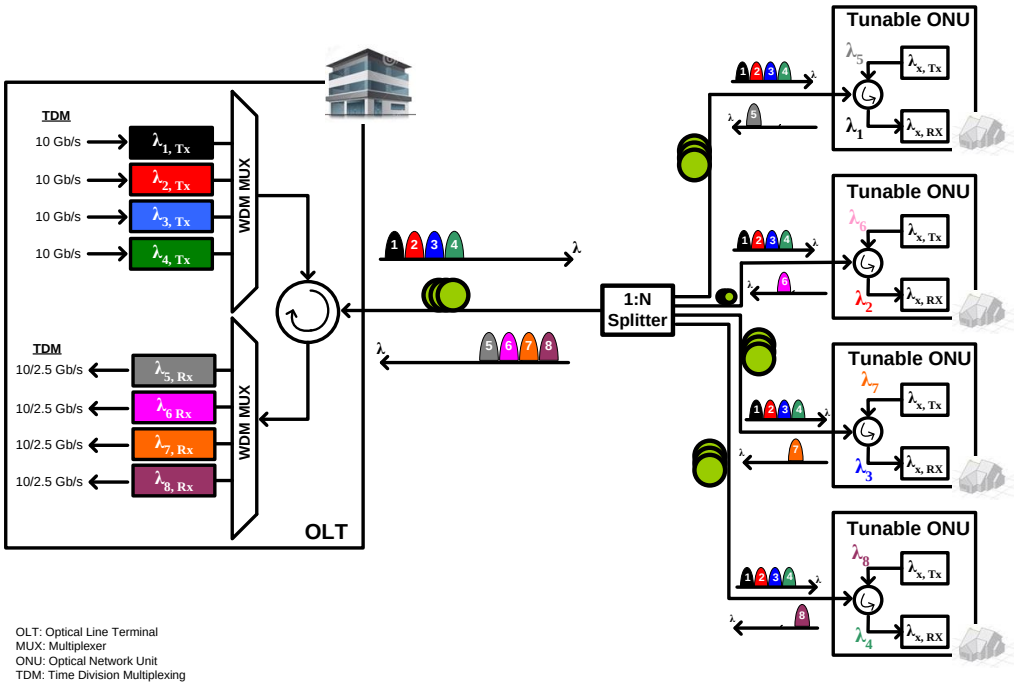

Figure 1.13. Typical TWDM-PON architecture

the transmitter and receiver adds to the complexity and costs compared to the legacy 10 G capable systems, although these costs are expected to be justified by the increase in throughput. The hybrid TWDM-PON is a smooth migration step from TDM-PON towards WDM-PON while maintaining some attractive characteristics from both network infrastructures. TWDM retains the power splitter and feeder fibre employed in the legacy 10G PON systems, this factor makes TWDM a viable route for the carrier for move towards WDM based access networks.

Considering the evolution of bandwidth demands through new applications and devices in the future, the evolution of access networks from NG-PON2 also needs to be addressed through further research and standardization. Such networks require extended reach, cost efficiency, higher split ratios and higher deliverable bandwidths. These systems will most likely be based on data rates beyond 100 Gb/s, and with advances in semiconductor and electro-optical industry, schemes such as OFDM, WDM, DWDM and coherent systems can contribute to such envisioned technologies.

An important aspect of access evolution is the consolidation of metro and access networks in one unified entity entailing passive technologies. By taking this approach, numerous active network-interfaces are removed from the architecture, which in turn lowers the CAPEX and OPEX. This consolidation can be made possible by extending the reach of next generation PON systems beyond 60 km [42] and forming Long Reach PON (LR-PON) systems. This LR-PON will penetrate deep into the aggregation network and terminate on a core edge node. Figure 1.14 presents an example of LR-PON (solid lines) where a large number of users are served by a single central office in the core network through a local exchange which consolidates multiple central offices which were supported by a metropolitan aggregation network (dashed lines).

A significant issue for consideration when designing LR-PON is the link power budget, since this topology covers a wider geographical region and possibly higher number of users, which translates into a higher split-ratio. The power budget can be increased by

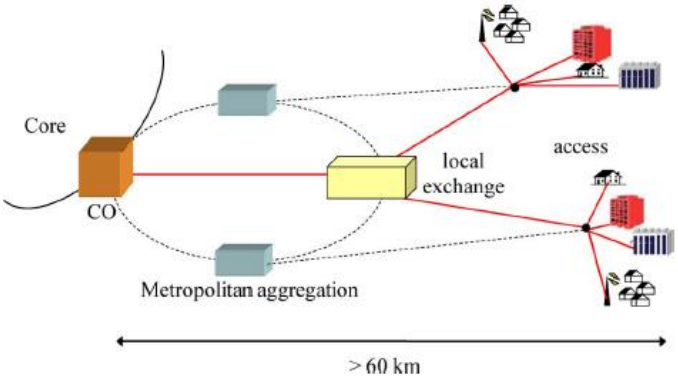

Figure 1.14. Schematic of LR-PON consolidating Central Offices [42]

using higher power transmitters and more sensitive receivers at the OLT and ONU. This approach requires significant alteration to the transceivers at the far-ends of PON, thus, it is least preferable. A more powerful approach is the employment of amplifiers such as EDFAs, Semiconductor Optical Amplifiers (SOAs) or Raman Amplifiers at either the OLT or the local exchange (mid-span reach extenders) [42]. Coherent receivers combined with DSP schemes have gained research attention in recent years for long reach applications [100, 101]. In these coherent schemes, the frequency selectivity and wavelength channel switching offered omits the need for narrowband filters and on the contrary allows the use of already installed passive splitters. These advantages can lead to the possibility of simultaneous migration towards LR dense or ultra-dense WDM-PON applications. The main obstacle hindering the emergence of coherent detection schemes combined with DSP into optical passive networks is possibly the considerable investment on high performance components (Local Oscillators (LOs), Optical hybrids and balanced-photodetectors, DSP processors, etc.…) in each ONU and OLT. This concern suggests that the exploitation of coherent detection techniques despite its potential and attractiveness for LR-PON might stay in the research and development stage and might not be ready for commercial deployment in the near future [42].

Another potential candidate for LR-PON is identified as OFDM. Besides its high spectral efficiency and resources agility, OFDM is able to show a high resilience towards chromatic dispersion in fibre which is a major impairment in LR networks [66] compared to TDM based services. OFDM used in simple intensity modulated systems has the capability of providing high per wavelength data rates at LR distances as it was demonstrated in [102] where a 33 Gbps intensity modulated OFDM band was transmitted over 60 km achieving a 32 dB loss budget.

1.5 Summary

In this chapter, the general forecasted trends on global and regional IP traffic were reviewed. In response to the explosive global data growth, optical based core and metropolitan networks are being continuously fed the technological advancements striving towards re-configurability and higher link capacities. The introduction of fibre, deep in the access networks was not seen viable in the 1980s due to the high economical costs and lack of demand, although all optical access topologies were seen as beneficial. With the emergence of the bottleneck in access networks, created by legacy co-axial and copper cables, service providers have been pushing fibre technologies ever closer to the user, by

replacing the copper-based systems by FTTH systems. FTTH has already been specified in the context of PONs that uses TDM technology. OFDM is one promising technology for use in next generation PON's due to its bandwidth efficiency, resilience to optical channel effects such as dispersion and a greater level of configurability. This technology will be a key focus of this thesis and will be described in more detail in later chapters.

Chapter 2

Hybrid Wired/Wireless Access Networks

This chapter discusses the role of Radio over Fibre (RoF) systems in hybrid wired/wireless access networks. The chapter starts with an overview of technological progress in cellular communication technologies and is followed by a brief introduction to key components in a RoF system. The chapter finally closes with a discussion on possible methods for integrating wired/wireless services over optical access networks using RoF techniques.

2.1 Introduction

User demand for high bandwidth fixed services continues to grow without any signs of slowdown1. In addition, governments around the globe have recognized that the broadband network is a major player for the emerging digital economy and are willing to invest or directly assist in an accelerated deployment of broadband optical access networks capable of providing broadband connectivity at high data rates [76]. Such changes in the access network will in turn drive more development in the metropolitan and core optical networks necessary to satisfy the needs of such a broadband infrastructure. In parallel to these progresses, a growing user demand for access ‘anywhere’ to data services over mobile and wireless networks is also necessitating a sustained improvement of the wireless access networks towards the provision of wireless connectivity at high data rates capable of

delivering data intensive streaming applications. As wireless access networks have continuously evolved to meet capacity and coverage demands with the introduction of new technological trends (i.e. 3G, 4G, 5G), network costs are exploding [103]. In response to the increase in data traffic over the wireless networks, operators have been looking to increase capacity in the form of acquiring more spectrum, increasing spectral efficiency, or increasing the densification of cells. However, delivery of high bandwidth wireless services requires a high bandwidth backhaul to connect the Base Stations (BSs) to the core cellular network. However, with the increasing number of BSs and their associated capacities, and with the growing access to existing optical fibre infrastructure, it is becoming favourable to adopt fibre technology to backhaul wireless services [104]. As the deployment of both optical and wireless access network infrastructure starts to proliferate throughout the globe, the idea for the possibility of consolidation of these two network infrastructures is raised. When these two topologies converge to a highly integrated network via a common optical feeder network, network operators can benefit from lowered operating costs associated with access networks and reduce capital costs required for future upgrades [105]. As the BSs account for most of the energy footprint in a wireless network, such converged access network can offer lower energy consumption levels through simpler and more cost-effective BS architectures [106]. RoF signal transport has been extensively studied in the past as a possible solution for the simplification of the BS's architecture. This simplification has been achieved through the reallocation of key functional properties of a conventional BS to a central location. BSs could then be simplified into Remote Antenna Units (RAUs) which are connected to a central office by an optical network [1]. This in turn has led to the use of optical fibre as an efficient and cost effective medium for radio network distribution over long distances, where the large bandwidth provided by fibre can accommodate current and future wireless applications operating at various frequency bands. Furthermore converged optical-wireless access networks will also co-exist with the legacy technologies providing wired-access.

2.2 Wireless Technologies

In the last number of years, the wireless industry has seen a tremendous growth in terms of both new technological breakthroughs and subscriber numbers. Since the introduction of the earliest cellular systems in the late 1970s, numerous cellular wireless generations have come into existence, each providing advanced means of communication and services. The evolution of wireless access technologies have now paved the way for introduction and deployment of 4th Generations (4G) [107] technologies and it has also initiated the path for

research and planning towards 5th Generation (5G). Looking at the past, wireless access technologies have taken different evolutionary paths toward a common vision of higher levels of performance and efficiency in the realms of mobile communications. 1st Generation (1G) technologies provided only mobile voice services whilst 2nd Generation (2G) introduced higher capacities and means for digital data transfer. The aim of 3rd Generation (3G) was to provide higher data rates and open the door for "mobile broadband". Currently (4G) is building on the vision of 3G by increasing the available data rates through new technologies.

1G cellular technologies used analogue communication techniques that are similar to those used in traditional analogue radios. The first cellular system based on 1G was deployed by NTT in Japan in 1979. Cellular communications reached the United States by 1982. These systems used Frequency modulation (FM) for transport of voice calls and Frequency Division Multiple Access (FDMA) for traffic multiplexing [108]. 1G technologies were only able to provide voice services and their high costs, limited their use amongst business users only. 2G systems started to be introduced in the late 80s, these systems had evolved from the analogue based system to digital, and this transmutation enabled efficiency in spectrum usage and cheaper devices. Similar to 1G, 2G products were also intended for voice calls but later were enhanced to support Short Message Service (SMS) and circuit switched data communication. The two popular 2G systems are Global System for Mobile Communications (GSM) and cdmaOne. GSM was intended as a pan-European technology but it became popular over the world where as cmdaOne became the dominant technology in USA. These technologies use multiple access schemes such Time Division Multiple Access (TDMA) or Code Division Multiple Access (CDMA). The first 3G network was launched by NTT in Japan in 2001 [108], and by 2006 these systems started to be deployed widely [109]. The original proposition of 3G was that end users want more capabilities from their handset such as video calls, playback of video and transfer of large files. In Europe, the 3G variant was called Universal Mobile Telecommunication Systems (UMTS), while cdma2000 is the American 3G variant. Cdma2000 and UMTS were both based on CDMA technology. The key characteristic of 3G includes the ability to carry video calls and video streaming capabilities at data rates up to 384kbit/s in both packet and circuit switched modes. 3G was later enhanced for data applications in 3.5G by technologies known as High Speed Packet Access (HSPA) in UMTS and High Rate Packet Data (HRPD) in cdma2000.

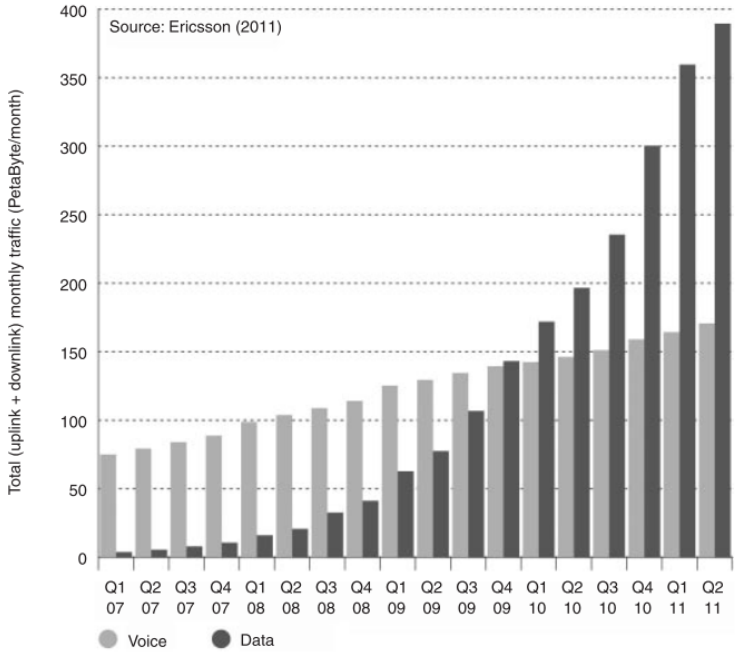

Figure 2.1. Global voice and data mobile traffic from Jan 2007 to July 2011 [110]

For many years voice communications dominated the global mobile traffic, but these trends changed by the year 2010 (Figure 2.1), where mobile data traffic started to surpass voice traffic. The emergence of such disparity can be credited to technological progressions and operator's incentives. The wide availability of 3.5G systems at the time and the introduction of Apple and Android smartphones in 2007-2008, and along with their capability of supporting 3rd party applications, resulted in an explosive increase in the number of applications used. At that time, operators also motivated the end-users to use data by offering flat-rate fees for their services, this created a situation where neither the end-user or service providers were motivated to limit their services [110]. It was already known by the service providers that the demand for higher data rates in mobile services

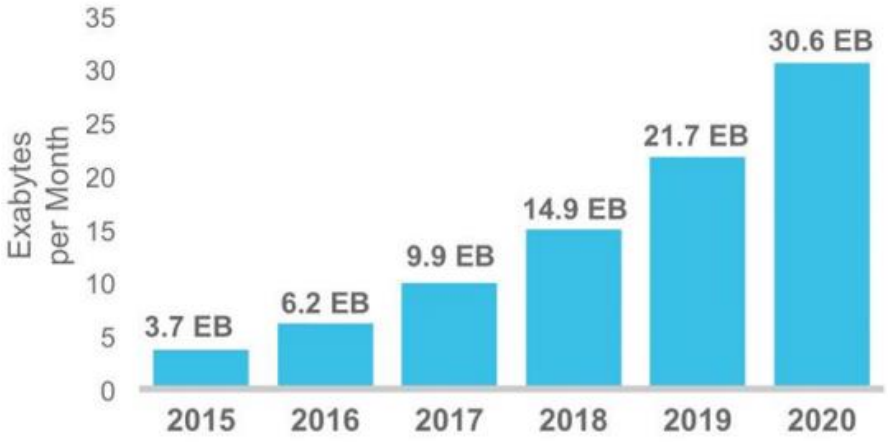

Figure 2.2. Global Mobile traffic estimates (2015-2020) [111]

would grow continuously (as projected in Figure 2.2 [111]). Such factors encouraged operators to seek higher capacities in future by initiating the 4G system. In light of these maters a new architecture called Evolved Packet System (EPS) was created. EPS accounts for two work items which namely are System Architecture Evolution (SAE) and Long Term Evolution (LTE). SAE involved the work in the core network which enabled all communications through packet switching techologies. And LTE refered to the evolution of the air interface from UMTS to Evolved UMTS Terrestial Radio Access Network (E-UTRAN). LTE systems initially were requiried to provide peak data rates of 100 Mbp/s downlink and 50 Mbp/s uplink, these requirements were eventually excceded in the final sytem delivering 300 Mbps in downlink and 75 Mbp/s in the uplink [110].

In the late 1990s the ITU declared its requierments for 3G systems under the name Internatonal Mobile Telecomunications (IMT) 2000. The same approach has also been taken by ITU for 4G systems under the name IMT-advanced. The new requierments set by IMT-advanced set the peak data rates for 4G systems at 600Mbp/s and 270 Mbps/s in downlink and uplink in a bandwidth of 40 MHz [110]. In response to these requiremetns for 4G, 3GPP strived towards finding specificiations for a system fulfilling the IMT-advanced requirements and the two proposals presented were LTE-Advanced and WiMax under IEEE 802.16m, known as WiMax 2.0. At the time these trends did not stop the marketing community from defining technologies such as LTE and mobile WiMax as 4G. Thus ITU in 2010 allowed 4G to represent any technology that had a substantially better performance than their 3G counterparts such as LTE, WiMax and HSPA+ [112].

The next evolutionary step in 4G systems was the move towards LTE-advanced. In this evolved technolgy the set required peak data rates are 1000 Mbp/s in downink and 500 Mbp/s in the uplink, these rates are envisioned to eventually increase 3000 Mbp/s and 1500 Mbp/s in downlink and uplink [110]. The radio reception and transmission in LTE is based on Orthogonal Frequency Division Multiple Access (OFDMA). OFDMA is also applied to several other communication standards such as Wirleess Local Area Network (WLAN, IEEE 802.11 a, g, n) and WiMax. OFDMA can carry out the same operations as other multliple access techniques but it is more roboust towards issues related to fading and ISI. This resilience to ISI is due to OFDMA subdividing the aviliable bandwidth into finite tributaries called subcarriers. Compared to single carrier systems each subcarrier in OFDMA has a longer symbol period thus it suffers from a lower level of ISI. To reduce the ISI even further these OFDM based systems use guard bands in time in the form of a Cyclic Prefix. Extra linear channel impairments which manifest themselves as amplitude or phase shifts at various subcarriers can be accordingly fixed in the frequency domain using equalizers. The equalization process operates by transmission of a known set of “reference

symbols" at different time-frequency locations which are then compared to their received copies. The comparision between transmitted and received symobls leads to channel estimates that can subsequntly be used to fix amplitude and phase variations. A key aspect of OFDM which is cruicial in spectrum-scarce wireless communications is its high spectral efficency. The spectral efficent nature of OFDM is achieved by the removal of guard bands that were previously employed in FDM systems and permitting subcarriers to overlap each other in frequency without interfering with one another.

The next major phase of mobile communication standards beyond 4G and LTE-Advanced is 5G. The existing wireless systems will be incapable of meeting the demands of future mobile netowrks traffic which is anticipated to increase by 1000 folds by the year 2020 [113]. This forecasted increase in bandwidth is contirbuted to – by the introduction of new applications and services such as 3D multimedia, HDTV and gaming. In this context, 5G systems are seen to have the capability to support 1000s time higher data volumes per unit area, achieving peak data rates up to 10 Gb/s [107].

2.3 Hybrid Wired/Wireless Optical Access; a Motivation

Currently, in response to increasing data traffic over cellular networks, cellular service providers in this sector are also seeking for technological solutions to increase the available capacity over their wireless access network for meeting the end-user's demands. Some of the proposed solutions are the increase of spectral efficiency, increasing the density of available cell sites and migration to other available operational frequencies [114]. An increase in spectral efficiency entails a better utilization of the available bandwidth which has invoked the employment of modulation formats such as OFDM in conjunction with spatial diversity schemes in wireless access systems such as Long Term Evolution (LTE) and LTE-Advanced [110]. On the other hand increasing the number of available cell stations in a geographical region can provide a higher level of capacity as the resources of one cell site are shared amongst a smaller number of users; this approach is currently being sought under the Heterogeneous Networks (HetNet) type architectures [114]. The present-day spectrum used by cellular communications is highly congested, making it very hard for cellular standards to achieve a substantial level of bandwidth extension. However the large bandwidths available at higher operational RF bands have sparked an interest in their exploitation for next generation cellular communication systems.

In a move to simplify the BSs in 3G cellular systems, a new architecture has been introduced whereby the conventional BS is separated into a radio unit and a signal processing unit. The radio unit called the Remote Radio Head (RRH) or Remote Radio Unit (RRU) is usually positioned on top of the communication mast and is responsible for providing an electrical interface to the Antenna and an optical interface to the signal processing unit or the Base Band Unit (BBU). The BBU is responsible for the radio resource allocation and control of multiple RRHs [115], and the means of communication between the RRH and the BBU is usually referred to as fronthauling. This new split BS architecture apart from simplifying the BS has the benefit of lowering OPEX by eliminating the high power amplifiers previously required at the bottom of the traditional BSs for overcoming the high loss associated with RF cables providing the interface between the amplifier and the antenna on top of the mast. The BBU can further be located in a location far from the RRH (up to 40 km), which results in further reductions in the OPEX due to the elimination of possible site rentals required for storing BS equipment at the base of the radio mast and the need for high power electrical cables needed to cool and serve baseband processing units.

In response to future increases of capacity in cellular access networks, and densification of cell sites, BSs will be required to achieve a better time and frequency synchronization and also they need to accommodate for higher data rates over inter-BS interfaces [114]. One of the main contributing factors to this requirement is the emergence of a higher level of inter cell interference which needs to be eradicated. To address such issues a new Radio Access Network (RAN) has emerged, this new architecture is called Cloud-RAN (C-RAN) and it aims at concentrating multiple BBUs in a centralized location, or concentrating the functionality of multiple BBUs in a single functional entity. C-RAN is envisioned to have a potential role in emerging high capacity cellular access networks.

In Both C-RAN and contemporary RANs operating based on the split BS architecture, the common protocol used in the interface between the BBU and RRH is called Common Public Radio Interface (CPRI) [116]. The transmission of this interface can be supported both over electrical and optical cabling, however due to the possible high bandwidths and long propagation lengths, optical transmission is preferred. The CPRI interface is a continuous stream OOK signal which is created by the digitization of the In-Phase (I) and Quadrature (Q) components of the wireless signal in baseband using Analogue to Digital converters (ADCs). The high ADC resolutions used in this process along with the possible overhead from the line encoders employed can lead to link rates that are orders of magnitudes larger than the net data rates carried by the wireless I-Q channels. A major disadvantage of using CPRI in high capacity RANs is the extremely high data rates that are

needed to be carried by the fronthaul links, which rapidly increases with the number of supported MIMO channels, sectors and channel bandwidths, which in most cases requires the intervention of high cost WDM technology and protocols commonly used in core and metropolitan networks. To solve this issue numerous methods have been proposed to compress the CPRI signal, and compression ratios up to 50% have been demonstrated [116, 117], however this approach can further the complexity of the system design due to the need of extra equipment at both the transmitter and receiver sides.

To compensate for the resulting high data rates that will be inferred by using CPRI, a new architecture termed Midhaul has recently emerged [118]. The Midhaul proposal entails moving a number of functional blocks in the BBU close to the RRH which leads to shorter CPRI connections and lowered data rates over the Midhaul interface. Such architecture still entails high data rates over the CPRI link and leads to higher complexities at the BS due to the migration of extra equipment from the BBU.

The exploitation of digital transmission over fronthaul links, as in the CPRI interface can in consequence lead to a number of architectural complexities. Apart from high link data rates, one can anticipate a complex BS due to the various complex functionalities housed in the RRH such as a high resolution Analogue to Digital Converters (ADCs) / DACs and high bandwidth optical receivers and transmitters. To overcome complexities of DoF schemes, Analouge over Fibre (AoF) architectures can replace the conventional CPRI based fronthualing interfaces technological challenges of next generation high capacity wireless access networks. In AoF techniques instead of transmitting a digitalized copy of the I-Q constituents of the wireless signal, the RF cellular signal in its native form is optically transmitted over the fronthaul link. Moreover AoF techniques will lead to a simple BS architecture, where the key functional blocks that are housed in the BS will be an optical transceiver, high gain amplifier, antenna and other RF equipment. However despite all the advantages offered by AoF techniques they are known to be susceptible to device nonlinearities and dispersive effects in fibre compared to their Digital counterparts. But careful system design can limit the impact of fibre dispersion and nonlinearities emerging from the electrical or optical subsystems. Thus AoF alongside DoF techniques has the potential to address numerous

Over the past number of decades, a substantial amount of work has been carried on the potential applications of AoF in cellular communications, for the delivery of microwave signals with frequencies up to tens of GHz over an optical infrastructure [119-121]. These studies have looked at various aspects of AoF technologies such as the impact of standard as well as novel direct and external modulation techniques on the quality of transmission

[122, 123], optical generation of high frequency RF signals, impact of fibre dispersion on transmission along with its enhancement [121], the employment of phase modulation instead of intensity modulation for the delivery of cellular signals and optical multiplexing schemes for provisioning MIMO schemes .

The increased availability of FTTX services for the provision of wired services. Moreover, the reliance of next generation cellular access networks on high bandwidth optical technologies for fronthualing and backhauling has created interest in the unification of wireless access with wired optical access architectures such as PONs, which has the potential for lowering the costs associated with deployment and operations of the unified system.

The provision of PONs for the accommodation of the CPRI interface has been proposed in recent years [83], however a number of obstacles need to be overcome before this can be realized. Firstly, in PONs in order to utilize the available resources efficiently, the bandwidth is dynamically assigned to each user, however CPRI requires a fixed bandwidth thus in order to use PONs for the transmission of CPRI certain alterations are needed to be made to the protocol scheme used to adhere to the stringent requirements set by CPRI. Secondly, as it was stated earlier the use of CPRI can lead to high link data rates, where in some cases the full resources of a PON channel must be dedicated to one cell site, changing the PON architecture from a point to multi point (p2mp) to point to point (p2p) type architecture. In more recent PON standards such as TWDM-PON this aspect has been addressed by allocating a number of wavelength bands just for p2p communications. Nevertheless using currently available PON standards for fronthualing CPRI channels especially in a C-RAN type of architecture can substantially exhaust the available fibre resources. To reduce the bandwidth challenges imposed by CPRI, proposals have been made to employ spectrally efficient modulation formats such as OFDM for CPRI [67].

The employment of AoF techniques for fronthauling in PONs can eliminate many of the challenges of DoF techniques. The removal of the digitization process in AoF removes the high overheads and high link rates. This use of AoF allows for a true hybrid high capacity wired/wireless access system, where the bandwidth needs of multiple wired and wireless entities/users are simultaneously meet. However, hybrid PONs based on AoF need to deal with the issue of inter-band interference management, which is a consequence of the presence and coexistence of digital and analogue signals sharing a single optical channel. Common approaches taken so far to manage such interference have been the introduction of frequency plans and using WDM schemes.

2.4 Radio over Fibre (RoF) Link Components

Microwave links play an important role in telecommunications today, but microwave RF signals experience high levels of attenuation in cables and waveguides as their operating frequencies increase especially in the millimetre wave region. RoF techniques can be used to carry microwave signals by modulating them onto optical carriers that are intensity modulated. These optically modulated signals are then transported to optical receivers via optical fibres. Thanks to the low-loss profile of optical fibres today, RF signals that can consist of an electrical carrier modulated by either digital or analogue information can be transmitted over long distances by using RoF. A typical practical example of RoF is the transmission to/from remotely located antennas or the distribution of TV signals to users using optical fibre.

A simple setup of a RoF system is illustrated in Figure 2.3. A typical RoF system requires some means for transferring the RF electrical signals onto the optical domain, such electro-optical conversion usually is achieved by using external modulators such as MZMs and EAMs or in other cases by directly modulating a laser. Following fibre propagation the optical signals are converted back to the electrical domain using a photodiode. The objective of RoF topologies is to achieve the same functionalities as conventional microwave links but with longer distances, reduced complexities, support of higher frequencies and better performance. In microwave links, performance degradation can be contributed to RF power loss, frequency response of equipment, and device nonlinearities. RoF systems on the other hand can also suffer from signal deterioration through the effects of fibre transmission and additional noise sources originating from the laser diode and the photodetector. Nonlinearity present during the electro-optical conversion process in RoF can also lead to signal distortion. In this section, the impact of various elements, in a RoF system, on signal transmission is presented.

2.4.1 Transmitters

Electro-optical conversion can be achieved by either Direct Modulation (DM) or external modulation. In direct modulation, the electrical RF signal-carrying analogue or digital

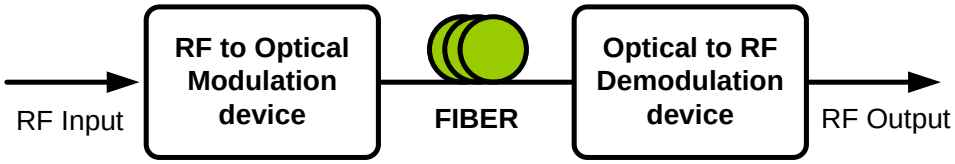

Figure 2.3. Typical RoF system

information is superimposed on a DC signal used to bias the laser. In external modulation, a Continuous Wave (CW) laser is coupled to a modulator that manipulates either the phase or amplitude of light in response to an electrical driving signal that is applied to the modulator.

2.4.1.1 Direct modulation

The attractiveness of directly modulated lasers in RoF stems from their compactness, and low bias/drive required currents. Since the power output of a laser is dependent upon the current feed to it, a P-I curve can characterise the emission properties of a laser. The P-I curve can identify the threshold point of the laser diode along with the current required to obtain a certain optical power. A typical Power-Current (P-I) curve for a laser is shown in Figure 2.4. Biasing the laser above the threshold current at I_B (mA) results in a CW optical signal with average power (P_0). Assuming the laser is directly modulated with a single frequency signal ($\cos(\omega_m t)$), where ω_m is the microwave modulation frequency of the electrical signal, the time varying electrical drive signal I_L and the optical power emitted from the laser P_L can be written as

$$I(t) = I\left(1 + m.\cos(\omega t)\right) \tag{2.1}$$

$$P(t) = P\left(1 + m.\cos\left(\omega t\right)\right) \tag{2.2}$$

Where m is the modulation index and P_0 the average optical power obtained upon the application of the DC bias I_B. The slope efficiency s_L with units (W/A) is dictated by the linear portion of the P-I curve and is given by $s_L = \delta P_L / \delta I_L$, therefore the average optical

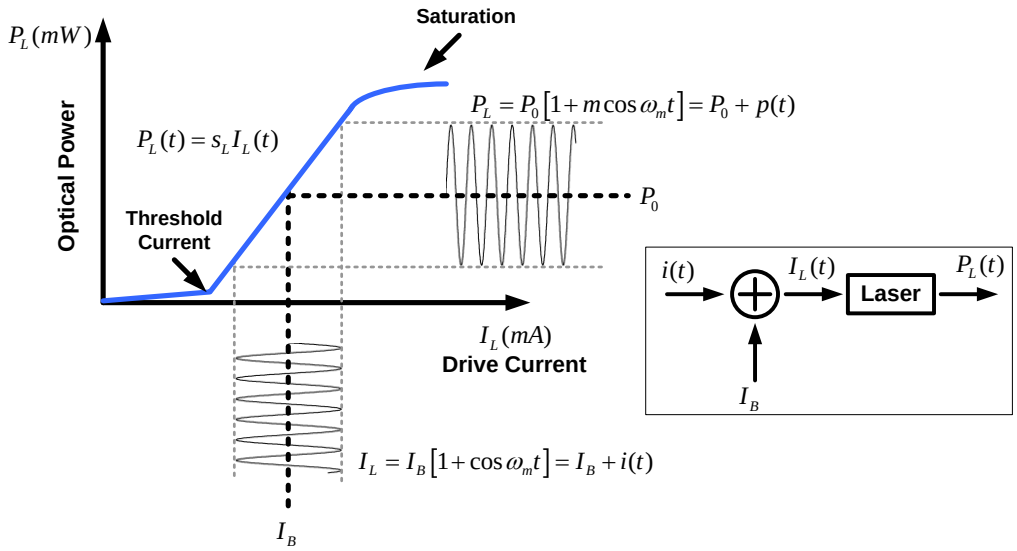

Figure 2.4. Typical P-I characteristics for a laser diode

power at the DC bias point can be written as $P_0 = s_L I_B$. If it is ensured that I_L operates above the threshold point and below the saturation point, the laser output follows the drive current; such restrictions on the drive current will also ensure signal clipping due to the threshold point and distortion due to the nonlinear saturation can be overcome. An interesting point that can be made for directly modulated laser is the fact that s_L is frequency dependent. This frequency dependence of s_L determines the modulation bandwidth of the laser and sets the limit on the maximum RF frequency attainable in a directly modulated laser. Figure 2.5 presents the simulated frequency response of a DFB laser for various bias currents (I_B). This frequency dependent response is the consequence of the interaction between carrier recombination and photon emission in the laser itself [122]. The peak observable at the relaxation oscillation frequency is as result of the intrinsic response of the device. Operating the laser at these frequencies will lead to performance deterioration as result of the laser nonlinearity at these frequencies [98]. Thus, the driving current I_L should have frequency components lower than the relaxation oscillation frequency. Normally this relaxation oscillation peak can be moved to higher frequencies by increasing the bias current thus increasing the modulation bandwidth of the laser. The progress towards higher bandwidth laser has led to demonstration of Multi Quantum Well (MQW) lasers at 1550 nm with 30 GHz bandwidth [57] and Distributed Bragg Reflector (DBR) laser with 37 GHz of bandwidth [124]. The modulation bandwidth of lasers can be extended further by optical injection of light from a secondary laser

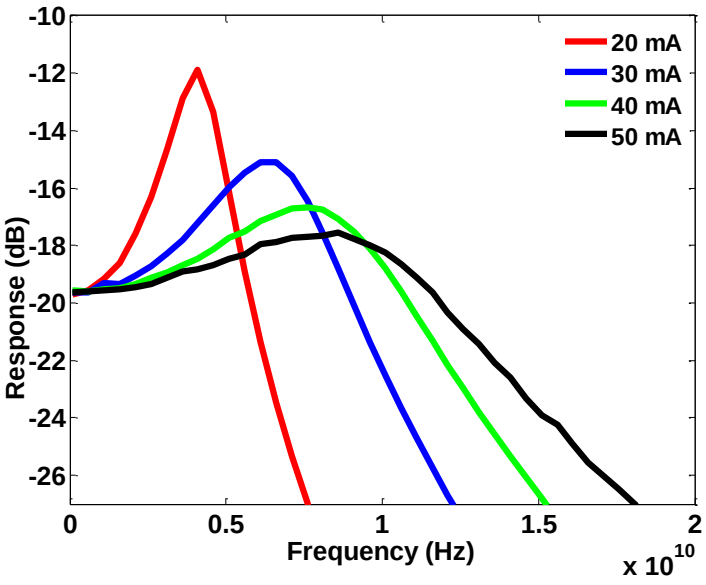

Figure 2.5. Simulated modulation frequency response of a typical DFB laser as function of modulation frequency at various bias current

(master). The bandwidth enhancement possible is a function of the injected optical power and the optical frequency difference between the two devices. Enhancements in modulation bandwidth up to 44 GHz for DFB lasers [125] and 50 GHz for Vertical Cavity Surface Emitting Laser (VCSEL) have demonstrated [126].

The main contribution of laser noise is due to spontaneous emission. Each spontaneously emitted photon adds a small field component with a random phase to the coherent field (established by stimulated emission), and thus results in fluctuations in both the phase and amplitude of the optical source. The unwanted random intensity variations are known as Relative Intensity Noise (RIN) whereas the variation in the phase leads to a finite linewidth when the laser is biased at a constant bias current (I_B). RIN in RoF systems employing intensity modulation and direct detection can act as a degrading factor by reducing the available SNR. RIN is frequency dependent, at lower frequencies it exhibits constant power levels and peaks at the resonance frequencies [9]. Thus in multi-carrier RoF applications, sub-channels operating close to the resonance frequencies can experience higher levels of intensity noise due to RIN.

In direct modulation, the applied drive current I_L results in the modulation of the emitted wavelength, this is due to the fact that the change in carrier density in the cavity as result of I_L has an impact on the cavity's refractive index [35]. This dependency between the emission frequency and drive current leads to time varying frequency fluctuations in the laser's nominal emission frequency which is known as the frequency chirping. Laser chirping in RoF systems can degrade performance by limiting fibre propagation lengths and creating discontinuities in the transmission spectrum [127]. The direct method for reduction of laser chirping is the design of semiconductor lasers with small value of linewidth enhancement factor or to use external injection locking to stabilize the frequency deviations [10].

2.4.1.2 External Modulation

As the names suggest, external modulation make use of an external device (modulator) to vary either the intensity or phase of the light emitted from a CW laser diode. The main drawbacks of external modulation are increased costs and complexities, power losses due to coupling and the increase in footprint size compared to direct modulation. However external modulation can provide higher modulation bandwidth. Thus external modulation is favourable in RoF systems operating at high frequencies. External modulation schemes can also allow control over the modulation process which can lead to alterations to the optical spectral content, achieving optical carrier and side-band suppression schemes.

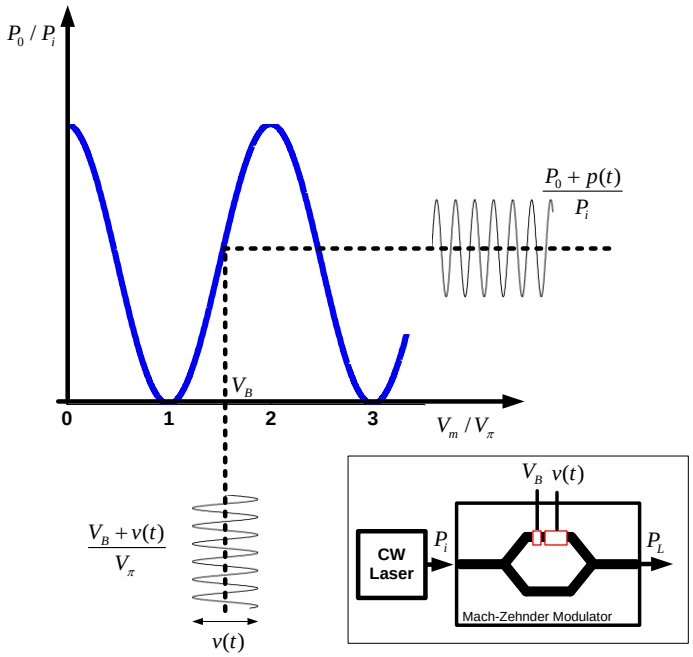

Figure 2.6. Mach-Zehnder Modulator and its transfer function

Unlike direct modulation, external modulation does not suffer from the problem of chirp, but the laser intensity noise is still present and can impact the system's SNR [122]. There are two principles of external modulation used in optical communications; these two namely are electro-optic and electro-absorption effects. The electro-optic effect entails a phase shift inside a $LiNbO_3$ waveguide as result of the electric field which originates from the drive voltage, this device can be used as a phase modulator. To construct an amplitude modulator a Mach-Zehnder interferometer (MZI) can be employed, where each arm is equipped with $LiNbO_3$ modulators. Electro-absorption based modulators make use of Franz-Keldysh effect, according to which the bandgap of a semiconductor decreases as an electric field is applied across it. Thus a transparent layer begins to absorb light when its bandgap is reduced electronically by applying an external electric field [35].

The structure and transfer characteristics of a Mach-Zehnder modulator are presented in Figure 2.6 where the input light is split in two paths (upper and lower waveguide). In this structure the optical phase of the upper arm is then varied with respect to the lower waveguide, the optical fields from the two waveguide are subsequently recombined. In absence of an applied external voltage, the optical fields in both arms experience an identical phase shift, which results in constructive interference. On the other hand, an additional phase shift introduced to one arm can destroy the constructive nature of the interference and results in lowering the transmitted intensity. The transfer characteristics for the MZM modulator is given by

$$\frac{P_0}{P_i} = \frac{T}{2}\left(1+\cos\left(\frac{\pi V_m}{V_\pi}\right)\right) \tag{2.3}$$

Where $V_m = V_B + v(t)$, with V_B being the bias voltage and V_π the voltage required to induce a phase shift of π between the two modulator arms, and T is the insertion loss that the MZI induces into the system (when biased at maximum transmission point). For intensity modulated RoF systems employing MZM, one suitable biasing point is located at $3V_\pi / 2$ as shown in Figure 2.6, employing a drive signal $v(t)$ in this biasing point can ensure that variations in drive voltage occur over a quasi-linear part of the characteristic transfer function of the modulator. The link gain or slope efficiency here is dependent on both the CW power (P_i), and the V_π therefore, it is of interest to employ higher power lasers and modulators with smaller V_π. Apart from related implementation complexities and high costs, the non-linear transfer function of MZM can reduce the dynamic range in an RoF system [9].

2.4.2 Optical Fibre Links

The two key parameters that influence performance after fibre transmission in RoF systems apart from fibre-nonlinearities are attenuation and dispersion. The main motivation behind the employment of fibre optics for transportation of microwave signals is due to electrical cabling exhibiting excessive losses when operated over any appreciable distances. Single mode fibres with their relatively low losses, typically 0.5 dB/km or 0.2 dB/km for 1330 nm and 1550 nm windows respectively, have paved the way for transmission of microwave signals over many 10's of km without the need for in-line amplification [128]. When a microwave signal is modulated on an optical carrier for an IM-DD RoF system, it results in

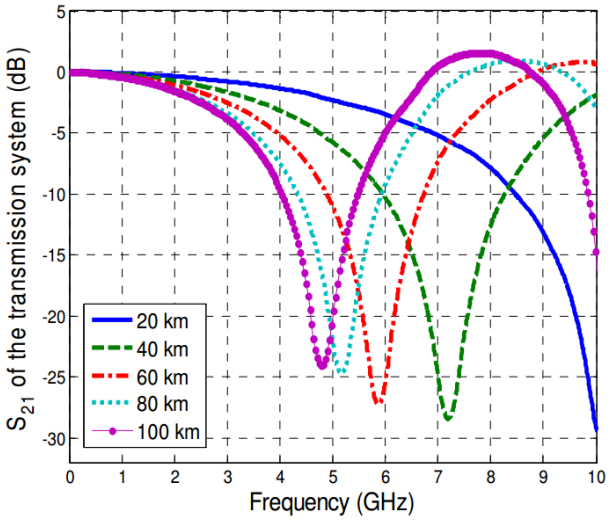

Figure 2.7. Frequency Response of 20-100 km ODSB based SMF transmissions [128]

a Double-Side-Band-with-Carrier (ODSB) modulation format. The sidebands in ODSB signals are located on two sides of the optical carrier with spacing equal to the operating frequency of the microwave signal. The propagation of an ODSB signal over a dispersive fibre will result in the two side-bands experiencing different amounts of phase shift with respect to the optical carrier. At the receiver upon detection at the photodetector, the square law process generates two beat components at the desired RF frequency, and the generated RF electrical power varies depending on the relative phase difference between the two beat components. This variation in the RF power is dependent on the fibre dispersion parameter, the fibre propagation distance and the RF frequency. Using a Network Analyser (NA) the frequency response of an EAM based system with ODSB with transmission over 20-100 km of SMF is presented Figure 2.7. From the trends presented it can be seen that the RF power varies in a periodic manner with complete power suppression occurring at specific frequencies [121]. Increasing fibre lengths in such a scenario leads to shift of the first RF power null to lower frequencies and reduction of the bandwidth available in baseband. This factor induces limitations in allowable transmission distance and lowers operating frequencies in a RoF system. Directly modulated lasers also produce an ODSB signal and can suffer from dispersive fading. However the chirp produced by the directly modulated laser can limit a RoF system even further by pushing the first electrical RF power null to lower frequencies. This limitation decreases the available bandwidth at baseband frequencies as well as the maximum propagation distance [127], and this may force system designers to up convert RoF signals at frequencies above the first power null [129]. The simplest approach to diminish the impact of dispersion on ODSB signals is to remove one of the optical sidebands, which leads to optical-single-side-band-with-carrier (OSSB). This can be done by directly filtering one of the side bands [130] which for lower RF frequencies requires a narrow bandwidth optical filter. At the detector in the receiver, the optical carrier beats with the optical side band to produce a beat component at the required RF frequency, which does not suffer from dispersive fading. An OSSB-plus-the-Carrier (OSSB+C) formatted signal can also be produced via the cancellation of the unwanted sideband within an external modulator. This can be done by the employment of a dual-electrode Mach-Zehnder Modulator (DEMZM) biased at the quadrature with the drive voltage applied to both electrodes with a 90^{o} phase shift between the two electrodes [131]. Another technique to alleviate the limitation imposed by dispersion in RoF systems is obtained by supressing the optical carrier in ODSB formatted signal. In this method, the carrier is supressed to generate two sidebands separated by twice the operating RF frequency. At the receiver these two sidebands beat together to generate a beat component at twice the drive signal's RF frequency, as a result this implementation will only require half of the desired modulation frequency to be applied to the modulator [132]. This scheme

is achievable by biasing a single electrode MZM at the minimum transmission point of the transfer function, as biasing the device at this point results in the elimination of the optical carrier. Despite the advantages of this scheme the drive signal requires a large RF power to obtain desirable modulation depths [121].

2.4.3 Optical Receivers

In intensity modulated RoF systems, requiring direct detection, an O/E transducer such as a photodiode is sufficient for reversing the E/O conversion by converting the incoming light into corresponding variations of current. In optical communications, two widely used types of photodetectors are PIN photodiode and Avalanche Photodiodes (APDs). These E/O photodiodes for RoF applications are required to have high conversion efficiency and high bandwidths. The responsivity of a photodiode, R is defined as the ratio between the generated photocurrent, I_g to the incident optical power P_i;

$$R = \frac{I_g}{P_i} \tag{2.4}$$

R is also known as the DC responsivity, thus it does not account for frequency dependence of the device given the dynamic nature of photodiodes. The typical PIN diode photodetector is created by sandwiching an intrinsic layer between doped p and n layers. The resulting photo-generated electron-hole pairs are then swept by the bias electric field to device's electrical contacts to produce a photocurrent [35].

Achievable sensitivities with PINs can be enhanced by using APDs. Unlike PINs this structure can offer an internal gain through an avalanche effect, hence improved receiver sensitivity without the need for external amplification. One disadvantage of APD's is that there is a fixed gain-bandwidth product from the fact that for higher multiplication factors there is an increase in the time required for the avalanche effect to build up within the device [122]. Therefore, there is a trade-off between gain and bandwidth in APD's. PIN devices are relatively cheaper and require a lower bias voltage compared to APDs, however the employment of an APD is preferred when there are high losses in the system.

2.5 Distortion in RoF Systems

Signals in a RoF system can be degraded by either noise or distortion. Optical sources usually introduce some unwanted intensity variations defined as RIN, while optical fibres on the other hand do not add noise to the signal but rather degrade the signal through attenuation and dispersion and introduce distortion through fibre nonlinearities. Many optical links also include optical amplifiers which increase the signal level but also degrade the SNR. At the receiver, the usual noise sources are the shot noise, photodetector dark current noise and thermal noises from the load resistor and amplifier unit. Apart from noise sources in a RoF system, signal distortion can also lead to performance limitations. In RoF systems distortions are caused by nonlinearities and these can be due to the intensity-current relationship of laser diodes as well-as its dynamics or the raised cosine transfer function of the external modulators. The non-uniform gain profile of an in-line optical amplifier can also cause distortions. At the receiver end, the nonlinearities present in the electrical amplifiers used in conjunction with a photodetector can also give rise to some level of distortion. The distortions that are caused by nonlinearity can be defined as nonlinear distortions, which can then be broken down into Harmonic Distortion (HM), and Intermodulation Distortion (IMD). Harmonic distortion refers to the case where new frequency components are generated at integer multiples of the original frequencies due to nonlinearity. These HM signals may fall in band causing interference with the broadband RoF signal causing performance degradation. IMD refers to new signal components generated as a result of introducing two signals at f_1 and f_2 to a nonlinear system. IMD are generated at the sum and difference of integer multiples of the transmitted frequencies i.e. ($f_1 + f_2, f_1 - f_2, 2f_1 + f_2, 2f_1 - f_2, \ldots$). The generation of spurious signals because of

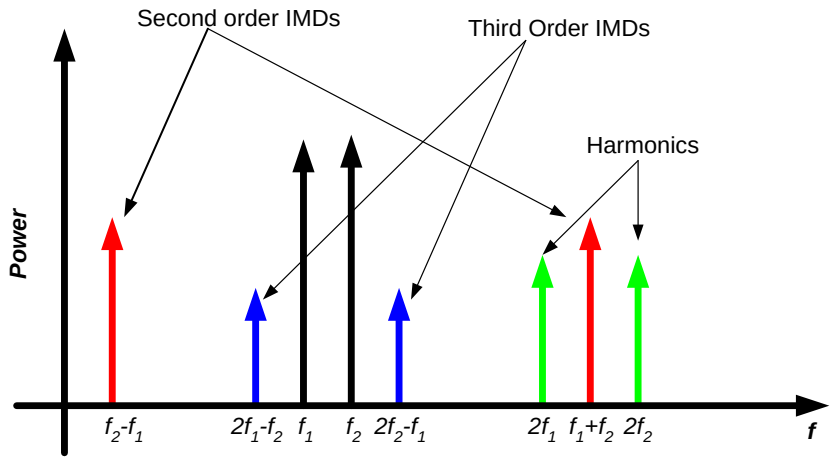

Figure 2.8. Intermodulation and harmonic distortions

feeding a nonlinear system with two tones with equal amplitudes operating at f_1 and f_2 is illustrated in Figure 2.8. For a passband signal the second order IMD usually falls out of band and can be simply filtered out, this leaves the spurs at $2f_1 - f_2$ and $2f_2 - f_1$. These spurs are known as the Third Order Intermodulation Distortion (3IMD) products and generally fall close to the original frequencies and can directly affect the RoF system through signal distortion.

2.6 Wireless services in Access Networks

The limited reach of wireless technologies along with the congested operating spectrum within which they operate, strongly diminishes the possibility of transmitting high bandwidth services over long distances to many users. Although the reduction of radio cell sites improves the wireless network's capacity (access rates for the end-user) [106]. On the other hand, the reduction in distance between the transmitting and receiving antennas because of cell-size reduction translates into lower energy levels required for the radio propagation, which leads into energy efficiency. With the increased number of cell sites in a given geographical region, the expenditure costs related to the deployed equipment in BSs also increases. Thus the economic feasibility of such topologies can be strongly improved by simplifying BSs and migrating complex radio functions and processing to a centralized location from where RoF techniques feed radio signals to the BSs. The connection over which RoF signals are transferred in such scenarios is referred to as "front-hauling" [133].

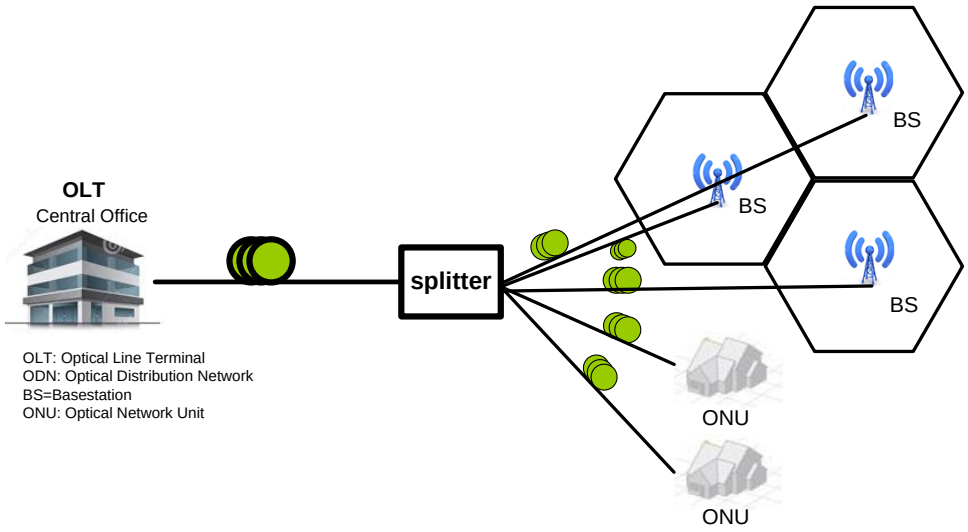

Figure 2.9. Hybrid wireless-optical access architecture

The demand for bandwidth in fixed services over past decades has pushed optical technologies closer to the end user in form of a FTTx, where high capacity passive optical links are used to transmit data between the service provider and end users. The interest in FTTx made possible standardization, commercialization and mass worldwide deployment of Gigabit capable PON topologies such as GPON and GE-PON. These technologies have significantly reduced the physical distance between the end user and the nearest optical network and already have well defined upgrade routes towards 10 to 40+ Gb/s capacity extensions [134, 135]. The bandwidth and reach attributes of FTTx has made integration of wireless access in PON's an attracting approach for delivery of high quality services along with high data rates. Given the vast deployment of PON technologies, along with it's passive, low loss and high bandwidth characteristics, this topology is identified as one of the most competent economical solutions for accommodating next generation wireless broadband access networks [136]. A typical hybrid wireless-optical access architecture based on the PON topology is presented in Figure 2.9. In this architecture front-hauling between the central office and the BS is provided by the optical feeder fibre, ODN and the distribution/drop fibre. Such networks are of upmost importance because this convergence between the wireless and wired services will generate savings in CAPEX (i.e. single fibre is deployed for fixed and mobile users) and in OPEX (i.e. single unified network leads to a more efficient network utilization) [105].

As illustrated in Figure 2.10 numerous methods can be employed for optical transportation of wireless channels at the physical layer, and they can be categorized in two groups based on either analogue or digital methods adopted. These are known as AoF and DoF. Analogue means are straight forward to implement, although they suffer from nonlinearities, noise sources and dispersion present in the transmission channel [121]. The two generic analogue schemes can be described as Radio-over-Fibre and IF-over-Fibre

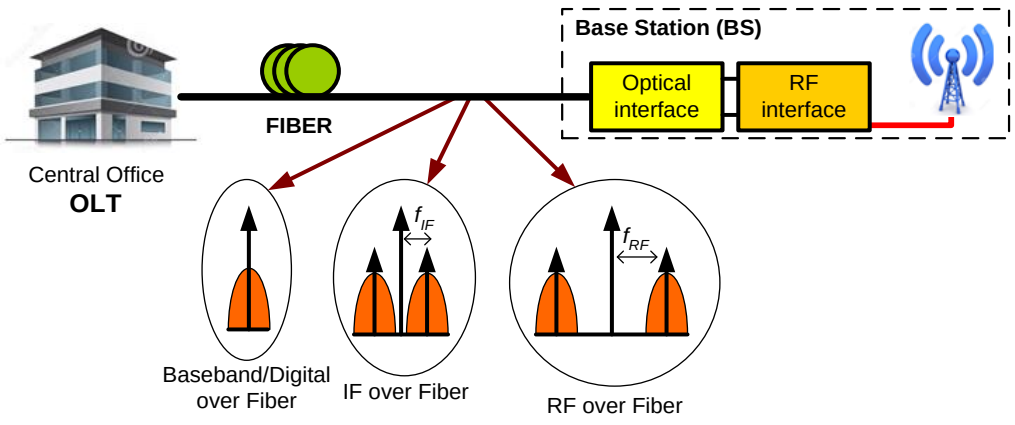

Figure 2.10. Optical transport schemes for Radio signals

(IFoF). The stated shortcomings of analogue techniques can be optimized to a level, by digitalizing wireless bands prior to their transmission at the expense of extra ADC's, DAC's, overheads, mixers and oscillators [120, 123]. Intensity modulation is the simplest scheme that can be used in RoF systems, and this can be achieved by the employment of external modulators or directly modulated lasers in the BS and the centralized station. As it was stated earlier, systems employing CPRI, operate by splitting the conventional BS into a RRU and a BBU. The connection between the RRU and BBU, which operates based on CPRI, provides the front-hauling solution. The provision of front-hauling by CPRI based DoF solutions had been initially sought for 4G systems but it can also be applied to 2G, 2.5G and 3G standards [115]. DoF implementations offer the advantage of exploiting mature digital optical communications hardware and network interfaces while enabling microwave signal distribution. Front-hauling through PON's can be also achieved by using CPRI [83, 117]. However, as result of digitization, the data rate of the optical channel will be a product of the sampling resolution and the sampling frequency, which results in net data rates with magnitudes higher than that delivered by the wireless band itself. Thus with increasing number of cells and antennas in a geographical location in next generation wireless access networks [84, 85], a high demand on required bandwidth is placed on PON's solely for providing access for wireless services. AoF techniques on the other hand avoid increased bandwidths by providing a cost effective, simple and transparent method for front-hauling wireless services over optical access infrastructures [137-139].

The co-existence of converged wireless services with fixed data channels in PON is an important matter that also needs to be addressed at the physical layer. This factor allows the new optically generated wireless services to merge/integrate within the existing infrastructure and ensure transparency in the remote access nodes. In essence, the allocation of a dedicated wavelength to each wireless and fixed band in PON links [83] as demonstrated for NG-PON2 [83], would transform the multiplexing complexity from the electronic domain into optics. Service-dedicated wavelengths promote upgradability in PON's, although with the rising number of antennas and wireless channels the number of required wavelengths also needs to be increased proportionally. This increase in the wavelength count leads to increased costs, inventory and management. Multiplexing fixed services along-with analogue wireless bands in one optical channel is also possible, alleviating the requirement for costly WDM equipment. Although guard bands are required spectrally between fixed services and the wireless bands, for interference reduction, nevertheless this can lead to bandwidth extensions, necessitating high bandwidth electro-optical equipment.

2.6.1 Analogue over Fibre (AoF)

RoF by analogue means is probably the most straightforward radio signal distribution scheme. The simplicity offered by AoF is due to the radio signals traveling through the fibre at their original carrier frequency with their modulation properties intact. Thus once these AoF signals are detected at the optical interface, in the receiver, no further up/down conversion or conversion between digital and analogue is required at the remote antenna BSs. This scheme simplifies the BS, by limiting the number of operational equipment in the BS to filters, amplifiers and antennas only. Figure 2.11 identifies the hardware required at the CO and BS for transmission of radio signals. In such systems a single or several RF bands carrying information are electrically summed and are superimposed on an optical signal. At the BS, the RoF is signal detected, filtered, amplified and radiated for air transmission. For upstream transmission of radio signals from the BS to CO, the system requires a method of E/O conversion at the BS and some means of optical detection at the CO. As it can be seen in Figure 2.11, such a transport scheme enables centralized control and remote monitoring of the radio signal distribution via a fibre based network which in turn reduces the complexity and costs associated in the BS [123].

IFoF can also achieve the same functions of RoF, the minor difference of this method with the prior technique comes from the employment of extra LOs at the receiver and transmitter ends. These LO will be used for down-conversion of radio signals to an IF. IF over Fibre allows the possibility for low-cost low-bandwidth optical subsystems to be employed in AoF systems. It can also allow wired and/or multiple wireless services operating at the same nominal frequencies to share a common fibre link. The architecture of an AoF system employing IF over fibre is shown in Figure 2.12. In this architecture, the transmitter may require extra local oscillators to shift the frequency of the existing

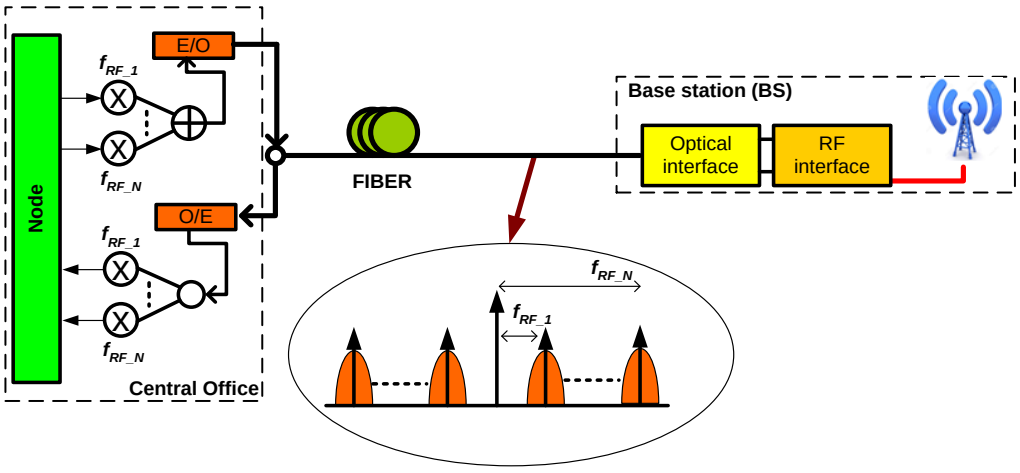

Figure 2.11. CO and BS hardware in RoF system

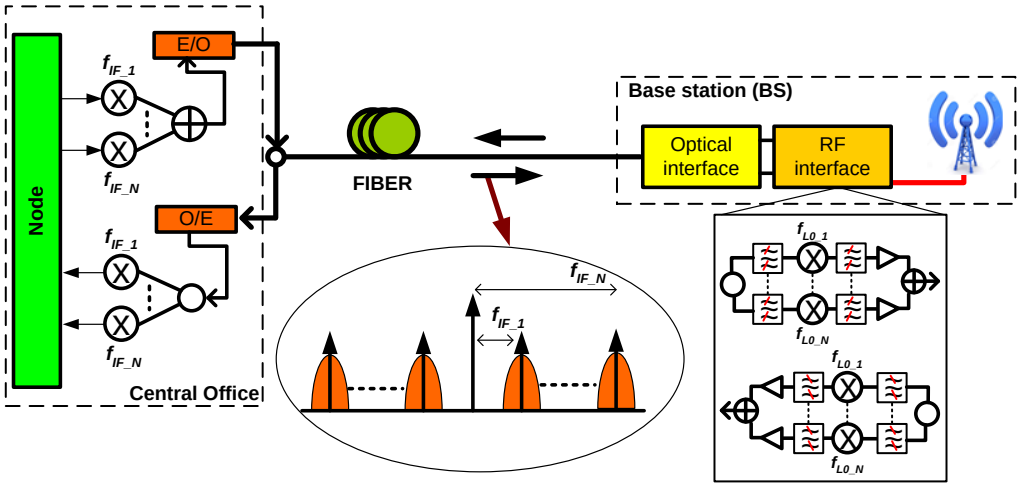

Figure 2.12.CO and BS hardware in IF over Fibre system

analogue waveform; otherwise, the data is directly modulated on an IF. At the receiver side after the photo-detection stage each IF band is filtered and is applied to a distinct LO which in turns produces a mixing product at the required RF band which is subsequently filtered and is radiated out, and for the uplink the process is reversed.

The IFoF architecture leads to increased complexity in the system, since extra LOs are required to be introduced in the BS. By moving toward higher operating frequencies such as those in millimetre range, the complexities are set to increase even further.

Due to the dramatic increase in demand for wireless services at the customer premises environment, a low cost, high capacity optical solution to deliver wireless services for both access and in-home networks is required. This demand can be met by AoF technologies that can provide low loss and large bandwidths for transmission. The exploitation of AoF in optical access networks for the transportation of wireless services is attracting a significant level of attention [140, 141] given the mass deployments of FTTH architectures which has

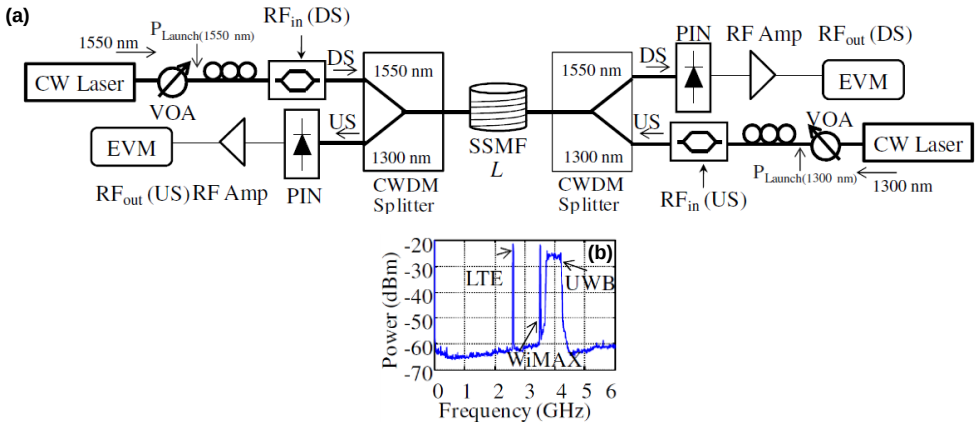

Figure 2.13. a) Experimental setup of a Bi-directional PON for transportation of three AoF radio services, b) electrical spectra of three combined radio services [2]

already provided the optical fibre infrastructure required by RoF. In [2] the idea of exploiting PON for the distribution of analogue RoF services was experimentally examined where Ultra Wide Band (UWB), WiMAX and LTE radio services were jointly transported over various lengths of an unamplified bi-directional link composed of SSMF. The experimental setup of the system employed is presented in Figure 2.13(a). The electrical signal driving (RF_{in}) the MZM that had been biased at the quadrature point is composed of the three radio signals. Upon fibre propagation, the optical signal is detected by a photodetector and subsequently has its performance evaluated in terms of Error Vector Magnitude (EVM). In the uplink direction, the same process as the downlink is repeated by a different laser operating at 1300 nm. The spectral content of RF_{in} is presented in Figure 2.13 (b), the LTE band had a bandwidth of 20 MHz and was set to operate at 2.6 GHz, the WiMAX signal was operating at 3.5 GHz with a bandwidth of 24 MHz, and the UWB was operating at 3.96 GHz with 528 MHz of bandwidth. Both LTE and WiMAX signals used 16 QAM. The experimental results for this system showed acceptable level of performance reached in downlink for all three services for link spans over 100 km and over 50 km in uplink. The lower reach in uplink can be related to higher losses at 1300 nm which dictate that the SNR is reduced more rapidly with increasing fibre lengths than in the 1550 nm path [2].

In [142] the provisioning of multiple wired and wireless services in LR-PON's was studied.

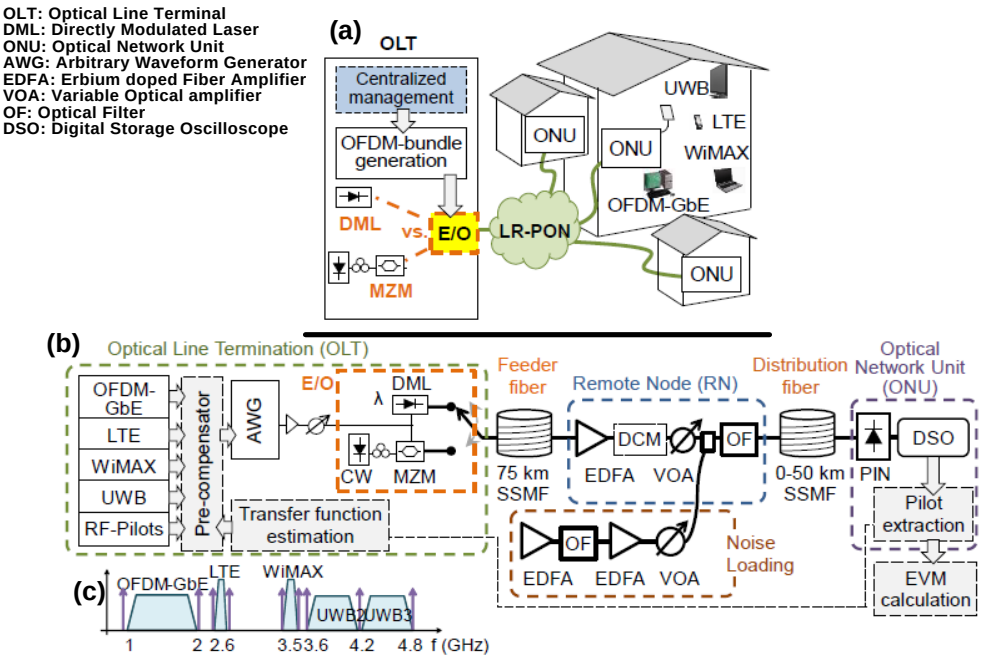

Figure 2.14. Hybrid wire/wireless LR-PON (a) system architecture (b) Experimental setup (c) Spectral content [142]

In this work a novel integrated access network for the provision of a quintuple-play (5PLAY) service (including broadband wired Internet, phone, HDTV, wireless data and home security services) to end users using a single hybrid LR-PON was demonstrated. The wireless services employed here were UWB, LTE and WiMAX, the wired services were allocated to a custom OFDM-based signal for Gigabit-Ethernet connectivity (OFDM-GbE). The wireless signals are transmitted using RoF in coexistence with the wired band. The envisioned system architecture is presented in Figure 2.14 (a). The OLT is responsible for the management and generation of the downlink signals and in order to improve cost efficiency it is also equipped and tested with a directly modulated DFB laser. The experimental setup and the transmitted electrical spectrum are further shown in Figure 2.14 (b-c). The optical amplifier housed in the RN acts as a reach extender for PON [42], and the extra pilot tones included at the edge of each band are used to correct for channel impairments. QPSK was used for all services employed, and experimental evaluation demonstrated acceptable performance limits being reached after transmission over 90 km in both directly and externally modulated cases.

These two above examples demonstrated the transmission of singular wireless bands over a PON infrastructure. Although given the number of active BSs and antennas in a region covered by a PON, it may be required for one optical link to carry multiple Analogue RoF bands. Due to scarce spectrum resources used by the wireless services, the neighbouring BSs will be operating at the same frequencies [110], thus overlaying RoF signals for all base-stations on a single wavelength channel will lead to a severe interference. In such scenarios, IFoF can allow for the co-existence of multiple wireless bands on one

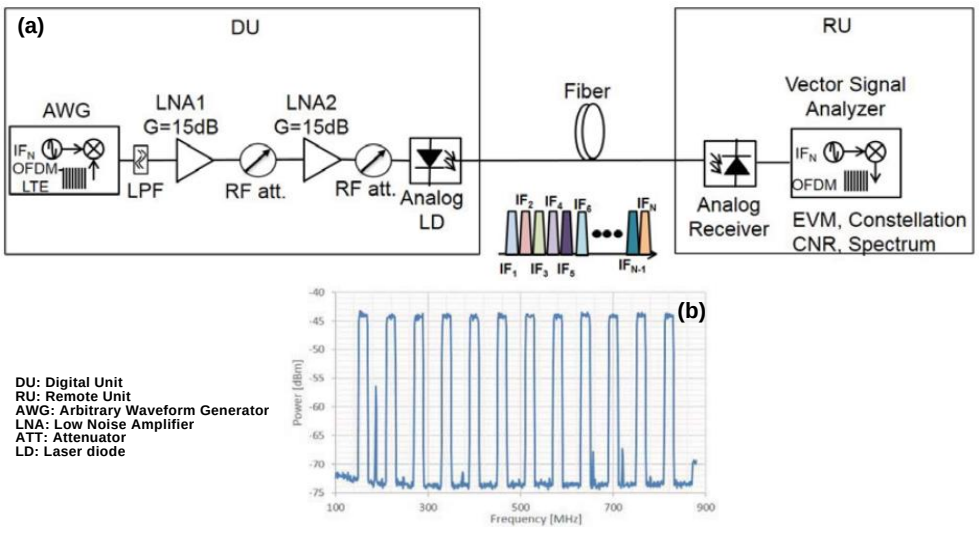

Figure 2.15. Mobile fronthualing using IFoF, (a) Experimental Setup, (b) generated electrical spectrum [138]

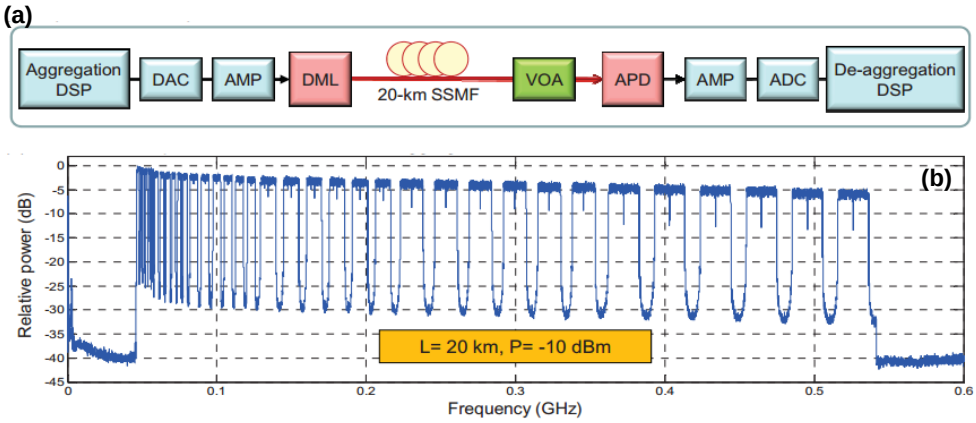

Figure 2.16. Mobile fronthualing of 36 LTE bands using IFoF, (a) Experimental Setup, (b) generated electrical spectrum [137]

wavelength channel in PON, were the radio signal for each antenna is re-allocated to a predetermined frequency grid, which is then re-shifted at the BS, using LOs. In [138] IFoF was employed to provide front-hauling for twelve 64 QAM modulated LTE radio signals which were generated using a directly modulated laser and transmitted over 20 km of SSMF. Figure 2.15 (a) shows the experimental setup used, an AWG was used to generate the twelve IF bands which covered less than 900 MHz of bandwidth (Figure 2.15(b)), the signal was then used to drive a DFB laser diode housed in the CO. After 20 km of fibre propagation, the optical signal is photodetected and is analysed using a vector signal analyser, which showed acceptable performance both in back to back and fibre transmission cases. In [137] IFoF was again used for front-hauling of 36 LTE like Analogue RoF signals, with transmission over 20 km of SSMF. The experimental setup and the received electrical spectrum are shown in Figure 2.16. The 36 bands were composed of six 1.4, 3, 5, 10, 15 and 20 MHz LTE bands that covered less than 600 MHz of bandwidth. The experimental results showed acceptable levels of performance over 20 km of fibre for QPSK, 16 QAM and 64 QAM modulation formats employed.

Front-hauling of LTE-advanced services using IFoF have also been demonstrated in [139] where twelve 100 MHz bands each composed of five 20 MHz carriers aggregated LTE bands were generated using a MZM and transferred over 40 km of SSMF. The transmission was evaluated for QPSK, 16QAM and 64 QAM modulation formats, and acceptable performance limits were achieved in each case. The above-mentioned method clearly demonstrates the capability of the passive link in PON for use in front-hauling schemes.

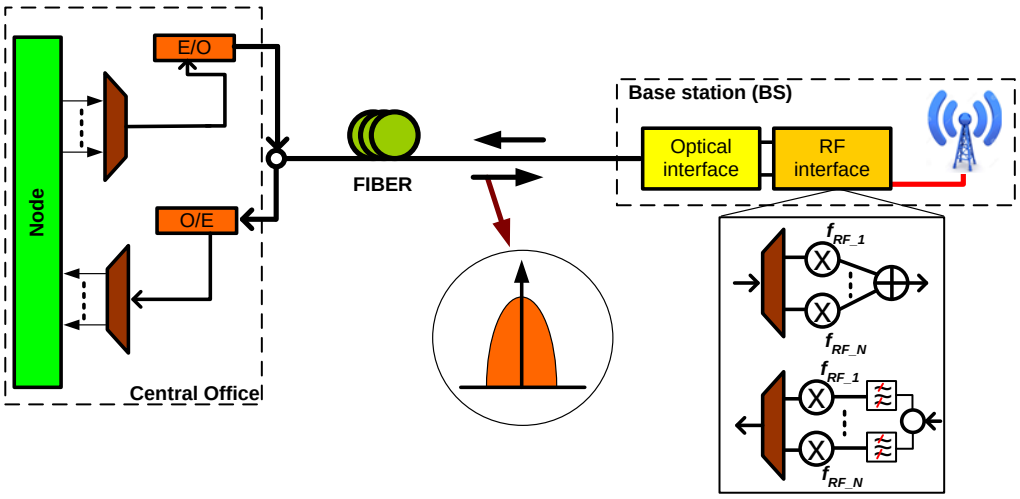

Figure 2.17. CO and BS hardware in Digital over Fibre system

2.6.2 Digital over Fibre (DoF)

The transport of radio signals over fibre by digital means is depicted in Figure 2.17. As shown here, the radio information for the radio carriers is transported to the BS as a TDM digital data stream. The individual data channels are then demultiplexed and unconverted to the required radio frequency using LOs at the BS prior to amplification and air transmission. DoF systems can readily exploit the use of mature and reliable RF and digital hardware for signal processing at the CO and BS [123]. However, similarly to IFoF, the need for frequency conversion at the BS complicates the BS architecture, especially as air interface radio frequency increases.

RoF links employing analogue subsystems are known to suffer from inter-modulation distortion arising from the nonlinearity of both microwave and optical components that make up the system [122, 123]. The digitalized RoF systems have therefore been developed to overcome such issues with AoF system [104]. The protocol used for front-hauling in DoF systems is typically the CPRI [116], which basically is a TDM based protocol that carries digital samples of the analogue signals to and from the antennas. In such schemes A/D converters are used to digitalize the analogue services prior to their optical transmission, this in-turn necessitates D/A converters at the air interface for air transmission. CPRI is a constant bit rate signal, which is structured as a multiplexing hierarchy of digital streams generated by sampling, quantization and binary encoding the analogue radio signals. It is defined at different line rates, ranging from 614.4 Mb/s to 9.83 Gb/s and can be considered independent of the specific radio service used [143]. Due to the digitalization process and extra overheads, the data rates required for CPRI for a particular wireless technology can be an order of magnitude higher compared to the net data rate

RAN	GSM 1T1R	GSM 1T2R	WCDMA 1T1R	WCDMA 1T2R	LTE 10MHz 2X2	LTE 10MHz 4X2	LTE 20MHz 2X2	LTE 20MHz 4X2
CPRI Data rate	12.304 Mb/s	24.608 Mb/s	307.2 Mb/s	614.4 Mb/s	1228.8 Mb/s	2457.6 Mb/s	2457.6 Mb/s	4915.2 Mb/s

Table 2.1. Typical data rates of CPRI in function of radio technology[115]

transferred by the wireless service itself. Table 2.1 presents some typical data rates required for different Radio Access Network (RAN) technologies using various antenna configurations.

Achieving front-hauling using CPRI in optical access has been discussed widely [103, 105, 133]. Given the high CPRI data rates for multi antenna technologies used in 4G Cellular communication systems, 10G capable PON systems have been seen fit to support the mobile front-hauling for such systems [136, 144], where dedicated wavelengths carrying CPRI data are routed to the BS's site. The transport of CPRI over 10G capable PON systems is envisioned to be achieved by native OOK modulation formats, although the use of highly spectral efficient modulation formats such as OFDM have been proposed [145, 146].

2.7 Summary

In response to the continuous increase of data traffic over wireless communication networks numerous cellular wireless generations (1G, 2G, 3G, 4G) have come into existence, with the common aim of offering increased capacity. To support these higher wireless capacities, it becomes necessary to adapt higher bandwidth communication links between the BSs and the wireless backbone. Optical fibre networks are seen as an attractive candidate for fulfilling this purpose thanks to their low loss and high bandwidth characteristics. The employment of RoF techniques in such optical-wireless links has been seen as an approach for simplifying the BSs through centralization of key components in a central location far from the BSs. The simultaneous growth of wireless access networks and optical access network in the form of PON's has now created the potential of convergence of the two topologies into a unified network. This approach will allow for lower operational costs through hardware sharing and energy savings.

RoF techniques can be subdivided into two variants (Analogue and Digital over Fibre). Analogue over fibre techniques can lead to simple architectures and can provide a transparent means of transportation for the wireless services although they suffer from intermodulation distortions arising from the nonlinearity of both microwave and optical components that make up the link. On the other hand Digital over Fibre techniques can be employed to enhance the RoF systems performance at the expense of higher required data rates created and complexities introduced at the transmission and reception nodes.

Chapter 3

Hybrid Wired/Wireless OFDM-PON

3.1 Introduction

To accommodate the growing demand in capacity, future optical access technologies will need to employ various multiplexing techniques and advanced modulation formats [147]. Furthermore, the convergence of wire-line and wireless services in PON's is very attractive as it offers increased network flexibility, increased capacity and simultaneous reduction of overall costs in the access domain [148]. The use of A-RoF techniques can enable the seamless transmission of wireless services to the Optical Network Units (ONUs) in PON's. With A-RoF techniques there is no need for frequency up/down conversion or extensive processing, as detected wireless signals can be directly radiated out using simple remote antennas [3].

From an economical point of view, the use of direct modulation in PON's is crucial [149], since using external modulators will result in increased costs, reduced overall power budgets and polarization dependencies. To further reduce the costs in a PON system, the use of inexpensive lasers should also be considered [150]. Nevertheless, the limited bandwidth available from such low cost transmitters means that conventional modulation

formats cannot achieve high data rates. Thus, highly spectrally efficient Orthogonal Frequency Division Multiplexing (OFDM) as a modulation format can be used in order to achieve the required data rates and propagation distances for next generation PON's. A limiting factor associated with such directly modulated systems is the increased nonlinearity that occurs at the resonance peak of the laser's modulation response. Given the moderate bandwidth of cost effective laser, these nonlinearities can emerge at lower modulation frequencies, thus directly modulating such lasers with OFDM type signals can severely degrade the performance of this multicarrier system [5], through the creation of significant interfering spurious signals in the higher frequency OFDM channels. The nonlinear distortion of an OFDM signal causes the loss of orthogonality between neighbouring subcarriers which reside in the vicinity of the nonlinear region; this in turn results in inter-carrier interference [151] and loss of perfomance. The nonlinear distortion, can also lead to spectral regeneration [152], which can cause interference in nearby operational channels. As analogue modulation of the optical carrier is used in these systems, the intrinsic Relative Intensity Noise (RIN) from the directly modulated laser can also be expected to influence the performance of the multicarrier OFDM band. The RIN degrades the performance by introducing additional amplitude fluctuations to the composite signal, thereby further reducing system's SNR [153].

Optical Injection can be used as a remedy for the shortcomings of inexpensive moderate bandwidth devices by enhancing their modulation bandwidth which in turn reduces both the inherent nonlinearities, and the RIN, at the frequencies of operation [10, 154]. Typical setups required to injection lock a laser have a large footprint, thus it is advantageous to use integrated devices when employing optical injection, as this will lead to a compact and simple transmitter module.

Cellular communication systems commonly use frequency bands below 3 Ghz for their air interface, this factor can influence the hybrid wired/wireless access networks through interference leading to performance degradation. This interference arises if wired and wireless services sharing a common wavelength operate at similar frequencies. Such interference cannot be easily eliminated, since wired services are usually operated at the baseband. The multi-carrier nature of OFDM allows for nulls in its spectrum by deactivating individual subcarriers. This can prove beneficial in hybrid wired/wireless OFDM-PON's, as subcarriers in the wired OFDM-band are de-activated at frequencies corresponding to the required A-RoF bands. This leads to spectral notches in the spectrum of the wired band which can be used for transmission of wireless services. Integrating OFDM based wireless services such as LTE in such an architecture can similarly to the wired band be affected by the nonlinearity present in the system [155], however optical

injection can also aid in reducing the impact of nonlinearity on this OFDM base wireless band arising from the directly modulated laser.

The work presented in this chapter for the first time looks at a hybrid wired/wireless OFDM PON system that accommodates for multiple in-band AoF signals carrying LTE services. The work also for the first time studies the performance of such a hybrid system in conjunction with integrated low cost integrated Discrete Mode (DM) laser devices with optical injection. Numerical studies are further used to identify the impact of RIN and nonlinearity on the performance of this system.

3.2 OFDM

Orthogonal Frequency Division Multiplexing (OFDM) is a Multi Carrier (MC) modulation technique, which allows the transmission of data over many subcarriers, which are harmonically related. Frequency Division Multiplexing (FDM) typically uses frequency guard bands between the adjacent subcarriers in order to alleviate possible interference between subcarriers. By using the concept of orthogonality in OFDM this guard band is eliminated, which reduces the frequency spacing between adjacent subcarriers to the baud-rate frequency; hence subcarriers overlap each other in the frequency domain. Given the orthogonal relationship amongst neighbouring subcarriers in OFDM, the overlapping of subcarriers does not result in Inter Carrier Interference (ICI). The overlap of subcarriers in-turn allows for higher spectral efficiencies, since more subcarriers are accommodated in the available bandwidth.

The first proposal to use orthogonal frequencies for transmission of data appeared in a 1966 patent by Chang of Bell Labs [156]. The next two major breakthroughs for OFDM were the utilization of a Fast Fourier Transform (FFT) as an efficient means to generate orthogonal subcarriers and a cyclic prefix to combat channel impairments [157, 158]. OFDM began to be considered for wireless applications in the 1980s by Cimini of Bell Labs [63]. In this work, Cimini studied the performance of OFDM over the air propagation. The application of OFDM for wireline communication was pioneered by Cioffi [159] where the potential of OFDM for DSL application was demonstrated. OFDM now forms the basis of many wireless systems such as LTE and WiMax. OFDM also has become the basis for most DSL standards, but in DSL applications the baseband OFDM signal is not modulated on a passband carrier frequency, in this context OFDM is usually called Discrete Multitone (DMT) [66].

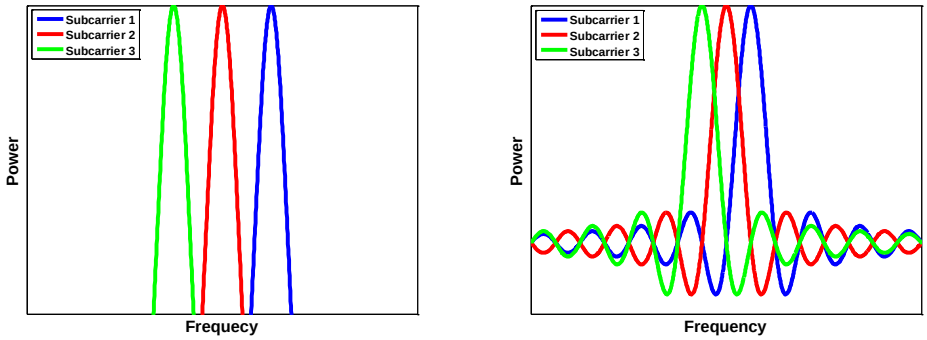

Figure 3.1. Spectrum of (a) WDM or FDM signals (b) OFDM Signals

The high spectral efficiency of OFDM along with its resilience to chromatic dispersion, has promoted OFDM to emerge as a dominant R&D area in the field of high-speed optical communications. Research interest on this topic has grown rapidly, with OFDM being used in different subsystems, from Plastic Optical Fibre (POF) applications [160] to hybrid wired/wireless access networks [3] and optical super channels [38].

3.2.1 System description

Figure 3.1 (a-b) show the spectrum of FDM and OFDM systems. The advantage of this "parallelized" FDM approach is that symbols on the each of these multiplexed tributaries or subcarriers have longer durations. These time elongated symbols make FDM systems less vulnerable to linear distortion effects such as chromatic dispersion, which become worse with increases to the symbol rate. The trade-off for this performance enhancement is a loss of spectral efficiency due to the insertion of guard band between the individual tributaries or subcarriers, which are required to prevent interference.

OFDM is able to counteract the issue of reduced spectral efficiency seen by FDM systems by reducing the previously used guard bands in FDM, such that neighbouring modulated subcarriers overlap one another. In such a scenario, interference can be eliminated by using the principle of orthogonality between subcarriers, which can be achieved by careful selection of OFDM's subcarrier frequencies $f_m, \{m = 0,1,2.....,M-1\}$ [67]. For example, assuming that f_1 is a sinusoidal carrier that has been modulated with a complex QAM symbol $X_1 = A_1 - jB_1$, where A_1 and B_1 are obtained by taking the real ($\Re$) and imaginary ($\Im$) parts of the complex point on a QAM constellation. The modulated subcarrier for one symbol period can be defined as

$$s_1(t) = A_1 \cos(2\pi f_1 t) - B_1 \sin(2\pi f_1 t) \tag{3.1}$$

The first and second terms of the above equation, respectively are the in-phase and quadrature portions of the signal at f_1. To ensure orthogonality between this subcarrier and a second subcarrier, let say f_2 the following condition must be met:

$$\int_0^T s_1(t)s_2(t)dt = 0 \tag{3.2}$$

However, in an OFDM system more than two subcarriers can exist. Thus the orthogonality condition in equation (3.2) must hold for all possible combinations of $s_m(t)s_l(t)$ where $m = \{0,1,2,...,M-1\}, l = \{0,1,2,...L-1\}$ and $m \neq l$. To meet this requirement, subcarrier frequencies f_m should be defined as harmonics over the symbol period as

$$f_m = \frac{m}{T} + f_{RF} \quad \text{for} \quad m = 0,1,2,...,M-1 \tag{3.3}$$

f_{RF} here is the frequency of the RF carrier, to which the baseband OFDM signal is up-converted to prior to transmission. In a special case for some OFDM systems $f_{RF} = 0$, this is true for DMT systems, which operate at the baseband. The resulting electrical time-domain OFDM signal may be expressed mathematically as

$$s(t) = \sum_{m=0}^{M-1} A_m h(t)\cos(2\pi f_m t) - B_m h(t)\sin(2\pi f_m t) \tag{3.4}$$

Where $h(t)$ represents the impulse response of the pulse shaping filter that is used on the I and Q channels. This pulse can be a rectangular pulse given as $h(t) = 1, \{0 \le t \le T\}$ and zero elsewhere. This particular choice of the pulse shaping function gives the Sinc shaped spectral content to each OFDM subcarrier as seen in Figure 3.1 (b).

In OFDM systems, the available bandwidth can be subdivided amongst 10's to 100's of subcarriers. In an analogue implementation, the difficulties related with such high numbers of subcarriers become more apparent. For example for an OFDM signal with M=512 subcarriers in order to implement equation (3.4), 511 synchronized analogue oscillators are required both at the transmitter side and the received end. Fortunately, this modulation complexity can be translated from the analogue domain into the digital domain. The Inverse Fast Fourier Transform (IFFT) operation at the transmitter and the Fast Fourier Transform (FFT) operation at the receiver make up the main components in this digital realization of an OFDM communication block. The input to the IFFT at the transmitter is a vector of complex entities $\bar{X} = [X_0, X_1, ..., X_{N-1}]^T$ thus, the vector has N elements and

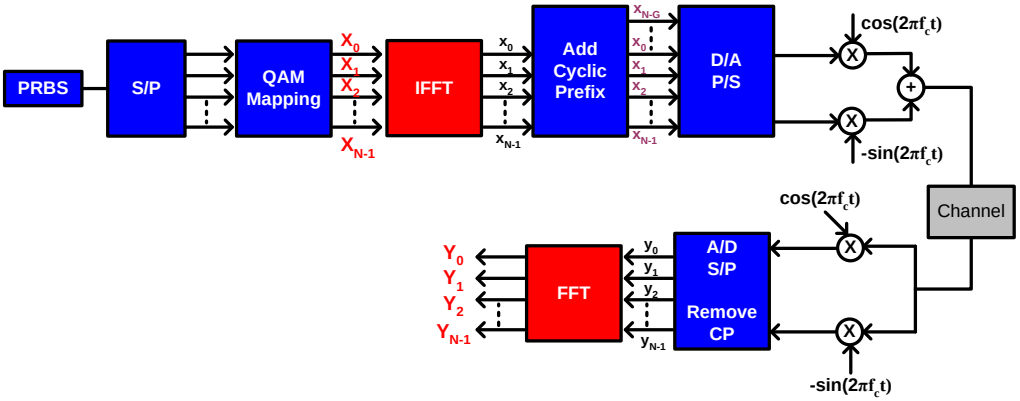

Figure 3.2. Block Diagram of OFDM communication system for RF wireless applications

the size of the IFFT is N . The elements X_k are complex elements representing a point on the QAM constellation, which will be modulated on the kth subcarrier (Capital letters here represent frequency domain entities and lower case represents those in the time domain, bars above letters signify vectors). The output of the IFFT is a complex vector $\bar{x} = [x_0, x_1, ..., x_{N-1}]^T$ where each element x_p in this vector is a discrete time-domain signal. The IFFT operation can then be represented as

$$x_p = \frac{1}{\sqrt{N}} \sum_{k=0}^{N-1} X_k \exp\left(\frac{j2\pi kp}{N}\right) \quad \text{for } 0 \le p \le N-1 \tag{3.5}$$

And similarly the FFT operation corresponds to

$$X_k = \frac{1}{\sqrt{N}} \sum_{k=0}^{N-1} x_p \exp\left(\frac{-j2\pi kp}{N}\right) \quad \text{for } 0 \le k \le N-1 \tag{3.6}$$

Figure 3.2 shows an example of an OFDM communication block along with input and outputs of the IFFT and FFT blocks. The PRBS block generates the binary data, which is then parallelized into multiple paths. The QAM mapper based on a given selection of binary bits produces a representative QAM symbol. The output of the QAM-Mapping block produces the vector $\bar{X}$, which is then fed to the IFFT block. The IFFT operation creates the vector $\bar{x}$. At the receiver, after down-conversion and Cyclic Prefix (CP) removal, the vector $\bar{y}$ is fed to the FFT block, this vector is the received version of $\bar{x}$ which had been subjected to noise and distortion in the communication system. The FFT block then produces the vector $\bar{Y}$ based on discrete time entities in $\bar{y}$. This vector ($\bar{Y}$) contains the received QAM symbols Y_k . In absence of noise and distortion in the channel or the transmitter and receiver front-ends, the following condition holds $\bar{Y} = \bar{X}$.

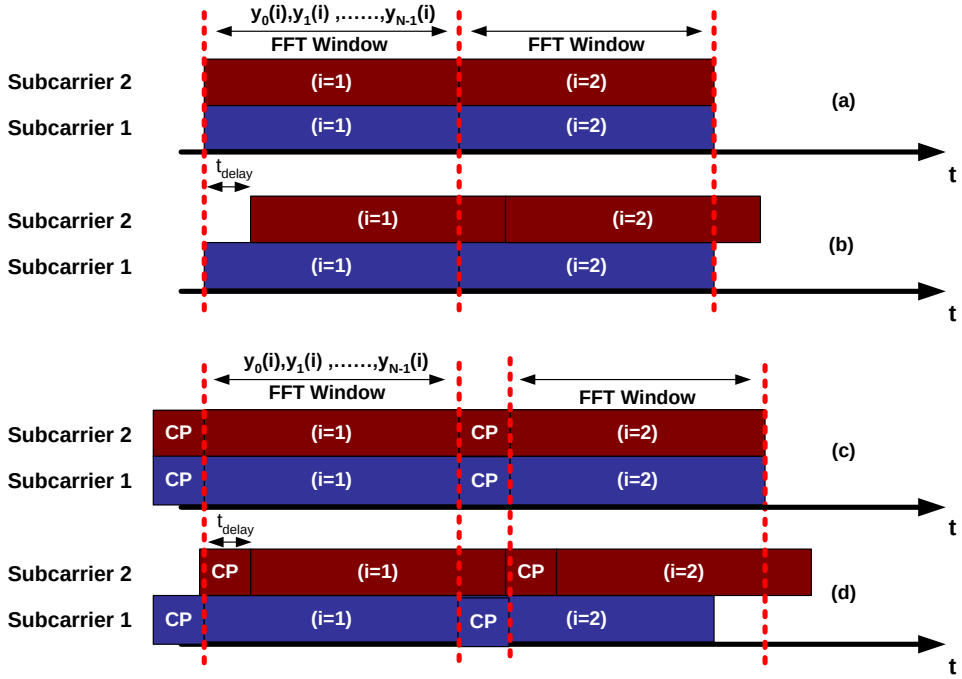

Figure 3.3. Impact of CP in a OFDM system with two symbols i=1,2. Containing two subcarriers. (a) "CP-less" with no delay, (b) "CP-less" with delay, (c) "with-CP" with no delay, (d) "with-CP" with delay

3.2.2 Cyclic Prefix

OFDM is so widely used because, when CP is employed, any distortion caused by a linear dispersive channel can be corrected using a 'single tap' equalizer [66]. OFDM symbols are denoted as $\bar{x}(i) = \left[x_0(i), x_1(i), ..., x_{N-1}(i)\right]^T$ where $\bar{x}(i)$ represents the output from the ith IFFT operation. The inclusion of CP requires the appending of G samples to the start of $\bar{x}(i)$, where G is the length of the CP. The new sequence as can be seen in Figure 3.2 takes on the following form $\bar{x}_{CP}(i) = \left[x_{N-G}(i), ..., x_{N-1}(i), x_0(i), x_1(i), ..., x_{N-1}(i)\right]^T$. The use of CP can eliminate both Inter Symbol Interference (ISI) and Inter Carrier Interference (ICI) from the received signal. To elaborate on this we take an example of two received consecutive OFDM symbols $\bar{y}(i), i = \{1,2\}$ which contain only two subcarriers. Figure 3.3 (a) shows this symbol pair where the contribution of each subcarrier to the OFDM signal is illustrated separately. With the absence of delay, both subcarriers arrive at the same time at the FFT window. This precise match of the OFDM window ensures that the FFT operation returns $\bar{Y}$, where with the absence of noise and distortion in the system it is ensured that $\bar{Y} = \bar{X}$. Figure 3.3 (b) illustrates a scenario where the channel imposes a delay t_{delay} on one of the subcarriers. This result in one of the subcarriers to be truncated at the FFT window, this leads to Inter (OFDM) Symbol Interference (ISI). This issue can be resolved by appending

a guard interval in which no signal is transmitted before or after each OFDM symbol. However, since the delayed subcarrier is truncated at the FFT window, the system will suffer from Inter Carrier Interference (ICI). But now by introduction of CP as shown in Figure 3.3 (c-d), each OFDM subcarrier is represented by a continuous sinusoid of the appropriate frequency throughout the main symbol period and the CP. Thus, as long as the t_{delay} does not exceed the CP used, the OFDM symbols can be retrieved free of ISI and ICI.

In a practical system, the $\bar{Y} = \bar{X}$ identity no more holds, due to the impact of noise and the distortion caused by the linear dispersive channel. However, when a CP is used, distortions caused by a linear dispersive channel can be corrected by simply using a 'single-tap' equalizer. To counteract the impact of the channel on $\bar{Y}$ and recovering a close approximation to $\bar{X}$, the response of the channel over various subcarriers (k) must be retrieved. Knowing how the effects of channel response and noise in the system effect the received complex symbols $\bar{Y}$ as $Y_k = H_k X_k + W_k$, where H_k and W_k are the response of the channel and noise present at the k th subcarrier, the approximation to X_k can be retrieved by

$$\hat{X}_k = \frac{Y_k}{H_k} = X_k + \frac{W_k}{H_k} \tag{3.7}$$

Thus to counteract the effects of the channel, the received symbols should be equalized by being multiplied by $1/H_k$.

3.3 Optical Injection Locking

The introduction of external coherent light from a master laser into the cavity of a slave laser has been termed Optical Injection locking (OIL) and has been widely investigated. OIL has been shown to achieve numerous advantages such as reduction in laser chirping [161], RIN [162], nonlinear distortions [5, 163] and also increase in the modulation bandwidth and enhancement of the resonance frequency [10]. Reduced chirping in RoF systems can allow for longer propagation distances by reducing the impact of fibre dispersion on directly modulated systems. Lower levels of RIN can enhance the performance in a RoF system by improving SNR levels. The interaction between electrons and photons in the laser cavity give rise to the nonlinear distortions in operating frequencies close to the resonance frequency.

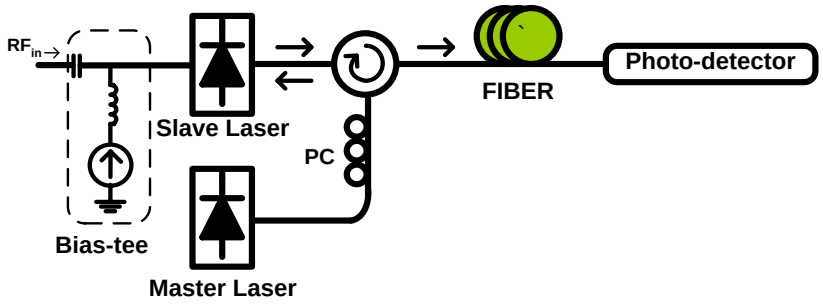

Figure 3.4. Typical Optical Injection Setup

Practical setups for optical injection are quite bulky, as they comprise of passive devices and two separate laser-transmitters operating in a master/slave configuration. A common setup used to achieve optical injection is presented in Figure 3.4, where the same output-facet of the slave laser is used to inject external light. To match the polarization of two laser devices a Polarization Controller (PC) is used after the master laser, and the resulting light is then routed to the slave laser's cavity by using an optical circulator.

The master and the salve lasers in an OIL system can operate at different wavelengths, but once stably injection-locked the slave laser tracks the master's emission wavelength within a specific detuning range. As the frequency difference between the two lasers becomes large, further increase to the detuning frequency results in the slave laser not being stably injection locked. The unlocking between the master and slave lasers, results in both devices operating at their nominal wavelengths. Apart from the detuning frequency the power of the injected signal also plays a significant rule in determination of the OIL characteristics [122].

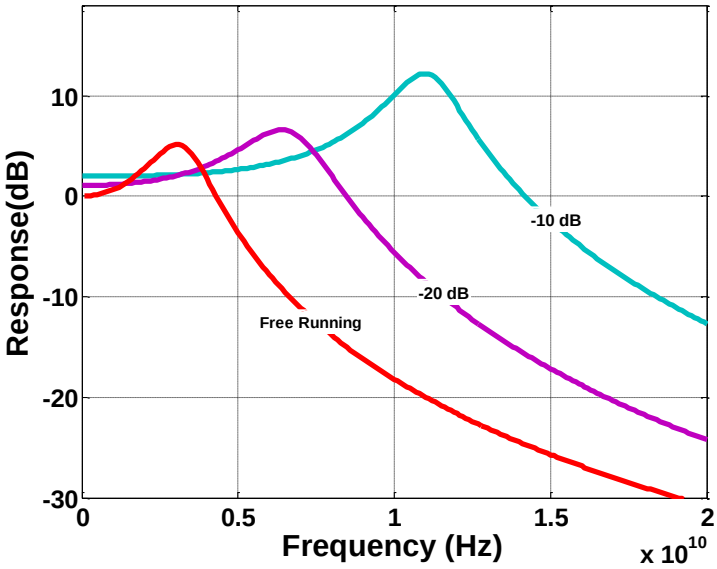

Figure 3.5.Simulated frequency responses of a slave laser under free running and optical injection at various injection ratios. ($\Delta\omega$ = -2 GHz)

The advantages achieved by OIL can improve the performance of directly modulated systems in transmitting of both analogue and digital signals. The 3-dB bandwidth or the modulation bandwidth of a laser is an important figure that characterizes the performance of the lasers. Modulation bandwidth of a directly modulated semiconductor laser is limited by its relaxation oscillation frequency, which, in turn, is related to the bias current of the laser. In RoF systems when lasers are modulated by signals containing frequency components close to the relaxation oscillation frequency, the laser experiences nonlinear coupling between carriers and photons. This nonlinear coupling produces signal distortions, resulting in the degradation of system performance. Therefore, high speed modulation of semiconductor lasers is limited by the relaxation oscillation frequency [122]. Many authors have reported modulation bandwidth enhancements by the employment of OIL both theoretically and experimentally [10, 164] . These improvements were achieved by the enhancement of the relaxation oscillation frequency of the free-running laser. Such enhancement in the relaxation oscillation frequency is dependent on the detuning frequency and the injection ratio. The detuning frequency $\Delta\omega \equiv \omega_{inj} - \omega_{fr}$ is the difference between the master laser's optical emission frequency ω_{inj} and that of the free running laser ω_{fr}. The injection ratio is the ratio between the steady state photon densities of the injected light entering slave laser's cavity to the steady state photon density of the slave laser. The simulated responses presented in Figure 3.5, shows the frequency response of a slave laser with and without optical injection. The figure clearly demonstrates that the application of optical injection can enhance the modulation bandwidth by moving the relaxation oscillation peak to higher frequencies.

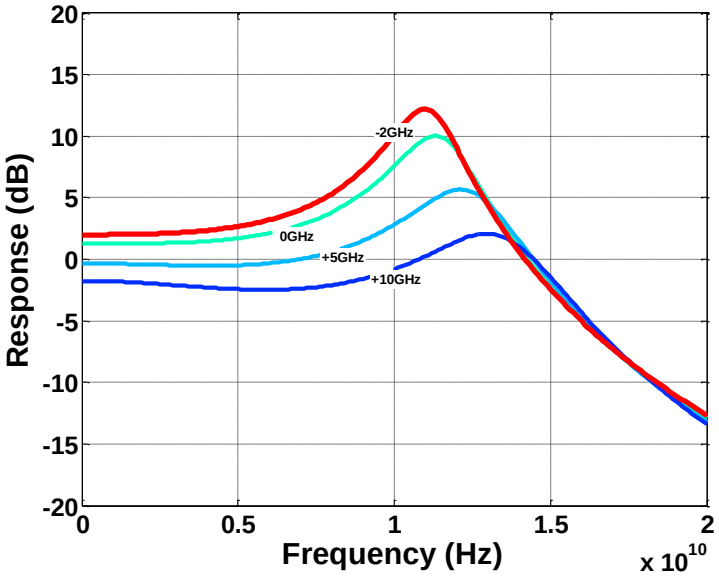

Figure 3.6. Simulated frequency responses of a slave laser under optical injection at various detuning frequencies. (Injection Ratio = -10 dB)

The increase in bandwidth of the slave laser because of enhancements to the relaxation oscillation frequency is depicted in Figure 3.6 for various detuning frequencies. In this figure, the shift in the resonance frequency to higher values is observed, as the detuning move towards higher positive frequencies.

3.4 Directly Modulated Hybrid wired/wireless OFDM-PON with optical injection

In this section the transmission of OFDM based wired services for hybrid PON's using direct laser modulation is studied. To overcome the limitations imposed by direct modulation of cost effective low bandwidth laser transmitters, we make use of novel monolithically integrated DM lasers that use optical injection. The wired OFDM signal used in this work is set to operate at 12.5 Gb/s. By deactivating a number of OFDM subcarriers in the wired band, a spectral notch is created which is subsequently used to carry either single or multiple 20 MHz bandwidth A-RoF signals carrying LTE services. This system's performance is evaluated for various relative power ratios of the wired/wireless signals. Additionally, the impact of Relative Intensity Noise (RIN) and laser nonlinearity on such a hybrid system is studied through computer simulations.

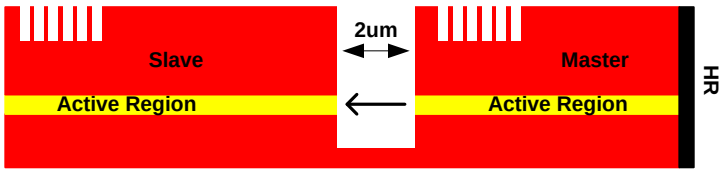

Figure 3.7. Physical structure of the two integrated DM lasers operating in master/slave configuration

3.4.1 Monolithically integrated device

Giving the complexity of the setup, which involves optical injection, it is advantageous to use integrated devices when employing optical injection, as this will lead to a compact and simple transmitter module for PON systems. The realization of an integrated device incorporating optical injection has been previously studied [11, 165]. This integrated device has two DM lasers, and it operates in a master-slave configuration. Such integration allows for all photonic coupling to occur within a common substrate, where all functions are confined to one operating device [5]. This provides a cost effective device with a small footprint and eliminates issues such as polarization dependencies and lower power budgets (which is usually attributed to coupling losses). The structure of the dual section laser used here is presented in Figure 3.7. The device is a ridged waveguide laser with a ridge width of 2.5 μm. The ridge and index perturbation were created with standard etching techniques used to fabricate Fabry-Pérot ridge waveguide lasers. The laser cavity is 700 μm and is divided into two sections (slave/master), each being a ridged waveguide laser with index perturbations, as shown in Figure 3.7. The slave section is 400 μm in length and the master is 300 μm [165]. The two sections are separated from each other by a 2 μm deep etched trench. This isolation allows each section to be biased independently. Etching such a slot, between the cavities, provides optical feedback in the device, which potentially sets up

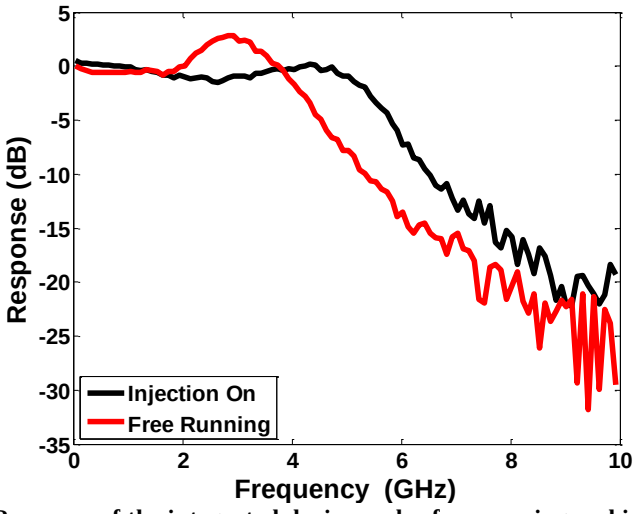

Figure 3.8. Response of the integrated device under free running and injected regimes

further unwanted optical cavities. To limit the impact of reflections on the optical performance of the device, the slots were etched at an angle of approximately 7° relative to the waveguide structure. The additional etched features created on each section's ridges restrict the optical gain to a single operational mode, enforcing single mode operation in that particular section [5]. The lasing frequency of each section is controlled through its temperature and bias current, for this work we kept a constant temperature for both sections and chose 30mA and 22mA respectively for slave and master sections of the integrated device. This bias setting, which resulted to the modulation responses shown in Figure 3.8, leads to the resonance peak appearing at 2.9 GHz in the free running case, 4.5 GHz in the injected case.

3.4.2 In-band wireless integration for OFDM-PON

Along with the evolution of PON's, there is an increasing demand for wireless access with a greater bandwidth offering. An approach to meet this demand is to miniaturize the wireless cell size in order to increase network capacity. However this approach gives rise to high cost backhauling requirements [166]. With the increasing deep penetration of PON infrastructure into users' premises, A-RoF can be realized by placing low-power remote antennas at the ONU's. This design is cost effective as it reduces hardware complexity since base stations with long reach are not required. As it was investigated in the previous chapter, much work had been carried in exploring the possibility of integrating A-RoF in the PON environment. From a multiplexing point of view, WDM-PON offers much flexibility for integration of RoF services by offering a dedicated wavelength for the transport of narrowband Radio signals for each antenna [119]. However, such designs results in high costs as the system will require sources with dedicated wavelengths at each ONU and multiple receivers at the OLT. Furthermore, the number of wavelengths increases in proportion to the number of wireless cells and wired serviced points. For the simultaneous support of mixed wireless and wired services on one optical wavelength, other approaches use high-frequency subcarriers to transport the RF signal, while wired data remains in the baseband [167]. This method successfully integrates both signals at the expense of high frequency components due to the required guard band between the baseband and RF signals. In other applications, the need for high frequency components as a result of employing guard bands is eliminated, with the help of highly spectral efficient modulation formats [2, 135]. But in these approaches the baseband data-rates are limited as further increases cause a reduction in the guard-band between them and RF bands, which forces the system designer to reallocate the RF signal to a higher IF band.

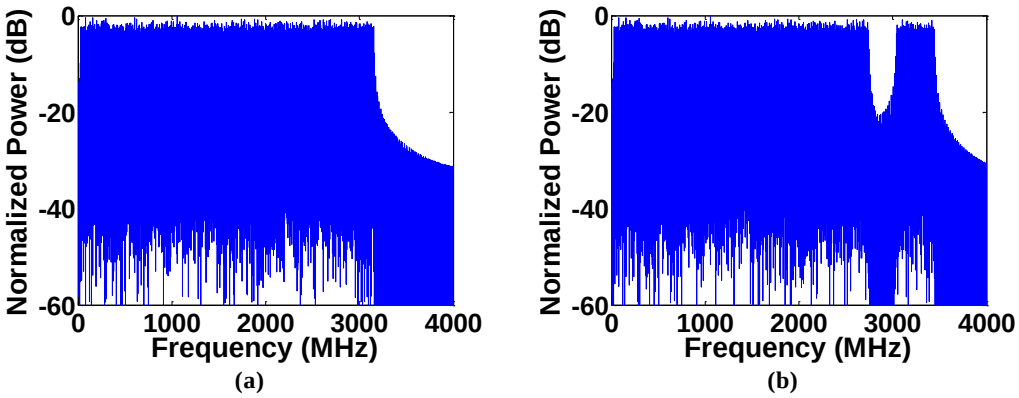

Figure 3.9. Electrical Spectrum of a OFDM signal operating at 12 Gbps (a) Without (b) With deactivated subcarriers

One inherent property of MC systems such as OFDM is the independent operation of each subcarrier. In these systems, each separate subcarrier can be allocated a different QAM format and a different power level without effecting neighbouring subcarriers. Interestingly, individual subcarriers can also be turned off; this de-activation of subcarriers is carried by nulling individual inputs to the IFFT block that coincide to frequencies of interest. This affects the system only by reducing the available net data rate in a given bandwidth, and it spectrally manifests itself as a spectral notch in the continuous OFDM band. These spectral notches can benefit hybrid wired/wireless OFDM-PON architectures that are carrying A-RoF services. In an OFDM-PON the wired band can extend from close to DC to several GHz, depending on the data rate and hardware employed. Creating spectral nulls in the wired OFDM band's spectrum at the A-RoF operating frequencies through the de-activation of individual subcarriers allows for A-RoF signals to co-exist with the wired band on a single shared wavelength without suffering from the impact of interference.

Figure 3.9 (a) presents the electrical spectrum of an OFDM band with 160 subcarriers, delivering 12.5 Gbps. As it can be seen, it will not be possible to incorporate any A-RoF bands below 3 GHz due to the potential for high interference with the wired band. Figure 3.9 (b) presents a case where 15 subcarriers around 2.9 GHz were deactivated this resulted to a spectral notch with a bandwidth of 290 MHz. This spectral notch can subsequently be used for accommodation of A-RoF services. This scheme provides a flexible architecture for integrated wired/wireless networks since the wired band can be reconfigured easily to create spectral notches with an arbitrary bandwidth at various frequencies.

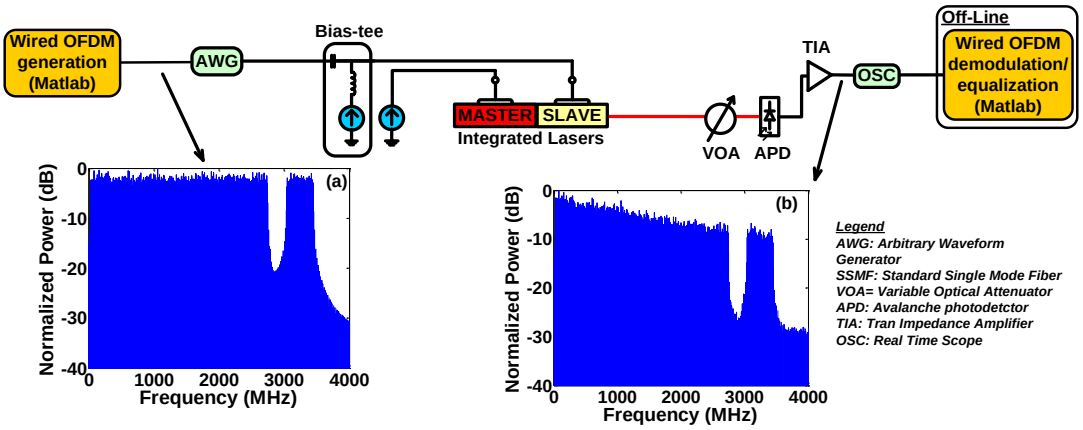

Figure 3.10. Experimental setup of the wired OFDM-PON, (a) Generated electrical spectrum (b) received electrical spectrum

3.4.3 Wired OFDM-PON

3.4.3.1 System Setup

In this section, the performance of a directly modulated wired OFDM system is evaluated. The laser that was presented in section 3.4.1 is employed in this work, and it is operated with/without injection locking. Figure 3.10 shows the full experimental setup that was used, the goal of this setup is to evaluate the overall impact that the transmitter and receiver have on the performance of the wired band in the presence and absence of optical injection, thus the fibre transmission is excluded from this setup. The generated wired OFDM signal occupied a bandwidth of 0.04~3.4 GHz as shown in the inset (a) of Figure 3.10 (parameters used to create the OFDM signal are listed in Table 3.1). This signal had an IFFT size of

Parameter	Value
Sampling rate	10 GSa/s
IFFT size	512
No. of active subcarriers	160
Modulation format	16 QAM
Frequency spacing	~ 20 MHz
No. of nulled subcarriers close to DC	2
Hermitian symmetry	Yes
Training sequence length	1 OFDM symbol
Number of OFDM symbols per frame	7000
Windowing	No
CP overhead	1.56 %
Total number of QAM symbols per frame	1120000
No. of frame transmitted per evaluation	10
Net data rate	12.5 Gb/s

Table 3.1. Parameters used for the wired OFDM signal

512, and the 160 subcarriers used for data transmission were encoded with 16 QAM symbols. The use of large IFFT blocks is required in OFDMA topologies for provision of high granularity in the available bandwidth. This high granularity allows for the precise control of bandwidth, which is allocated to the end users and the incorporated spectral notches. The extra 352 unused IFFT points out of the 512, were used to demonstrate the possibility of a gradual increase in the number of supported ONU's and their relative bandwidths by the activation and assignment of these unused subcarriers, this approach eliminates the need for major upgrades in transmitter and receiver ends. The sampling rate was set at 10 GSa/s resulting in a net data rate of 12.5 Gb/s. A Cyclic Prefix (CP) with 6.25% overhead was used which is sufficient to overcome dispersive effects of fibre lengths that will be used in this chapter. Since the laser diode is directly modulated, the wired signal was created using Hermitian symmetry [66] which resulted in 'real' valued waveforms. During the assignment of data to

the subcarriers, 15 IFFT inputs were intentionally nulled to create a spectral null with a bandwidth of approximately 290 MHz centred at 2.9 GHz (as shown in the inset (a) of figure 2) in order to accommodate for RoF services.

Following the generation of the values for the samples for the wired OFDM signal in Matlab, it was then sent to the AWG, whose output was used to directly modulate the slave laser. The experimental parameters used in this experimental setup are listed in Table 3.2. The resulting optical signal was detected with an Avalanche Photodetctor (APD), which was packaged with a trans-impedance amplifier. The APD was biased to results into an M-factor or multiplication factor of three, higher used M-factors will degrade the SNR and bandwidth of the device. The received electrical signal (as shown in inset (b) of

Parameter	Value
AWG used	AWG7122C
DAC sampling rate	10 GSa/s
DAC resolution	8 bits
Drive voltage	0.8 Vp-p
Master DM section bias	22 mA
Slave DM section bias	30 mA
3dB bandwidth before optical injection	4.3 GHz
3dB bandwidth after optical injection	5.5 GHz
APD used	Oclaro AT10XGC
M-factor APD	3
DSO used	Tektronix DPO71254B
ADC sampling rate	25 GSa/s

Table 3.2. Experimental parameters employed

Figure 3.10) was then routed to a Real Time Scope (RTS) for analogue to digital conversion. Subsequent digital signal processing was undertaken offline in Matlab.

To assess the enhancements that can be achieved by using optical injection with the integrated device, the performance of the system was evaluated by transmitting the OFDM signal using the directly modulated laser diode under free running (master laser section turned off) and injected (master and slave laser turned on) conditions. The directly modulated laser was driven under conditions that were presented in section 3.4.1. The frequency response of the laser with and without injection is also presented in Figure 3.8. In the free running case, the resonant peak appears at 2.9 GHz. This peak is a clear indication of frequencies at which laser nonlinearities are observed. These nonlinearities can severely degrade the performance of the wired OFDM. This degradation in performance is due to the intermixing of subcarriers, which generates new interfering frequency components such as third order intermodulation products. Optical injection from the master section can be used to move the nonlinear region of the laser to higher frequencies beyond those that are used for the wired and wireless transmission; this can reduce the nonlinear effect at the frequencies of interest and enhance overall performance. As can be seen in Figure 3.8, upon application of optical injection the resonance frequency is shifted to 4.5 GHz.

3.4.3.2 Experimental Results & Discussions

Figure 3.11 shows the performance of the wired signal in terms of average Error Vector Magnitude (EVM) per subcarrier for the laser diode with/without optical injection from the master laser where the average received optical power is set to -18dBm. Comparisons of the two graphs shows a severe penalty for the free running case especially at higher subcarriers where the signal sits close to the resonance peak as shown in Figure 3.8 (as the nonlinearity is largest at these frequencies). This performance degradation mainly results

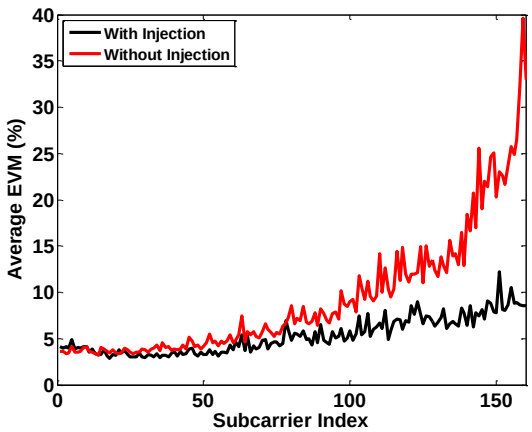

Figure 3.11. Average EVM per subcarrier for the wired OFDM band, with/without optical injection

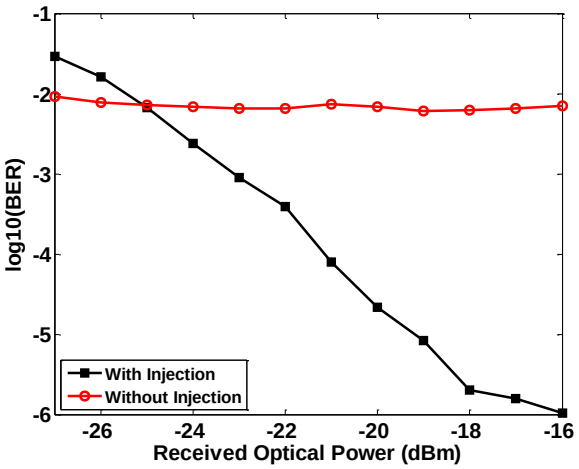

Figure 3.12. Received optical power versus log10(BER)

from interference caused by intermixing of OFDM subcarriers as a result of nonlinearities in the laser cavity. As mentioned previously, optical injection from the master laser can be used to shift the relaxation oscillation frequency of the slave laser beyond the frequencies used for data transmission, thus reducing laser nonlinearity and enhancing the system performance, as is also visible in Figure 3.11. These enhancements present themselves as a reduction in EVM values of the higher subcarriers.

The performance of the wired signal in terms of BER with respect to received optical power was then evaluated while operating the laser diode with/without optical injection and the results are plotted in Figure 3.12. It should be noted that each transmitted frame consisted of 7000 OFDM symbols, where to increase the confidence level, at the receiver 10 consecutive frames are evaluated to study the performance of the system in terms of BER or EVM. The system with the free running laser displays an error floor close to 10^{-2} for all received powers, and this degradation can be attributed to the nonlinearities present in the laser. Correcting for these device shortcomings using optical injection can result in significant performance gains as evident in Figure 3.12.

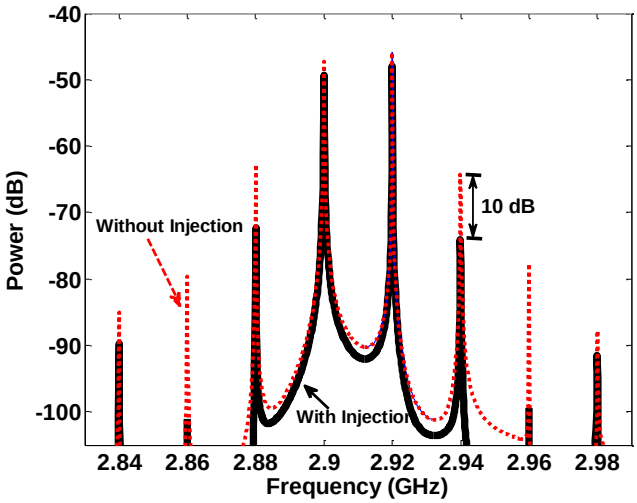

Figure 3.13. Simulated two tone test for the directly modulated laser with/without injection

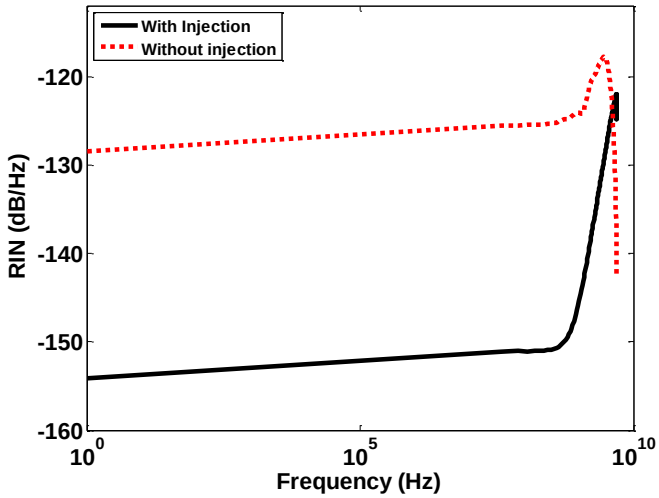

Figure 3.14. Relative Intensity Noise (RIN) of the laser transmitter with/without injection

3.4.3.3 Simulation studies & Discussions

In order to evaluate the degree of impairment that laser nonlinearity and RIN have on the performance of the OFDM signals used in this work, the setup shown in Figure 3.10 was modelled in Matlab. The laser model employed in these simulations was based on standard laser rate equations with injection parameters to describe the optical injection process [168]. To evaluate the impact of spur signals created as result of nonlinearity present in directly modulated lasers, a two tone test is carried via simulations by placing the fundamental tone at ω_1=2.9 GHz and the second tone at ω_2=2.92 GHz. The 20 MHz spacing between the two test tones reflect the subcarrier spacing we used in the wired OFDM band. The third order Intermodulation Products (IMPs) are of interest here as they lie close to the original subcarriers and might interfere with other subcarriers. Figure 3.13 presents the third order IMPs at $2\omega_1 - \omega_2$ and $2\omega_2 - \omega_1$ for cases with/without optical injection used. As the trend in this figure shows, employing optical injection results in the reduction of the third order IMPs by 10dB. Thus, optical injection can reduce the nonlinear degradation on directly modulated OFDM signals. In Figure 3.14 the simulated RIN profile of the laser with/without injection is demonstrated, where the reduction of RIN through optical injection [10] and amplification of RIN in the vicinity of resonant peak is clearly demonstrated.

3.4.4 Hybrid wired/wireless OFDM-PON

3.4.4.1 System Setup

To study the performance of the hybrid wired/wireless system, an A-RoF signal is introduced to the OFDM-PON systems described in the last section. The aim of this

Parameter	Value
Sampling rate	30.72 MSa/s
IFFT size	2048
No. of active subcarriers	1022
Modulation format	16 QAM
Frequency spacing	15 KHz
RF frequency	2.9 GHz
Training sequence length	1 OFDM symbol
Number of OFDM symbols per frame	4
Windowing	No
CP overhead	Normal CP
Total number of QAM symbols per frame	4088
No. of frame transmitted per evaluation	10
Net data rate	~ 60 Mb/s
Bandwidth	~ 20 MHz

Table 3.3. Parameters used for the wireless OFDM signal

experimental setup is to evaluate the performance of the proposed hybrid wired/wireless OFDM PON system in terms of the interference experienced form each band and the impact of device nonlinearity and RIN on performance. This wireless signal operated at 2.9 GHz and was configured to emulate an LTE signal (the parameters used to generate this signal are listed in Table 3.3). The generated wireless signal had an IFFT size of 2048, sampling rate of approximately 30.72 MSa/s, and a subcarrier spacing of 15 kHz. Normal CP (as defined in 3GPP standards) is used [169], and the 1022 data carrying subcarriers are encoded with 16 QAM symbols. This RoF signal was also generated in Matlab and was subsequently added to the wired OFDM signal that was programmed into the AWG. The operating frequency of the LTE signal coincides with the spectral notch created in the wired band (inset (a) Figure 3.15). To achieve Electro-optical conversion, the output of the AWG is used to directly modulate the slave laser. The resulting optical signal is transmitted through 50 km of fibre and is detected with an Avalanche Photodetector which is packaged with a trans-impedance amplifier. The received electrical signal (as shown in inset (b) of Figure 3.15) is then routed to a real time scope for analogue to digital conversion, and subsequent digital signal processing is undertaken offline in Matlab.

Prior to processing of the wired signal in DSP, the wireless signal needs to be rejected by filtering in order to eliminate its interference on the wired band. In this test-bed, notch filtering was employed to reject the LTE bands. A drawback associated with implementing the notch filter at the operating region of the wireless signals is that the sidelobes of the nearby wired subcarriers are suppressed: resulting in a loss of orthogonality between these subcarriers and other subcarriers in the wired OFDM signal. A Butterworth notch filter

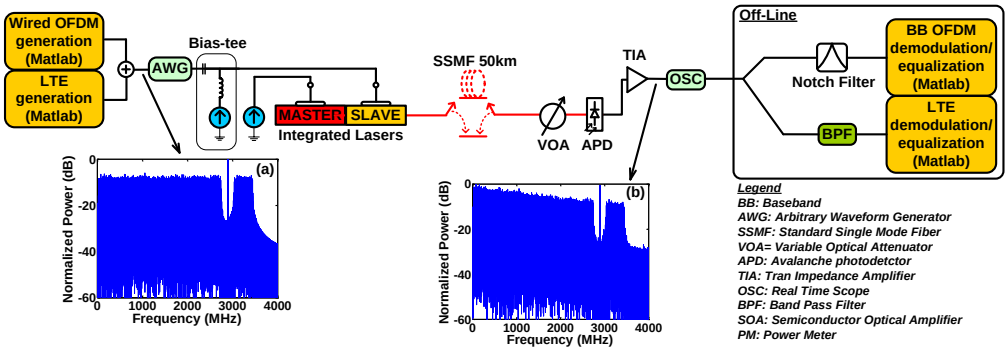

Figure 3.15. Experimental setup of the hybrid wired/wireless OFDM-PON with one A-RoF band. (a) Generated electrical spectrum (b) received electrical spectrum

with 400 taps was used in the experimental work to reject the wireless signal before processing the wired signal. The large number of taps used here for the notch filter helped to achieve nearly perfect rejection of the LTE signal with minimum amount of interference to wired band. Similarly, to isolate the received LTE band for processing it is filtered from the wired band by a four-tap Chebychev bandpass filter centred at 2.9 GHz.

Since two different electrical bands are sharing a common modulator, consideration must be taken as to relative power levels of the wired and wireless signals. This factor creates a trade off in performance of the wired and wireless signals, in terms of the interference they experience from one another due to their overlapping side lobes, resilience to noise and level of nonlinearity they experience. Here we use the average power in each signal to express the Wired-to-RF Power Ratio (WRPR) which is defined as

$$WRPR = \frac{average\_power(wired\_OFDM)}{average\_power(wireless\_OFDM)} \tag{3.14}$$

WRPR was tuned by varying the average power in wireless_OFDM with respect to the average power in wired_OFDM band, the resulting composite signal was then scaled to a predetermined drive level at the output of the AWG for all various test scenarios. The scaling of the composite signal results in a change in average powers in both bands, which in turn leads to SNR variation in both.

3.4.4.2 Experimental Results & Discussions

Figure 3.16 shows the performance of the wired signal under various WRPR levels in a back to back scenario, where the laser diode operated with injection from the master laser. The optical injection allows the system to operate under weaker influence from laser nonlinearity. As the figure suggests, the performance of the wired signal improves as WRPR increases, indicating a decrease in the level of interference received from the wireless bands. As the WRPR is increased beyond 12 dB the increase in performance of the wired signal is no longer significant as the interference from the wireless signal becomes

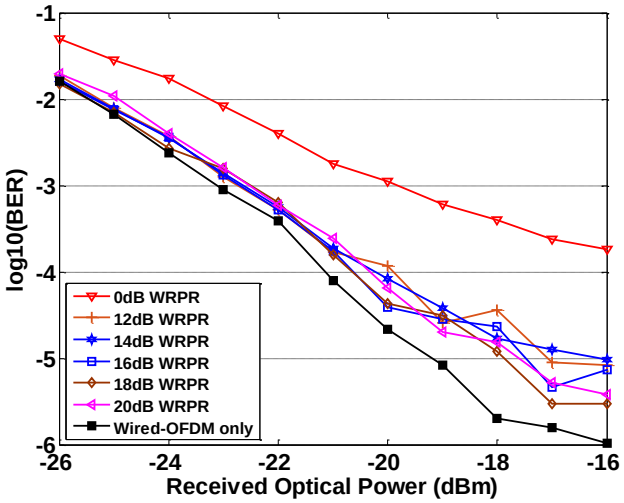

Figure 3.16. Performance of the wired band in the hybrid system in terms of log10(BER) vs Received optical power

negligible. The inclusion of the wireless signal introduces some level of degradation. This degradation accounts for approximately 0.5-1 dB of penalty at BER of 10^{-4} for WRPRs between 12-20 dB and a penalty of greater than 5dB at 0dB WRPR.

The performance of the in-band LTE signals in terms of Error Vector Magnitude (EVM) for various WRPR ratios is also illustrated in Figure 3.17. The performances of this A-RoF signal with respect to WRPR follow a dissimilar trend as the wired band. In this case as WRPR decreases, the interference originating from the wired band decreases leading to lower EVM levels and better performance.

The performance of the wired signal at 16 dB was then evaluated for back to back and transmission through 50 km of SSMF while operating the laser diode with/without optical injection and the results are plotted in Figure 3.18. The system with the free running laser displays an error floor close to 10^{-2} for all received powers, for both back to back and fibre

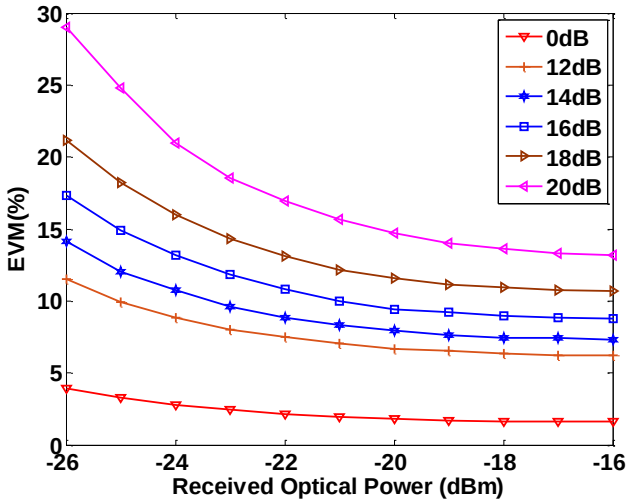

Figure 3.17.Performance of the wireless band in the hybrid system in terms of EVM vs Received optical power

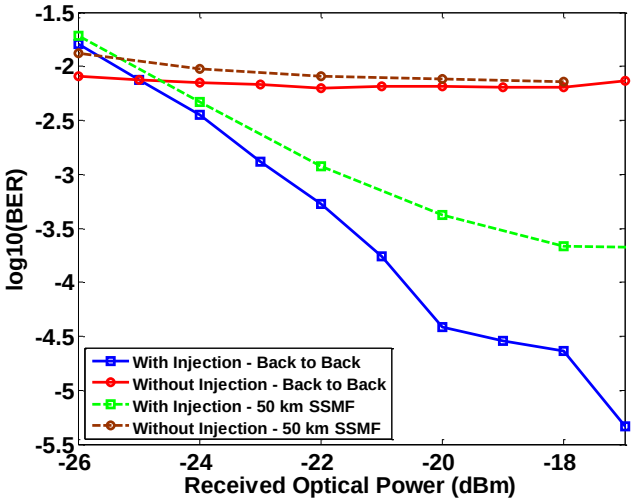

Figure 3.18. Performance of the wired band in terms of BER vs Received optical power at 16 dB WRPR

transmission scenarios. This degradation can be attributed to the nonlinearities present in the laser. Correcting for these device shortcomings using optical injection results in significant performance gains both for back to back and fibre transmission as evident in Figure 3.18. The difference in performance for the injected case with fibre transmission can be attributed to effects of dispersion in fibre.

The received LTE signal's performance was also evaluated and the results are presented in Figure 3.19**.** For the received optical powers shown, device nonlinearities prevent the signal from reaching the performance required for a 16 QAM LTE signal as recommended by 3GPP standards [169], but with the injection applied acceptable performance levels are achieved for received powers above -23dBm.

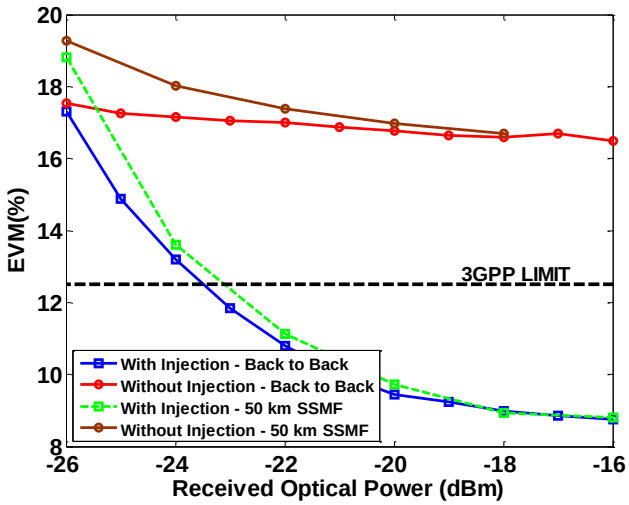

Figure 3.19. Performance of the LTE signal in terms of EVM vs Received optical power at 16 dB WRPR

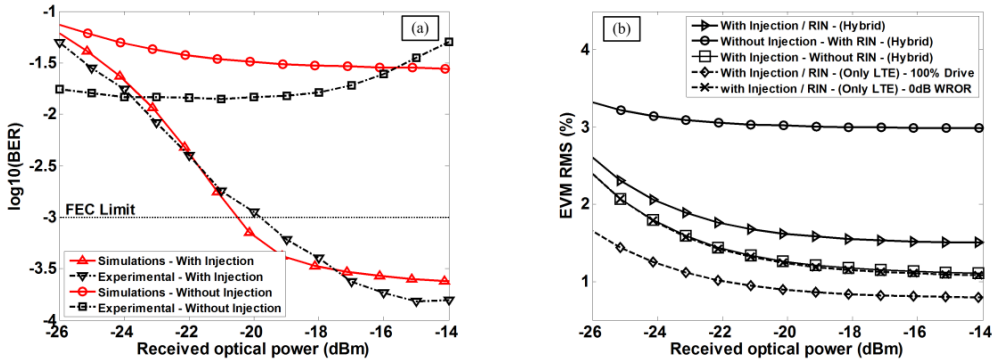

Figure 3.20. Simulated a) back to back performance of the wired signal at 0 dB WRPR (single LTE band), b) back to back performance of the wireless band at 0dB WRPR

3.4.4.3 Simulation Results & Discussions

Numerical simulations were also carried out on this system, in order to evaluate the degree of impairment that laser RIN and nonlinearity have on the performance of the composite OFDM signals used in this work. The drive current used for the laser device in these simulations was set to represent an electrical composite waveform containing 7000 wired and 4 LTE OFDM symbols. A system of coupled differential equations with/without injection representing the optical injection setup was then solved numerically using ODE solvers. Subsequently a model of an avalanche photo-detector equipped with a TIA along with expressions for thermal and shot noises as-well as dark current was used to convert the optical signal into electrical waveforms for demodulation and processing.

Figure 3.20 (a) presents the experimental and simulated results for the wired band with/without injection, in terms of BER versus received optical power. Simulation and experimental trends are shown to be in agreement for both cases where the laser was operated with/without optical injection. The results of various studies carried out for the wireless band are presented in Figure 3.20 (b). The interference from the wired band resulted in no significant changes in performance of the single LTE signal operating solely at the chosen WRPR, whilst driven by the same power level used for the wireless band in 0 dB WPRR. Scaling the LTE signal to the maximum available power level demonstrates the decrease in SNR which leads to an EVM enhancement to around 1%. No significant degradation is observed as a result of including RIN in an optically injected system, but the emergence of an error floor above 3% EVM is clear with the elimination of external injection, which is a result of additional nonlinearity in the system.

To analyse and separate the impact of RIN and nonlinearity on performance, the hybrid system was simulated under injected/non-injected scenarios along with/without the inclusion of RIN. By observing the simulated results for the wired band, shown in

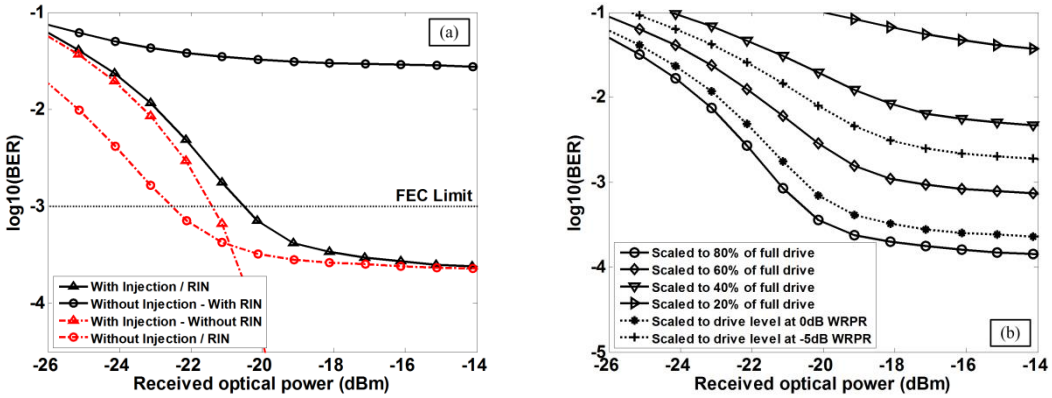

Figure 3.21. Simulated back to back performance of the wired band, a) at 0dB WRPR showing the impact of RIN and nonlinearity, b) with respect to relative drive levels and it's impact on SNR

Figure 3.21 (a), it is clear that the RIN in the injected case was responsible for the error floor at BER of $10^{-3.5}$, as excluding it results in the elimination of the error floor and enhanced BERs at lower received optical power levels. Next, the effect of nonlinear degradation on performance is shown for the scenario where neither RIN nor injection was employed. As the trend suggests, the interference created by nonlinearity in the un-injected case leads to the emergence of an error floor at BER of $10^{-3.5}$ for received optical powers above -17 dBm. The inclusion of RIN in the un-injected case further degrades the performance and results in an error floor at BER of $10^{-1.5}$ for average received optical powers above -20dBm.

The impact of intra-band interference due to WRPR modifications is presented in Figure 3.16. Variations of WRPR also impose SNR changes due to power variations in the operational bands. For instance, a reduction of WRPR leads to reductions in the wired OFDM band's average power levels which in turn reduce SNR, Figure 3.21 (b) illustrates the performance degradations obtained as a result of reducing power levels in the wired band whilst operating without any wireless signals present. Drive levels equal to those used in 0dB and -5dB WRPR scenarios along with signals scaled to 20-80% of full drive levels were used. The degradation of SNR with reduced WRPR presents itself as an increase in BER levels for the wired band.

To evaluate the impact of RIN, the performance of each individual subcarrier of the wired signal is assessed in the presence of RIN, and compared to that of the experimental results in Figure 3.22. Here, the average received optical power was set to -16 dBm for all scenarios. By comparing the simulated scenarios, with/without the presence of RIN, in Figure 3.22 (a) (where optical injection was used); it is noticeable that higher frequency subcarriers suffer more from the effects of RIN, as EVM increases from around 5% for lower frequency subcarriers to 20% at higher frequency subcarriers. This can be attributed to the increasing RIN as the subcarrier frequencies approach the resonant peak. Similarly

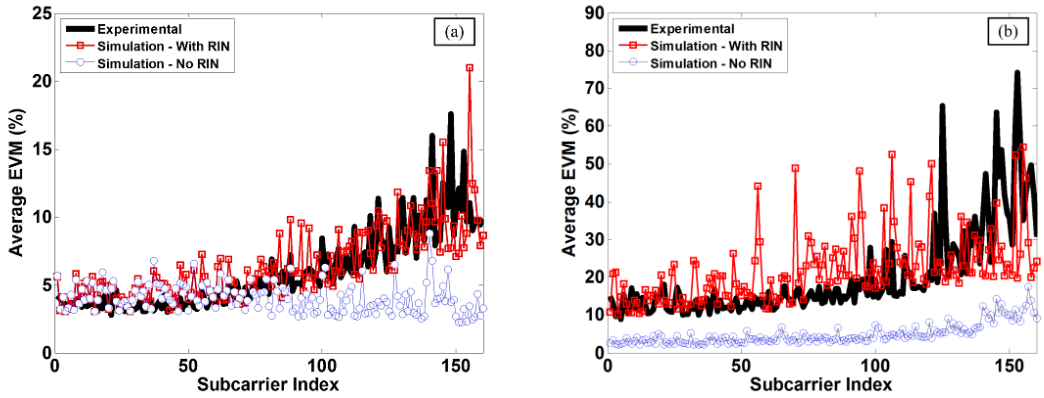

Figure 3.22. Back to back performance of the wired signal in terms of average EVM per subcarrier, (0dB WRPR, -16 dBm average received optical power), a) with injection from the master section, b) without injection from the master section.

the performance of the wired band operating with no optical injection (both experimental and simulation) is shown in Figure 3.22 (b). By contrasting simulation and experimental results, RIN is seen to have a greater impact on higher frequency subcarriers, with EVM increasing from approximately 15% on low frequency subcarriers to 45 % on higher frequency subcarriers in the case where no injection is used.

Nonlinear distortion in the region of the resonant peak was indicated as a source of performance degradation on multicarrier systems such as OFDM. The elimination of RIN in the simulation model used here, results in a system dominated mainly by the receiver's noise and nonlinear distortions. Comparing simulation results in Figure 3.22 (a-b), for scenarios where no RIN was applied, increased EVM values can be seen for subcarriers operating at higher frequencies. EVM extends to 20% in the non-injected case, and approximately 7% in the injected case. This increase in EVM is as a result of subcarrier intermixing which is due to the impact of laser nonlinearity on the OFDM system.

The accompanying LTE bands' performances are evaluated and presented in Figure 3.23. Good matches, between experiment and simulation can also be seen in the presence of RIN

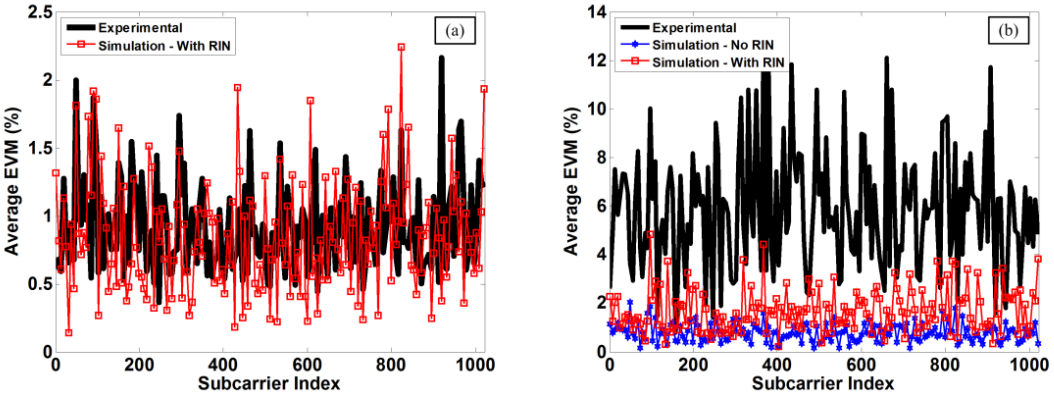

Figure 3.23. Back to back performance of the wireless signal in terms of average EVM per subcarrier, (0dB WRPR, -16dBm average received optical power), a) with injection from the master section, b) without injection from the master section.

when optical injection is employed (Figure 3.23 (a)). The wireless signal exhibits good performance, as expected in this case, with average EVMs below 2%, across all LTE sub carriers. The discrepancy between simulation and experimental results for the non-injected scenario (Figure 3.23 (b)), can be attributed to the laser model failing to accurately replicate the resonant peak or the nonlinear region of the free running laser correctly since standard laser rate equations where used rather than a detailed model of this novel device. Nevertheless, the simulation results do clearly show the performance enhancement of the wireless signal when injection is employed and when RIN is turned off. The combination of the experimental and simulation results clearly show that the performance of the directly modulated OFDM system is determined by both RIN and nonlinearity in the directly modulated laser.

Comparing the experimental trends in Figure 3.23 (a-b), the LTE signal has not been degraded significantly by nonlinearity, even though it operates at the nonlinear region. Without the inclusion of injection or RIN in the model, the EVMs achieved are very low, suggesting that the minor degradation is due to interference caused by nonlinearity. It should be recognized that even though the average power in both the wired and wireless bands is equal (0dB WRPR), the power per subcarrier in the wireless band is significantly lower compared to the wired band. This is due to the higher number of subcarriers in the wireless band. The limited power in wireless OFDM subcarriers operating at frequencies close to the resonant peak lessens the impact of nonlinearity, as compared to that experienced by wired band subcarriers.

The LTE band is also seen to be affected less significantly in the presence of RIN compared to the wired band (as can be seen in Figure 3.22-Figure 3.23) especially in the absence of optical injection. This is due to the small bandwidth of the LTE signal and its subcarriers. Each OFDM subcarrier in the wired band occupies a bandwidth of 20 MHz, compared to 15 KHz in the wireless band. The smaller bandwidth of LTE subcarriers suggest a reduced accumulation of RIN power per subcarrier, leading to less severe degradations.

3.4.5 Hybrid wired/wireless OFDM-PON with multiple A-RoF services

Typically in hybrid PON's adopting A-RoF a single wavelength may be required to provide services to multiple BSs. In this part we use the spectral notch that was created in wired OFDM PON's spectral content to carry three A-RoF signals carrying OFDM based LTE services.

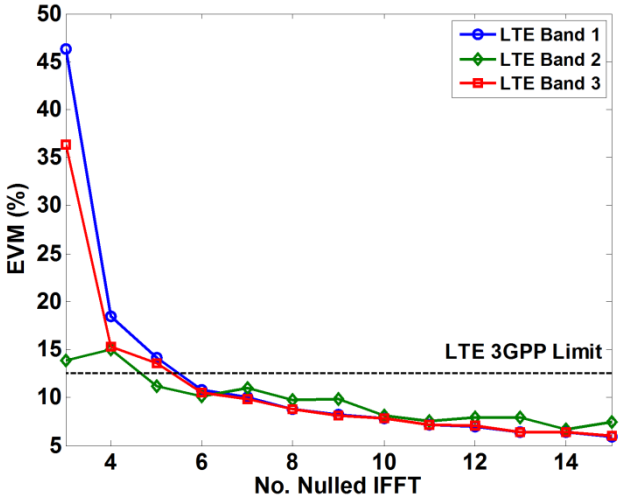

Figure 3.24. Electrical Back-to-Back performance of the wireless bands with respect to Number of nulled IFFT inputs

3.4.5.1 System Setup

The generated wireless signals were centred at 2.86/2.89/2.92 GHz. Each of the LTE signal take on parameters similar to that, which are listed in Table 3.3. Each LTE band had an IFFT size of 2048, sampling rate of approximately 30.72 MSa/s, and a subcarrier spacing of 15 kHz. Normal CP [169] was used for these LTE signals, and the 1022 data carrying subcarriers in each band were encoded with 16 QAM symbols. Due to availability of only one AWG, the wired and wireless bands were again added together electrically prior to the DAC, thus the composite waveforms from each band needed to match one another closely in time. The wired band in this section takes on a similar format as in the previous section. In the wired band, 15 IFFT inputs were again intentionally nulled to create a spectral null with a bandwidth of approximately 290 MHz centred at 2.9 GHz. De-activating less than 15 IFFT inputs results in a spectral null with a bandwidth smaller than 290 MHz, which necessitates the employment of higher order band-pass and notch filters with steeper roll offs at the receiver. Figure 3.24 shows the performance of the three LTE bands in terms of Error Vector Magnitude (EVM) for an electrical back-to-back scenario for various number of nulled IFFT inputs. In this illustration we used the same bandpass filter used in carrying out the rest of this work. As the figure suggests, reducing the nulled bandwidth results in deterioration of the wireless band's performance as result of interference from the wired band which had not been rejected by the bandpass filter, leading to EVM values above the level recommended for 16 QAM LTE bands by 3rd Generation Partnership Project (3GPP) [169].

Figure 3.25 represents the full experimental setup; the aim of this setup is to investigate the proposed hybrid system with multiple Of signals in presence of interbank interference as well as nonlinearity and RIN from the laser transmitter. The three uncorrelated LTE signals

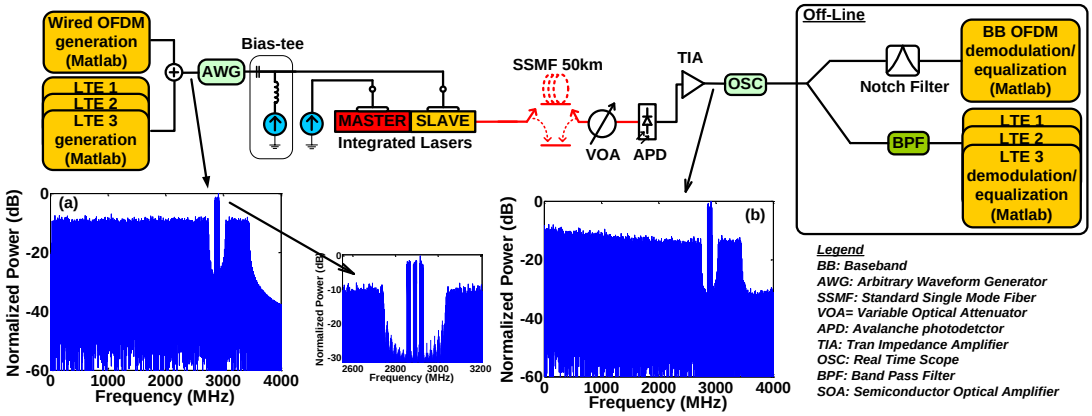

Figure 3.25. Experimental Setup. a) normalized spectrum of transmitted signal, b) normalized spectrum of received signal (laser with injection)

are added to the wired band prior to being loaded unto the AWG. The output of the AWG was then used to drive the slave section of the dual-section laser. The optically generated signal is then routed through 50 km of SSMF and is detected by an APD packaged with a TIA. The received electrical signal is then subjected to a notch filter and bandpass filter prior to the processing of the wired and wireless signals.

3.4.5.2 Experimental Results and Discussions

Figure 3.26 (a) shows the performance of the wired signal under various WRPR levels in a back to back scenario, where the laser diode operated with injection from the master laser. As the figure suggests, the performance of the wired signal improves as WRPR increases, indicating a decrease in the level of interference received from the wireless bands. As the WRPR is increased beyond 5 dB the increase in performance of the wired signal is no longer significant as the interference from the wireless signal becomes negligible.

The performance of the three in-band LTE signals in terms of EVM for WRPR values used in Figure 3.26 (a), is illustrated in Figure 3.26 (b). The performances of all three RF bands

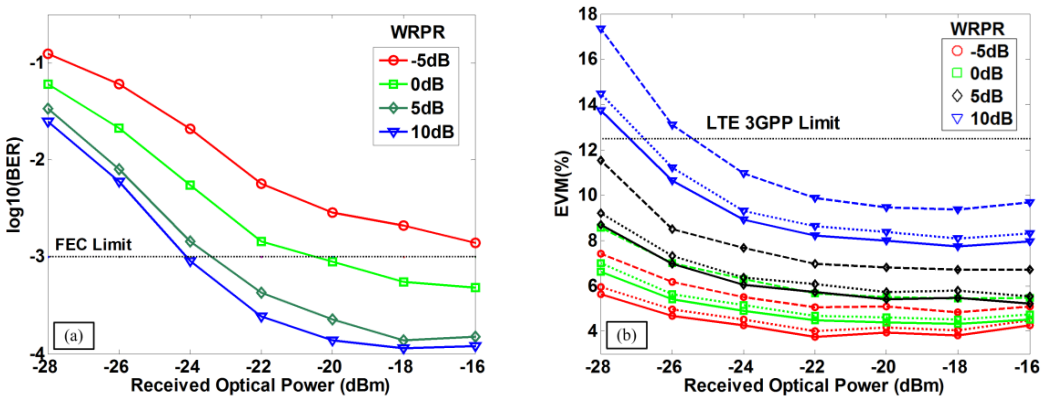

Figure 3.26. Back to Back performance of the a) wired signal with salve laser under optical injection, b) in-band LTE signals with slave laser under optical injection (lines: LTE band 1, broken lines: LTE band 2, dotted lines: LTE band 3)

in each case follow a similar trend. The reduction of interference experienced by the wireless signals can also be seen in Figure 3.26 (b) as the performance of the LTE channels increases as the WRPR is decreased.

Comparing Figure 3.8 and Figure 3.25 (inset (a)), it can be noted that for the free running laser, the wireless signals and part of the wired signal will operate in the vicinity of the resonant peak, and operating at these frequencies will cause the creation of spur signals as nonlinearities are largest at this region. The existence of Relative Intensity Noise (RIN) which is maximised at the vicinity of the resonant peak [9, 153]will also cause performance degradation in the non-injected case.

Results for the wired band in the presence and absence of fibre transmission, and optical injection, are plotted in (a) for the wired signal operating at 0 and 10 dB WRPR. The aforementioned shortcomings related to the free running laser (without injection) result in poor system performance, leading to an error floor for the wired signal above a BER of 10^{-2} as shown in figure Figure 3.27 (a). It is notable that operating at a WRPR of 10 dB results in approximately 4 dB of performance improvement compared to operating at WRPR of 0 dB, both for back-to-back and fibre transmission cases when the injection from the master laser is turned on. The difference in performance between the back-to-back and fibre transmission, in the injected case, can be attributed to dispersive fading which is due to the double side band nature of the transmitted signal [5]. Also shown in the same figure, performance levels below the FEC limit were achieved but only at received powers above -20 dBm, for both back to back and fibre transmission cases, operating at a WRPR of 0 dB. Interference minimization, attained by operating at higher WRPRs, can result in enhanced performance in the wired band, but this is traded off against poorer performance of the wireless signals, as stated previously.

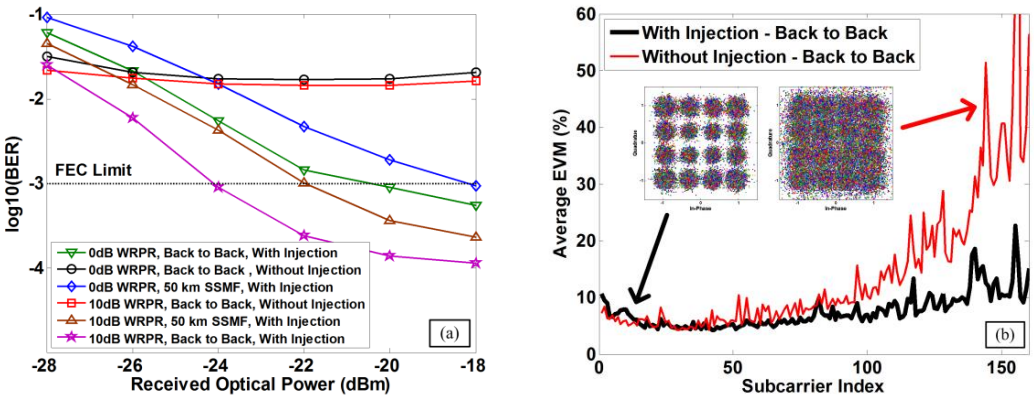

Figure 3.27. a) Performance of the wired signal for back to back and fibre transmission, and performance enhancement using optical injection., b) Average EVM per subcarrier for Wired signal at 0dB WRPR and -20dBm average received optical power.

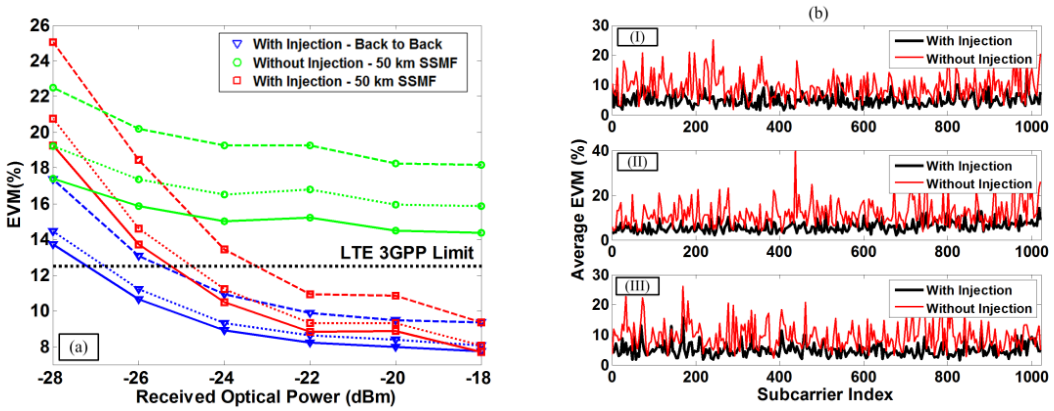

Figure 3.28. a) Performance of the three LTE bands, for back to back and fibre transmission, and performance enhancement using optical injection. (lines: LTE band 1, broken lines: LTE band 2, dotted lines: LTE band 3), b) Average EVM per subcarrier for wireless signal at 10dB WRPRP I) band 1; II) band 2; III) band 3

The degradations imposed by the free running laser are further demonstrated in Figure 3.27 (b), which presents the wired band's performance in terms of average EVM per subcarrier for the laser diode with/without optical injection, along with constellation diagrams. For 0 dB WRPR the average received optical power in this case was set to -20dBm. Severe penalties can be observed when injection is not employed, especially at higher frequency subcarriers where the signal resides close to the resonant peak. This performance degradation is contributed to, in part, by the effects of RIN and the interference caused by intermixing of in-band wired and out-of-band wireless (LTE) OFDM subcarriers.

The three wireless LTE signals' performances, were also evaluated for a WRPR of 10 dB with the results plotted in Figure 3.28 (a). For the case where the laser was operated without injection, it is clear that all three wireless signals failed to provide sufficient performance levels, as recommended by 3GPP [169], for 16 QAM LTE signals. This is due to the system degradations (RIN and nonlinearity), inherent to the free running laser, combined with the interference experienced from the wired band. By employing optical injection, system performance can be improved to well below the required EVM limit set

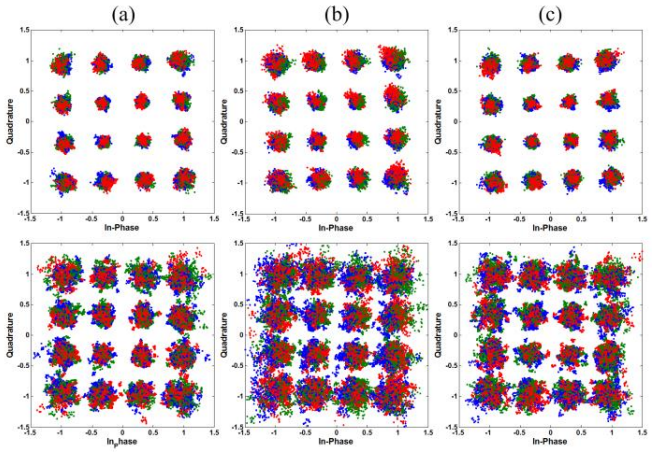

Figure 3.29. Constellation diagrams for the three wireless bands shown in figure 9. Top row with injection, bottom row without injection for a) band 1; b) band 2; c) band 3.

by 3GPP, both for back to back and transmission through 50 km of fibre.

The performance degradation of the wireless bands when injection is not employed, are further clearly outlined in Figure 3.28 (b), which shows average EVM per subcarrier, for 10dB WRPR and received average optical power of -20 dBm. Significant degradation to all 3 channels is apparent, whilst operating the laser without injection, with the average EVM residing around 18%. The figure also shows that the application of optical injection results in the improvement in performance of all three LTE sub-bands, with average EVM's reduced to around 7%. The constellation diagrams for the scenarios shown in Figure 3.28 (b) are plotted in Figure 3.29.

3.5 Discussions

Table 3.4 presents a brief summary of the key results obtained from the experimental setup, which assessed the performance of the hybrid system with one AoF signal only. As it can be seen either in Back to Back (B2B) case or transmission through 50 km of SSMF, the absence of optical injection can result in an error floor above the FEC limit for the wired band, however the application of injection, allows for the FEC limit ($1x10^{-3}$) to be reached at all WPRR ratios employed. The transmission of this hybrid signal over fibre under optical injection was further evaluated at 16 dB WPRR and it was found that the propagation through 50 km of SSMF resulted in approximately 1 dB of performance penalty. The in-band AoF signal also achieved an acceptable performance level up to 16 dB WPRR whilst operating under optical injection. As the results suggest, for the 16dB WRPR case the wireless signal performance is below the limit required for 3GPP when no optical

Signal (WRPR)	With injection (B2B)	Without injection (B2B)	With injection (50 km)	Without injection (50 km)
Wired Only	-23 dBm	Above FEC limit	-	Above FEC limit
Wired 0dB	-19.8 dBm	Above FEC limit	-	Above FEC limit
Wired 16dB	-22.65 dBm	Above FEC limit	-21.7 dBm	Above FEC limit
Wired 20dB	-22.55 dBm	Above FEC limit	-	Above FEC limit
Wireless Only	Below limit	-	-	-
Wireless 0dB	Below limit	-	-	-
Wireless 16dB	-23.5 dBm	Above limit	-23.1 dBm	Above limit
Wireless 20dB	Above limit	Above limit	-	Above limit

Table 3.4. Summary of experimental results from the hybrid system with one AoF signal, in terms of received optical power at which the FEC limit or the 3GPP limit was reached. (Below/above limit: performance at all received optical powers is below/above 3GPP limit. Above FEC limit: performance at all received optical powers is above the FEC limit)

Signal (WRPR)	With injection/With RIN	Without injection/With RIN	With injection/Without RIN	Without injection/Without RIN
Wired Only 0dB	-20.2 dBm	Above FEC limit	-20.8 dBm	-22.5 dBm

Table 3.5. Summary of simulation results from the hybrid system with one AoF signal, in terms of received optical power at which the FEC limit or the 3GPP limit was reached. (Above FEC limit: performance at all received optical powers is above the FEC limit)

injection is used, however optical injection can remedy this. Comparing the B2B and fibre transmission scenarios it was clear that only 0.4 dB of performance penalty was experienced by the wireless LTE signal.

Table 3.5 summarises the set of simulation results, which were used to study the impact of RIN and nonlinearity on the performance of the hybrid signal operating at 0 dB WRPR, along with the enhancement in performance achievable by optical injection. As is stated, the removal of optical injection and the emergence of higher RIN levels in low bandwidth laser devices results in BER levels above the FEC limit. However, the complete removal of RIN in simulations, such that the only deteriorating factor remaining is the device nonlinearity, leads to enhanced performance and the FEC limit is achieved at -22.5 dBm. Thus, the excess nonlinearities experienced in the non-injected case only account for 2.3 dB of performance degradation; whereas the RIN in the non-injected case is responsible for the majority of performance deterioration observed causing an error floor above the FEC limit. The effect of lower levels of RIN in the injected case are also determined by eliminating the RIN in simulations, such that according to Table 3.5 the RIN only account for 0.6 dB of performance deterioration in the injected case.

Table 3.6 summarises the experimental results obtained from the hybrid system containing

Signal (WRPR)	With injection	Without injection	With injection (50k)	Without injection (50k)
Wired Only	-23 dBm	Above FEC limit	-	Above FEC limit
Wired -5dB	Above FEC limit	Above FEC limit	Above FEC limit	Above FEC limit
Wired 0dB	-20.5 dBm	Above FEC limit	-18 dBm	Above FEC limit
Wired 5dB	-23.6 dBm	Above FEC limit	-	Above FEC limit
Wired 10dB	-24 dBm	Above FEC limit	-22 dBm	Above FEC limit
Wireless -5 dB	Below limit	-	-	-
Wireless 0dB	Below limit	-	-	-
Wireless 5dB	Below limit	-	-	-
Wireless 10dB	-27.3 / -25.8 / -25 (dBm) *(band 1/2/3)*	-	-25.2 / -23 / -24.4 (dBm) *(band 1/2/3)*	Above limit

Table 3.6. Summary of simulation results from the hybrid system with three AoF signals, in terms of received optical power at which the FEC limit or the 3GPP limit was reached. (Above FEC limit: performance at all received optical owners is above the FEC limit)

three AoF signals carrying LTE services. Again, without injection the wired signal reaches a BER error floor above the FEC limit in both B2B and 50 km transmission case. In the injected case, the interference also leads to an error floor in the wired band for WRPRs at and below -5 dB. However, reasonable performance is achieved for WRPRs above 0 dB WRPR, both for B2B and 50 km transmission scenario, with approximately 2–2.5 dB performance penalty experienced as result of propagating through 50 km of fibre. The performance of the wireless signal was analysed in B2B for the injected case for WRPRs ranging between -5dB to 10 dB, for all the received optical powers analysed, and the performance levels achieved were below the 3GPP limit. The results also suggest that, with the propagation through 50 km of SSMF, the three in-band LTE signal at 10 dB WRPR were capable of achieving the required performance, with a maximum penalty of 2.8 dB compared to the B2B case.

3.6 Summary

The integration of wireless services in future PON infrastructures is a beneficial approach as it has the ability to meet ongoing demands of the end user for higher bandwidths. Using OFDM based modulation formats for wired services in hybrid PON's provides high spectral efficiencies. This factor allows the use of cost effective, low bandwidth components in the transmission link. Replacing external modulation techniques with direct modulation is a highly cost effective solution for PON's, but the nonlinearity and noise mechanisms such as RIN in low bandwidth laser transmitters can severely limit the performance of directly modulated OFDM signals. The multicarrier nature of OFDM can allow for individual control over operational subcarriers. It was shown that by deactivation of a number of subcarriers it is possible for in-band A-RoF wireless signals to co-exist with wired OFDM signals in a common spectral band.

In this chapter through experiment and simulations, it was demonstrated that the use of optical injection in an integrated device could enhance the performance of a directly modulated hybrid wired/wireless OFDM systems by reducing the effects of device nonlinearity and RIN at the operating frequencies of interest. The transmission systems was comprised of a wired OFDM signal delivering 12.5 Gb/s, accompanied by either one or three 20 MHz bandwidth LTE signals. By the employment of optical injection, the relaxation oscillation frequency of the directly modulated laser employed was enhanced by 1.6 GHz. This allowed for considerable reduction in distortion originating from the nonlinearity and RIN of the device. The experimental results showed the emergence of

error floors approximately at BER of 10^{-2} for the wired band and 17 % EVM for the wireless LTE band, in back to both back and 50 km fibre transmission scenarios as a consequence of nonlinearity and RIN in the device. Upon the application of optical injection, the error floors were eliminated and the trends show that the BER of 10^{-3} for the wired band and the EVM of 12.5 % for the LTE band was reached at -23 and -23.5 dBm of average received optical power accordingly, for a system operating at 16dB WRPR. Inclusion of 50km fibre transmission in this optically injected system resulted to approximately 1dB performance penalty at BER of 10^{-3} for the wired system and approximately 0.5 dB of penalty for the wireless band at the EVM level of 12.5 %.

Chapter 4

Line Coding Techniques in Hybrid Wired/Wireless PONs

This chapter starts by providing a general and brief overview on line coders with DC balanced and minimum bandwidth properties. Subsequently a system of interleaved 8B/10B encoders with a DC balanced property, and a system of MB810 encoders with both DC balanced and minimum bandwidth properties are used to form multiple notches in a 10 Gb/s OOK signal representing the wired band in a PON system for the accommodation of a single A-RoF band delivering LTE services. Furthermore experimental and simulation results are provided to show performance gains possible as function of encoding, encoding order and power ratios between the wired and wireless signals sharing a common transmission wavelength.

4.1 Introduction

The insertion of one or more spectral notches in the wired service's operational band was seen as a potential approach for the accommodation of Analogue Radio over Fibre (A-RoF) services [98]. These spectral notches create the basis for a Passive Optical Network (PON) infrastructure that enables the simultaneous coexistence of wired and wireless services, by creating a transparent medium for the transport of A-RoF services in PON architecture. In

such a scenario, the A-RoF band is not required to be shifted to an IF or baseband in order to minimize inter-band interference between the wired and wireless signals, thus a filter, amplifier and antenna are only needed on the physical layer at the receiver side for wireless transmission.

As was mentioned in earlier chapters, standardized PON technologies employ single carrier OOK modulation schemes at line rates up to 10 Gb/s per wavelength channel. The establishment of currently standardized PON systems around TDM and On-Off keying (OOK) [42], motivates our interest in the methods for creation of spectral nulls in such On-Off keyed serial channels for in-band accommodation of wireless services. The solution proposed here uses the concept of line coding that is commonly used to shape the spectrum of digital single carrier systems. Here we will investigate the use of such line coding techniques to create spectral notches in the PON baseband spectrum for the accommodation the A-RoF signals.

In digital transmission of binary signals, the power spectrum of the pulse train can be shaped through the introduction of redundancies. Usually in so doing, the amplitude of the spectrum can be made small near certain frequencies. One frequency commonly chosen is DC [15], which leads to line codes identified to have a DC balance property. In this chapter we assume OOK as the modulation format for the PON and make use of DC balanced encoders such as 8B/10B and MB810 which have a minimum bandwidth property, to create one or more notches in the spectrum of the OOK data stream operating at 10 Gb/s by interleaving the encoders. Furthermore, one of these notches is then used for the transmission of a single wireless band, delivering Long Term Evolution (LTE) services. The performance of this system is studied for various power ratios between the wired and wireless signals and encoding orders through experiments and numerical simulations.

PON standards already make use of DC balanced coding schemes to enhance their overall system performance. Standards such as GE-PON and 10 GE-PON, make use of coders such as 8B/10B and 64B/66B [42]. Thus, the pre-existence of DC-balanced line encoders, in PONs, makes the creation of in-band notches feasible, with alterations required only to the encoding scheme.

The work presented in this chapter looks at possible means for the creation of in-band spectral notches in OOK based PON systems. In this work, these notches are created through the employment of various line encoding schemes. The work undertaken in this chapter for the first time looks at the employment of line encoding schemes for the creation of such spectral notches in TDM-PONs which are subsequently used to accommodate for Analogue over Fibre (AoF) signals carrying LTE services. This work also for the first time,

employs a new class of encoders called MB810 for the creation of in-band spectral notches in OOK based TDM-PONs.

4.2 Encoding

Various line-coding techniques may be used to alter the properties of a signal's spectrum by rearranging its binary sequence. In fibre optic communications, it can be advantageous to use line codes that suppress the DC component, as they can aid clock recovery at the receiver [170], and also help to eliminate data dependent heating in the laser diode [171]. Such codes are called DC-free or DC-balanced codes.

To fulfil the DC-free condition, the coding scheme needs to produce a sequence that takes finite values for its inherent Running Digital Sum (RDS) at DC [18], which is defined as

$$RDS_{DC}(\boldsymbol{\alpha}) = \sum_{l=0}^{N} \alpha_l \tag{4.1}$$

for the code string $\boldsymbol{\alpha} = \{a_0, a_1, ..., a_N\}$, where the individual elements in $\boldsymbol{\alpha}$ represent binary data and appropriate values were chosen to represent the coded symbols in this subset [17, 172]. There are numerous NB/MB line coders that transform N bits of data to M specific bits that can satisfy the DC free condition. Some of these coders namely are 8B/10B, 5B/6B, 7B/8B and 9B/10B, and in order to maintain certain coding properties, the M code strings are predefined [173]. 8B/10B is capable of achieving the highest reduction in low frequency components among other stated NB/MB coders [173], this is mainly due to the stringent requirements imposed on this coder [174]. The elimination of the low frequency components with the help of 8B/10B encoding is presented in Figure 4.1 for an OOK signal operating at 10 Gb/s.

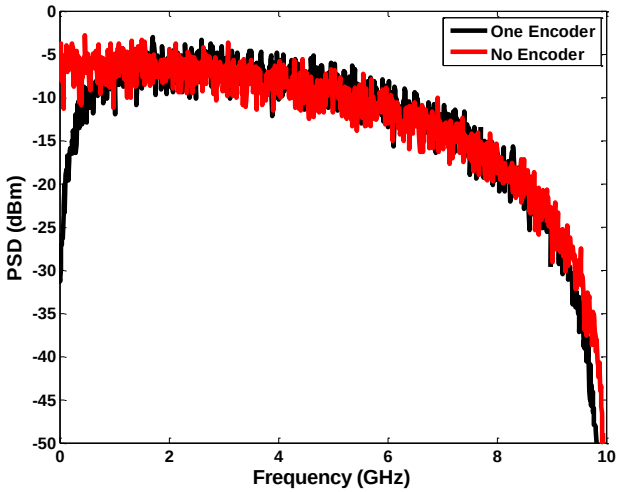

Figure 4.1. Electrical spectra of a 10 Gb/s OOK signal with/without 8B/10B encoding

Initially motivated by insertion of in-band pilot tones, the concept of finite RDS at DC can be extended to passband frequencies, in which the sequence $\boldsymbol{\alpha}$ requires finite values for its RDS at $f = kf_s / n$ [16, 18], with f_s being the symbol rate, and where RDS at f is defined as

$$RDS_f(\boldsymbol{\alpha}) = \sum_{l=0}^{N} \alpha_l e^{-i2\pi kl/n} \tag{4.2}$$

Various coding methods can be used to achieve single or multiple in-band notches [13, 16], but it has been shown that a null can be produced at f_s / m, and its harmonics, by demultiplexing the input data stream to m DC balanced line-coders then interleaving the m output sequences, [16, 18]. This produces m DC free sequences, $\alpha^{(1)}, \alpha^{(2)}, ..., \alpha^{(m)}$ each with length $x+1$, serialized to produce a stream of form

$$\left\{ \begin{matrix} \alpha_0^{(1)}, \alpha_0^{(2)}, ..., \alpha_0^{(\mathrm{m})}, \alpha_1^{(1)}, \alpha_1^{(2)}, ..., \alpha_1^{(\mathrm{m})}, \\ ....., \alpha_x^{(1)}, \alpha_x^{(2)}, ..., \alpha_x^{(\mathrm{m})} \end{matrix} \right\} \tag{4.3}$$

In order to have a notch at f_s / m, and its harmonics, the incoming bit stream prior to the encoder has to be parallelized into m steams, where each stream is encoded by a separate DC-balanced encoder. The parallel streams are combined to form a single serialized stream, as was indicated in Eq. (4.3). The resulting serialized stream is then used for modulation. The practical arrangement of encoders that is required to achieve the stream defined in Eq. (4.3) is presented in Figure 4.2 . Each encoder employed, is required to have a DC balanced property which results in a data stream with m spectral notches spread across its spectrum. At the receiver end similar entities such as parallel to serial converters (P/S), serial to parallel converters (S/P) and m interleaved decoders are required to recover the original binary sequence. Figure 4.3 represents the electrical spectrum of a 10Gb/s OOK stream passed through two or four interleaved 8B/10B encoders, in all cases the removal of the DC component is evident as-well-as the emergence of the in-band notches at f_s / m and its harmonics.

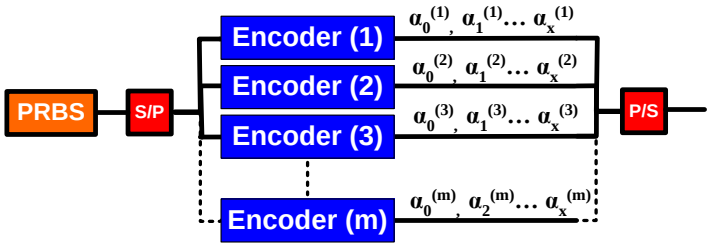

Figure 4.2. System of interleaved encoders for realization of in-band notches

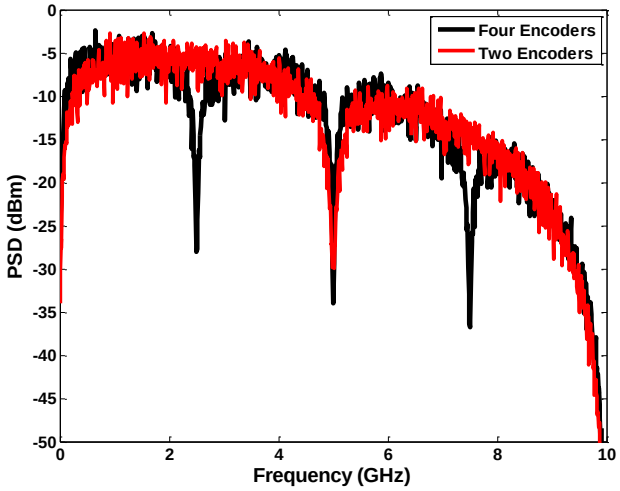

Figure 4.3. Electrical spectra of a 10 Gb/s OOK signal with two and four interleaved 8B/10B encoders

A class of codes is identified as being minimum-bandwidth (MB). Such MB codes have a Nyquist-free property which manifests itself as a spectral null at the Nyquist frequency ($f_N = f_S / 2$) in the encoded signals continuous spectrum [175]. Such MB codes can also be designed to be DC free, which in-turn leads to the creation of a coded-stream which has a spectral nulls both at DC and f_N [17, 175, 176].

To satisfy the MB property the inherent Alternating Sum Variation (ASV) is required to acquire a finite value over the entire length of the generated coded stream [17, 172].

$$ASV = \max_{P,Q,\{\alpha_i\}} |RAS| \tag{4.4}$$

Where the Running Alternate Sum or RAS is defined as the alternate sum over an arbitrary interval P-Q in the generated coded stream α_i

$$RAS = \sum_{i=P}^{Q} (-1)^i \alpha_i \tag{4.5}$$

Codes with a finite ASV, apart being MB, also exhibit a Nyquist-free property which manifests itself as a spectral null at f_N in the signal's continuous spectrum [175]. Such MB codes apart from having a finite ASV can also be designed to be DC free, which in-turn leads to creation of a coded-stream which has spectral nulls both at DC and f_N [17, 175, 176].

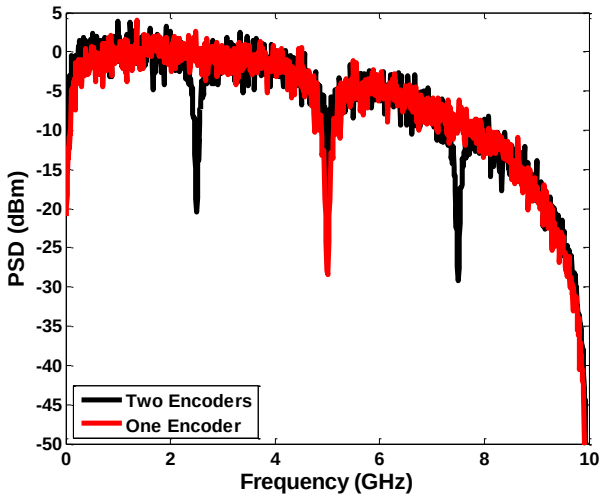

Figure 4.4. Electrical spectra of a 10 Gb/s OOK signal encoded by one and two interleaved MB810 encoders.

MB codes with a DC free property can also be interleaved similarly to encoders only with a DC free property as was suggested in Eqn. (4.3), but interleaving encoders with both MB and DC-free property leads to the doubling of the number of evenly spaced nulls in the resulting spectrum which in turn reduces the number of required encoders.

MB810 is a coding scheme that was initially proposed for the use in 10 GbE (Gigabit Ethernet) [172], this code was designed to be MB and DC-free which in-turn lead to generation of spectral nulls at DC and the Nyquist frequency. The spectrum of an OOK stream operating at 10 Gb/s coded with MB810 is shown in Figure 4.4, the presence of spectral nulls at DC and 5 GHz are clearly visible. Figure 4.4 also shows the resulting electrical spectra obtained by processing the original bit-stream through an interleaved system of MB810 encoders for $m=2$, where the doubling of spectral nulls is clearly seen.

To create a spectral null at a required frequency band, the m- factor should be chosen carefully such that one of the created spectral notches coincides with the band of interest. Although it is also possible to design line-encoders capable of producing spectral nulls at any arbitrary frequency [13], but this will require the design and implementation of separate encoders for each specific frequency band.

4.3. Line coding in hybrid wired/wireless PON's

In this chapter we experimentally make use of interleaved DC balanced 8B/10B encoders, and use numerical simulations to further study the performance of interleaved 8B/10B and MB810 encoders in a hybrid system.

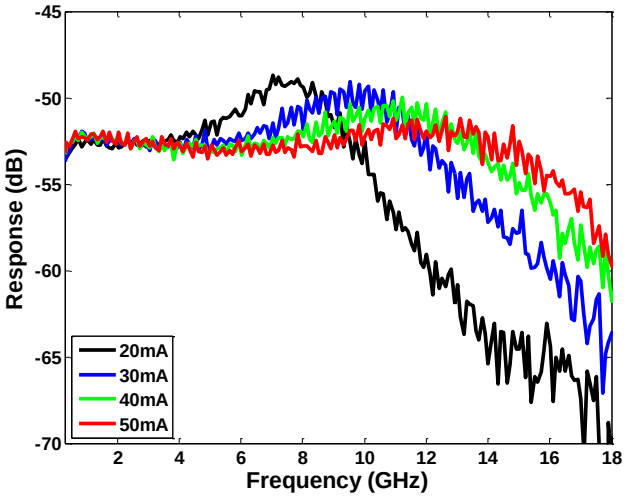

Figure 4.5. Frequency response of the DFB laser as function of bias current

4.3.1 System Setup

In the experimental work, the wired band used, was set to deliver information by directly modulating a DFB laser with a 10Gb/s encoded/un-encoded OOK signal. The encoded data stream used to program the Pulse Pattern Generator (PPG) was created offline. This encoded stream was created by interleaving and parallelizing a PRBS code-word of length of 2^{26}-1 into m streams, each encoded by a separate 8B/10B encoder and finally interleaved together. The structure of the encoder implemented is presented in Figure 4.2. The frequency response of the DFB laser used here is illustrated in Figure 4.5 for various bias currents.

In order to simultaneously transmit a wireless signal operating at 2 GHz, with minimal interference, it is necessary to create a notch at this frequency in the OOK spectrum, using the proposed encoding scheme. Given the fact that the OOK stream employed in this work operates at 10 Gb/s, creating a notch at 2 GHz, requires the incoming data to be parallelized

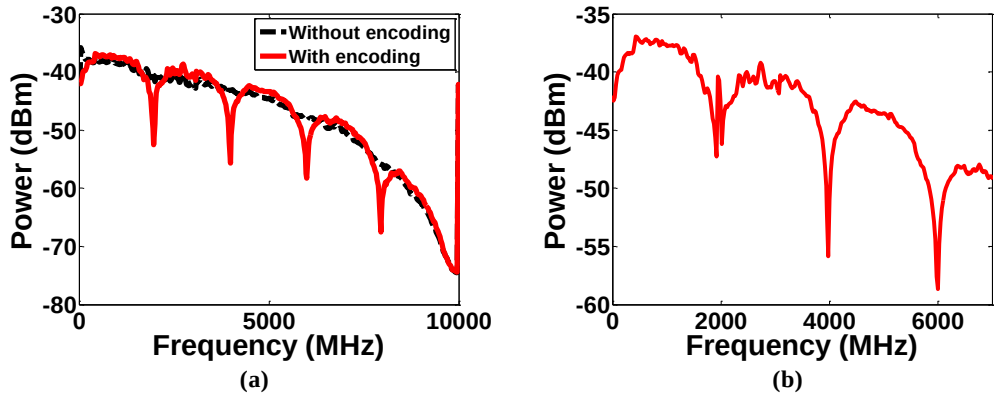

Figure 4.6. Electrical spectra of experimentally generated 10 Gb/s OOK signal using a) no encoders and five interleaved 8B/10B encoder, b) five interleaved encoders with an integrated LTE band at 2 GHz

Parameter	Value
Sampling rate	30.72 MSa/s
IFFT size	2048
No. of active subcarriers	1200
Modulation format	16 QAM
Frequency spacing	15 KHz
RF frequency	2 GHz
Training sequence length	1 OFDM symbol
Number of OFDM symbols per frame	4
Windowing	No
CP overhead	Normal CP
Total number of QAM symbols per frame	4800
No. of frame transmitted per evaluation	10
Net data rate	~ 72 Mb/s
Bandwidth	~ 20 MHz

Table 4.1. Parameters used for the in-band wireless OFDM signal

into 5 streams (m =5). Figure 4.6 (a) shows the resulting measured spectra with notches introduced at 0, 2, 4, 6 and 8GHz. The spectrum of the encoded signal with the wireless signal inserted at 2GHz is also shown in Figure 4.6 (b).

The wireless signal was generated in Matlab according to the requirements set by 3GPP standards [98, 169]. The parameters used to generate this wireless band are listed in Table 4.1. This OFDM based multicarrier signal had a bandwidth of 20MHz, with 1200 operational subcarriers, each modulated by 16 QAM symbols. The LTE band had an IFFT size of 2048 and a sampling rate of approximately 30.72 MSa/s with the subcarrier spacing was set to 15 kHz. A normal CP (as defined in 3GPP standards for LTE signals [169]) as opposed to an extended CP was used. The resulting LTE signal was digitally up-converted to the desired RF channel.

The wireless LTE signal was loaded into an Arbitrary Waveform Generator (AWG), whose output was electrically added to the output signals generated by the PPG. As can be observed in Figure 4.7, to overcome electrical reflections, and further interference, an attenuator was placed between the AWG and the electrical adder. The main aim of the experimental setup shown in Figure 4.7, which subsequently will also be used in numerical simulations, was to study and identify the possible performance enhancement achievable by the creation of in-band spectral notches in OOK hybrid PONs. This experimental setup will also be used to shed some light on the limiting factors of the line encoding schemes employed. Some of the key parameters regarding the experimental setup are listed in Table 4.2.

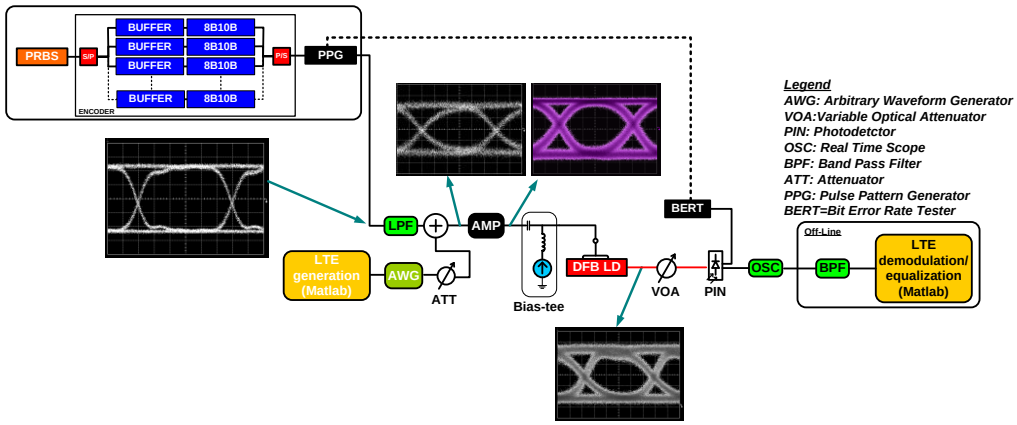

Figure 4.7. Experimental Setup and eye diagrams at various points on the system

The combined electrical signal was then amplified and used to directly modulate a DFB laser whose 3-dB bandwidth was approximately 15 GHz. The bias current of the laser was set to 50mA. The resultant optical signal was subsequently sent to a PIN photodiode package with a transimpedance amplifier (TIA). To evaluate the performance of the wired band, the received electrical signal was sent to a Bit Error Rate Tester (BERT). The electrical signal from the PIN-TIA was also sent to the Real Time Scope (RTS) where it was sampled and saved for offline processing, which included filtering to isolate the LTE signal prior to Error Vector Magnitude (EVM) measurements of the LTE signal. The EVM measurements were carried out to determine the impact of noise and distortion affecting the LTE signal. To obtain the EVM the received QAM symbols in each subcarrier after normalization were compared with the transmitted QAM symbols which were made known to the receiver.

The communication system presented in Figure 4.7 was also modeled in Matlab for numerical simulations. The electrical signal used to drive the laser model was composed of

Parameter	Value
PPG / BERT used	Anritsu AWG7122C
Line encoders	8B10B / MB810
Drive voltage (PPG)	0.8 Vp-p
AWG used	Tektronix AWG70002A
DAC sampling rate	10 GSa/s
DAC resolution	8 bit
Laser used	DFB
Laser bias point	50 mA
Laser 3dB bandwidth	15 GHz
Electrical amplifier used	JDSU H301
DSO used	Tektronix DPO71254B
ADC sampling rate	12.5 GSa/s
Photodetector	Nortel PP-10G (PIN)

Table 4.2. Experimental parameters employed

an amplified OOK signal, an LTE signal and a noise source associated with the electrical amplifier. The laser model used was a system of coupled rate equations representing a standard DFB laser [177]. The laser model was then numerically solved by the Runge-Kutta algorithm for a drive current represented by the generated electrical signal. The resulting optical signal was then converted to the electrical domain by a model of a PIN-TIA with appropriate added noise values.

The received simulated wireless signal after filtering was passed through the same off-line processing unit which was used in experimental work, and EVM calculations are used to study its performance levels and to assess transmission properties of the OOK band, where Direct Error Counting (DEC) was used to measure BER values.

4.3.2 Relative Power Ratio

Given that the wireless signal was inserted within the bandwidth of the wired signal, the interference they experience from each other becomes a major degrading factor in this particular system. As was mentioned above, the proposed encoding schemes can alleviate this interference to a degree. The performance of both the wired and the wireless bands, with respect to the level of interference they each experience was experimentally examined, with and without encoding for a system of interleaved 8B/10B encoders with m =5. The level of interference is significantly dependent on the respective drive power levels of both the wired and wireless signals. To examine the impact of interference, the wired signal was assigned a constant power level, whereas the power in the wireless band was varied by controlling the output of the AWG. From here on we refer to the relative power in the two signals, as the Wired to RF Power Ratio (WRPR), which is defined as

$$WRPR = \frac{P_{OOK}}{P_{RF}} \tag{4.6}$$

With P_{OOK} representing the total power in the wired band and P_{RF} representing the total power in the RF band. This ratio had been set prior to the amplification stage after the two electrical signals are combined, and it was experimentally varied from 7 dB to 13 dB, and was limited by the maximum output power level of the AWG. During the measurement of this system's performance, the power in the OOK signal was set to -5 dBm and the wireless power was varied. However, Figure 4.8 shows various eye diagrams captured prior to the amplification of the encoded 10 Gb/s OOK signal, which were obtained by varying both the OOK and wireless signals power levels. As the figure suggests, different WRPRs are obtained by varying the power levels in the OOK and wireless bands. It is clear that at high WRPR levels the power in the wireless band are negligible and this does not result in

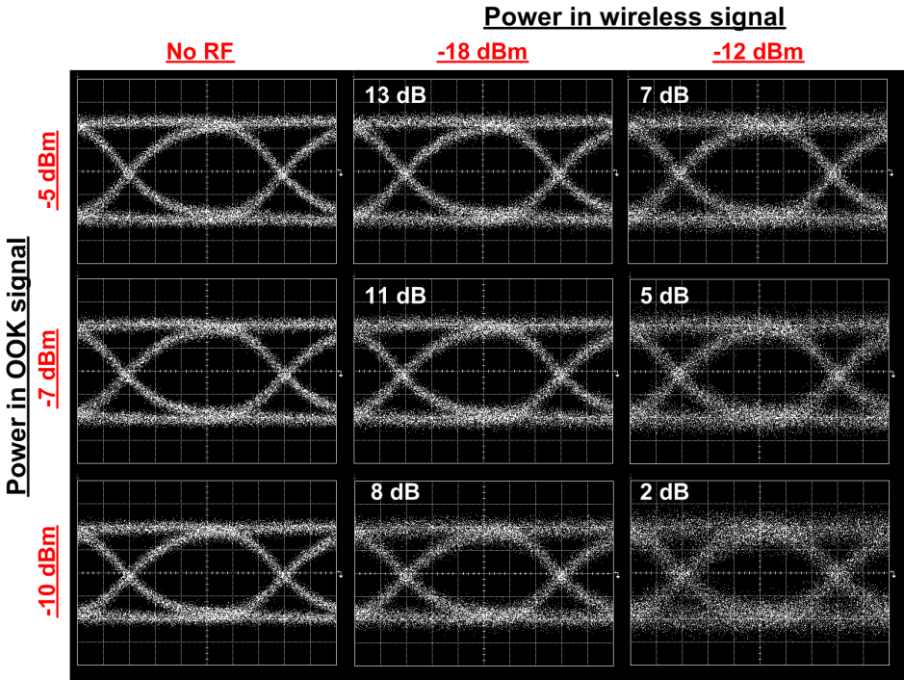

Figure 4.8. Encoded eye diagram for various WRPR ratios prior to amplification

significant distortion of the eye opening, but with decreasing WRPR levels a decrease in SNR and eye opening is evident.

4.3.3 Results and Discussions

Figure 4.9 shows the measured BER versus received optical power for the wired signal, with and without encoding, and at various WRPR values. As the figure suggests, error free performance can still be achieved with the introduction of the wireless signal when the wired signal has been encoded. Indeed, only a 1-dB penalty is observed at BER of 10^{-9} for cases where the LTE band was operated at maximum drive power (7-dB WRPR) relative to the case where no LTE signal had been present. Using an un-encoded stream, of similar

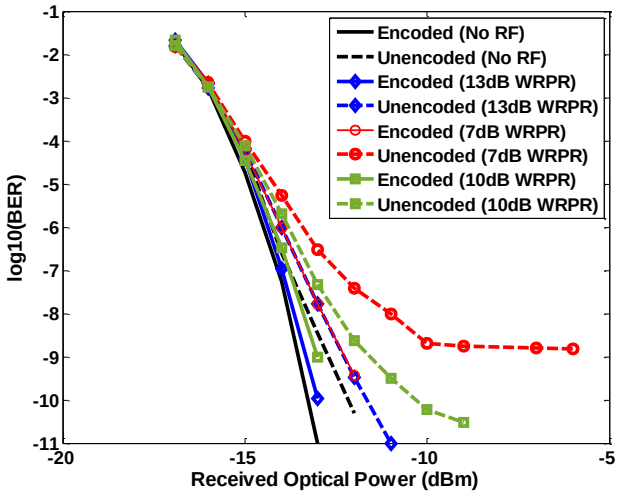

Figure 4.9. Experimental performance of the wired band in the hybrid system employing interleaved 8B/10B encoders with m =5.

PRBS length, results in elimination of the spectral notch, and further errors in the wired signal are encountered due to the interference from the LTE band. As outlined in Figure 4.9 it results in error floors, which are visible for WRPR ratio of 7 dB.

Figure 4.9 also shows a difference in performance between the encoded and un-encoded wired signals, where no wireless signal has been used, with slightly better performance for the encoded signal. The improvement in system performance for the encoded signal at higher received optical powers (where the system was no longer dominated by receiver noise), shows how DC balanced encoders such as 8B/10B can enhance performance, which can be due to a reduction in effects of the low frequency cut-off of RF amplifiers used in the system.

The performance degradation evident in Figure 4.9 caused by the insertion of the wireless signal is of the order of 0.5dB for a WRPR of 13dB. This degradation is due to the direct interference from the LTE signal.

The simulated results presented in Figure 4.10, show that insertion of the LTE signal without encoding has minimal impact at 13dB WRPR, due to the low power levels in the narrowband signal. Although decreasing WRPR to 6dB leads to an increase in interference experienced by the wired band and decreasing WRPR levels below 6-dB results in an error floor approaching BERs of 10^{-6} and 10^{-3} at 5 and 2-dB WRPR respectively. These results indicate that the impact of the LTE signal on the OOK signal was independent of the encoding, but rather had been dependent on its relative magnitude as expected. Transmission through 20 km of Standard Single Mode Fibre (SSMF) is also presented.

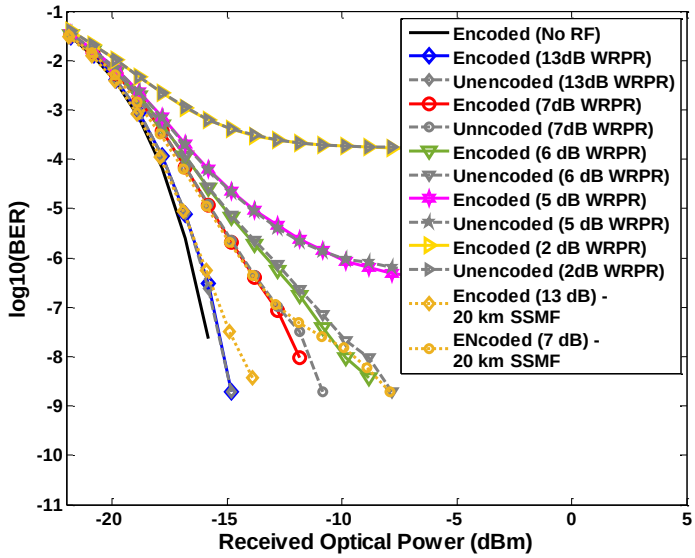

Figure 4.10. Simulated results for the wired band with/without interleaved 8B/10B encoding with m =5.

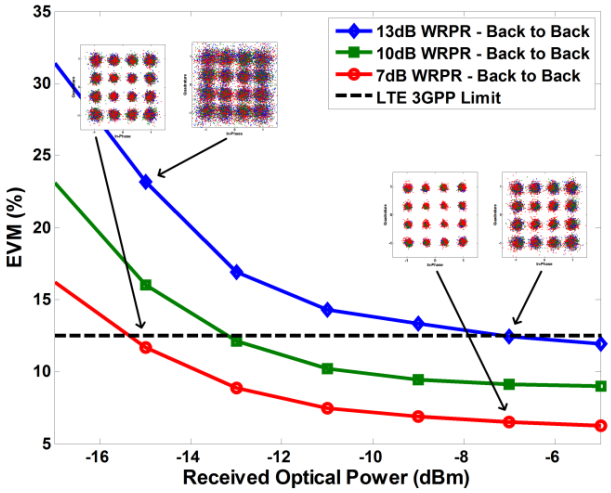

Figure 4.11. Experimental performance of the LTE band in the hybrid system employing interleaved 8B/10B encoders with m =5.

Fibre transmission resulted in degradation of approximately 1 and 2.3 dB at BER of 10^{-8} for 13 and 7 dB WRPR respectively, this degradation can be attributed to fibre dispersion and it's interaction with chirp form the directly modulated lasers.

The experimentally evaluated performance of the accompanying LTE band for various WRPR ratios is presented in Figure 4.11 in terms of Error Vector Magnitude (EVM), at different average received optical power levels. EVM values below that which are required by 3GPP standards were achieved for all three different WRPR ratios ranging between 7 and 13 dB, for the scenarios where encoding was employed. A constant increase in EVM is seen in the trends as WRPR grows, which suggests an increase of interference from the wired band, with EVM values reaching above 30 % for 13 dB WRPR and 15 % for the 7-dB WRPR at the lowest received optical powers.

The addition of the wireless band to an un-encoded wired band, results in severe penalties, creating error levels above 80% EVM for 7 dB WRPR and 120% for 13-dB WRPR, as

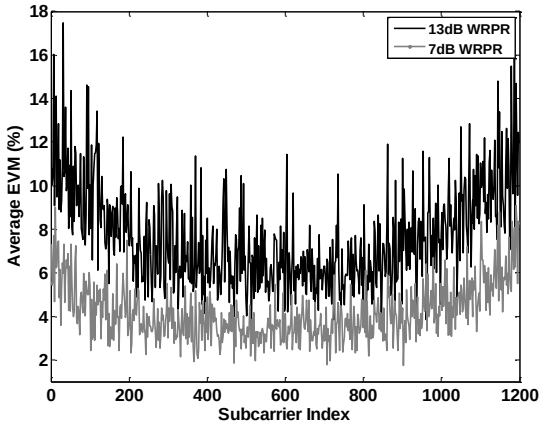

Figure 4.12.Performance of the LTE signal in presence of encoded wired signal, in terms of average EVM per subcarrier. (Average received optical power =-7dBm). At m =5

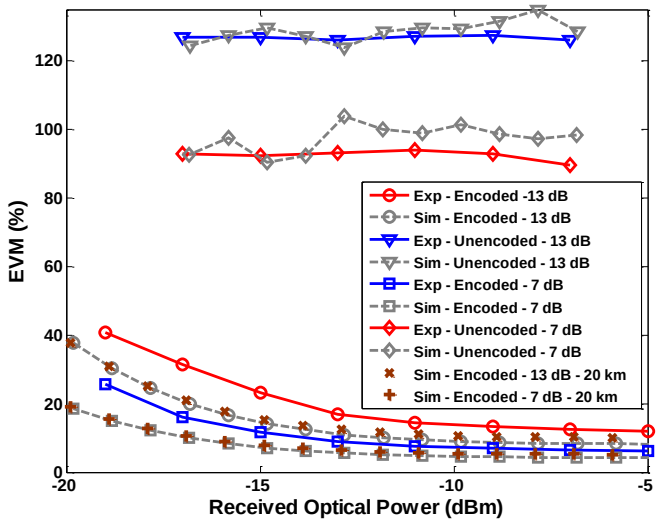

Figure 4.13. Simulation and experimental results for performance of LTE band with/without interleaved 8B/10B encoding with m =5, At 7 and 13-dB WRPR.

presented in Figure 4.13, this signifies the sensitivity of this multicarrier system to interference from the wired signal when it has not been encoded to create the spectral nulls. This also presents the significantly improved results obtained by numerical simulations for the LTE band in a system employing 5 interleaved encoders; the simulation trends show good agreement with the measured experimental results in both encoded and un-encoded scenarios. Transmission of this LTE signal through 20 km of SSMF results in a negligible difference in performance; this can be attributed to the resilience of OFDM to dispersion.

Figure 4.12 shows the EVM per subcarrier of the LTE signal that was evaluated in Figure 4.11 (with coding used for the wired signal). LTE subcarriers in the middle of the band display the lowest EVM values. This is the frequency at which the null in the interfering wired signal, due to the encoding, has the maximum suppression. Due to the increased levels of interference from the wired signal at the edges of the wireless signal band, the EVM performance worsens with a variation of approximately 10 % in EVM across the band for the case where WRPR is 7-dB, and 4% when a WRPR of 13-dB is used. Since the position of the notches is determined by the signaling rate f_s and the interleaving order m, for the accommodation of a wireless band operating at 2 GHz, five interleaved 8B/10B encoders were employed. The m factor also creates a trade-off between performance of wired and wireless services by altering levels of interference experienced by each. As it was illustrated in Figure 4.3 two interleaved 8B/10B encoders operating at 10 Gb/s resulted in a spectral notch at 5 GHz, using this nulled frequency band for transmission of a 20 MHz LTE band at 13-dB WRPR resulted in minor performance deterioration in contrast to a wired band with 5 notches as suggested in Figure 4.15. Out-of-band spurious signals created due to the RF signal interacting with the nonlinearity in the

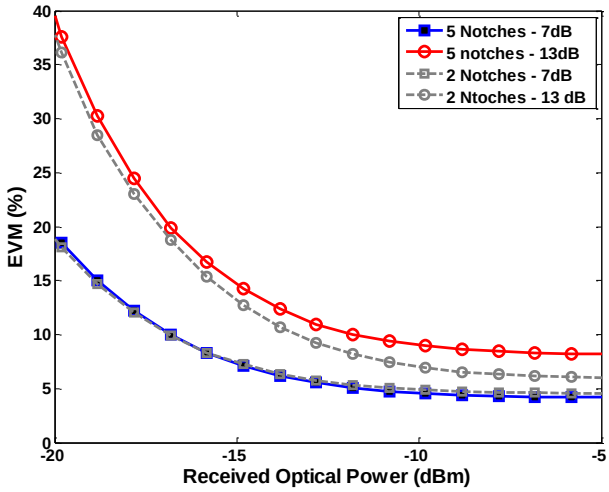

Figure 4.14. Simulation results for the Wireless signal using interleaved 8B/10B encoding with two and five notches at 7 and 13-dB WRPR.

channel coincide with the spectral notches at harmonics of f_s / m along with changes in shape of the spectral nulls as a result of variations to the m-factor, determine the performance improvement seen in the wired band with increasing m.

A slight deviation in performance is seen at low WRPR values for the LTE band operating with 2 or 5 encoders (Figure 4.14), although a reduction in interference as a consequence of lowering the m-factor is clear for higher WRPR levels. A closer look at the simulated performance of the wireless band Figure 4.17 suggests spectral broadening of the spectral null with the reduction in the number of interleaved encoders. The spectral broadening manifests itself as a decrease in EVM by a factor of two at low and high subcarrier numbers when an encoder with m=2 was employed. While a slight increase in EVM at the mid-band region for m=2, suggests a decrease in depth of the spectral null, this factor is

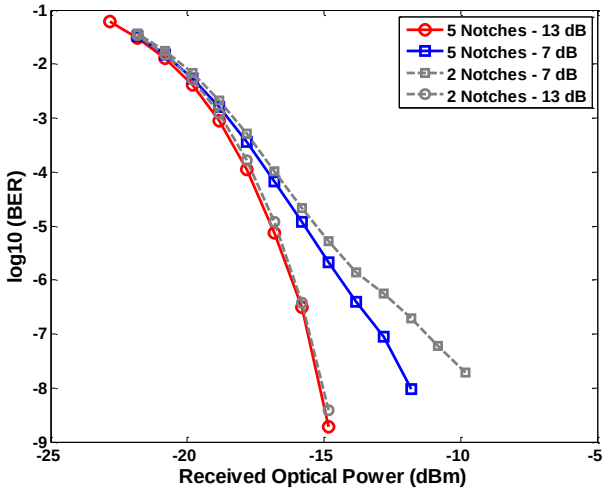

Figure 4.15. Simulation results for the wired band using interleaved 8B/10B encoding with two and five notches at 7 and 13-dB WRPR.

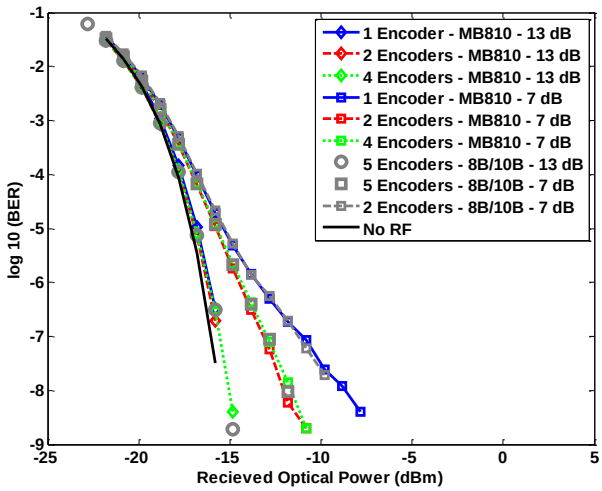

Figure 4.16. Simulation results for the Wired bands using various interleaved orders of MB810 and 8B/10B encoders for 7 and 13-dB WRPR.

observable in the spectrums in Figure 4.3 where two and four interleaved encoders were compared.

Next, the performance of a hybrid system employing interleaved MB810 encoders is evaluated via simulations, the obtained trends are further compared with scenarios were 8B10B was employed. The performance trends for the wired band using either 8B10B or Mb810 (Figure 4.16) converge at the high WRPR ratio of 13-dB irrespective of the m-factor or the encoding scheme used. Although at 7-dB WRPR, the performance deteriorates when only one MB810 encoder was employed, the same performance trend is also seen in the case where two interleaved 8B/10B encoders were used. Significant interference reduction is achieved at 7-dB WRPR when the m-factor is increased to two and four for MB810 and 8B10B scenarios respectively.

In case of the wireless band, the increase in the number of interleaved MB810 encoders

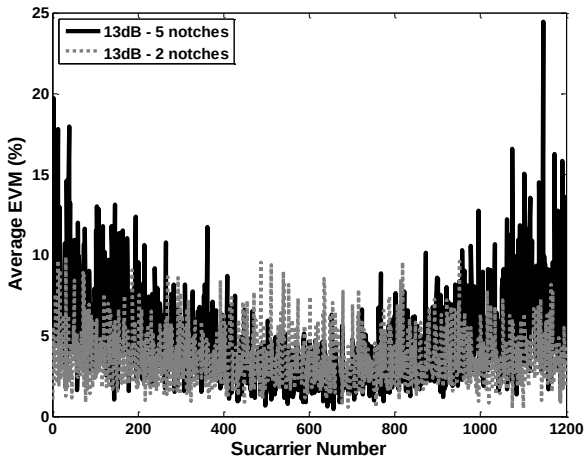

Figure 4.17. Simulated LTE band evaluated at 13-dB WRPR and -7dBm average received optical power.

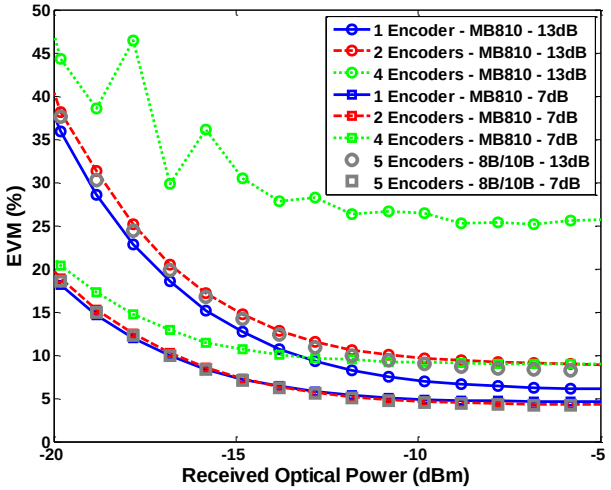

Figure 4.18. Simulation results for the Wireless band using various interleaved orders of MB810 and 8B/10B encoders for 7 and 13-dB WRPR.

leads to EVM deterioration as seen in Figure 4.18. This rise in EVM is an indication of an increase in interference level, which comes from variations in the width, and depth of the spectral null. The worst performance is observed for the occasions were four interleaved encoders were employed indicating an error floor at approximately 10% and 25 % EVM for 7-and 10-dB WRPR respectively.

4.4 Discussions

Table 4.3 summarises all of the key results that were obtained through the experimental work and the numerical simulations, which were set to study the performance of the hybrid

Signal (WRPR)	Without Encoding (Exp)	With Encoding (Exp)	Enhancement (Exp)	Without Encoding (Sim)	With Encoding (Sim)	Enhancement (Sim)
No RF	-13.25 dBm	-13.8 dBm	0.55 dB	-	-15.5 dBm	-
Wired-13dB	-12.9 dBm	-13.6 dBm	0.7 dB	-15.1 dBm	-15.2 dBm	0.1 dB
Wired-10dB	-12.5 dBm	-13.4 dBm	0.9 dB	-	-	-
Wired-7dB	-11 dBm	-12.9 dBm	1.9 dB	-11.4	-11.8 dBm	0.4 dB
Wired-6dB	-	-	-	-8.9 dBm	-9.8 dBm	0.9 dB
Wired-5dB	-	-	-	Above limit	Above limit	-
Wireless-13dB	Above limit	-15.4 dBm	-	Above limit	-13.8 dBm	-
Wirleess-10dB	Above limit	-13.2 dBm	-	Above limit	-	-
Wireless-7dB	Above limit	-7 dBm	-	-	-17.9	-

Table 4.3. Summary of Experimental (Exp) and Simulation (Sim) results from the hybrid system with one AoF signal, in terms of received optical power at which the BER limit (set at 10-8) or the 3GPP limit was reached. (Below/above limit: performance at all received optical powers is below/above 3GPP or FEC limit)

system using 8B10B encoders. The performance levels in this table are presented in terms of power levels at which either the chosen BER limit (10^{-8}) or the 3GPP limits were reached. The BER limit here is chosen to be at 10^{-8}, because some of the results failed to reach the BER of (10^{-9}), this new FEC limit will allow for an adequate comparison of results obtained. As the table suggests, encoding the wired OOK signal and excluding the AoF signal results in 0.55 dB of performance enhancement compared to the un-encoded case. This enhancement in the wired band can be attributed to the elimination of low-frequency component associated with the OOK signal that in the non-encoded case was filtered by the in-line electrical amplifier causing distortion to the wired signal. The addition of the AoF signal to the wired band results into additional levels of distortion, which are successfully alleviated by the encoding process. As the results show, at 13 dB WRPR the encoding process achieved 0.7 dB of performance enhancement. Decreasing the WRPR to 7 dB, leads to the reduction of the available power in the wired band and an increased level of interference from the wireless signal, however, the inclusion of encoding allows for 1.9 dB of performance gain.

In the simulation model employed, the filtering effect of the in-line amplifier was not specified thus the wired OOK signal operating at 10 Gb/s without the AoF band will exhibit a similar performance with or without encoding. However, as it can be seen, the decrease of WRPR in simulations also produces higher levels of interference on the wired band, which is similarly alleviated by the encoding architecture employed. As the trends in the table above suggest, up to 0.9 dB of performance enhancement is achieved by simply using line encoding. The lower levels of enhancement achieved for the wired band in the simulated case compared to the experimental scenarios can in part be attributed to the filtering effects of the in-line amplifier not being included in the simulations. On the contrary, through both simulations and experiments, it was shown that the removal of encoding leads to the wireless signal not being detectable anymore. The inclusion of encoding of the wired signal allowed for significant performance gains, and the 3GPP limit for the wireless signal to be reached.

Table 4.4 presents an overview of the results obtained from the simulations that were

Signal (WRPR)	5 Notches	2 Notches	Performance deterioration
Wired 13 dB	-15.1 dBm	-15 dBm	0.1 dB
Wired 7 dB	-11.8 dBm	-9.4 dBm	2.4 dB
Wireless 13 dB	-13.9 dBm	-14.72	- 1.72 dB
Wireless 7 dB	-17.8 dBm	17.9 dBm	- 0.1 dB

Table 4.4. Summary of simulation results, showing the impact of a reduction of the interleaving on the performance of the wired and wireless signals in terms of received optical power at which the BER limit (10^{-8}) or 3GPP limit was reached.

carried out to study the effect of variations in the interleaving order on performance. These simulations were based on 8B10B line encoders. The variations in performance as result of an increase or decrease to the interleaving order can be attributed to changes in spectral size of the spectral notches generated in the OOK signal's spectrum. The trends clearly show a 2.4 dB deterioration in performance of the wired band at 7 dB WRPR when the number of notches is decreased from 5 to two. When the interference on the wireless band is maximum (i.e. 13 dB WRPR), decreasing the number of notches to 2 results in a performance enhancement for the wireless signal of 1.72 dB. The apparent enhancement in the performance of the LTE signal when the interleaving order is reduced can be associated with an increase in the width of the spectral notches in the wired signal which consequently results in lower interference levels on the lowest and highest subcarriers of the LTE signal, as was demonstrated earlier in the chapter. In the case of the wired OOK signal however, the opposite is seen, with the performance degrading as the interleaving order is decreased. This can be attributed to a decrease in the depth of spectral notches with every subsequent reduction made to the number of interleaved encoders, which results in higher levels of interference being experienced by the wired OOK signal from the narrowband LTE band.

4.5 Summary

Both deployed and standardized PON technologies available today employ On-Off-Keying (OOK) in conjunction with Time Division Multiplexing (TDM). This chapter explored the idea of using line-coding techniques for the creation of spectral notches in the spectrum of an OOK modulated signal in a PON system. The aim of these notches was to allow for the simultaneous existence of wired/wireless services on a single wavelength. In order to create such spectral notches in the spectrum of 10 Gb/s OOK signal representing the wired band in a PON system, a special arrangement of multiple interleaved 8B/10B and MB810 line encoders was used. The in-band wireless signal used in this work was set to deliver LTE services. Experimental and simulation results showed that in absence of spectral notches, the interference caused a complete deterioration of the LTE signal however with the inclusion of spectral notches and the reduction of interference, reasonable performance was achieved for the wireless LTE signal at all examined Wired to RF Power Ratios (WRPRs). Similarly, performance deterioration was observed in the wired band as result of operating the hybrid system in absence of spectral notches, experimental results suggested the emergence of an error floor above the BER of 10^{-9} at 7 dB WRPR. It was also found that, it would be possible to double the number of in-band notches by using an interleaved

structure of MB810 encoders compared to 8B10B encoders, provided by their minimum bandwidth and DC balanced properties.

Chapter 5

Filter Bank Multicarrier in PONs

5.1 Introduction

Orthogonal frequency division multiplexing (OFDM) has become popular in both wired and wireless communications as well as optical communications [66]. The benefits of OFDM in optical communication come from its inherent high spectral efficiency and its resilience to chromatic dispersion. This resilience to dispersion arises from the Multi Carrier (MC) nature of OFDM along with its employment of a Cyclic Prefix (CP). But the inclusion of this CP entails a waste in the transmitted power as well as a reduction in the spectral efficiency. This reduction in spectral efficiency, in a practical optical systems can increase with the accumulation of chromatic dispersion [178], requiring longer CP lengths. Furthermore, The multi carrier nature of OFDM along with its particular choice of a prototype function can also increase its sensitivity to non-ideal conditions imposed on the channel such as frequency and time offsets. This increased sensitivity is due to the fact that each subcarrier in OFDM exhibits a Sinc-shaped frequency response across all subcarriers [23], which results in Inter Carrier Interference (ICI) between a target and many of the neighbouring subcarriers at the receiver under non ideal channel conditions.

To mitigate these drawbacks, a new class of MC modulation schemes, termed Filter Bank Multicarrier (FBMC) systems have recently attracted increased attention for both wired and

wireless applications [19, 20]. FBMC offers a better spectral efficiency, and better spectral containment compared to OFDM [179]. FBMC has appeared in the wireless literature based on numerous variants [19], and Staggered Multi Tone (SMT) is one example. The initial work on SMT was carried out by Saltzberg [180] in 1967. In this work Saltzberg showed that by the proper design of a transmit pulse-shape in a multichannel QAM system, and by introducing a half symbol delay between the in-phase and quadrature components (Offset Quadrature Amplitude Modulation (OQAM)), it is possible to achieve a baud-rate frequency spacing between adjacent subcarrier channels and still recover the information symbols, free of Inter Symbol Interference (ISI) and ICI. The OQAM property allows for well localized prototype filters in time and the frequency domains to be employed, thus increasing the system's resilience to frequency offsets [179]. Unlike OFDM, FBMC does not use any guard intervals or CP to combat channel distortion. This absence of a guard interval in FBMC results in improved bandwidth efficiency. Furthermore, due to the inherent properties of FBMC, the overlap between subcarriers is mostly restricted to the adjacent channels unlike OFDM, where there is a significant overlap among many subcarriers. As a result, FBMC is less prone to synchronization issues such as carrier offset and time offsets. More importantly, in Orthogonal Frequency Division Multiple Access (OFDMA) architectures, were individual users are allocated a subset of subcarriers available from an continuous OFDM band, any loss of synchronization between the users and the receiver can lead to a significant loss of performance [20], due to the significant overlap amongst neighbouring subcarriers.

FBMC and its applications have recently attracted a lot of attention in the field of optical communications. This interest has been fuelled by the superiority of FBMC over OFDM. There have been numerous studies on the feasibility of FBMC for various optical architectures. In [181], by using intensity modulation at the transmitter and direct detection at the receiver, 100 Gb/s FBMC based system were experimentally transmitted over 320 km of SSMF in a WDM architecture. FBMC in conjunction to intensity modulation was also exploited in [182] for transmission of 10 Gb/s signals over 50 km of SSMF. FBMC in coherent optical systems was studied and analysed through experimental examination and numerical simulations in [178, 183, 184]. To achieve higher spectral efficiencies in [185] by numerical simulations, the properties of FBMC in a Polarization Multiplexed optical coherent architecture was studied. The requirements for a channel equalizer capable of alleviating the impact of Polarization Mode Dispersion (PMD) and Chromatic Dispersion (CD) were also presented in this work. The impact of chromatic dispersion on FBMC based systems was studied in [186], and in [187] the properties of MC FBMC signalling was analysed in the presence of a large accumulation of dispersion as a result of transmission

through thousands of km of SSMF. A comparative study between OFDM and FBMC based transmission in presence of CD was presented in [187, 188]. Digital and analogue real-time implementation of FBMC based systems have also been carried out in [189, 190].

Despite the advantages of FBMC, there has not been much work on its applications in Passive Optical Networks, were high spectral efficient and cost effective means of transmission are required. In the downlink PON, FBMC and OFDM can be very beneficial as they can provide high spectral efficiencies without the need for high bandwidth electrical/optical equipment. Moreover, FBMC can show a better spectral efficiency than OFDM as transmission is possible without a CP. The reduced side-lobes of FBMC and the control over individual subcarriers can also lead to simultaneous existence of wired FBMC systems with in-band wireless signals. This can be accommodated by the de-activation of a few wired subcarriers [28], which can subsequently can be modulated by RF carriers transmitting wireless services. The reduced sidelobes of subcarriers in wired FBMC signals can then allow for reduced levels of interference on the accommodated wireless signal, compared to using OFDM for the wired band.

There have been many studies that demonstrate the effectiveness of OFDM for optical access, mainly aimed at the downlink communication [67], and the majority of work carried out at the uplink has been involved in alleviating the Optical Beat Interference at the OLT [67, 191]. To best of our knowledge, in most work exploring OFDM-PON in the uplink, guard bands are intentionally placed in frequency, between the subcarriers from different ONUs [192, 193]. These guard bands allow the neighbouring ONUs not to suffer from ICI in the presence of synchronization errors that can arise from carrier frequency offsets and timing delays. However in [194] a experimental system was devised to study the performance of CP based OFDMA for uplink PON, without the integration of frequency guard bands. In this work, a finite number of QPSK modulated subcarriers were assigned to a number of ONUs. Furthermore, Multi Access Interference (MAI) which resulted from the non-orthogonal conditions amongst neighbouring subcarriers that are received at the OLT, was mainly contributed to by relative timing delays between the ONUs. Thus to correct for this factor, an algorithm was created to measure the imposed signal propagation delays at the OLT which were subsequently corrected for at the ONU's for the next transmission frame. More recently, this work was also implemented in a field trial [195], however no detailed insight was provided on the impact of MAI and its alleviation using delay tracking. The employment of FBMC for uplink PON with frequency guard bands was studied and compared to OFDM recently in [27]. In this work, it was identified that because of the supressed side lobes of subcarriers in FBMC, a single guard band with subcarrier spacing was sufficient to alleviate any possible MAI - unlike OFDM.

This study was further analysed in the presence of relative timing variations and it was found that FBMC was not affected by MAI.

The inclusion of a frequency guard band in an optical architecture such as PON to eliminate MAI may lead to high losses in bandwidth efficiency as the number of users increases. In FBMC based systems, it was found that a single guard band with subcarrier spacing is sufficient to eliminate possible MAI unlike OFDM. However, because of the large subcarrier bandwidth that might be employed in PON, the accumulation of guard bands can still result in significant losses in bandwidth efficiency. FBMC is a great candidate for such architecture, since compared to OFDM it can provide a higher tolerance to frequency offset and in the presence of MAI, interference at worst effects inter-ONU adjacent subcarriers.

This work for the first time looks at the employment of FBMC in directly modulated long reach PONs, with propagation lengths over 75 km and data rates over 14 Gb/s. The work also for the first time looks at the resilience of FBMC to MAI in uplink PON where frequency guard bands have been excluded, and subsequently comparisons are drawn to a similar system employing OFDM.

5.2 Filter Bank Multicarrier

To improve channel utilization, multicarrier modulation techniques have been proposed, which allowed for the parallel transmission of data. An example of such techniques is OFDM, which has been widely employed in wireless and wired standards such as Digital Audio Broadcasting (DAB), Digital Video Broadcasting (DVB) and Wireless LAN (WLAN). OFDM has recently gained a lot on interest in fibre-optic communications [66] and is considered for future network topologies such as PONs [67]. The benefit that OFDM brings to fibre-optics is its resilience to fibre dispersion. This resilience arises from the parallelization of data into smaller tributaries and the employment of a CP. These characteristics also lead to a simplified channel equalization scheme. In a dispersive channel, the modulated symbols in each data tributary or subcarrier undergo a smaller amount of broadening because the symbols have larger duration compared to a serial stream. Under fibre dispersion, the orthogonality between neighbouring subcarriers can also be disturbed and give rise to ISI and ICI, but the employment of a guard interval in the form of a CP with an appropriate length can reduce these shortcomings. However, as it was stated earlier the extra overheads as result of the employed CP and the sensitivity to synchronization issues have motivated research on other MC system such as FBMC.

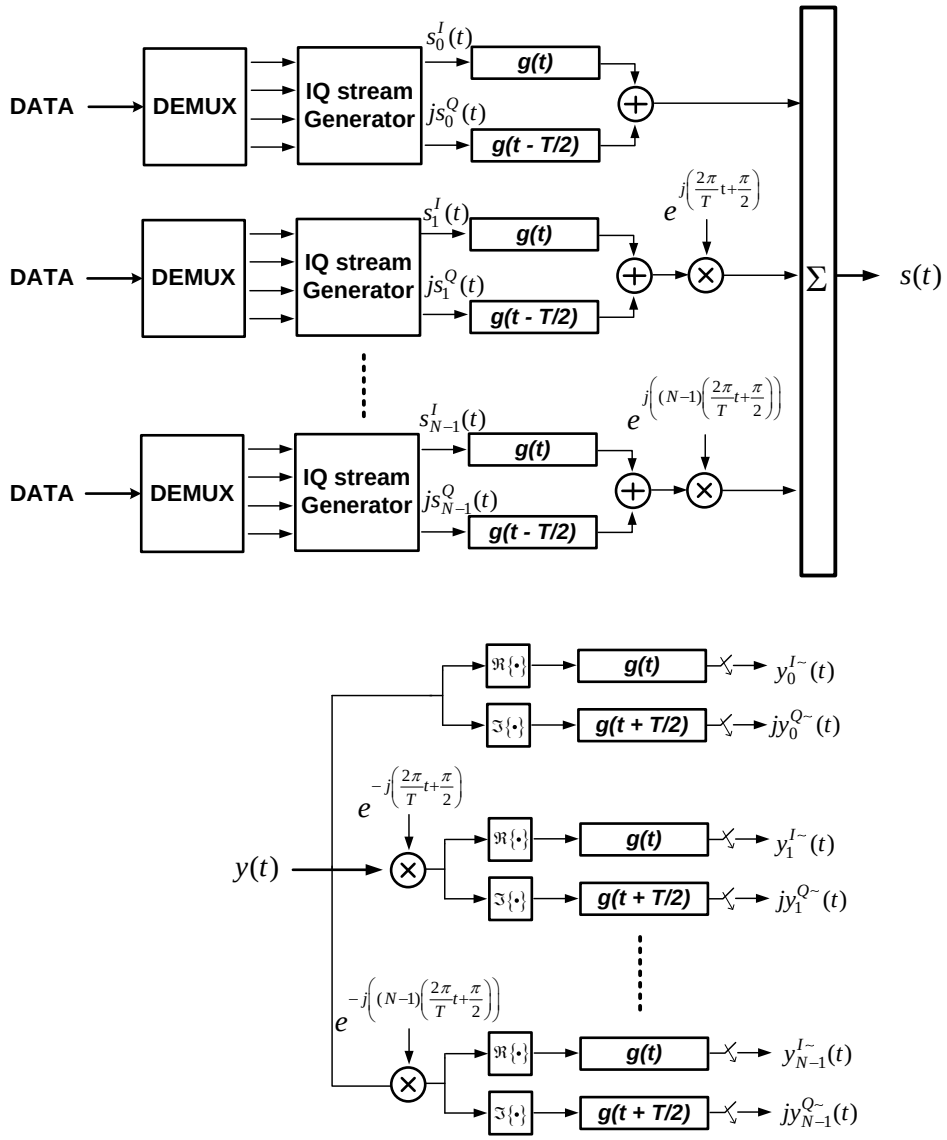

Figure 5.1. FBMC system architecture

5.2.1 System Description

The transmitter and the receiver pair for a SMT system is presented in Figure 5.1. At the transmitter, the binary data for each subcarrier is de-multiplexed into multiple tributaries. Based on these individual branches, the IQ stream generators create the multi-level I and Q data points which are then fed to the pulse shaping filters with the impulse response $g(t)$. The continuous-time SMT signal generated at the output of the transmitter shown in Figure 5.1 can be expressed as

$$s(t) = \sum_{n=1}^{N_s} \sum_{m=0}^{N-1} a_{m,n} \underbrace{g\left(t - n\tau_0\right) e^{j2\pi m v_0 t} e^{j\frac{\pi}{2}(m+n)}}_{g_{m,n}(t)} \tag{5.1}$$

N_s here denotes the number of SMT blocks transmitted, N is the total number of active subcarriers in the system and $a_{m,n}$ equals the real valued transmitted symbol of the subcarrier m at time index n. Due to the OQAM property here, two consecutive elements of $a_{m,n}$ at subcarrier m represent a QAM symbol, the values for each of these two elements is obtained by taking the real ($\Re\{\bullet\}$) or imaginary ($\Im\{\bullet\}$) parts of the complex QAM symbol that is required to be transmitted within one SMT symbol. The elements for $a_{m,n}$ are generated by the output of the IQ stream generator $S_m^I(t)$ and $S_m^Q(t)$ as shown in Figure 5.1. If τ_0 and v_0 represent the SMT block duration and the subcarrier spacing, then the SMT symbol duration within which a complex QAM symbol is transmitted is denoted as $T = 2\tau_0$ therefore the frequency spacing between each subcarrier is set to $v_0 = 1/T = 1/2\tau_0$. The extra term $e^{j\frac{\pi}{2}(m+n)}$ in equation (5.1) ensures the required $\frac{\pi}{2}$ phase shift between the staggered in-phase and quadrature terms in each subcarrier and their adjacent subcarrier, in the SMT system presented in Figure 5.1 this phase shift is realized by applying the $j = \sqrt{-1}$ term to the quadrature branch prior to the filter $g(t - T/2)$. The extra $\frac{\pi}{2}$ phase shift between each subcarrier is also realized in the SMT system by including the $\frac{\pi}{2}$ to the modulator block as shown in Figure 5.1. Furthermore, the expression $g_{m,n}(t)$ represents the shifted version of the prototype filter in both time and frequency.

The shortcomings of OFDM, such as its sensitivity to synchronization errors and the need for a guard interval arise from its particular choice of the prototype function $g(t)$ which in OFDM is a rectangular pulse in the time domain. This particular choice of a prototype function results in the Sinc shaped frequency spectrum, which guarantees orthogonality in the complex domain. To alleviate the shortcomings of MC systems such as OFDM, the prototype function modulating each subcarrier must be well localized in the time domain, to limit the ISI. Moreover, it can be chosen to be well localized in the frequency domain, to limit the inter-carrier interference. The function must also guarantee orthogonality between the neighbouring subcarriers in a MC system. Functions having these characteristics exist but they can only guarantee orthogonality in the real domain [196]. The existence of orthogonality only in the real field, unlike OFDM eliminates the possibility of modulating each subcarrier with complex QAM symbols. Thus to achieve orthogonality in such systems the symbol rate at each subcarrier is doubled and OQAM is employed. The OQAM modulation in each subcarrier is carried by time staggering of two Pulse Amplitude

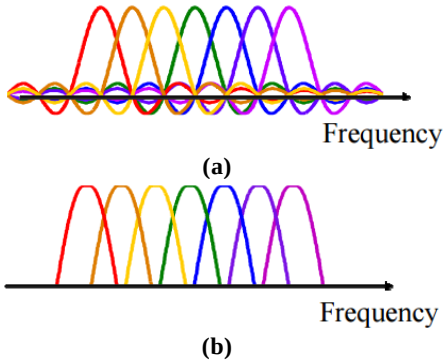

Figure 5.2. Spectra of (a) OFDM and (b) SMT system

Modulation (PAM) symbols which are obtained by taking the real ($\Re\{\bullet\}$) and imaginary ($\Im\{\bullet\}$) products of a QAM symbol after one another. Each of these PAM symbols represents either the in-phase or the quadrature signals and the duration of each is equal to τ_0. The OQAM property is realized in Figure 5.1 by delaying the porotype function in the quadrature branch by τ_0 or $T/2$. The Square-Root-Raised-Cosine (SRRC) function, well known for being ISI free in single-channel systems, when combined with OQAM can provide orthogonality amongst neighbouring subcarriers, and also restricts the possible ICI between adjacent subcarriers by limiting a significant portion of its spectral overlap over adjacent channels that are only distant by no more than one channel spacing [197]. Figure 5.2 shows the generated spectra of OFDM and SMT systems. The Sinc spectrum of the OFDM subcarriers stretches over all other subcarriers, but due to the orthogonality condition between all subcarrier it does not result in ICI or ISI in the time domain. However if some subcarriers are subjected to synchronization errors in OFDM, the resulting loss of orthogonality can affect all other subcarriers. The use of a well-localized prototype function $g(t)$ in SMT systems as shown in Figure 5.2 (b), results in orthogonal subcarriers with a limited spectral overlap.

As was stated earlier, the particular choice of the prototype function in SMT systems leads to an orthogonality condition only in the real part [196], the following expression demonstrates this fact. Assuming a perfect channel, perfect reconstruction of real symbols is achieved due to the real orthogonality condition:

$$\begin{aligned}\Re\left\{\left\langle g_{m,n}, g_{m+p,n+q}\right\rangle\right\} &= \Re\left\{\int g_{m,n}(t)\, g_{m+p,n+q^*}(t)dt\right\} \\ &= \Re\left\{j^{-[(p+q)+p(2n+q)]} A_g\left(-p\tau_0, -qv_0\right)\right\} \\ &= \begin{cases}1, & (p,q)=(0,0)\\ 0, & (p,q)\neq(0,0)\end{cases}\end{aligned} \tag{5.2}$$

In the above equation A_g is the ambiguity function of the $g(t)$ [19]. This ensures that there is no interference on the real symbol at position (m,n), from the neighbouring Frequency-Time positions. This equation further implies that in the absence of channel distortion and synchronization errors, there will be some ICI/ISI at the output of the matched filter at the receiver [179], however it is purely imaginary. This pure imaginary term can be defined as $\left\langle g_{m,n}, g_{m+p,n+q} \right\rangle = j\left\langle g \right\rangle_{m,n}^{m+p,n+q}$ (the term $\left\langle g \right\rangle_{m,n}^{m+p,n+q}$ has a real value and corresponds to the ambiguity function of $g(t)$) [198].

When passing through the channel composed of a dispersive fibre, the transmitted SMT signal is influenced by the fibre's Chromatic Dispersion (CD) and noise from various electro-optical components within the link. By defining the CD induced impulse response as $h(t)$ and the noise in the systems as $w(t)$, the demodulated signal at the receiver can be expressed as

$$\begin{aligned} r_{x,m} &= \int g_{m,n}^{*}(t)\left\{h(t) \otimes s(t)\right\} dt + \int g_{m,n}^{*}(t) w_x(t) dt \\ &= \int g_{m,n}^{*}(t)\left\{\int_0^{\Delta} h(u)s(t-u)du\right\} dt + \int g_{m,n}^{*}(t) w_x(t) dt \end{aligned} \tag{5.3}$$

The term $g_{m,n}^{*}(t)$ here represents the impulse response of the matched filter at the receiver for the frequency-time at the position (m,n), in Figure 5.1 this step is carried out in the receiver block by applying the appropriate IQ demodulation followed by filters $g(t)$ and $g(t+T/2)$. The symbol $\otimes$ in equation (5.3) stands for convolution in time. The signal at the output of the channel can be written as $y(t) = h(t) \otimes s(t) + w_x(t)$ (where $w_x(t)$ represents the combined contribution of $w(t)$ and the photodetector noise). Moreover the length of the prototype filter $g(t)$ is defined as T_g , this value is equal to or is greater than the SMT symbol length T [185]. Then we assume that we have a flat fading channel at each subcarrier, which means that $1/T_g$ is less than the coherence bandwidth of the channel $B_c \approx 1/(2\Delta)$ (Δ is maximum delay spread of the channel and is usually small for fibre [185]). Based on these statements we can then assume that the prototype function has low variation in the time interval $t \in [0, \Delta]$. That is $g(t - n\tau_0 - u) \approx g(t - n\tau_0)$ for $t \in [0, \tau]$ [198] , then we get

$$
\begin{aligned}
s(t-u) &= \sum_{n=1}^{N_s}\sum_{m=0}^{N-1} a_{m,n} g\left(t-n\tau_0-u\right) e^{j2\pi m v_0 t} \times e^{-j2\pi m v_0 u} e^{j\frac{\pi}{2}(m+n)} \\
&\approx \sum_{n=1}^{N_s}\sum_{m=0}^{N-1} a_{m,n} e^{j2\pi m v_0 t} e^{j\frac{\pi}{2}(m+n)} \times g\left(t-n\tau_0\right) e^{-j2\pi m v_0 u}
\end{aligned}
\tag{5.4}
$$

By substituting equation (5.4) into (5.3) we can obtain the following expression for the demodulated signal after the match filtering stage

$$
r_{m,n} = \sum_{(p,q)} a_{m+p,n+q} \int_0^{\Delta} h(u) e^{-j2\pi m v_0 u} du \times \left\langle g_{m,n}, g_{m+p,n+q} \right\rangle + w_x \tag{5.5}
$$

Where $w_x = \int g_{*_{m,n}}(t) w_x(t) dt$ and by defining the CD induced channel response as $h_{m,n} = \int_0^{\Delta} h(u) e^{-j2\pi m v_0 u} du$, equation (5.5) is reduced to

$$
r_{m,n} = h_{m,n} a_{m,n} + \sum_{(p,q)\neq(0,0)} h_{m+p,n+q} a_{m+p,n+q} \left\langle g_{m,n}, g_{m+p,n+q} \right\rangle + w_x \tag{5.6}
$$

Now considering the fact that the channel is slowly time varying, we can assume for the first order neighbours of the SMT block $(m+p,n+q)((p,q)\in\Omega_{1,1})$, the following assumption for the channel response is satisfied [185]

$$
h_{m+p,n+q} \approx h_{m,n} \tag{5.7}
$$

Furthermore assuming that the prototype function has a good Time and Frequency localization the following equality can be obtained [179]

$$
\left\langle g_{m,n}, g_{m+p,n+q} \right\rangle \approx 0, \quad (p,q) \notin \Omega_{1,1} \tag{5.8}
$$

This means that the purely imaginary interference is mainly affected by the first order Time and Frequency neighbouring blocks. By defining the index of these blocks as $\Omega^*_{(1,1)} = \Omega_{(1,1)} - (0,0)$, equation (5.6) can be modified to

$$
r_{m,n} = h_{m,n} a_{m,n} + \underbrace{\sum_{(p,q)\in\Omega^*_{1,1}} h_{m+p,n+q} a_{m+p,n+q} \left\langle g_{m,n}, g_{m+p,n+q} \right\rangle}_{IMI} + w_x \tag{5.9}
$$

The expression above for $r_{m,n}$ is the final expression for the received and demodulated SMT block at frequency-time indices (m,n). In Figure 5.1 the values for these demodulated received signals are represented by variables $y_m^{\sim I}$ and $y_m^{\sim Q}$. This expression presents the impact of noise, imaginary interference (assuming perfect channel) from neighbouring time-frequency blocks (denoted as Intrinsic Imaginary Interference (IMI)) along with the

distortion induced by chromatic dispersion in fibre, whose response for different SMT blocks is denoted as $h_{m,n}$. Thus in a practical optical transmission system by using channel estimation techniques to retrieve an expression for channel response $h_{m,n}^{est}$, assuming that a well localized prototype function is used, the transmitted PAM symbols $a_{m,n}$ can be approximated by

$$\hat{a}_{m,n} = \Re\left\{\left(h_{m,n}^{est}\right)^{-1} r_{m,n}\right\} \tag{5.10}$$

5.2.2 Channel Estimation

As it was demonstrated in earlier chapters, in a conventional OFDM system the impact of the channel in an optical communication system, which usually consists of various opto-electronic devices and a dispersive fibre can be corrected for by channel estimation techniques. In QAM based OFDM systems the value for this complex estimate $h_{m,n}^{est,OFDM}$ at frequency-time location (m,n) is estimated by comparing received complex QAM symbols $\alpha_{m,n}$ to the transmitted symbol at that frequency-time location $\beta_{m,n}$ (i.e. $h_{m,n}^{est,OFDM} = \alpha_{m,n} / \beta_{m,n}$ for perfect demodulation and channel conditions). OFDM accommodates this since, unlike SMT, it allows for the orthogonality condition to exist in the complex domain [196]. However due to the existence of the orthogonality condition in the real field and the existence of an IMI in SMT and FBMC systems, the channel estimation in such systems is not as straight forward as in OFDM.

As was derived in the last section for SMT, in presence of an ideal channel $h(t) = \delta(t)$, that is $h_{m,n} = 1$, and neglecting the impact of noise, the received SMT block can be re-written as

$$r_{m,n} = a_{m,n} + \underbrace{\sum_{(p,q)\in\Omega_{1,1}^{*}} a_{m+p,n+q} \left\langle g_{m,n}, g_{m+p,n+q} \right\rangle}_{IMI} \tag{5.11}$$

Where, IMI is the interference arising from the in-phase and quadrature tributaries of the first order neighbouring subcarriers ($m^{th}, (m+1)^{th}, (m-1)^{th}$). Due to the real orthogonality condition of the prototype function, the term (IMI) in equation (5.11) is imaginary, thus for simplicity this equation can also be written as

$$r_{m,n} = a_{m,n} + \underbrace{j \sum_{(p,q)\in\Omega_{1,1}^{*}} a_{m+p,n+q} \left\langle g_{m,n}, g_{m+p,n+q} \right\rangle}_{IMI} \tag{5.12}$$

Thus after the application of the $\Re(\bullet)$ operator in the receiver this term disappears leading to the reconstruction of the transmitted PAM symbol free of crosstalk.

$$\hat{a}_{m,n} = \Re(r_{m,n}) = \Re\left(a_{m,n} + \underbrace{j \sum_{(p,q)\in\Omega_{1,1}^{*}} a_{m+p,n+q} \left\langle g_{m,n}, g_{m+p,n+q} \right\rangle}_{IMI} \right) \tag{5.13}$$

Although in the case of a non-ideal channel such as an optical communication channel, as stated in equation (5.9) the complex channel response $h_{m,n}$ apart from effecting the term $a_{m,n}$ can also force the IMI terms to become complex. Thus after application of the $\Re(\bullet)$ operator, this can result in the demodulated signal to contain the signal power along with cross talk terms from the IMI, which now is complex. The crosstalk can be supressed and the impact on $a_{m,n}$ can be reversed by retrieving $h_{m,n}^{est}$. This will lead to the following expression when noise is neglected

$$\frac{r_{m,n}}{h_{m,n}^{est}} \approx a_{m,n} + \underbrace{j \sum_{(p,q)\in\Omega_{1,1}^{*}} a_{m+p,n+q} \left\langle g_{m,n}, g_{m+p,n+q} \right\rangle}_{IMI} \tag{5.14}$$

Methods used in QAM-based OFDM to retrieve the channel estimates cannot be used in SMT due to the existence of the IMI. In the literature, there have been numerous methods, which aim at achieving channel equalization in FBMC systems. In [196] a pilot aided method is proposed where, by using prior knowledge of the prototype function, the IMI at the frequency-time position of the pilot symbol (m,n) is forced to zero by careful assignment of coefficients to first order neighbours to the pilot symbols at $(m+p,n+q)((p,q)\in\Omega_{1,1})$. To reduce the complexity of this Zero Forcing (ZF) method, in [198] the Interference Approximation Method (IAM) was proposed. In the IAM method, channel estimates are obtained at the receiver by determining the IMI using information about the prototype function and pre-known transmitted preambles. More recently, Zhao discussed a Modified Least Square (M-LS) and Modified Least Mean Square (M-LMS) channel estimation methods. In the proposed M-LS and L-MS methods, odd and even channel responses are estimated individually using a custom-made training sequence that helps to minimize the IMI on the pilot tunes used for the channel estimation.

5.2.3 FBMC in the presence of an optical channel

A significant achievement in FBMC compared to OFDM was identified as its capability to operate in the absence of a guard interval. As stated in [178] fibre dispersion can impact

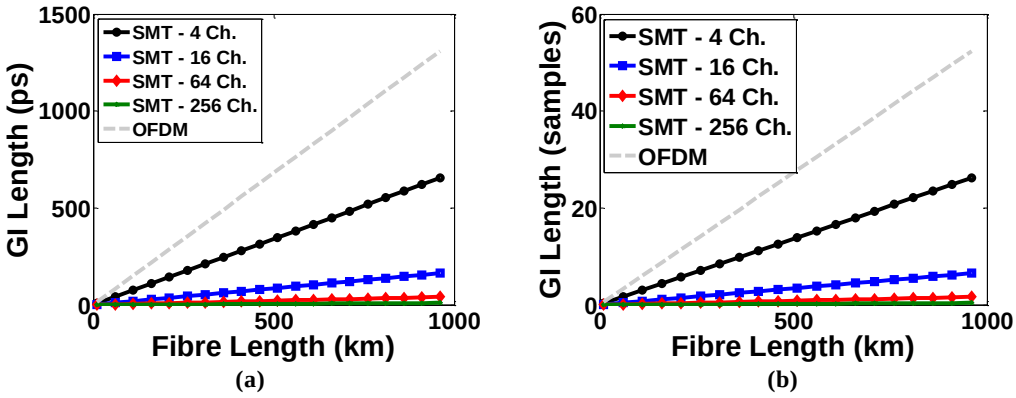

Figure 5.3. Required length of a guard interval for a 10 GHz OFDM and FBMC Signal in terms of (a) seconds (b) digital sample number

multicarrier orthogonal systems by 1) broadening the pulse in each channel and 2) causing a relative time delay amongst different subcarriers. The impact of the first factor is negligible especially for fine granularity in bandwidth (i.e. large number of subcarriers). In QAM-based OFDM the second factor in a system were no GI is employed causes the de-multiplexing filter at the receiver to no longer be orthogonal to other subcarriers in the OFDM signal resulting in ICI (or ISI) to the target subcarrier (or the target OFDM symbol). However, the introduction of a guard interval in the form of CP can avoid the ICI and ISI. The length of the guard interval τ_{GI} employed should correspond to the delay difference between the lowest frequency and highest frequency subcarrier in the OFDM band [186], that is

$$\tau_{GI} \geq \left| L\beta_2 \Delta\omega \right| \tag{5.15}$$

Where $\Delta\omega = \left(\omega_{N-1} - \omega_0\right)$ is the full bandwidth of the QAM based OFDM signal, L is the length of fibre and β_2 is the second order dispersion value. In contrast, in FBMC, thanks to the well-localized prototype functions, the value $\Delta\omega$ in (5.15) reduces to $\Delta\omega = \left(\omega_2 - \omega_0\right)$, making $\left| L\beta_2 \Delta\omega \right|$ much smaller for the FBMC compared to QAM based OFDM. The length of guard interval for FBMC can even be further scaled down by reducing the subcarrier spacing, thus his scheme may support transmission without the GI [186]. Figure 5.3 illustrates the required GI length in SMT and OFDM systems alike to ensure ICI and ISI free reception at various propagation distances, calculated based on equation (5.15). These trends assume the full bandwidth of these signals to be 10 GHz, $\beta_2 = -21.7\ ps^2/km$, and a digital sampling rate at 40 GS/s. The trends in Figure 5.3 (a) shows a linear increase of the required GI length for OFDM as the fibre length increases. However, in the SMT system the tolerance to dispersion increases with decreasing subcarrier width or an increase in bandwidth granularity. As can be seen in Figure 5.3 (b)

after propagating through 1000 km of fibre, OFDM requires a GI, which is equivalent to 60 discrete time domain digital samples or 1200 ps however, the SMT system with 256 carriers requires a GI, which is approximately equivalent to zero digital samples in length. With this property of SMT, according to [178], the frequency domain channel response of the system by neglecting the impact of phase noise in the system can be represented as

$$H(\omega_m) = \exp\left(j\beta_2 L\omega_m^2 / 2\right).H_{b-b}(\omega_m) \tag{5.16}$$

Where $H_{b-b}(\omega_n)$ is the back-to-back system response accounting for optoelectronic devices. The combined effect presented in equation (5.16) can then be corrected for by channel estimation techniques and single tap equalizers at the frequency domain [183]. The resilience of FBMC and OFDM systems to fibre dispersion in absence of a guard intervals was examined both theoretically and experimentally for optical coherent systems in [178, 183, 187] where FBMC was found to be superior.

5.3 FBMC in intensity modulated PON's

The multicarrier nature of OFDM and its capability to reach a high distance/bandwidth product has promoted the study of its use in point to multi point (p2mp) architectures such as PONs [67, 98], where efficient bandwidth sharing is required. Since in the downlink channel each user in the PON is required to receive and process the full OFDM bandwidth, dynamic carrier assignment can be made possible here, which if combined with Wave Division Multiplexing (WDM) and Time Division Multiplexing, this dynamic allocation of bandwidth can be further made flexible [42, 147]. Amongst various methods available for optical modulation, Intensity Modulation (IM) in conjunction with Direct Detection (DD) can allow for cost efficiencies in PONs. The matter of cost effectiveness is usually placed at the forefront of PON requirements; due to the fact that a large portion of costs in an optical network is formed by the access topology. As it was pointed out in the earlier chapters, IM can be achieved by either external or direct modulation schemes. In comparison, direct modulation in conjunction with low-cost lasers can contribute further to the cost effectiveness [128], given its lower footprint and independency from polarization issues. Thus in this work the effectiveness of SMT in downlink intensity modulated PONs is evaluated, with the help of direct and external modulation schemes.

5.3.1 System Setup

The experimental setup used for this section is shown in Figure 5.4. The main aim of this experimental setup was to evaluate the performance of FBMC in intensity modulated long

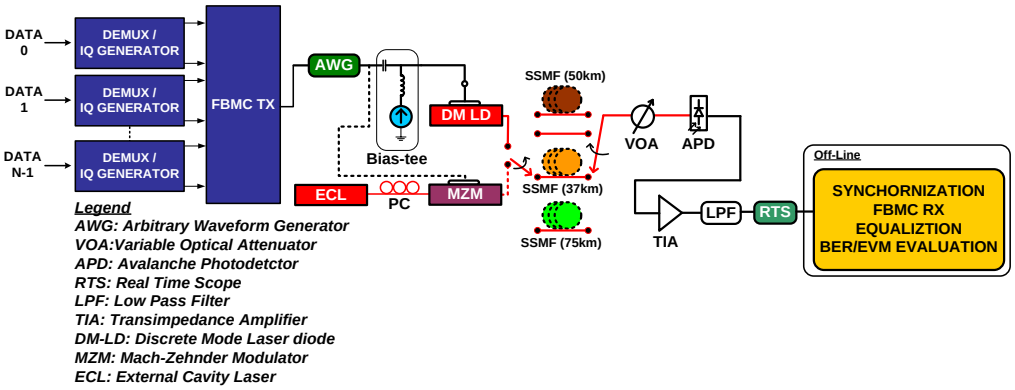

Figure 5.4. Downlink SMT experimental setup

reach PONs operating based on either external or direct modulation. Results obtained will shed light on the impact of RIN and nonlinearities on the performance. Moreover, by examining the performance concerning varying lengths of fibre and data rates, the limitations of such intensity-modulated system in terms of dispersive effects in fibre can be identified. For direct modulation a cost effective Discrete Mode (DM) [11] laser was used, the performance of an external modulator (MZM) was also evaluated for this system. At the transmitter side, the binary data for N subcarriers were fed into I-Q stream generators. The system subsequently processed the I-Q information accordingly to create the SMT signal with N partially overlapping subcarriers. Table 5.1 provides a list of parameters that were used in the generation of the FBMC signal. The prototype function employed here was a Square-Root Raised Cosine (SRRC) with a roll-off factor equal to 0.5. The frequency spacing between each subcarrier was set to $v_0 = 100MHz$ and each subcarrier was modulated by 16 QAM symbols. The system is then examined for various numbers of subcarriers which ranged from 21-37, this yields a net data rate between 8.4 – 14.8 Gbps in

Parameter	Value
Frequency spacing (v_0)	100 MHz
Number of active subcarriers (N)	21 / 25 / 31 / 37
Net data rates	8.4 / 10 / 12.4 / 14.8 Gb/s
Modulation format	16 QAM
Assigned frequency to first subcarrier	100 MHz
Prototype function $g(t)$	SRRC
Roll off factor α	0.5
Number of OFDM symbols per frame	1024
CP overhead	0 %
Total No. of QAM symbols per frame	21504 / 25600 / 3174 / 37888
Overheads for training sequence	4 %
No. of frame transmitted per evaluation	30

Table 5.1. Parameters used for the generation of the FBMC signals

2.1 – 3.7 GHz of bandwidth. Channel estimation and synchronization at the receiver-end is achieved by appending a pre-known training symbol that avoids the impact of IMI. These training symbols are appended to the start of the FBMC's Transmission frame, and the training symbols only account for 4% of the overall transmission frame. The waveforms which are created offline in Matlab are loaded onto an Arbitrary Waveform Generator (AWG) equipped with a DAC operating at 10 GSa/s whose output is then ac coupled and used to drive either a DM laser or a MZM biased at the Quadrature point. Table 5.2 provides a list with details of the subsystem that were employed in this experimental setup. The directly modulated laser is driven by the output of the AWG that is set to 0.8 Vp-p, this electrical signal is however amplified by an electrical amplifier in order to achieve the necessary drive levels required by the external modulator. The modulated optical signal is subsequently routed through 0 / 37 / 50 or 75 km of SSMF. The received optical signal is subsequently received by an APD equipped by a TIA. The received electrical signal is digitalized by using a Real Time Scope equipped with a ADC operating at 10 GSa/s, the resulting digital samples are then processed offline in Matlab. The off-line process carries out signal synchronization, equalization and BER/EVM evaluations. Furthermore in order to overcome the power roll-offs imposed by the transmission system the high frequency subcarriers are intentionally pre-emphasized. The modulation response of the DM laser under test was obtained by using a network analyser; this normalized response is shown in Figure 5.5 for two bias currents. The obtained 3dB bandwidth at these two bias points (18 and 20 mA) accordingly was 5.5 and 6.1 GHz. The intensity modulation schemes that are used here both result in an Optical Double Side Band (ODSB) signal.

Parameter	Value
AWG used	AWG7122C
DAC sampling rate	10 GSa/s
DAC resolution	8 bits
Drive voltage	0.8 Vp-p
Directly modulated laser used	DM single section
Direct modulated lase bias point	20 mA
External modulator used	EOM OC192 LiNbO3
External modulator driver	JDSU H301
APD used	Oclaro AT10XGC
M-factor APD	3
DSO used	Keysight DSO80404B
ADC sampling rate	10 GSa/s
Input optical power to fibre	~ 0 dBn

Table 5.2. Experimental parameters employed

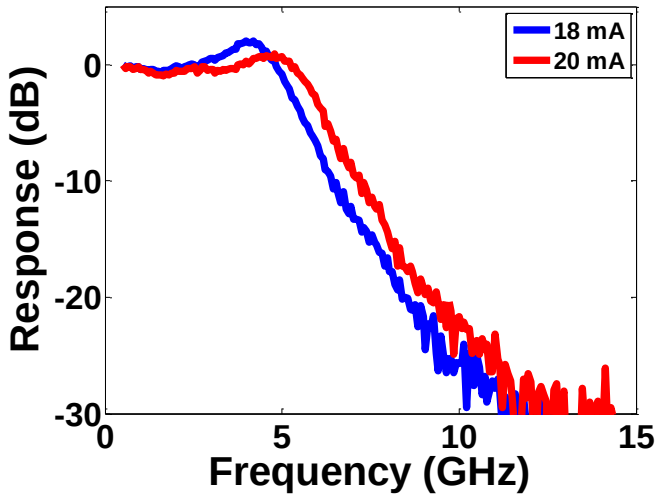

Figure 5.5. Measured frequency response of the DM laser at two bias points

5.3.2 Experimental Results

5.3.2.1 Transmission at 8.4 Gb/s

In the first case, a SMT with 21 subcarriers was generated. The net data rate representable by this MC signal was 8.4 Gbps and it occupied 2.1 GHz of bandwidth. The electrical and optical spectrums at various points in the system are shown in Figure 5.6. , in both electrical and optical spectra, the large side lobe suppression is clearly visible. The

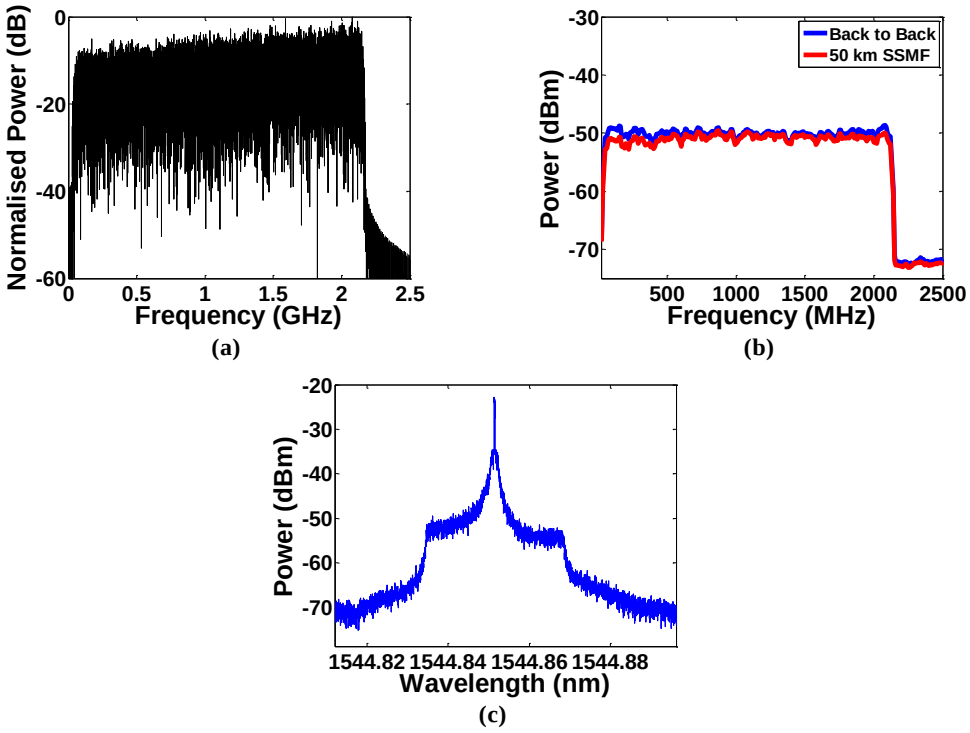

Figure 5.6. (a) Electrical Spectrum of 21 subcarriers at output of the AWG (b)Electrical spectrum for back to back and 50 km transmission and (c) optical spectrum after direct modulation

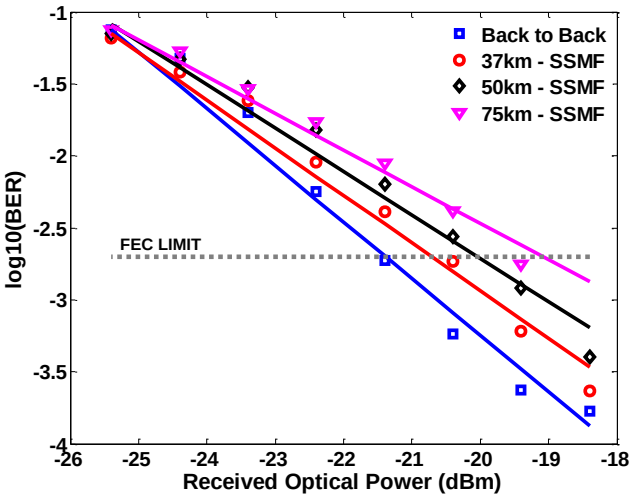

Figure 5.7. Experimental performance of the FBMC systems with 21 subcarriers in terms of BER vs Received Optical Power for back to back and fibre transmission scenarios

application of pre-emphasis to the SMT signal is also visible in Figure 5.6 (a) , which helps to achieve a constant power over the full bandwidth of the signal after its propagation through the system as is visible in Figure 5.6 (b). The DM LD in this section was set to 20mA, this bias point ensured that the FBMC signal was not clipped at the laser threshold.

The experimental performance of the directly modulated FBMC system for various received optical powers levels are explained in Figure 5.7. Assuming a FEC limit at $2x10^{-3}$, in the back to back arrangement this limit was reached at approximately -21.4 dBm of average received optical power. The transmission of the ODSB signal modulated by 21 SMT subcarriers through 37 and 50 km of SSMF resulted in approximately 0.7 and 1.4 dB of performance penalty compared to the fibre-less transmission. Such negligible levels of degradation in performance clearly demonstrate the resilience of this CP-less MC modulation format to transmission impairment in an intensity-modulated system. The 8.4 Gbps data load was also transmitted through 75 km of SSMF, as trends in Figure 5.7 suggest, this resulted in approximately 2.3 dB of performance penalty at the FEC limit.

The experimental results following equalization and synchronization are also evaluated in terms of Error Vector Magnitude (EVM). Performance trends in terms of EVM are also presented in Figure 5.8, along with constellation diagrams measured at -19.4 dBm of received optical power.

By studying Figure 5.7 and Figure 5.8, it is clear that performance degradation increases for longer lengths of SSMF employed. This trend can be attributed mainly to the existence of intermodulation products created by the interaction of higher frequency subcarriers with laser nonlinearities, along with Signal to Signal Mixing Interference (SSMI) and dispersive

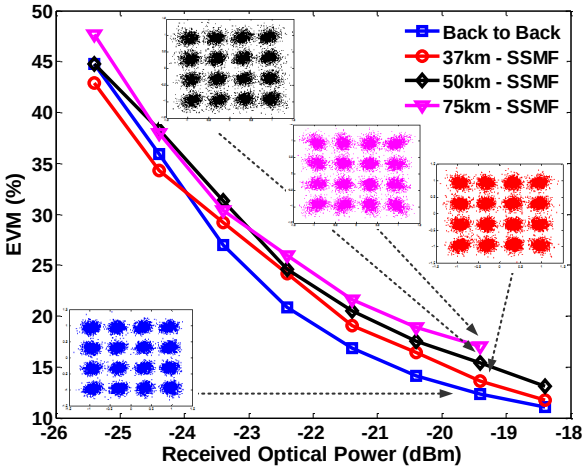

Figure 5.8. Experimental performance of the FBMC systems with 21 subcarriers in terms of EVM vs. Received Optical Power for back to back and fibre transmission scenarios. Constellation diagrams measured at -19.4 dBm

fading. The newly created spurious signals that are by-products of laser nonlinearity can interact further with fibre dispersion, causing a performance penalty, which is dependent on the propagation distance [199]. Figure 5.9 provides a better insight into this issue. This figure represents the performance of 21 quasi-overlapping subcarriers at -19.4 dBm of received optical power in terms of EVM vs. the subcarrier index. By studying Figure 5.5 and Figure 5.6 (a) it can be observed that the high frequency subcarriers in this SMT signal are being influenced by laser nonlinearity that sits close to the relaxation oscillation frequency. The impact of these spurious signals, which are significant for higher frequency subcarriers, is clearly visible in the back-to-back transmission as shown in Figure 5.9 for subcarriers 13-21, where EVM increases by 3-4%. However, with the inclusion of increasing fibre transmission, an increase in performance penalty at these subcarriers is evident. Similarly, the lower subcarriers 1-10 also show a performance penalty in the back-to-back scenario, this penalty mostly can be attributed to the fact that a small guard band

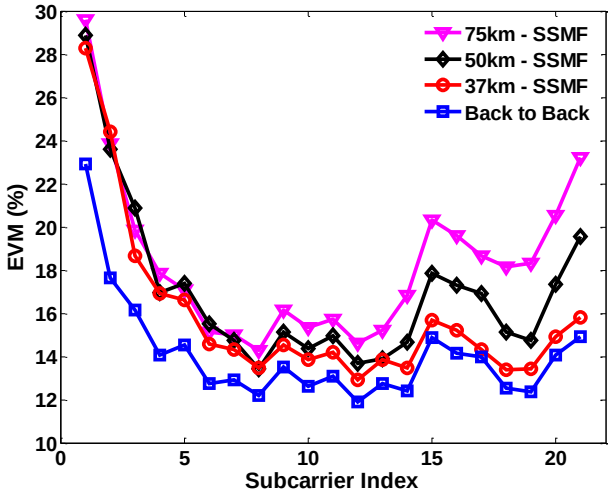

Figure 5.9. Experimental performance of the FBMC system with 21 subcarriers. In terms of EVM with respect to subcarrier index. Measured at -19.4 dBm.

was inserted between DC and the first subcarrier. In MC transmission systems like OFDM, which use DD, a common issue is the emergence of SSMI which lies close to DC. Thus, due to the absence of a large guard band close to DC, the lower frequency subcarriers are subjected to SSMI as well as to Second Order Intermodulation products (2IMDs) which also cause performance deterioration. By further examination, it is notable that the inclusion of fibre in the system also leads to the worsening of performance in the low frequency subcarriers. SSMI at low frequencies and dispersive fading at higher frequencies allow for the reduction of SNR at the affected subcarrier but their impact on the training sequence can also lead to an un-reliable estimate of the transmission channel. This inaccurate estimation may cause some crosstalk as a result of the IMI terms being filtered by the $\Re(\bullet)$ operator as was pointed out earlier in the previous subsections. Second and third order IMPs also impact the data and training symbols in the affected subcarriers but their impact is also known to be dependent on propagation lengths [199]. Consequently, the performance difference which is observed in Figure 5.9 between back to back and fibre transmission scenarios (37-50 km) can be attributed to the SSMI and the IMPs. However, at 75 km of transmission the higher subcarriers are also affected by some power attenuation as a result of dispersive fading, which cause a higher level of deterioration for higher subcarriers.

From the previous discussion, it can be concluded that fibre dispersion, solely does not pose a significant penalty to the CP-less SMT system. Thus, the equality that was expressed in equation (5.15) is validated for this experimental SMT signal propagating through such long lengths of fibre. To further clarify this issue the MC signal described in this section is modulated onto an optical carrier by an external MZM modulator. External modulators such MZMs compared to directly modulated lasers can provide a better performance in terms of nonlinearity, provided by their quasi-linear transfer function [122]. The results for this particular system are plotted in Figure 5.10, were negligible differences

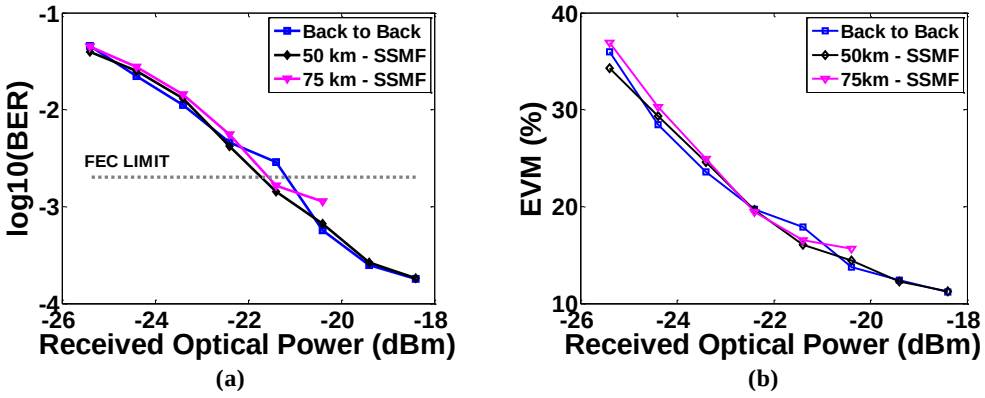

Figure 5.10. Performance of the SMT system with 21 carriers modulated using a MZM in terms of (a) BER vs received optical power and (b) EVM vs. received optical power

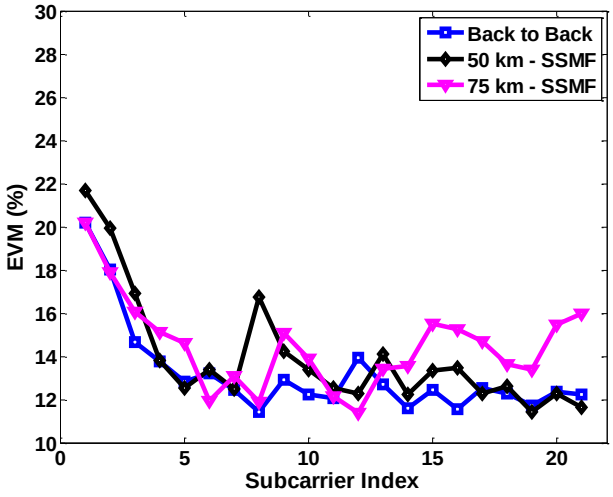

Figure 5.11. Experimental performance of the FBMC system with 21 subcarriers modulated by an MZM. In terms of EVM with respect to subcarrier index. Measured at -20.4 dBm

can be seen back to back and fibre transmission scenarios (numerical simulations are also presented in later chapters). The performance of this system is also expressed in terms of EVM vs subcarriers for various transmission schemes in Figure 5.11. By comparing this figure to Figure 5.9, the deterioration previously seen as a result of intermodulation products is significantly reduced. The reduced impact of third order IMDs (3IMDs) leads to a constant EVM at higher frequency subcarriers 10-21 with very slight increase in EVM with increasing fibre length. The reduced impact of 2IMDs also leads the performance in lower frequency subcarriers to be dominated mainly by SSMI, which seems to have a lower impact on channel estimation. The emergence of dispersive fading at 75 km is evident at higher subcarriers here.

5.3.2.2 Transmission at 10 Gb/s

In this case, a total of 25 subcarriers are assigned to the SMT signal which is subsequently directly modulated onto the DM laser biased at 20mA. The first subcarrier was modulated at 100 MHz, creating a guard band at DC. The net data rate was 10 Gb/s. The spectra at various points on the system are presented in Figure 5.12, and the high frequency powers were once again pre-emphasised to counteract the impact of power roll-offs. As Figure 5.12 (b) suggests, the propagation through 50 km SSMF results into approximately 5dB of power attenuation at highest frequency subcarriers as result of interaction of the ODSB signal with fibre dispersion leading to dispersive fading.

The performance for the directly modulated system is once again evaluated in terms of BER and EVM. Figure 5.13 presents these trends in terms of BER, in the back to back scenario the previously assumed FEC limit at $2x10^{-3}$ was reached at approximately -20.1 dBm of received optical power. Thus, the system has experienced a 1.3 dB penalty in back

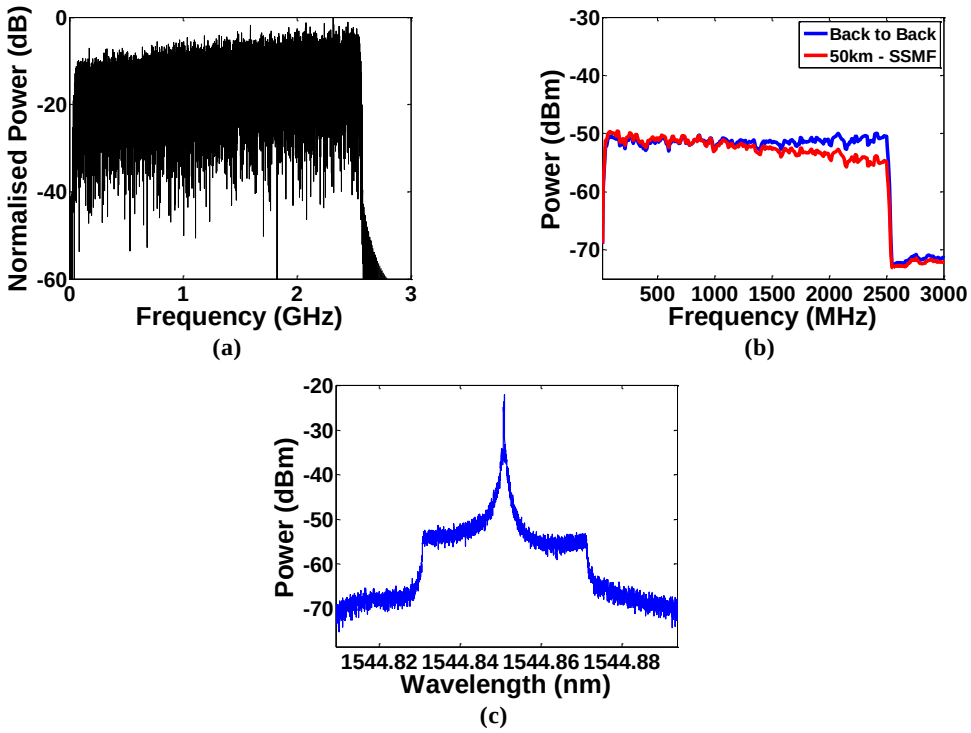

Figure 5.12. (a) Electrical Spectrum of 25 subcarriers at output of the AWG (b)Electrical spectrum for back to back and 50 km transmission and (c) optical spectrum in back to back (direct modulation)

to back by increasing the data rate from 8.4 to 10 Gb/s. Propagating the ODSB through 37 and 50 km of SSMF resulted in 0.5 and 0.6 dB of penalty respectively. Due to low optical power levels injected into the high losses arising from loss connectors in the system, enough power was not available to reach the FEC limit at the 75 km transmission experiment, thus this trend is linearly fitted to identify an approximate intercept point. As Figure 5.13 suggests the transmission of this 10G system through 75 km resulted in

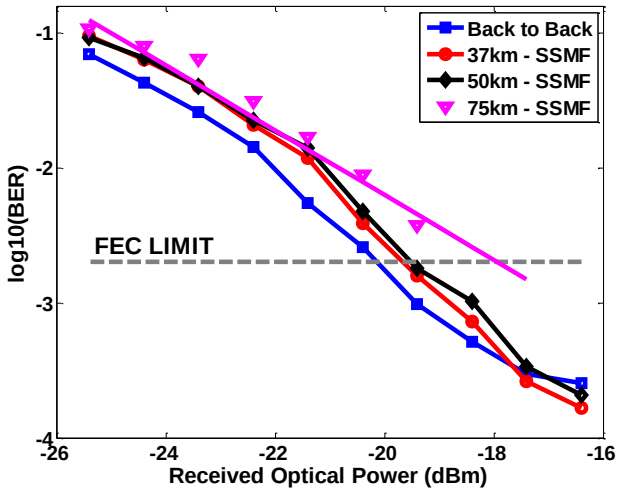

Figure 5.13. Experimental performance of the FBMC systems with 25 subcarriers in terms of BER vs Received Optical Power for back to back and fibre transmission scenarios

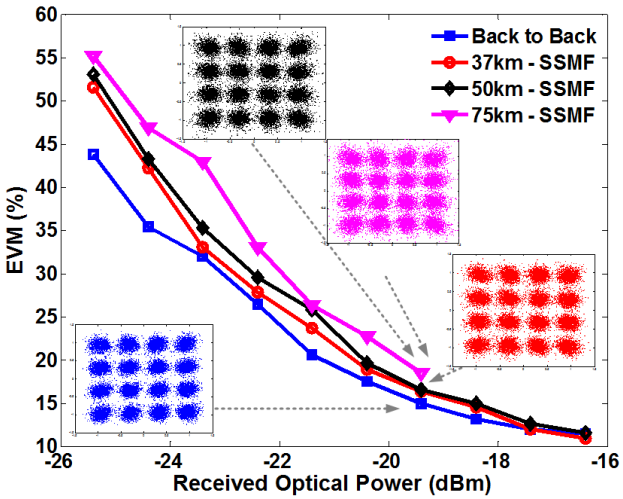

Figure 5.14. Experimental performance of the FBMC systems with 25 subcarriers in terms of EVM vs. Received Optical Power for back to back and fibre transmission scenarios. Constellation diagrams measured at -19.4dBm

approximately 2.2 dB performance penalty. The evaluated performance metrics in terms of EVM is presented in Figure 5.14 along with the measured constellation points.

Unlike the system with 21 subcarriers, the performance is not greatly affected after propagating though 37 and 50 km of transmission. This enhancement can be attributed to a reduction in strength of intermodulation products as result of a reduction in the average power per each subcarrier. The increase in the number of subcarriers results in a greater spread of the electrical drive power provided by the AWG across a larger bandwidth, which manifests itself as subcarriers with lower average powers. However, a degradation in system performance is observable for the 75 km transmission scenario at higher received optical power levels (-20 to -16 dBm), which is directly attributed to an increase in the impact of dispersive fading on the system.

5.3.2.3 Transmission at 12.4 Gb/s

In this section, the same laser diode biased at 20 mA is directly modulated with a total of 31 SMT overlapping subcarriers with symbol rate set at 100 MHz. The net data rate achieved was 12.4 Gb/s. Figure 5.15 shows the spectra at various points in the system. As can be seen in inset (b) of this diagram the higher subcarriers are also subjected to dispersive fading. Figure 5.16 shows the BER vs received optical power metrics for this setup. The FEC limit for the back to back system was reached at -19.8 dBm, compared to the 10 and 8.4 Gb/s systems, the figures show 0.3 and 1.6 dB of performance penalty respectively. Furthermore, transmission through 37 and 50 km induce an extra 1.9 and 2.6 dB penalty on the system. Figure 5.17 representes the performance in terms of EVM with respect to received optical power along with constellations at -18.4 dBm. Due to high

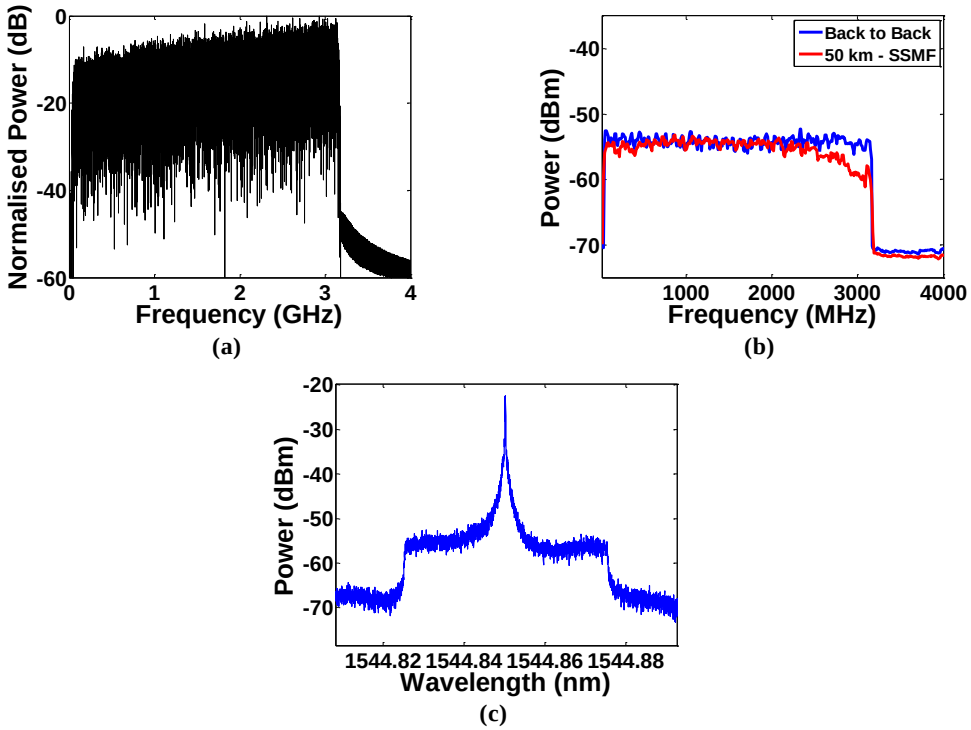

Figure 5.15. (a) Electrical Spectrum of 31 subcarriers at output of the AWG (b)Electrical spectrum for back to back and 50 km transmission and (c) optical spectrum in back to back (direct modulation)

losses as a result of dispersive fading, extra transmission lengths above 50km were eliminated from the system. With the increased number of active subcarriers and spread of available power across more tributaries, the strength of spurious signals are reduce, however with new subcarriers operating closer to the nonlinear region of the laser, nonlinearity will still exist in the system. As a result, the most effected subcarriers will be those at lower and higher frequencies. In the back-to-back scenario, SSBI and nonlinear terms will affect the lower set of frequencies and at high frequencies nonlinearity will

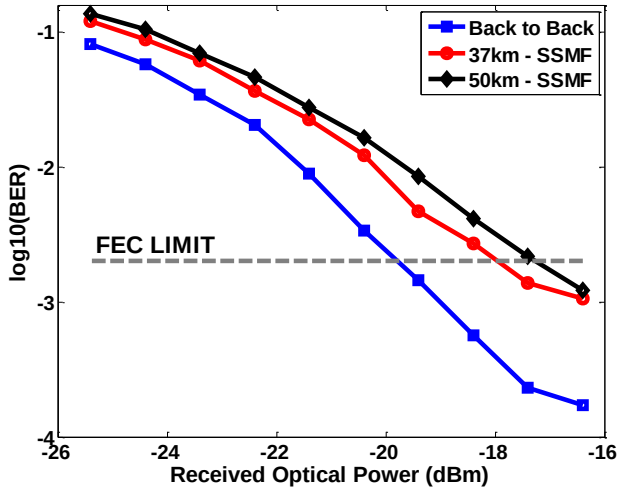

Figure 5.16. Experimental performance of the FBMC systems with 31 subcarriers in terms of BER vs Received Optical Power for back to back and fibre transmission scenarios

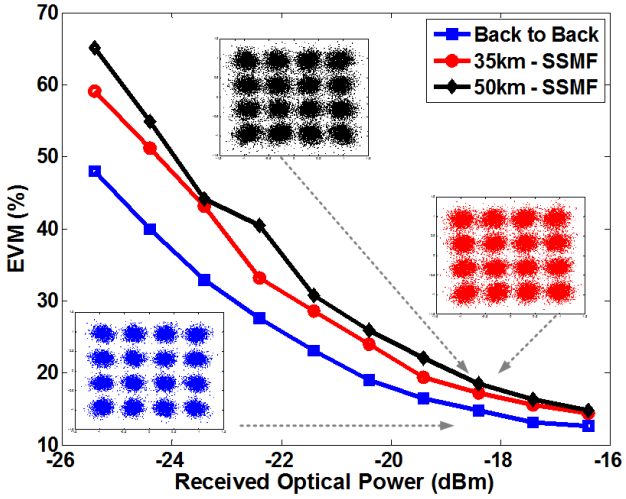

Figure 5.17. Experimental performance of the FBMC systems with 31 subcarriers in terms of EVM vs. Received Optical Power for back to back and fibre transmission scenarios. Constellation diagrams measured at -18.4 dBm

dominate. However, with inclusion of fibre transmission, higher frequencies can be further impacted by dispersive fading. These two mechanisms can affect the subcarriers at the two extremes by reducing the available SNR which may affect reliable channel estimation. The performance gains achievable by an external modulator are also tested in Figure 5.18, where negligible differences are seen between back to back and fibre transmission scenarios.

To investigate the origins of performance deterioration as a result of fibre propagation, each subcarrier is studied independently in Figure 5.19. In the back to back case, lower frequency subcarriers are dominated both by SSMI and some nonlinear terms, while the higher subcarriers are dominated by nonlinearity terms in the directly modulated case and reduced SNR levels in the external modulation case as a result of power roll-off imposed by the MZM at these subcarriers which are not compensated by the application of pre-emphasis. After transmission through 50 km the externally modulated subcarriers see a

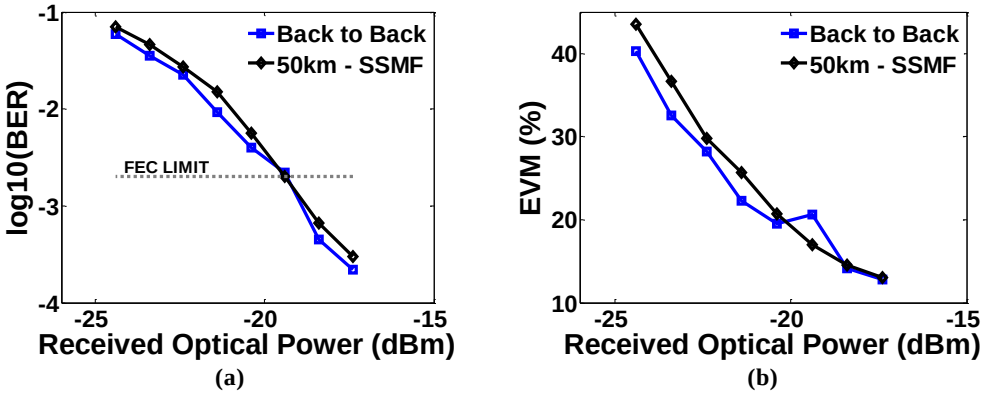

Figure 5.18. Performance of the SMT system with 31 carriers modulated using a MZM in terms of (a) BER vs received optical power and (b) EVM vs. received optical power

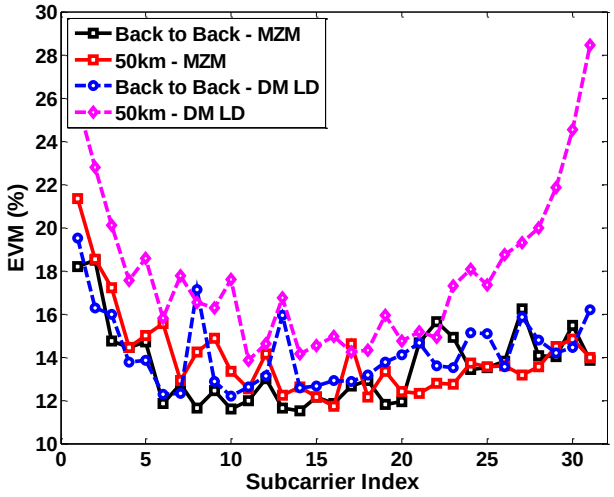

Figure 5.19. Experimental performance of the FBMC system with 31 subcarriers modulated by an MZM. In terms of EVM with respect to subcarrier index. Measured at -18.4 dBm

negligible degradation in terms of EVM over the complete band. However, in the directly modulated case, higher subcarriers exhibit a greater deterioration which can be attributed to RF power loss through dispersive fading and interaction of nonlinear terms with fibre dispersion. The exaggerated impact of dispersive fading on the system in comparison with the case were an external modulator was used is associated with laser chirping [127].

5.3.2.4 Transmission at 14.8 Gb/s

To push the limits of the SMT system proposed earlier, a total of 37 subcarriers are employed in this directly modulated system. This signal with 3.7 GHz bandwidth, delivered a net data rate equivalent to 14.8 Gb/s. Due to the impact of dispersive fading only 37 km of fibre transmission was possible in this setup. Figure 5.20 illustrates a set of electrical and optical spectra for this system; inset (c) also illustrates the existence of dispersive fading effecting subcarriers residing between 2.5-3.8 GHz. Figure 5.21 presents the back-to-back and fibre transmission system performances. In the back to back scenario the FEC limit was reached at -17.5dBm, Figure 5.21 indicates a 3.9/2.6 and 2 dB performance penalty compared to the 8.4Gb/s , 10 Gb/s and 12.4 Gb/s systems. At the FEC limit, negligible difference is seen in performance compared to the fibre transmission scenario.

The performance in terms of EVM along with constellation diagrams which were measured at -18.4 dBm of average received optical power are presented in Figure 5.22. The performance in each case is further studied in terms of EVM per subcarrier in Figure 5.23 at -18.4 dBm of average received optical power. In the back to back case we can see that the low subcarriers are again dominated by SSMI and nonlinear terms, subcarriers residing around index=31 are experiencing a similar performance compared to the system using 31

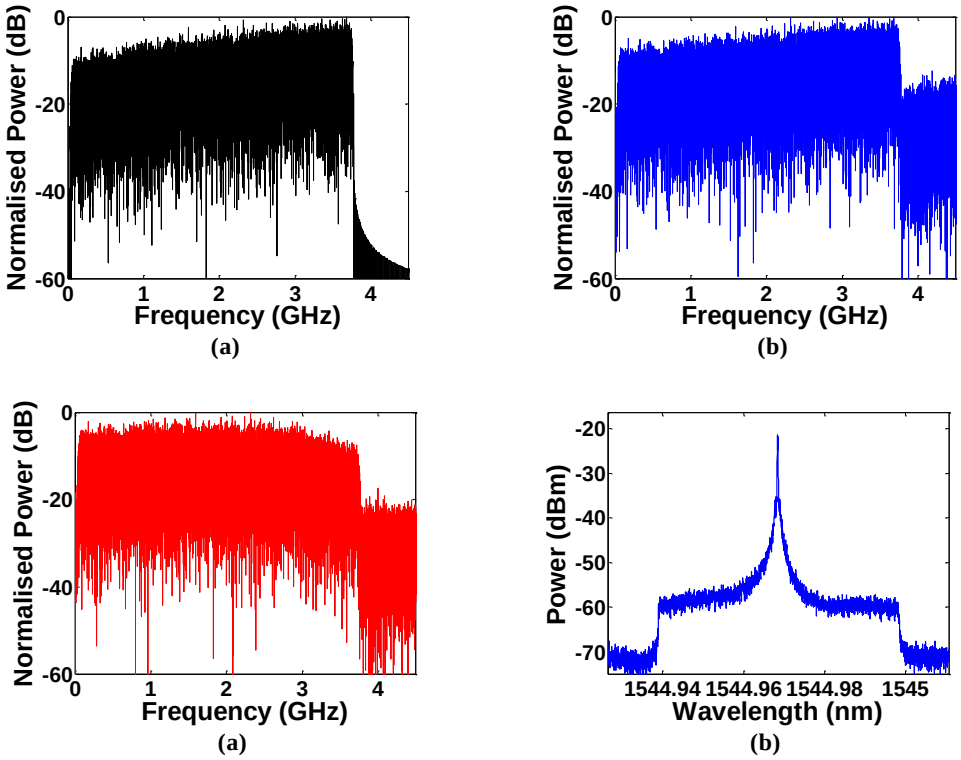

Figure 5.20. (a) Electrical Spectrum of 37 subcarriers at output of the AWG (b)Electrical spectrum for back to back and (c) 50 km transmission and (d) optical spectrum in back to back (direct modulation)

subcarriers (Figure 5.19), however this performance reaches 30 % EVM at index=37, which can only be attributed to the close approach to the relaxation oscillation peak and creation of stronger interfering spurious signals in the region. After propagating through 37 km of fibre, low frequency subcarriers (index=1-10) experience negligible performance difference however those operating at higher indexes do experience some deterioration as result of fading and nonlinear terms which apart from impacting raw data can interfere with

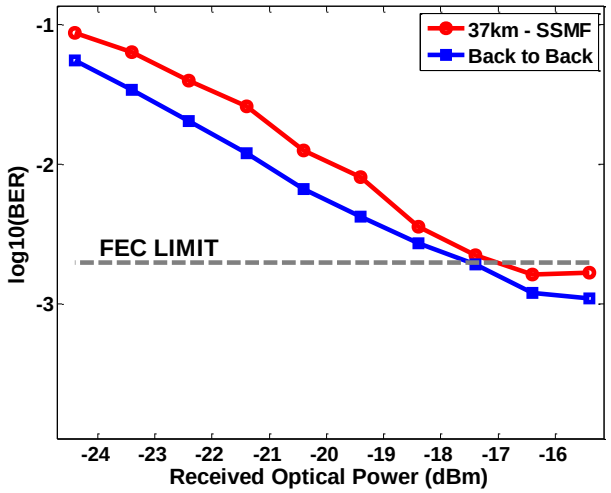

Figure 5.21. Experimental performance of the FBMC systems with 31 subcarriers in terms of BER vs Received Optical Power for back to back and fibre transmission scenarios

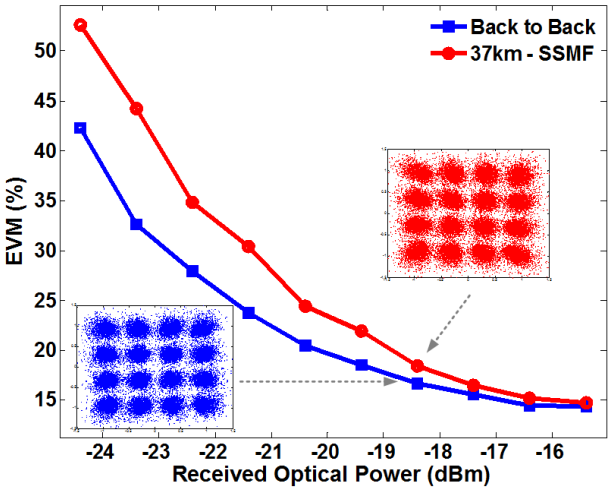

Figure 5.22. Experimental performance of the FBMC systems with 37 subcarriers in terms of EVM vs. Received Optical Power for back to back and fibre transmission scenarios. Constellation diagrams measured at -18.4 dBm

training symbols and subsequently give rise to miss-estimation of channel coefficients.

5.4 Exploitation of FBMC in uplink transmission in PON

The interest in MC systems such as OFDM, in point to multi point (p2mp) architectures such as PON, originates from their ability to subdivide the available bandwidth amongst multiple entities. This subdivision of bandwidth into individual tributaries in frequency allows for an efficient and flexible distribution of resources amongst multiple users. In highly efficient MC systems that employ orthogonality, apart from carrying out channel

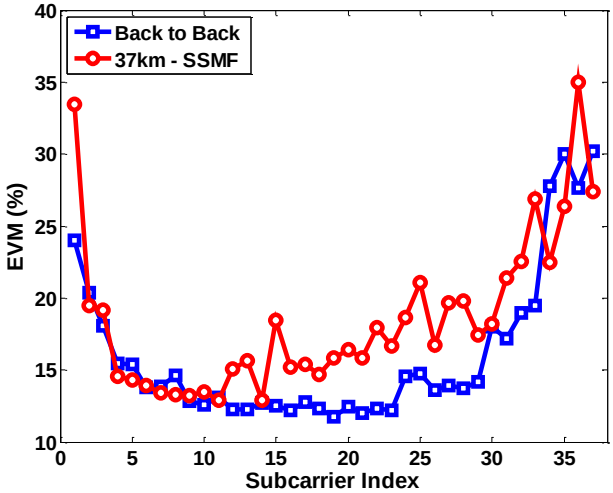

Figure 5.23. Experimental performance of the FBMC system with 37 subcarriers modulated by an MZM. In terms of EVM with respect to subcarrier index. Measured at -18.4 dBm

estimation, time and frequency synchronization is also required at the receiver-end in order to preserve that inherent orthogonality amongst multiple tributaries. Since in the downlink channel in a p2mp topology each user receives a complete copy of an OFDM band, the preservation of orthogonally via synchronization at each receiver becomes trivial and practical as it is the case in standardized technologies such as LTE. Similarly, at the uplink, orthogonality amongst all received subcarriers must also be preserved to omit any ISI or ICI. However, in the uplink, since each user transmits its own subset of subcarriers independently, individual frequency and timing de-synchronization is accumulated for each subcarrier subset. Thus, synchronization of the received subcarriers at the uplink receiver will not be as trivial as in the downlink; this is due to the fact that synchronizing the subcarriers from one user may cause miss synchronization of the subcarriers from the other users.

The field of optical communications has seen a tremendous exploitation of OFDM in various network topologies ranging from access to core [66, 67]. However, the majority of these studies have assumed a point-to-point type architecture. Most of studies on OFDM-PON have experimentally evaluated the multi user uplink architecture [192, 193, 200], but the largest portion of these studies was aimed at combating well known issues such as Optical Beat Interference (OBI) [67]. Therefore, these experimental demonstrations have neglected the possible impact of system de-synchronization and the resulting Multiple Access Interference (MAI) by means of creating guard bands in frequency between subsets of subcarriers, each originating from various ONU, along with assigning dedicated transmitter and receiver pairs to represent each ONU and OLT. The separation of ONUs in frequency alleviates the required orthogonality conditions to be met between neighbouring ONUs in frequency. In wireless communication standards the inclusion of empty guard bands in frequency may prove effective, provided by the high granularity in these system's bandwidth [30], which does not lead to high losses in bandwidth efficiency. However, adaptation of such techniques in the field of optical communication in topologies such as PON may lead to reduced bandwidth efficiencies with a rising number of uplink users, due to the large bandwidth assigned to each subcarrier. Such issues motivate the need for the elimination of frequency guard intervals in p2mp PON topology.

In PONs subsequent to ensuring synchronization amongst the transmitters at the ONUs and the receiver at the OLT, the possible contributors to MAI in a guard-band-less system become the Carrier Frequency Offset (CFO) from each ONU and the relative timing delays amongst the ONUs. The impact of CFO is attributed to the scenarios were coherent detection is used at the OLT in order to eliminate the OBI problem [67]. However the source of MAI can be reduce only to the impact of relative time delays between ONUs by

using intensity modulation at the ONUs and direct detection at the OLT [24]. Furthermore, as each ONU will be connected to the remote node by a geographically independent fibre cable, there will be a relative delay amongst all ONUs, and to add to the complexity here, the delay that each fibre experiences can also drift with respect to the temperature [194], this makes the propagating waveforms susceptible to environmental drifts as result of the thermo-optic effect in silica [201]. Therefore, in a practical system, adaptive techniques are required to measure and correct for this varying delay. Recently in [194], an adaptive method to alleviate MAI as a result of drifting temperatures was proposed for OFDMA-PON, where the system used the synchronization symbols along with estimated channel responses to approximate the delay at each ONU which were then used to time align each ONU independently. This method was also employed in a field trial, however insufficient results were supplied to demonstrate the effectiveness of the system compared to a guard-band-less system.

In a comprehensive work carried out in [27], the performance of OFDM for uplink PON using frequency guard bands was evaluated, and it was found that regardless of the guard band employed, MAI was still experienced. This resulting MAI emerges from the long side-lobes of subcarriers in neighbouring ONUs, which may require a frequency guard

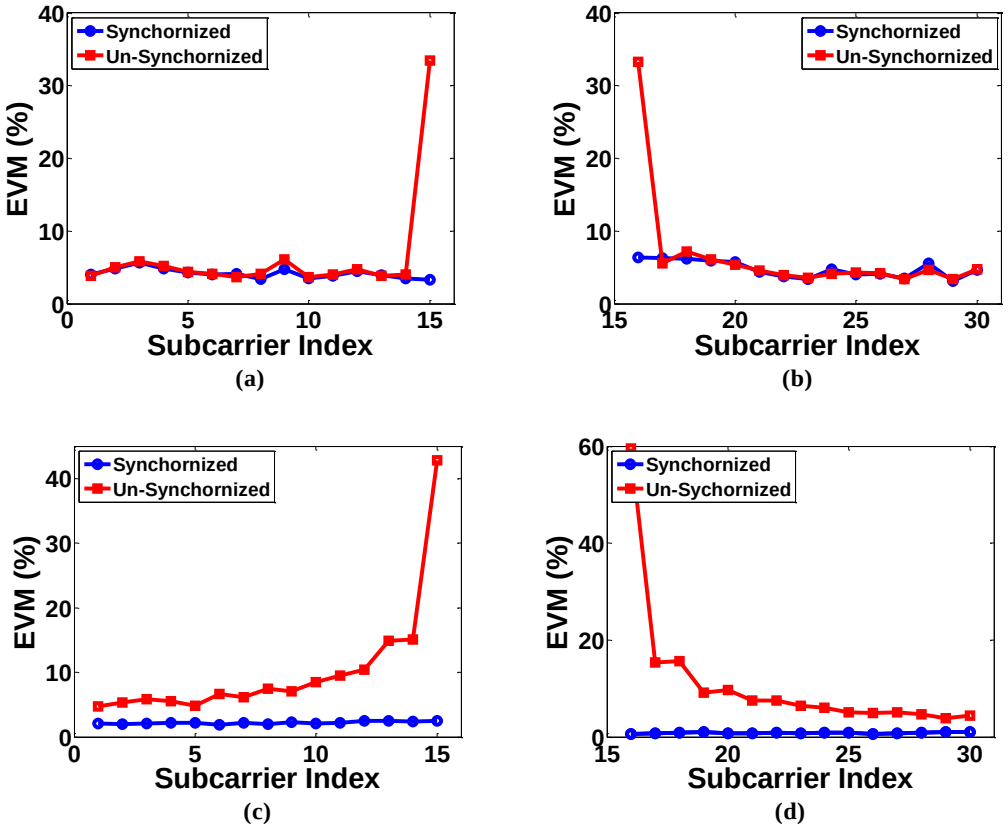

Figure 5.24. Numerical Simulations representing the performance of two sets of subcarriers from two users in terms of EVM with a synchronized and unsynchronized relative delay (a)FBMC subcarriers 1-15 (b) FBMC subcarriers 16-30 (c)OFDM subcarriers 1-15 (d) OFDM subcarriers 16-30

band with a size equal to multiple subcarriers spacing to be fully suppressed. The incapability to supress MAI with small guard bands in OFDM can significantly decrease the bandwidth efficiency in the uplink, where the need for bandwidth efficient means of data transport is significant [24]. However due to the well localized properties of the prototype functions used in FBMC, in [24] by using the Mirabbasi-Martin filter as was proposed by Phydas [202] for wireless systems, they were able to show that a guard band as narrow as one subcarrier spacing is sufficient to remove all MAI resulting from miss-synchronization between ONUs. This suggests that FBMC can have superior performance to OFDM even in guard-band-less system, where residual unaccounted synchronization errors can only affect neighbouring subcarriers.

To demonstrate FBMC's superiority with regards to synchronization errors, numerical simulations are carried on FBMC and OFDM based systems. The FBMC signal in this system takes on an architecture as was presented at the start of this chapter. In both the OFDM and FBMC systems two users are assumed, each users accounts for fifteen 16-QAM modulated subcarriers and a data rate equivalent to 6 Gb/s. The subcarriers are assigned to each ONU such that the highest frequency subcarriers from user one overlaps that lowest frequency subcarrier of user two, thus there is no guard band between the two. In this simulation, only the impact of timing errors as a cause for MAI is considered. Figure 5.24 (a-b) presents the results for this numerical simulation for the FBMC based system, in the presence of a timing delay between the two users, it is clearly visible that overlapping subcarriers (index 15-16) suffer from MAI, thanks to the well localized properties of prototype filters. However in the case of the OFDM, Figure 5.24 (b-c) it is clearly visible that nearly all subcarriers are affected by MAI as result of the Sinc profile of the subcarriers.

5.4.1 Experimental Setup

The experimental setup used to evaluate FBMC for uplink PON is depicted in Figure 5.25. Table 5.2 lists the physical parameters employed in this experimental setup. The aim of this experimental setup was to analyse the impact of MAI as a result of inter-ONU timing offsets on the performance in OFDM-PON and FBMC-PONs. The waveforms for each ONU are created offline using Matlab and are later loaded into an AWG. The common subcarrier spacing used for both ONU's is 100 MHz and all subcarriers are assigned to be modulated by 16 QAM. The parameters used to create the FBMC signals for each ONU are listed in Table 5.3. The operating frequencies of the subcarriers in each ONU are chosen such that it does not lead to any frequency guard bands, and hence, adjacent subcarriers from the two ONUs will overlap in frequency once they arrive to the OLT. The prototype

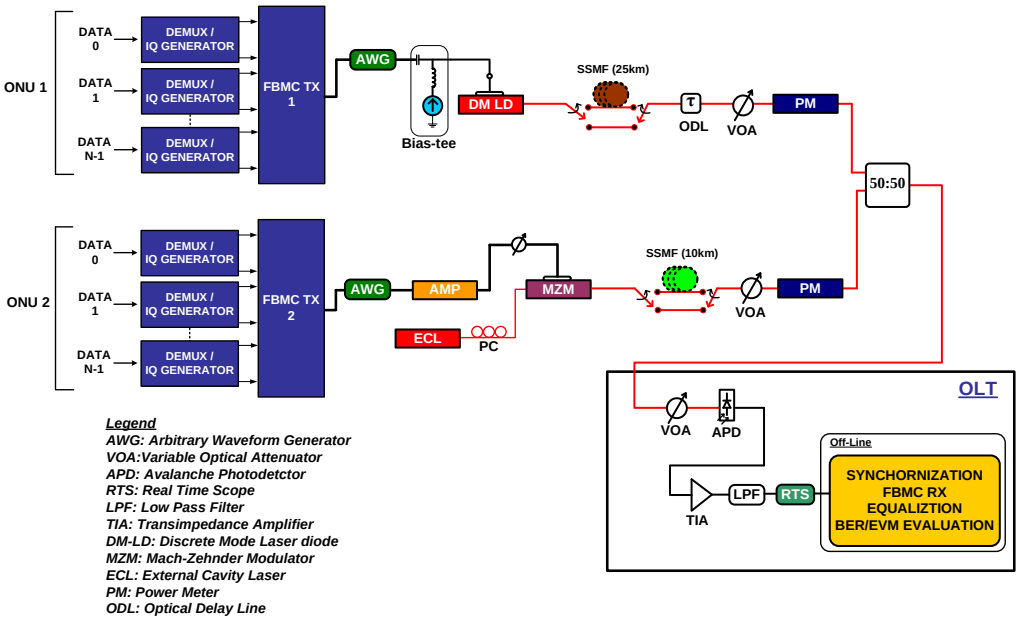

Figure 5.25. Uplink Experimental setup with two ONUs

function employed here is a SRRC with a roll-off-factor equal to 0.5. In this section unless stated, fifteen subcarriers were assigned to each ONU, which means a total of 12 Gb/s is received at the OLT.

The DM laser is biased at 20 mA, and is directly modulated by the output of the first AWG. The MZM is biased at the quadrature point. The drive signal for the MZM after being generated from the second AWG is electrically amplified and attenuated accordingly to generate the required drive voltage level allowing operation within the linear region of the

Parameter	Value
Frequency spacing (v_0)	100 MHz
Number of active subcarriers (N) per ONU	15 / 21
Net data rates per ONU	6 / 8.4 Gb/s
Modulation format	16 QAM
Assigned frequency to first subcarrier - ONU 1	100 MHz
Assigned frequency to first subcarrier - ONU 2	1.6 GHz
Prototype function $g(t)$	SRRC
Roll off factor α	0.5
Number of OFDM symbols per frame	1024
CP overhead	0 %
Total No. of QAM symbols per frame	15360 / 21504
Overheads for training sequence	4 %
No. of frame transmitted per evaluation	20

Table 5.3. Parameters used for the generation of the FBMC signals for uplink PON

MZM. The use of a directly modulated laser and a MZM for two different ONUs can represent the achievable diversity in uplink PON by FBMC. To avoid the effects of OBI, the wavelength difference between the DM laser and the ECL is chosen to be sufficiently large. Subsequently, the generated optical signal from the DM laser is passed through an Optical Delay Line (ODL) capable of providing delays up to 300 ps. The ODL here provides the means for manual correction of the loss of orthogonality between inter-ONU subcarriers which had been caused by a difference in the propagation delay of optical signals. Delays can also be introduced electrically, by delaying the waveforms at the AWG, but are limited by the sampling rate of the AWG, while the ODL can provide smaller delay steps. Given the high microwave frequency bands used here, a small difference in path lengths between the two ONU2 prior to reaching the 50:50 power combiner in the remote node combiner can lead to significant synchronization errors. Thus, in the back-to-back case, different length patch cords can also give rise to MAI. The uplink FBMC topology is also tested in the presence of fibre propagation after each ONU. Practical drop fibres in PONs take on short lengths prior to reaching the power combiner at the remote node, however assuming the worst case scenario here the two ONU's are propagated through 10 and 25 km of SSMF before being combined at the remote node. The two VOAs prior to the 50:50 combiners are used to match the signal power from the two ONUs prior to their arrival at the OLT. At the OLT the photo-detected signal is passed through an ADC, the resulting digital signals are then sent to Matlab for offline processing. In the offline processing stage the signal from each ONU is synchronized in time and is then sent to a common receiver where channel equalization for both ONUs is also carried out. Since direct detection had been employed at the OLT, the impact of CFO and laser noise can be neglected thus the MAI mainly emerges from the differential delay between the ONUs.

5.4.2 Experimental Results

In this section fifteen subcarriers are added to each ONU. The DM laser is modulated with the subcarriers operating at lower set of frequencies and given the large bandwidth of the MZM the subcarriers operating at higher frequencies (up to 3.1 GHz) are externally modulated onto the ECL by the MZM.

The measured electrical spectra received by the OLT for this uplink system using either OFDM or FBMC is presented in Figure 5.26. By looking at these spectra it is clearly notable that at the OLT the subcarriers from ONU1 and ONU2 experience some overlapping since no frequency guard band was employed here. However, these overlaps tend to extend over multiple subcarriers for OFDM but due to the superior attenuation of

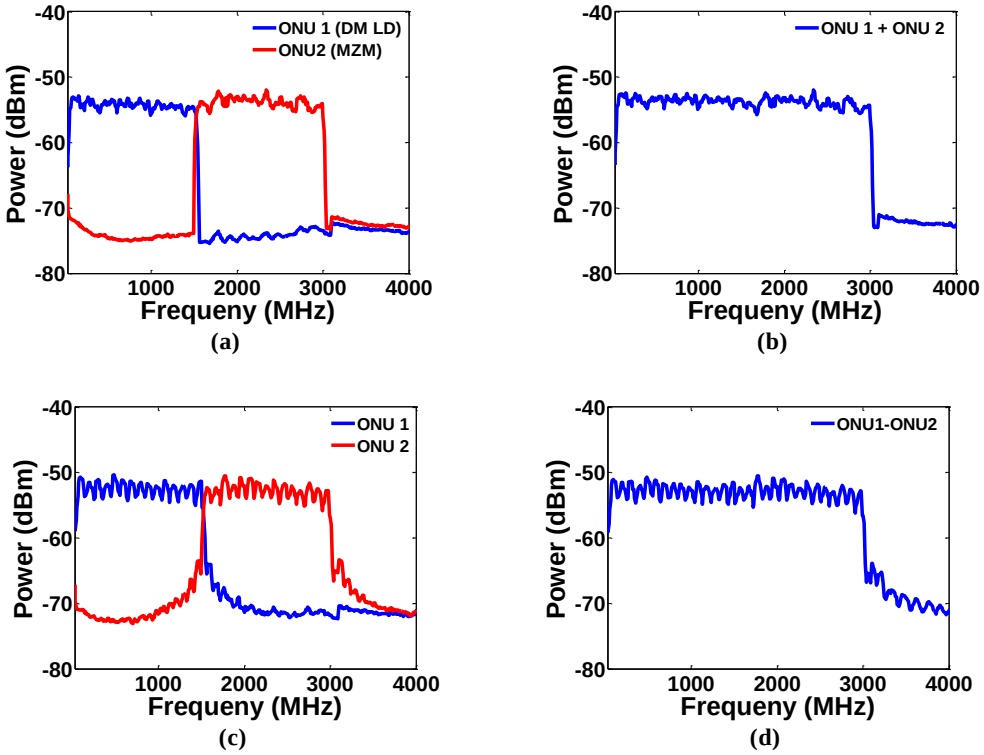

Figure 5.26. Measured Electrical spectra's received at the OLT for (a) only ONU1/ONU2 FBMC system (b) combined ONU1/ONU2 based on FBMC, (C) only ONU1/ONU2 based on OFDM, (d) combined ONU1 and ONU2 based on OFDM

side lobes in FBMC this overlap is restricted to one neighbouring subcarrier only. Furthermore in the case of ONU 2 in figures Figure 5.26 (a-c), the low frequencies exhibit a non-flat response, this in-fact is the SSBI rising from the MC system.

The numerical results that were presented in Figure 5.24 are next validated by using the experimental setup used in this section. The optical signal from each ONU is allowed to propagate through two un-match optical paths before reaching the power combiner. Upon arrival at the OLT, at a set received optical power of -14.4 dBm the signal from each ONU is then evaluated in terms of EVM vs subcarrier. The performance of each subcarrier is then evaluated in terms of extreme timing de-synchronization and synchronization, where timing synchronization between the two ONUs is achieved by either delaying the electrical signal at the ONU or by fine tuning the optical delay by using the ODL. By studying the trends in Figure 5.27, it can again be seen that MAI in FBMC only affects one subcarrier at most, where as in OFDM a series of subcarriers are affected.

The colormap in Figure 5.28 illustrates the performance of all 30 overlapping subcarriers from the two ONUs received by the OLT, whose' performance is evaluated in terms of EVM as a function of both subcarrier index and timing delay. The performance at each point is evaluated by setting the received optical power at the OLT to -14.4 dBm. This figure clearly indicates the performance of the uplink system in the presence of a timing

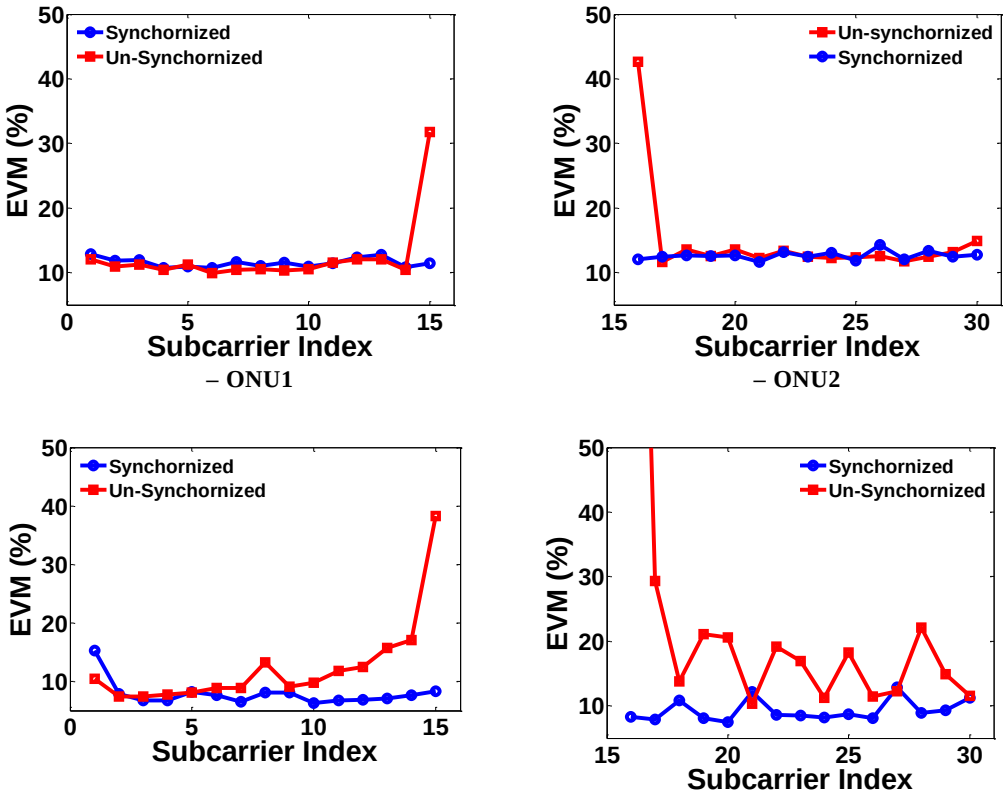

Figure 5.27. Experimental results representing the performance of two sets of subcarriers from two users in terms of EVM with a synchronized and unsynchronized relative delay (a)FBMC subcarriers 1-15 (b) FBMC subcarriers 16-30 (c)OFDM subcarriers 1-15 (d) OFDM subcarriers 16-30

error between the ONUs. However, it can also be seen that by using the ODL as shown in the experimental setup, it is possible to eradicate the timing errors and eliminate the MAI as shown in Figure 5.28 for the neighbouring subcarriers of ONU1 and ONU2. In this figure some other subcarriers apart from the neighbouring subcarriers also show some

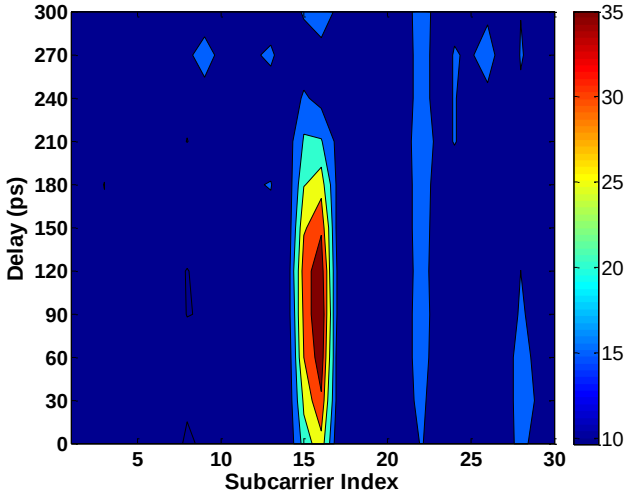

Figure 5.28. Performance of the 30 overlapping subcarriers received by the OLT from two ONUs in terms of EVM as function of subcarrier index and imposed timing delay

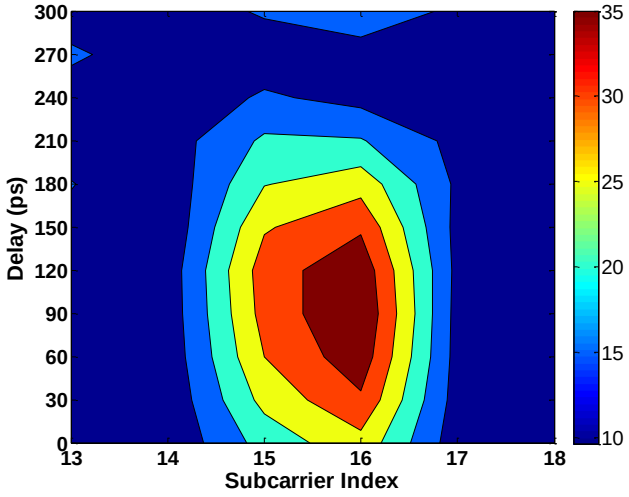

Figure 5.29. Performance of the neighbouring overlapping subcarriers received by the OLT from two ONUs in terms of EVM as function of subcarrier index and imposed timing delay

degradation in performance (i.e. subcarrier 8/22/29), that can be attributed to individual effects of the channel. Figure 5.29 illustrates a better view of the MAI of the system, as it was previously demonstrated by experimental and numerical results, MAI only significantly effects overlapping subcarriers which in the case of FBMC is only adjacent subcarriers, as this figure shows regardless of the imposed timing delay, only subcarriers 15-16 are deteriorated. Furthermore, it can be concluded that the performance of the subcarriers impacted by MAI in this case is a function of the timing delay.

In Figure 5.30, trends are also presented in order to evaluate the performance of each ONU in terms of their BER with respect to the received optical power at the OLT. In this figure, similarities can be seen between ONU1 and ONU2 operating individually in absence of the secondary ONU. By correcting for the timing delay between the two ONUs, and adjusting

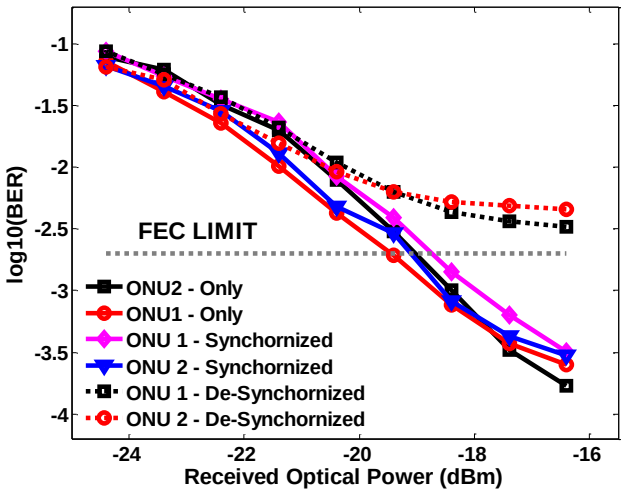

Figure 5.30. Performance of Each ONU in terms of BER vs Received Optical Power in presence and absence of a secondary ONU and in presence and absence of timing synchronization

the delay at the ONU from 1 to 270 ps according to Figure 5.28, the performance trends for the two simultaneously operating ONUs is similar to the scenario where each ONU had operated individually. This indicates to the disappearance of MAI and the preservation of orthogonality amongst the inter-subcarriers in ONU1 and ONU2. However, by eliminating the orthogonality between the two users by setting the imposed time delay to 90 ps, results in an error floor for both ONUs above the FEC limit.

According to Figure 5.29, by delaying ONU1 by 270ps the MAI which arises due to the loss of orthogonality between the two ONUs can be removed. However this required delay is not fixed, and can emerge in a periodic manner as the delay is increased, where the period is directly related to the frequency of subcarriers overlapping one another in ONU1 and ONU2. Due to the limited delay available from the ODL this factor was not illustrated in Figure 5.29. To illustrate this issue further, a further experiment was required, where the number of subcarriers per each ONU is raised to 21, increasing the net data rate from both ONUs at the OLT to 16.8 Gb/s. This increase in number of subcarriers results in the increase of the highest frequency subcarrier in ONU1 which overlaps the first subcarrier in ONU2. Figure 5.31 illustrates the performance of all 41 overlapping subcarriers from the ONU received at the OLT in terms of EVM as function of subcarrier index and relative imposed delay. The figure suggests that lowest subcarrier in ONU1 and highest subcarriers in ONU2 suffer from extra level of deterioration. In case of ONU 1 this can be attributed to a reduced level of power per subcarrier compared to the previous section, and an increase in power of nonlinear spurs. In the case of ONU2 this degradation at higher subcarriers can be attributed to power roll offs from the system and possible nonlinear terms from the directly modulated laser in ONU 1. However, by studying the neighbouring subcarriers 21-22, it is visible that cannot be attributed to MAI, since the same impact is not visible for

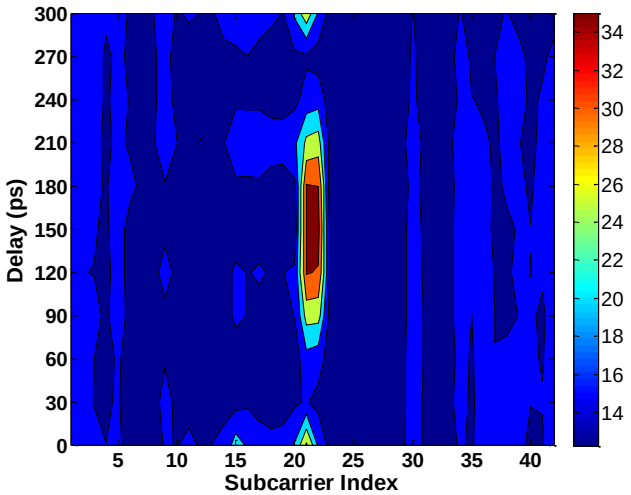

Figure 5.31. Performance of the 42 overlapping subcarriers received by the OLT from two ONUs in terms of EVM as function of subcarrier index and imposed timing delay

ONU2 and at relative delays at which MAI is maximum (i.e. 150ps of delay). In Figure 5.31, it is clear that MAI reduces at multiple points as the relative delay in increased, the period between these two points is approximately 227ps which corresponds to half of the period of the subcarrier operating at 2.2 GHz. In equation (5.1) it was noted that to be able to establish orthogonality a $\frac{\pi}{2}$ term was needed between adjacent subcarriers. The timing delays between the two ONU in fact results in deterioration of this imposed phase shift between the overlapping adjacent subcarriers, leading to MAI. Thus this factor implies that by the maximum and minimum MAI should be observed, periodically as the highest frequency in ONU1 is delays by quarter of it's period or $\frac{\pi}{2}$ radians. In the 21 carrier subcarrier case this time delay is 113ps, which is measurable in Figure 5.31 and in the 15 subcarrier case this required delay is 156ps which again is measurable from the experimental results in Figure 5.28.

In [187] the impact of dispersion on FBMC type signals was placed into three categories, 1) Delay between neighbouring subcarriers 2) Broadening of pulses in each subcarrier, 3)Linear impairment to each subcarrier in the form of a phase and amplitude shift. The third impairment caused here can be corrected for by channel equalization techniques as would be the case in OFDM systems. The tolerance to dispersion induced pulse broadening is high in MC systems such as OFDM and FBMC, due to the low subcarrier width employed, thus this tolerance can also be optimized at higher accumulated dispersion values by reducing the subcarrier's width. By reducing the subcarrier spacing, the delay experienced by neighbouring subcarriers can be further reduced and can lead to increased

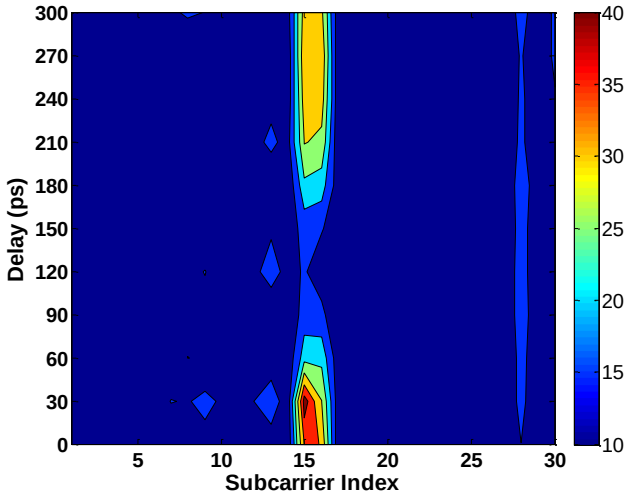

Figure 5.32. Performance of the 30 overlapping subcarriers received by the OLT from two ONUs after propagating drop fibres in terms of EVM as function of subcarrier index and imposed timing delay

performance for FBMC as it was pointed out to in Figure 5.3. Thus, the lead cause of MAI experienced by two neighbouring inter-ONU subcarriers as was presented in previous examples is analogous to the impact that dispersion has on delaying neighbouring subcarriers. In [187] the impact of a large accumulation of dispersion on FBMC systems was studied for cases were the CP-less transmission lead to performance deterioration. In this study it was found that the increased accumulation of dispersion which leads to large delays between neighbouring subcarriers can cause a loss of orthogonality and introduce crosstalk from neighbouring time-frequency points (i.e. IMI passing through the Real operator).

Next, drop fibres are also included to each ONU prior to being combined at the ODN. In order to examine the worst-case scenario, the signal from ONU1 is transmitted through 25 km of SSMF and the signal from ONU 2 is transmitted through 10 km of SSMF. Figure 5.32 presents the performance as a function of a timing delay introduced to ONU 1, were the impact of MAI on the system is clearly seen. These results demonstrate that in the presence of arbitrarily chosen large lengths of drop fibres MAI still affects the inter-ONU neighbouring subcarriers similar to the scenario where no drop fibres were employed, and again it can be fixed by adjusting the relative delay. Figure 5.33 presents an understanding of the performance of the two ONUs following propagation through different lengths of optical fibre. Operating each ONU independently results in comparable trends to the case where both ONUs operated simultaneously where synchronization was obtained by delaying ONU 1 by approximately 120 ps. However, operating with a relative delay between the two ONUs results in both ONU's performance reaching an error floor above

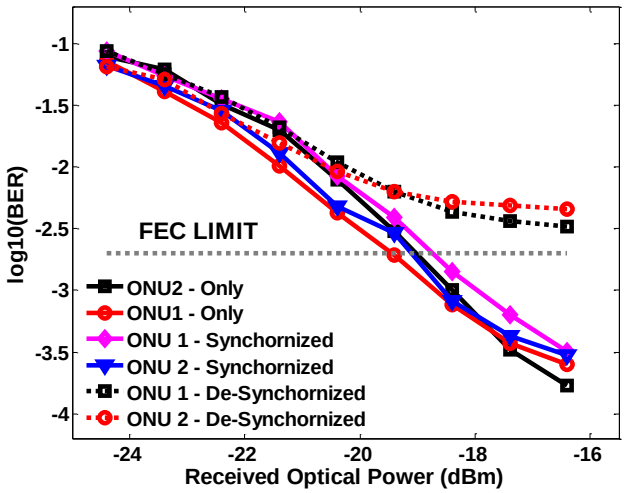

Figure 5.33. Performance of Each ONU in terms of BER vs Received Optical Power in presence and absence of a secondary ONU and in presence and absence of timing synchronization. With fibre transmission

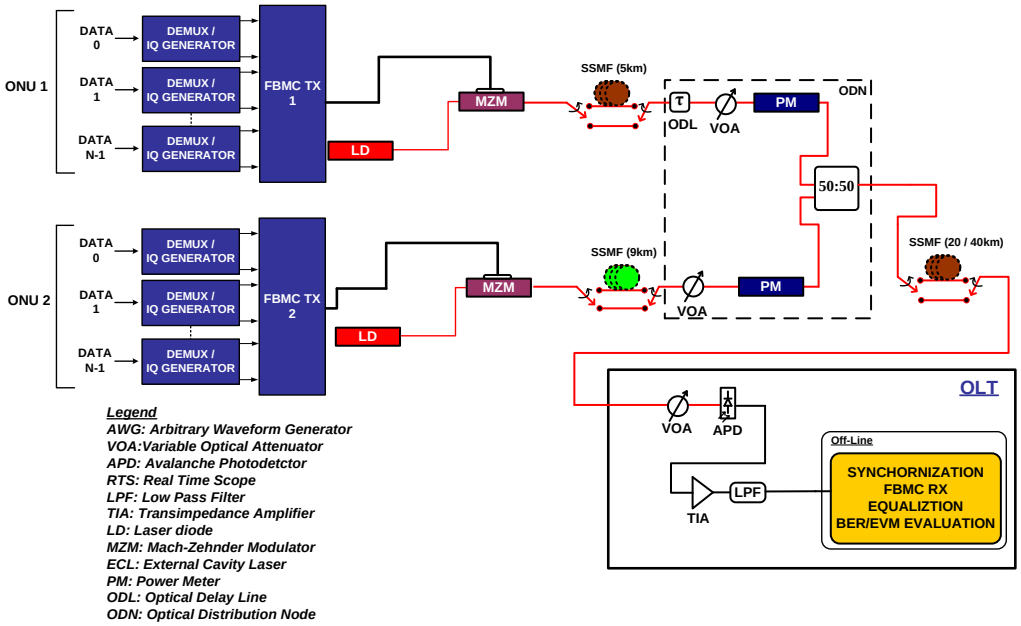

Figure 5.34. Uplink Simulation setup with two ONUs

the FEC limit. Comparing the trends in Figure 5.32 to the results obtained in the absence of fibre propagation (Figure 5.30) negligible difference is seen in both cases.

5.4.3 Simulation Results

In the previous section, small and large lengths of SSMF links were used for the drop fibres connecting the ONUs to the ODN and it was found that increasing the length of these links to the extremes does not result in an increase in MAI. In this section the impact of MAI is also studied on the system through numerical simulations. Trends are also provided for the inclusion of a feeder fibre between the ODN and OLT. Figure 5.34 shows the system setup that was implemented in Matlab for numerical simulation, to accommodate faster simulation times both ONUs are equipped with MZMs biased at the Quadrature transmission point. For simplicity, the impact of laser RIN and fibre nonlinearity are neglected here.

To understand how the numerical results will reflect the experimental trends, Figure 5.35 shows the experimental results of a FBMC system composed of 21 or 31 subcarriers modulated by a MZM intensity modulator for back to back and fibre propagation scenarios. These results show good agreement with the numerical results. Next, the system presented in Figure 5.34 is simulated, a similar subcarrier assignment as in the previous section is employed here with 15 subcarriers per ONU. By eliminating the feeder fibre and setting the received optical power at the OLT to -14.4 dBm and adjusting the optical delay at one ONU, the impact of MAI is measured and is plotted in Figure 5.36. These numerical results again show good agreement with the experimental results, indicating that MAI at most affects only the two neighbouring inter-ONU subcarriers. MAI is reduced as a result of a

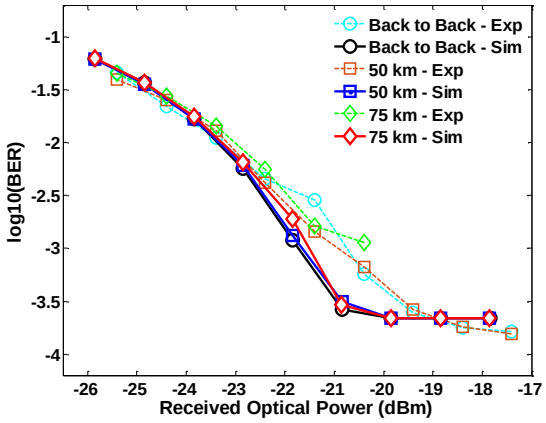

(a)

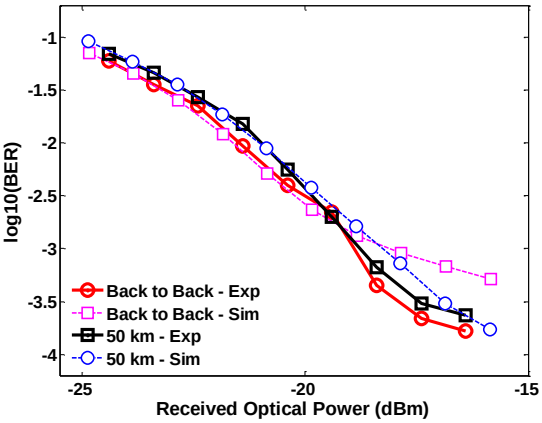

(b)

Figure 5.35. Numerical and experimental results for a FBMC system modulated by a MZM with (a) 21 subcarriers (b) 31 subcarriers

restoration in orthogonality of the two neighbouring subcarriers by adjusting the timing delay between each such that the $\frac{\pi}{2}$ phase shift between these two subcarriers is restored. As a result, MAI reduces in a periodic manner, which in this case has a period of approximately 312 ps. Subsequently the performance of each ONU is analysed in terms of

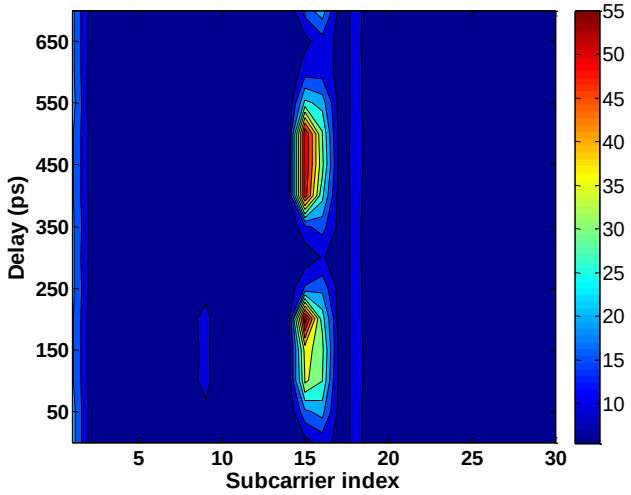

Figure 5.36. Numerical results for the 30 overlapping subcarriers received by the OLT from two ONUs in terms of EVM as function of subcarrier index and imposed timing delay

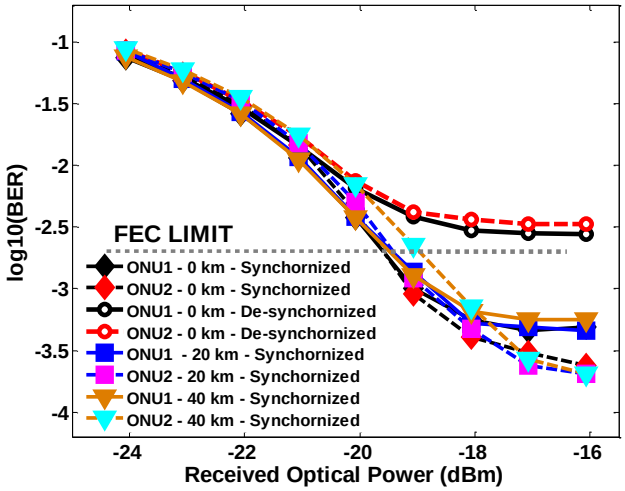

Figure 5.37. Simulated results for Each ONU in terms of BER vs Received Optical Power in presence and absence of a secondary ONU and in presence and absence of timing synchronization and 0/20 and 40 km of feeder fibre

BER with respect to the received optical power at the OLT for 0/20 and 40 km of feeder fibre lengths. In Figure 5.37 these BER trends are presented, without including a feeder fibre and operating the two ONUs at the point of maximum MAI results in an error floor for both ONUs above the FEC limit. However, as was found in the experimental work, restoring the orthogonality by adjusting the timing delay results in reasonable trends for both ONUs. The combined optical signal from the two ONUs is subsequently propagated through 20 and 40 km of a feeder fibre before reaching the OLT, showing that it leads to a negligible change in the performance.

5.5 Discussions

Figure 5.38 summarises the experimental results obtained from the setup used to study the performance of FBMC in long-reach intensity modulated PONs. The results are presented in terms of the receiver sensitivity at the FEC limit ($2x10^{-3}$) as function of the propagation length. To identify the limitations of this architecture, simulation results are also included in the Figure 5.38. As is evident from the experimental results in the directly modulated case, performance level better than the FEC limit was reached for data rates up to 10 Gb/s and propagation lengths up to 75 km. However the propagation length was limited to 50 and 37 km respectively in cases where data rates were set to 12.4 and 14.8 Gb/s. Moreover, in the directly modulated case a constant degradation in the performance as function of the propagation length is noticeable. As it was stated earlier, the FBMC system can operate in absence of a CP, thus, dispersion in the fibre cannot solely be responsible for the performance deterioration seen here. To clarify this point, the experimental results in Figure 5.38 (b) for the externally modulated system are presented. These show negligible

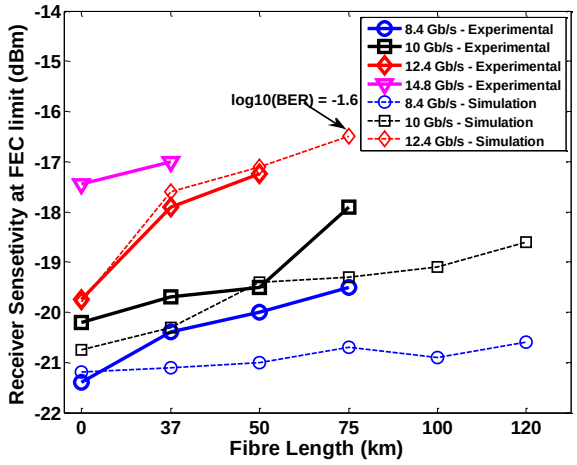

(a)

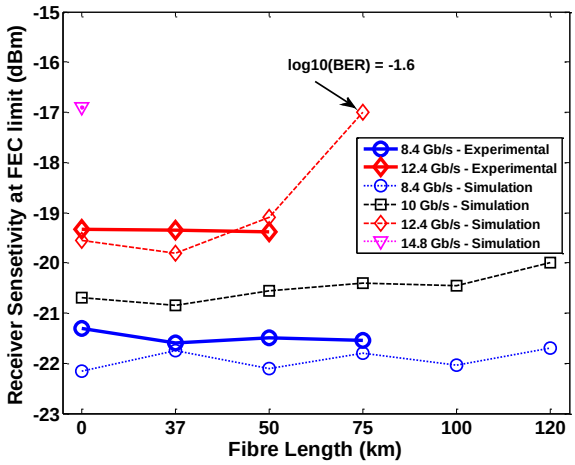

(b)

Figure 5.38. Receiver sensitivity at which the FEC limit was reached in (a) directly modulated (b) externally modulated system

degradation in system performance as a function of the accumulated dispersion. Thus, the degradation seen in the directly modulated case as function of the fibre propagation length can be attributed to fibre the higher levels of dispersive fading which emerge due to the chirping from the directly modulated laser.

Simulations results in Figure 5.38 show a similar trend compared to the experimental results. It can be seen that in both the directly modulated and externally modulated scenarios it was possible to extend the transmission length to 120 km whilst operating at 8.4 and 10 Gb/s. These results present the resilience of FBMC to accumulated dispersion in the system. A major factor limiting the propagation length at data rates above 10 Gb/s is the dispersive fading, which forced the experimental system operating at 12.4 Gb/s to have a limited reach of 75 km, above which the FEC limit could not be achieved. To identity the severity of performance degradation imposed after propagating the 12.5 Gb/s through 75 km of SSMF, the receiver sensitivity at the BER of $10^{-1.6}$ which is well above the FEC limit is plotted in Figure 5.38 for both the direct and externally modulated cases.

ONU (drop/feeder length)	Synchronized	Unsynchronized
ONU 1 (0 km / 0 km)-Exp	-19.1 dBm	Above limit
ONU 2 (0 km / 0 km)-Exp	-19.4 dBm	Above limit
ONU 1 (25 km / 0 km)-Exp	-18.75 dBm	Above limit
ONU 2 (10 km / 0 km)-Exp	-19.2 dBm	Above limit
ONU 1 (5 km / 0 km)-Sim	-19.6 dBm	Above limit
ONU 2 (9 km / 0km)-Sim	-19.6 dBm	Above limit
ONU 1 (5 km / 20 km)-Sim	-19.4 dBm	Above limit
ONU 2 (9 km / 20km)-Sim	-19.4 dBm	Above limit
ONU 1 (5 km / 40 km)-Sim	-19.5 dBm	Above limit
ONU 2 (9 km / 40km)-Sim	-18.9 dBm	Above limit

Table 5.4. Summary of the experimental and simulation results, showing the impact of desynchronization on each ONU. Performance in terms of receiver sensitivity at which the FEC limit was reached

The experiments carried with uplink PON earlier in this chapter were suggestive of superior performance levels in FBMC PON in comparison with OFDM. This superiority was attributed to the well-localized prototype filters employed in the FBMC based PONs which enhanced the resilience to MAI. Table 5.4 summarises some of the key results obtained from the experimental and simulation works carried on uplink PON earlier in this chapter. It is clear that under maximum levels of MAI or when the two ONUs are desynchronized, both fail to achieve a BER better or at the FEC limit for all received optical powers. The addition of drop fibres to each ONU as can be seen in the experimental results still allows for reliable synchronization to be achieved which compared to the back to back case endures performance penalties below 1 dB. As Table 5.4 suggest the simulation results closely match the experimental results and they further show that the addition of a feeder fibre with lengths up to 40 km does not disturb the synchronization between the two ONUs and leads to only 0.5 dB of penalty compared to the system with no feeder fibre.

5.6 Summary

MC modulation formats by using orthogonal properties can provide high levels of bandwidth efficiency. This concept is highly favourable in PONs where bandwidth efficient means of data transmission is required. The subdivision of available bandwidth in orthogonal tributaries can also allow for efficient and dynamic bandwidth allocation amongst multiple users. The employment of OFDM in PON has been widely studied; this scheme apart from being bandwidth efficient it can also show resilience towards chromatic dispersion by using overheads in form of a CP. However, OFDM is sensitive to CFO and the use of a CP leads to a loss of available bandwidth. Another family of MC modulation formats called FBMC are also able to provide similar advantages as OFDM with higher resilience to synchronization issues without the need for CP. The properties of FBMC can

provide advantages over OFDM in an intensity modulated PON both in downlink and uplink communication channels.

Experimental results showed that by using this CP-less FBMC system in conjunction with direct modulation of cost effective laser diodes, it had been possible to transmit a 10 Gb/s signal over 75 of SSMF and 14.8 Gb/s signal over 37 km of SSMF. Through experimental and numerical work, it was also found that in the case of desynchronization between neighbouring ONUs with overlapping orthogonal components, FBMC shows a better immunity to MAI compared to OFDM.

Chapter 6

Conclusion and Future Work

6.1 Conclusion

As the global demand for broadband services continues to grow, service providers and governments alike are incentivized to invest in higher capacity optical networks in order to meet customer requirements. In access networks, in order to eliminate technological barriers limiting the provision of higher bandwidths, optical networks need to be moved closer to the end user through the deployment of fibre-to-the-home (FTTH) topologies. However due to the associated costs of access networks, the candidate topologies need to be cost-effective while maintaining a degree of flexibility and scalability in order to accommodate for future upgrades.

To promote cost-effectiveness in optical access networks, the use of highly spectrally efficient modulation formats such as OFDM and FBMC can allow for the integration of low cost and low bandwidth electro-optical devices, these modulation schemes also show a high level of resilience to chromatic dispersion, which is highly advantageous in Long Reach PONs. Furthermore, with the increasing demand for higher bandwidth cellular applications, wireless service providers are deploying technologies that can meet the needs of end users, however, this necessitates higher bandwidth backhaul links. Using optical

access networks to consolidate these high bandwidth wireless backhaul links can lead to reduced expenditure and operational costs for the service provider.

In this thesis, highly spectrally efficient modulation formats such as OFDM and FBMC are proposed for access networks, which are capable of providing the data rates and spectral efficiencies required for next generation designs. The use of these two modulation schemes can provide a high tolerance to chromatic dispersion, enabling longer propagation lengths. This thesis, also provides an efficient means for accommodating wireless services in PONs using OFDM by subcarrier manipulation, and also in OOK based PONs by exploiting encoding schemes.

The following outlines some of the main results obtained:

In chapter 3, the transmission of directly modulated OFDM based hybrid wired/wireless PON is demonstrated. In this work single or multiple wireless LTE signals are integrated in the system by the de-activating number of in-band wired subcarriers. The effects of nonlinearity and RIN introduced by the directly modulated laser, through experiments and simulations are shown to be reduced by employing optical injection. In the experimental work, to achieve optical injection, a novel two section monolithically integrated device, which is suitable for low cost PONs is used. Experimental and simulation results clearly demonstrated, the formation of an error floor above the required FEC limit in presence of laser non-linearity and RIN for the wired OFDM band operating at 12.5 Gb/s. Similar experimental and simulation models also show the enhancement of performance in presence of optical injection which allowed for reliable data delivery over 50 km of SSMF. Results also show the deterioration of in-band wireless signals in presence of nonlinearity and RIN and its enhancement in performance upon optical injection. Furthermore, performance of this hybrid system is also studied with respect to relative power between wired and the wireless signals. The work presented in this chapter was the first demonstration of hybrid wired/wireless PON accommodating for in-band AoF signals carrying LTE services. This work also for the first time made use of integrated devices with optical injection for hybrid wired/wireless PON, where the impact of RIN and nonlinearity were analysed in detail.

In chapter 4, the in-band accommodation of LTE services through AoF single was for the first time demonstrated in OOK based PON. In this work, encoders with a DC free property and encoders with both DC-free and Nyquist free properties are exploited for the creation of spectral notches in the spectrum of OOK modulated serial streams running at 10 Gb/s. By using a structure within which encoders are interleaved, it was possible to create multiple harmonically related spectral notches. The two line encoders implemented in this

work were called 8B10B and MB810. In the experimental work, a 10 Gb/s OOK stream representing a TDM-PON channel was produced by a system of five interleaved 8B10B encoders, this resulted in narrow spectral notches at 0, 2, 4, 6 and 8 GHz. Furthermore, this electrical binary signal was combined with a wireless signal operating at 2 GHz which was then directly modulated onto a DFB laser. The wireless signal and the wired OOK signal were both evaluated in the presence and absence of line-encoding. It was found that with the removal of encoding, the in-band wireless signal was severely deteriorated as a result of the imposed interference from the wired band, regardless of the wireless signal's power level. The removal of line-coding and the elimination of spectral notches also showed the impact of the wired OOK band. Through simulations, MB810 was compared to 8B10B, and it was found that they both exhibited a similar performance with the main difference being that the interleaved MB810 encoders were capable of producing more spectral notches compared to interleaved 8B10 encoders owing to their extra Nyquist free property. Trough simulations the impact of fibre propagation on the performance was also studied.

In Chapter 5, an introduction to FBMC was presented. The use of FBMC for directly modulated PONs using cost effective discrete mode lasers was demonstrated experimentally for data rates ranging between 8.4 to 14.8 Gb/s over various lengths of SSMF fibre ranging from 37 to 75 km of SSMF. By the employment of external modulators such as MZM the high resilience of this CP-less modulation format to chromatic dispersion in intensity modulation PONs was also illustrated. The utilization of FBMC for uplink PON communication channels was demonstrated experimentally by using two separate ONUs each modulating the intensity of a separate optical carrier by either direct or external modulation. During the assignment of subcarriers, no frequency guard bands were employed between the two ONUs. The elimination of a frequency guard band between the two ONUS led to a situation where at the OLT's receiver the highest subcarrier from ONU1 overlapped the lowest frequency subcarrier of ONU2. To avoid multi access interference and eliminate any ICI, the orthogonality between the neighbouring subcarriers of ONU 1 and ONU 2 needs required to be preserved. In this system, it was identified that the loss of orthogonality could be attributed to a relative timing de-synchronization between the two ONU's as the result of a discrepancy between the propagation paths of ONU1 and ONU2 prior to their combination at the remote node. This time miss-synchronization was subsequently corrected either by an optical variable delay line connected to the output of one ONU or by electrically delaying the signal from one of the ONUs at the electrical transmitter. Experimental and simulation results were presented, which demonstrated the effectiveness of FBMC towards MAI compared to OFDM. In OFDM it was found that as result of its long side lobes, MAI influenced

multiple subcarriers whereas in FBMC only the adjacent neighbouring subcarriers were affected the most. Experimental and simulation results show that MAI in FBMC systems can still produce unwanted error floors. However, by adjusting the timing delay between neighbouring ONUs it is possible to correct for the MAI regardless of the lengths of the feeder or drop fibre lengths employed. This work for the first time demonstrated the use of directly modulated laser in long reach FBMC-PON with fibre propagation lengths up to 75 km. This work also for the first demonstrated the effectiveness of FBMC compared to OFDM in uplink PON.

6.2 Future Work

Work in this thesis has shown the potential for multicarrier modulation formats such as OFDM and FBMC in meeting the requirements of cost effective next generation optical access networks. This thesis also included some work on hybrid wired/wireless PONs which aimed at effective methods of delivering wireless services on a shared link. Below are some of the potential directions for continuation of this research:

- In integrating wireless services in this work by using Analogue Radio over Fibber (AoF), Single Input Single Output (SISO) architecture was envisioned. However, next generation optical access networks need to be able to account for Multi Input Multi Output (MIMO) type architectures. Thus, investigation of hybrid wired/wireless PON architectures that can accommodate for MIMO wireless topologies effectively is of interest.

- In this work, line encoders with DC free and Nyquist free properties were employed in an interleaved structure to create spectral notches for the accommodation of wireless services. However, creating a single encoder capable of producing spectral notches at arbitrary positions is also of interest.

- In the work carried out in this thesis for uplink PONs employing FBMC, only two ONUs were considered and the timing delay between the ONUs was adjusted manually. It will be of interest to study the performance in the presence of more than two ONUs with overlapping subcarriers and devising a reliable method for automatic compensation of inter ONU timing

References

[1] K. Ikeda, T. Kuri, and K. Kitayama, "Simultaneous three-band modulation and fiber-optic transmission of 2.5-Gb/s baseband, microwave-, and 60-GHz-band signals on a single wavelength," *Lightwave Technology, Journal of,* vol. 21, pp. 3194-3202, 2003.

[2] M. Morant, T. Quinlan, R. Llorente, and S. Walker, "Full standard triple-play bi-directional and full-duplex CWDM transmission in passive optical networks," in *Optical Fiber Communication Conference and Exposition (OFC/NFOEC), 2011 and the National Fiber Optic Engineers Conference*, 2011, pp. 1-3.

[3] M. Morant, T. Quinlan, S. Walker, and R. Llorente, ""Real world" FTTH optical-to-radio interface performance for bi-directional multi-format OFDM wireless signal transmission," in *Optical Fiber Communication Conference and Exposition (OFC/NFOEC), 2011 and the National Fiber Optic Engineers Conference*, 2011, pp. 1-3.

[4] J. J. V. Olmos, T. Kuri, and K. i. Kitayama, "Reconfigurable Radio-Over-Fiber Networks: Multiple-Access Functionality Directly Over the Optical Layer," *IEEE Transactions on Microwave Theory and Techniques,* vol. 58, pp. 3001-3010, 2010.

[5] C. Browning, K. Shi, S. Latkowski, P. Anandarajah, F. Smyth, B. Cardiff, *et al.*, "Performance improvement of 10Gb/s direct modulation OFDM by optical injection using monolithically integrated discrete mode lasers," in *Optical Communication (ECOC), 2011 37th European Conference and Exhibition on*, 2011, pp. 1-3.

[6] Y. C. Chi, P. C. Peng, H. H. Lu, and G. R. Lin, "Coherently injection-locked weak-resonant-cavity laser diode for optical 16-QAM-OFDM transmission at 4 Gb/s," in *2012 21st Annual Wireless and Optical Communications Conference (WOCC)*, 2012, pp. 138-139.

[7] H. Karkhaneh, A. Ghorbani, and J. M. Liu, "Broadband transmission over injection-locked optical OFDM systems: Theory and design," *IEEE/OSA Journal of Optical Communications and Networking,* vol. 5, pp. 475-483, 2013.

[8] Z. Liu, J. Y. Kim, D. S. Wu, D. J. Richardson, R. Slav, and x00Ed, "Homodyne OFDM with Optical Injection Locking for Carrier Recovery," *Journal of Lightwave Technology,* vol. 33, pp. 34-41, 2015.

[9] W. S. C. Chang, *RF Photonic Technology in Optical Fiber Links*: Cambridge University Press, 2002.

[10] E. K. Lau, W. Liang Jie, and M. C. Wu, "Enhanced Modulation Characteristics of Optical Injection-Locked Lasers: A Tutorial," *Selected Topics in Quantum Electronics, IEEE Journal of,* vol. 15, pp. 618-633, 2009.

[11] C. Herbert, D. Jones, A. Kaszubowska-Anandarajah, B. Kelly, M. Rensing, J. O'Carroll, *et al.*, "Discrete mode lasers for communication applications," *Optoelectronics, IET,* vol. 3, pp. 1-17, 2009.

[12] T. Kamisaka, T. Kuri, and K. Kitayama, "Simultaneous modulation and fiber-optic transmission of 10-Gb/s baseband and 60-GHz-band radio signals on a single wavelength," *IEEE Transactions on Microwave Theory and Techniques,* vol. 49, pp. 2013-2017, 2001.

[13] J. Cavers, R. F. Marchetto, and S. D. Carlson, "A new spectral notch generator for pilot tone systems," in *Vehicular Technology Conference, ,* 1990, pp. 547-552.

[14] J. Cavers, R. F. Marchetto, and S. D. Carlson, "A new spectral notch generator for pilot tone systems," in *Vehicular Technology Conference, 1990 IEEE 40th*, 1990, pp. 547-552.

[15] J. Franklin and J. Pierce, "Spectra and Efficiency of Binary Codes Without DC," *Communications, IEEE Transactions on,* vol. 20, pp. 1182-1184, 1972.
[16] K. A. S. Immink, "Spectral null codes," *IEEE Transactions on Magnetics,* vol. 26, pp. 1130-1135, 1990.
[17] C. Lee, D. Y. Kim, J. W. Kim, H. W. Jung, and H. H. Lee, "Method and apparatus for encoding MB810 line code with the characteristics of minimum bandwidth and DC-free," ed: Google Patents, 2002.
[18] B. H. Marcus and P. H. Siegel, "On codes with spectral nulls at rational submultiples of the symbol frequency," *IEEE Transactions on Information Theory,* vol. 33, pp. 557-568, 1987.
[19] B. Farhang-Boroujeny, "OFDM Versus Filter Bank Multicarrier," *Signal Processing Magazine, IEEE,* vol. 28, pp. 92-112, 2011.
[20] B. Farhang-Boroujeny, *Signal Processing Techniques for Software Radios*, 2nd ed. Salt Lake City: University of Utah, 2010.
[21] A. Sahin, I. Guvenc, and H. Arslan, "A Survey on Multicarrier Communications: Prototype Filters, Lattice Structures, and Implementation Aspects," *IEEE Communications Surveys & Tutorials,* vol. 16, pp. 1312-1338, 2014.
[22] G. J. González, F. H. Gregorio, J. Cousseau, R. Wichman, and S. Werner, "Uplink CFO compensation for FBMC multiple access and OFDMA in a high mobility scenario," *Physical Communication,* vol. 11, pp. 56-66, 6// 2014.
[23] H. Saeedi-Sourck, Y. Wu, J. W. M. Bergmans, S. Sadri, and B. Farhang-Boroujeny, "Sensitivity analysis of offset QAM multicarrier systems to residual carrier frequency and timing offsets," *Signal Processing,* vol. 91, pp. 1604-1612, 7, 2011.
[24] S.-Y. Jung, S.-M. Jung, H.-J. Park, and S.-K. Han, "Mitigation of timing offset effect in IM/DD based OFDMA-PON uplink multiple access," *Optics Express,* vol. 23, pp. 13889-13898, 2015/06/01 2015.
[25] A. Saljoghei, F. A. Gutierrez, C. Browning, and L. P. Barry, "FBMC for directly modulated passive optical networks (PON)," in *Microwave Photonics (MWP), 2015 International Topical Meeting on*, 2015, pp. 1-4.
[26] J. Sun-Young, J. Sang-Min, and H. Sang-Kook, "AMO-FBMC for Asynchronous Heterogeneous Signal Integrated Optical Transmission," *Photonics Technology Letters, IEEE,* vol. 27, pp. 133-136, 2015.
[27] J. Sun-Young, J. Sang-Min, and H. Sang-Kook, "AMO-FBMC for reduction of multiple access interference between asynchronous ONUs in PON," in *Optical Fiber Communications Conference and Exhibition (OFC), 2015*, 2015, pp. 1-3.
[28] J. Sun-Young, K. Soo-Min, J. Sang-Min, and H. Sang-Kook, "AMO-FBMC based RoF transmission for efficient wired/wireless converged optical networks," in *Microwave Photonics (MWP) and the 2014 9th Asia-Pacific Microwave Photonics Conference (APMP), 2014 International Topical Meeting on*, 2014, pp. 215-217.
[29] T. Fusco, A. Petrella, and M. Tanda, "Sensitivity of multi-user filter-bank multicarrier systems to synchronization errors," in *Communications, Control and Signal Processing, 2008. ISCCSP 2008. 3rd International Symposium on*, 2008, pp. 393-398.
[30] M. Bellanger. (2010, FBMC physical layer: a primer.
[31] T. H. Maiman, "Stimulated Optical Radiation in Ruby," *Nature,* vol. 187, pp. 493-494, 08/06/print 1960.
[32] K. C. Kao and G. A. Hockham, "Dielectric-fibre surface waveguides for optical frequencies," *Electrical Engineers, Proceedings of the Institution of,* vol. 113, pp. 1151-1158, 1966.
[33] F. P. Kapron, D. B. Keck, and R. D. Maurer, "RADIATION LOSSES IN GLASS OPTICAL WAVEGUIDES," *Applied Physics Letters,* vol. 17, pp. 423-425, 1970.
[34] A. M. Noll, "Accelerating Technology: The Pace of Transmission Systems," *Prometheus,* vol. 20, pp. 15-20, 2002/03/01 2002.

[35] G. P. Agrawal, *Fiber-optic communication systems*, 4 ed. Hoboken, New Jersey: Wiley, 2010.
[36] R. J. Mears, L. Reekie, I. M. Jauncey, and D. N. Payne, "High-gain rare-earth-doped fiber amplifier at 1.54 μm," in *Optical Fiber Communication*, Reno, Nevada, 1987, p. WI2.
[37] M. Seimetz, *High-Order Modulation for Optical Fiber Transmission*: Springer Berlin Heidelberg, 2009.
[38] P. J. Winzer, "High-Spectral-Efficiency Optical Modulation Formats," *Lightwave Technology, Journal of*, vol. 30, pp. 3824-3835, 2012.
[39] June 2009). Cisco Visual Networking Index: Forecast and Methodology, 2008–2013.Available: http://www.cisco.com/web/BR/assets/docs/whitepaper_VNI_06_09.pdf
[40] May 2015). Cisco Visual Networking Index: Forecast and Methodology, 2014–2019.Available: http://www.cisco.com/c/en/us/solutions/collateral/service-provider/ip-ngn-ip-next-generation-network/white_paper_c11-481360.pdf
[41] J. Prat, *Next-Generation FTTH Passive Optical Networks: Research towards unlimited bandwidth access*, 1 ed.: Springer, 2008.
[42] E. Wong, "Next-Generation Broadband Access Networks and Technologies," *Lightwave Technology, Journal of*, vol. 30, pp. 597-608, 2012.
[43] J. Sakaguchi, B. J. Puttnam, W. Klaus, Y. Awaji, N. Wada, A. Kanno, *et al.*, "19-core fiber transmission of 19x100x172-Gb/s SDM-WDM-PDM-QPSK signals at 305Tb/s," in *National Fiber Optic Engineers Conference*, Los Angeles, California, 2012, p. PDP5C.1.
[44] E. Lach and K. Schuh, "Recent Advances in Ultrahigh Bit Rate ETDM Transmission Systems," *Lightwave Technology, Journal of*, vol. 24, pp. 4455-4467, 2006.
[45] E. Wong, "Next-Generation Broadband Access Networks and Technologies," *Journal of Lightwave Technology*, vol. 30, pp. 597-608, 2012/02/12 2012.
[46] Chacin, x, M. ski, U. Westergren, B. Stoltz, R. Driad, *et al.*, "100 Gb/s ETDM Transmitter Module," *Selected Topics in Quantum Electronics, IEEE Journal of*, vol. 16, pp. 1321-1327, 2010.
[47] R. H. Derksen, U. Westergren, M. Chacinski, C. Schubert, H. G. Bach, R. Driad, *et al.*, "Cost-efficient high-speed components for 100 gigabit ethernet transmission on one wavelength only: results of the HECTO project," *Communications Magazine, IEEE*, vol. 51, pp. 136-144, 2013.
[48] S. K. Routray, "The Changing Trends of Optical Communication," *IEEE Potentials*, vol. 33, pp. 28-33, 2014.
[49] K. Schuh and E. Lach, "High-bit-rate ETDM transmission systems," in *Optical Fiber Telecomunications*. vol. V, I. P. Kaminow, T. Li, and A. E. Willner, Eds., 1 ed USA: Elsevier, 2008.
[50] G. Raybon, A. L. Adamiecki, P. Winzer, C. Xie, A. Konczykowska, F. Jorge, *et al.*, "Single-carrier 400G interface and 10-channel WDM transmission over 4,800 km using all-ETDM 107-Gbaud PDM-QPSK," in *Optical Fiber Communication Conference and Exposition and the National Fiber Optic Engineers Conference (OFC/NFOEC), 2013*, 2013, pp. 1-4.
[51] G. Raybon, A. Adamiecki, P. P. J. Winzer, M. Montoliu, S. Randel, A. Umbach, *et al.*, "All-ETDM 107-Gbaud PDM-16QAM (856-Gb/s) transmitter and coherent receiver," in *Optical Communication (ECOC 2013), 39th European Conference and Exhibition on*, 2013, pp. 1-3.
[52] T. Richter, M. Nolle, F. Frey, and C. Schubert, "Generation and Coherent Reception of 107-GBd Optical Nyquist BPSK, QPSK, and 16QAM," *Photonics Technology Letters, IEEE*, vol. 26, pp. 877-880, 2014.
[53] H. G. Weber, R. Ludwig, S. Ferber, C. Schmidt-Langhorst, M. Kroh, V. Marembert, *et al.*, "Ultrahigh-Speed OTDM-Transmission Technology," *Lightwave Technology, Journal of*, vol. 24, pp. 4616-4627, 2006.

[54] L. K. Oxenlowe, "Tutorial: Terabit/second OTDM systems," in *Photonics Conference (PHO), 2011 IEEE*, 2011, pp. 650-651.
[55] M. Nakazawa, T. Yamamoto, and K. R. Tamura, "1.28 Tbit/s-70 km OTDM transmission using third- and fourth-order simultaneous dispersion compensation with a phase modulator," *Electronics Letters*, vol. 36, pp. 2027-2029, 2000.
[56] C. L. Schow, A. Rylyakov, B. G. Lee, F. E. Doany, C. Baks, R. A. John, *et al.*, "Transmitter Pre-Distortion for Simultaneous Improvements in Bit-Rate, Sensitivity, Jitter, and Power Efficiency in 20 Gb/s CMOS-driven VCSEL Links," in *Optical Fiber Communication Conference/National Fiber Optic Engineers Conference 2011*, Los Angeles, California, 2011, p. PDPC6.
[57] Y. Matsui, H. Murai, S. Arahira, S. Kutsuzawa, and Y. Ogawa, "30-GHz bandwidth 1.55um strain-compensated InGaAlAs-InGaAsP MQW laser," *Photonics Technology Letters, IEEE*, vol. 9, pp. 25-27, 1997.
[58] A. Sano, T. Kobayashi, S. Yamanaka, A. Matsuura, H. Kawakami, Y. Miyamoto, *et al.*, "102.3-Tb/s (224 x 548-Gb/s) C- and Extended L-band All-Raman Transmission over 240 km Using PDM-64QAM Single Carrier FDM with Digital Pilot Tone," in *National Fiber Optic Engineers Conference*, Los Angeles, California, 2012, p. PDP5C.3.
[59] H. Takara, A. Sano, T. Kobayashi, H. Kubota, H. Kawakami, A. Matsuura, *et al.*, "1.01-Pb/s (12 SDM/222 WDM/456 Gb/s) Crosstalk-managed Transmission with 91.4-b/s/Hz Aggregate Spectral Efficiency," in *European Conference and Exhibition on Optical Communication*, Amsterdam, 2012, p. Th.3.C.1.
[60] L. Yuanqiu, Z. Xiaoping, F. Effenberger, Y. Xuejin, P. Guikai, Q. Yinbo, *et al.*, "Time- and Wavelength-Division Multiplexed Passive Optical Network (TWDM-PON) for Next-Generation PON Stage 2 (NG-PON2)," *Lightwave Technology, Journal of*, vol. 31, pp. 587-593, 2013.
[61] I. T. Union, "G.694.1 spectral grids for WDM applica- tions: DWDM frequency grid," Series G: Transmission Systems and Media, Digital Systems and Networks," ed, 2012.
[62] M. K. Smit, "New focusing and dispersive planar component based on an optical phased array," *Electronics Letters*, vol. 24, pp. 385-386, 1988.
[63] L. J. Cimini, "Analysis and Simulation of a Digital Mobile Channel Using Orthogonal Frequency Division Multiplexing," *Communications, IEEE Transactions on*, vol. 33, pp. 665-675, 1985.
[64] I. Koffman and V. Roman, "Broadband wireless access solutions based on OFDM access in IEEE 802.16," *Communications Magazine, IEEE*, vol. 40, pp. 96-103, 2002.
[65] U. Reimers, "Digital video broadcasting," *Communications Magazine, IEEE*, vol. 36, pp. 104-110, 1998.
[66] J. Armstrong, "OFDM for Optical Communications," *Lightwave Technology, Journal of*, vol. 27, pp. 189-204, 2009.
[67] N. Cvijetic, "OFDM for Next-Generation Optical Access Networks," *Lightwave Technology, Journal of*, vol. 30, pp. 384-398, 2012.
[68] *Optical Fiber Telecommunications V, B: Systems and Networks*: Elsevier, 2008.
[69] S. Kai, F. Smyth, D. A. Reid, C. Browning, B. Roycroft, B. Corbett, *et al.*, "Fast Switching Slotted Fabry-Perot Laser for Phase Modulated Transmission Systems," *Lightwave Technology, Journal of*, vol. 28, pp. 3409-3416, 2010.
[70] A. A. M. Saleh and J. M. Simmons, "Evolution toward the next-generation core optical network," *Lightwave Technology, Journal of*, vol. 24, pp. 3303-3321, 2006.
[71] R. Younce, J. Larikova, and W. Yajun, "Engineering 400G for colorless-directionless-contentionless architecture in metro/regional networks [invited]," *Optical Communications and Networking, IEEE/OSA Journal of*, vol. 5, pp. A267-A273, 2013.

[72] A. Balaban and A. Pitts, "Powering the Emerging Full Service Access Networks (FSAN)- the last mile challenge," in *Telecommunications Conference, 2005. INTELEC '05. Twenty-Seventh International*, 2005, pp. 137-143.

[73] M. D. Nava and C. Del-Toso, "A short overview of the VDSL system requirements," *Communications Magazine, IEEE*, vol. 40, pp. 82-90, 2002.

[74] ISP-Review. (2015). *UPDATE Can BT's Long Reach VDSL Fibre Broadband Help Rural Homes* [Online Article]. Available: http://www.ispreview.co.uk/index.php/2015/09/can-bts-long-reach-vdsl-fttc-fibre-broadband-help-rural-homes.html

[75] J. Segarra, V. Sales, and J. Prat, "Access services availability and traffic forecast in PON deployment," in *Transparent Optical Networks (ICTON), 2011 13th International Conference on*, 2011, pp. 1-6.

[76] G. Finnie. (2015, European FTTH Forecast, 2014-2019. Available: www.fftcouncil.eu

[77] K. Jeung-Mo and H. Sang-Kook, "A novel hybrid WDM/SCM-PON sharing wavelength for up- and down-link using reflective semiconductor optical amplifier," *IEEE Photonics Technology Letters*, vol. 18, pp. 502-504, 2006.

[78] Z. Jianyu, L. Feng, X. Mu, Z. Ming, M. I. Khalil, L. Jianguo, *et al.*, "Photonics-assisted microwave mixing and direct detection for dual-polarization and SCM based UDWDM-PON," in *Optical Fiber Communications Conference and Exhibition (OFC), 2015*, 2015, pp. 1-3.

[79] D. v. Veen, V. Houtsma, and H. Chow, "Demonstration of symmetrical 25 Gbps quaternary PAM/duobinary TDM-PON with multilevel interleaving of users," in *Optical Communication (ECOC), 2015 European Conference on*, 2015, pp. 1-3.

[80] K. Y. Cho, Y. Takushima, and Y. C. Chung, "Enhanced chromatic dispersion tolerance of 11 Gbit/s RSOA-based WDM PON using 4-ary PAM signal," *Electronics Letters*, vol. 46, pp. 1510-1512, 2010.

[81] J. R. Stern, J. W. Ballance, D. W. Faulkner, S. Hornung, D. B. Payne, and K. Oakley, "Passive optical local networks for telephony applications and beyond," *Electronics Letters*, vol. 23, pp. 1255-1256, 1987.

[82] I. T. U.-. T, "G.983.1, Broadband optical access systems based on Passive Optical Networks (PON) " in *SERIES G: TRANSMISSION SYSTEMS AND MEDIA, DIGITAL SYSTEMS AND NETWORKS*, ed, 2005.

[83] L. Yuanqiu, G. Jianhe, and F. Effenberger, "Next generation hybrid wireless-optical access with TWDM-PON," in *Wireless and Optical Communication Conference (WOCC), 2014 23rd*, 2014, pp. 1-5.

[84] J.-C. Guey, "To 4G mobile communication and beyond," in *VLSI Technology, Systems, and Applications (VLSI-TSA), 2013 International Symposium on*, 2013, pp. 1-2.

[85] A. Khayrallah, "4G/5G mobile technologies - Can they be a blueprint for optical networks?," in *Optical Fiber Communication Conference and Exposition and the National Fiber Optic Engineers Conference (OFC/NFOEC), 2013*, 2013, pp. 1-3.

[86] S. Jain, F. Effenberger, A. Szabo, Z. Feng, A. Forcucci, W. Guo, *et al.*, "World's First XG-PON Field Trial," *Journal of Lightwave Technology*, vol. 29, pp. 524-528, 2011/02/15 2011.

[87] (2013, BT and ZTE Are the First to Deploy XG-PON in a Live Customer Environment.Available: http://wwwen.zte.com.cn/endata/magazine/ztetechnologies/2013/no4/articles/201307/t20130717_402288.html

[88] G.-K. Chang, A. Chowdhury, Z. Jia, H.-C. Chien, M.-F. Huang, J. Yu, *et al.*, "Key Technologies of WDM-PON for Future Converged Optical Broadband Access Networks [Invited]," *Journal of Optical Communications and Networking*, vol. 1, pp. C35-C50, 2009/09/01 2009.

[89] Q. Guo and A. V. Tran, "Mitigation of Rayleigh noise and dispersion in REAM-based WDM-PON using spectrum-shaping codes," *Optics Express,* vol. 20, pp. B452-B461, 2012/12/10 2012.

[90] P. Chanclou, A. Cui, F. Geilhardt, H. Nakamura, and D. Nesset, "Network operator requirements for the next generation of optical access networks," *Network, IEEE,* vol. 26, pp. 8-14, 2012.

[91] H. Suzuki, M. Fujiwara, T. Suzuki, N. Yoshimoto, H. Kimura, and M. Tsubokawa, "Wavelength-Tunable DWDM-SFP Transceiver with a Signal Monitoring Interface and Its Application to Coexistence-Type Colorless WDM-PON," in *Optical Communication - Post-Deadline Papers (published 2008), 2007 33rd European Conference and Exhibition of*, 2007, pp. 1-2.

[92] F. J. Effenberger, J.-i. Kani, and Y. Maeda, "Standardization trends and prospective views on the next generation of broadband optical access systems," *IEEE J.Sel. A. Commun.,* vol. 28, pp. 773-780, 2010.

[93] L. Xu and H. K. Tsang, "Colorless WDM-PON Optical Network Unit (ONU) Based on Integrated Nonreciprocal Optical Phase Modulator and Optical Loop Mirror," *Photonics Technology Letters, IEEE,* vol. 20, pp. 863-865, 2008.

[94] T. Mitsui, K. Hara, M. Fujiwara, J. Kani, M. Tadokoro, N. Yoshimoto, *et al.*, "Simple and scalable WDM/TDMA-PON using spectral slicing and forward error correction," in *Optical Fiber Communication Conference and Exposition (OFC/NFOEC), 2011 and the National Fiber Optic Engineers Conference*, 2011, pp. 1-3.

[95] S. Dong Jae, Y. C. Keh, J. W. Kwon, E. H. Lee, J. K. Lee, M. K. Park, *et al.*, "Low-cost WDM-PON with colorless bidirectional transceivers," *Lightwave Technology, Journal of,* vol. 24, pp. 158-165, 2006.

[96] M. D. Feuer, J. M. Wiesenfeld, J. S. Perino, C. A. Burrus, G. Raybon, S. C. Shunk, *et al.*, "Single-port laser-amplifier modulators for local access," *Photonics Technology Letters, IEEE,* vol. 8, pp. 1175-1177, 1996.

[97] E. Wong, L. Ka Lun, and T. B. Anderson, "Directly Modulated Self-Seeding Reflective Semiconductor Optical Amplifiers as Colorless Transmitters in Wavelength Division Multiplexed Passive Optical Networks," *Lightwave Technology, Journal of,* vol. 25, pp. 67-74, 2007.

[98] A. Saljoghei, C. Browning, and L. Barry, "Hybrid wired/wireless OFDM-PON with direct modulation of integrated lasers employing optical injection," in *Microwave Photonics (MWP), 2013 International Topical Meeting on*, 2013, pp. 309-312.

[99] N. Cvijetic, Q. Dayou, H. Junqiang, and W. Ting, "Orthogonal frequency division multiple access PON (OFDMA-PON) for colorless upstream transmission beyond 10 Gb/s," *Selected Areas in Communications, IEEE Journal on,* vol. 28, pp. 781-790, 2010.

[100] P. M. Anandarajah, R. Zhou, R. Maher, D. Lavery, M. Paskov, B. Thomsen, *et al.*, "Gain-switched multicarrier transmitter in a long-reach UDWDM PON with a digital coherent receiver," *Optics Letters,* vol. 38, pp. 4797-4800, 2013/11/15 2013.

[101] D. Lavery, R. Maher, D. S. Millar, B. C. Thomsen, P. Bayvel, and S. J. Savory, "Digital Coherent Receivers for Long-Reach Optical Access Networks," *Lightwave Technology, Journal of,* vol. 31, pp. 609-620, 2013.

[102] C.-C. Wei, H. Y. Chen, H.-H. Chu, Y.-C. Chen, C.-Y. Song, I. C. Lu, *et al.*, "32-dB Loss Budget High-Capacity OFDM Long-Reach PON over 60-km Transmission without Optical Amplifier," in *Optical Fiber Communication Conference*, San Francisco, California, 2014, p. Th3G.1.

[103] A. Lometti, C. Colombo, S. Frigerio, and V. Sestito, "Network architectures for CPRI backhauling," in *Transparent Optical Networks (ICTON), 2012 14th International Conference on*, 2012, pp. 1-4.

[104] Y. Horiuchi, "Evolution of optical access network technologies in radio systems," in *Optical Communication, 2009. ECOC '09. 35th European Conference on*, 2009, pp. 1-4.
[105] D. Breuer, E. Weis, S. Gosselin, T. Mamouni, and J. Torrijos, "Unified access and aggregation network allowing fixed and mobile networks to converge," in *Optical Fiber Communication Conference and Exposition and the National Fiber Optic Engineers Conference (OFC/NFOEC), 2013*, 2013, pp. 1-3.
[106] A. M. J. Koonen, M. Popov, and H. Wessing, "Upper bound for energy efficiency in multi-cell fibre-wireless access systems," in *Optical Communication (ECOC 2013), 39th European Conference and Exhibition on*, 2013, pp. 1-3.
[107] E. Hossain, M. Rasti, H. Tabassum, and A. Abdelnasser, "Evolution toward 5G multi-tier cellular wireless networks: An interference management perspective," *Wireless Communications, IEEE*, vol. 21, pp. 118-127, 2014.
[108] S. Pankaj, "Evolution of Mobile Wireless CommunicationNetworks-1G to 5G as well as Future Prospectiveof Next Generation Communication Network," *International Journal of Computer Science and Mobile Computing*, vol. 2, pp. 47-53, August 2013 2013.
[109] W. Webb, *Wireless Communicatins: The Future*: Wiley, 2007.
[110] C. Cox, *An Introduction to LTE: LTE, LTE-Advanced, SAE and 4G Mobile Communications*: Wiley, 2012.
[111] May 2016). Cisco Visual Networking Index: Global Mobile Data Traffic Forecast Update, 2015-2020. Available: http://www.cisco.com/c/en/us/solutions/collateral/service-provider/visual-networking-index-vni/mobile-white-paper-c11-520862.pdf
[112] U. Varshney, "4G Wireless Networks," *IT Professional*, vol. 14, pp. 34-39, 2012.
[113] E. Dahlman, M. Gunnar, S. Parkvall, J. Peisa, J. Sachs, and Y. Selen, "5G radio access," *Ericsson Review*, 2014.
[114] A. Checko, H. L. Christiansen, Y. Yan, L. Scolari, G. Kardaras, M. S. Berger, *et al.*, "Cloud RAN for Mobile Networks;A Technology Overview," *IEEE Communications Surveys & Tutorials*, vol. 17, pp. 405-426, 2015.
[115] P. Chanclou, A. Pizzinat, F. Le Clech, T. L. Reedeker, Y. Lagadec, F. Saliou, *et al.*, "Optical fiber solution for mobile fronthaul to achieve cloud radio access network," in *Future Network and Mobile Summit (FutureNetworkSummit), 2013*, 2013, pp. 1-11.
[116] "Common Public Radio Interface (CPRI)," in *Interface Specification*, ed, 2013.
[117] N. Shibata, T. Tashiro, S. Kuwano, N. Yuki, J. Terada, and A. Otaka, "Mobile front-haul employing ethernet-based TDM-PON system for small cells," in *Optical Fiber Communications Conference and Exhibition (OFC), 2015*, 2015, pp. 1-3.
[118] T. Pfeiffer, "Next Generation Mobile Fronthaul and Midhaul Architectures [Invited]," *Journal of Optical Communications and Networking*, vol. 7, pp. B38-B45, 2015/11/01 2015.
[119] M. Bakaul, A. Nirmalathas, C. Lim, D. Novak, and R. Waterhouse, "Hybrid Multiplexing of Multiband Optical Access Technologies Towards an Integrated DWDM Network," *Photonics Technology Letters, IEEE*, vol. 18, pp. 2311-2313, 2006.
[120] L. Kazovsky, W. Shing-Wa, T. Ayhan, K. M. Albeyoglu, M. R. N. Ribeiro, and A. Shastri, "Hybrid Optical&Wireless Access Networks," *Proceedings of the IEEE*, vol. 100, pp. 1197-1225, 2012.
[121] C. Lim, A. Nirmalathas, M. Bakaul, P. Gamage, L. Ka-Lun, Y. Yizhuo, *et al.*, "Fiber-Wireless Networks and Subsystem Technologies," *Lightwave Technology, Journal of*, vol. 28, pp. 390-405, 2010.
[122] S. Iezekiel, *Microwave Photonics: Devices and Applications*: Wiley-IEEE Press, 2009.
[123] C. H. Lee, *Microwave Photonics*: CRC Press, 2006.

[124] L. Bach, W. Kaiser, J. P. Reithmaier, A. Forchel, T. W. Berg, and B. Tromborg, "Enhanced direct-modulated bandwidth of 37 GHz by a multi-section laser with a coupled-cavity-injection-grating design," *Electronics Letters*, vol. 39, pp. 1592-1593, 2003.

[125] E. K. Lau, S. Hyuk-Kee, and M. C. Wu, "Ultra-high, 72 GHz resonance frequency and 44 GHz bandwidth of injection-locked 1.55-/spl mu/m DFB lasers," in *Optical Fiber Communication Conference, 2006 and the 2006 National Fiber Optic Engineers Conference. OFC 2006*, 2006, p. 3 pp.

[126] L. Chrostowski, X. Zhao, C. J. Chang-Hasnain, R. Shau, M. Ortsiefer, and M.-C. Amann, "50 GHz directly-modulated injection-locked 1.55 μm VCSELs," in *Optical Fiber Communication Conference, 2005. Technical Digest. OFC/NFOEC*, 2005, p. 3 pp. Vol. 4.

[127] L. A. Neto, P. Chanclou, B. Charbonnier, A. Gharba, N. Genay, R. Xia, *et al.*, "On the interest of chirped lasers for AMOOFDM transmissions in long distance PON networks," in *Optical Fiber Communication Conference and Exposition (OFC/NFOEC), 2011 and the National Fiber Optic Engineers Conference*, 2011, pp. 1-3.

[128] A. Saljoghei, C. Browning, and L. Barry, "Performance enhancement of a hybrid wired/wireless OFDM based PON infrastructure using an integrated device with optical injection," in *Optical Communication (ECOC 2013), 39th European Conference and Exhibition on*, 2013, pp. 1-3.

[129] D.-Z. Hsu, C.-C. Wei, H.-Y. Chen, W.-Y. Li, and J. Chen, "Cost-effective 33-Gbps intensity modulation direct detection multi-band OFDM LR-PON system employing a 10-GHz-based transceiver," *Optics Express*, vol. 19, pp. 17546-17556, 2011/08/29 2011.

[130] J. Park, W. V. Sorin, and K. Y. Lau, "Elimination of the fibre chromatic dispersion penalty on 1550 nm millimetre-wave optical transmission," *Electronics Letters*, vol. 33, pp. 512-513, 1997.

[131] G. H. Smith, D. Novak, and Z. Ahmed, "Technique for optical SSB generation to overcome dispersion penalties in fibre-radio systems," *Electronics Letters*, vol. 33, pp. 74-75, 1997.

[132] J. M. Fuster, J. Marti, and J. L. Corral, "Chromatic dispersion effects in electro-optical upconverted millimetre-wave fibre optic links," *Electronics Letters*, vol. 33, pp. 1969-1970, 1997.

[133] K. Laraqui, "Small cell optical mobile backhauling: Architectures, challenges, and solutions," in *Optical Communication (ECOC 2013), 39th European Conference and Exhibition on*, 2013, pp. 1-3.

[134] ITU-T, "10-Gigabit-Capable Passive Optical Network (XG-PON) Systems: Definitions, Abbreviations, and Acronyms," in *G.987*, ed, 2009.

[135] R. Llorente, M. Morant, F. Martinez, T. Alves, A. Cartaxo, T. Quinlan, *et al.*, "Impairment compensation in long-reach integrated optical-wireless PON," in *Future Network & Mobile Summit (FutureNetw), 2012*, 2012, pp. 1-9.

[136] C. Ranaweera, E. Wong, C. Lim, and A. Nirmalathas, "Next generation optical-wireless converged network architectures," *Network, IEEE*, vol. 26, pp. 22-27, 2012.

[137] L. Xiang, F. Effenberger, N. Chand, Z. Lei, and L. Huafeng, "Demonstration of bandwidth-efficient mobile fronthaul enabling seamless aggregation of 36 E-UTRA-like wireless signals in a single 1.1-GHz wavelength channel," in *Optical Fiber Communications Conference and Exhibition (OFC), 2015*, 2015, pp. 1-3.

[138] C. Seung-Hyun, C. Hwan Seok, H. Changyo, L. Sangsoo, and L. Jong Hyun, "Experimental demonstrations of next generation cost-effective mobile fronthaul with IFoF technique," in *Optical Fiber Communications Conference and Exhibition (OFC), 2015*, 2015, pp. 1-3.

[139] Z. Ming, L. Xiang, N. Chand, F. Effenberger, and C. Gee-Kung, "High-capacity mobile fronthaul supporting LTE-advanced carrier aggregation and 8x8 MIMO," in

Optical Fiber Communications Conference and Exhibition (OFC), 2015, 2015, pp. 1-3.

[140] R. Llorente, M. Morant, T. Quinlan, N. Medina, and S. Walker, "Optical architectures evaluation for triple-play distribution in FIVER project," in *Future Network & Mobile Summit (FutureNetw), 2011*, 2011, pp. 1-8.

[141] A. Cartaxo, J. A. P. Morgado, and D. Fonseca, "A perspective on optical-wireless converged NG-FTTH networks using directly modulated lasers," in *Transparent Optical Networks (ICTON), 2011 13th International Conference on*, 2011, pp. 1-4.

[142] T. Alves, M. Morant, A. Cartaxo, and R. Llorente, "Wired-wireless services provision in FSAN NG-PON2 compliant long-reach PONs: Performance analysis," in *Optical Fiber Communication Conference and Exposition and the National Fiber Optic Engineers Conference (OFC/NFOEC), 2013*, 2013, pp. 1-3.

[143] A. Lometti and V. Sestito, "Optical access architectures for backhauling of broadband mobile networks," in *Telecommunications Network Strategy and Planning Symposium (NETWORKS), 2012 XVth International*, 2012, pp. 1-6.

[144] K. Grobe, "Next-Generation Access/Backhaul based on ITU G.989, NG-PON2," in *Photonic Networks; 15. ITG Symposium; Proceedings of*, 2014, pp. 1-6.

[145] M. Milosavljevic, P. Kourtessis, L. Wansu, and J. M. Senior, "Next generation PONs with wireless backhauling," in *Transparent Optical Networks (ICTON), 2011 13th International Conference on*, 2011, pp. 1-4.

[146] N. Cvijetic, A. Tanaka, M. Cvijetic, H. Yue-Kai, E. Ip, S. Yin, *et al.*, "Novel Optical Access and Digital Processing Architectures for Future Mobile Backhaul," *Lightwave Technology, Journal of*, vol. 31, pp. 621-627, 2013.

[147] N. Cvijetic, M. Cvijetic, H. Ming-Fang, E. Ip, H. Yue-Kai, and W. Ting, "Terabit Optical Access Networks Based on WDM-OFDMA-PON," *Lightwave Technology, Journal of*, vol. 30, pp. 493-503, 2012.

[148] J. Zhensheng, Y. Jianjun, H. Ming-Fang, R. L. Packham, and C. Gee-Kung, "Testbed Demonstration and Analysis for Delivering Dual Services Simultaneously in a Single Radio-over-Fiber Access Platform," in *Microwave Photonics, 2007 IEEE International Topical Meeting on*, 2007, pp. 108-111.

[149] J. A. P. Morgado, D. Fonseca, and A. V. T. Cartaxo, "Influence of spectrum location of Gigabit-Ethernet in coexistence with multi-band OFDM-UWB wireless signals on the long-reach PON performance using directly modulated lasers," in *Microwave Photonics, 2011 International Topical Meeting on & Microwave Photonics Conference, 2011 Asia-Pacific, MWP/APMP*, 2011, pp. 250-253.

[150] S. Huan, K. Byoung-Whi, and B. Mukherjee, "Long-reach optical access networks: A survey of research challenges, demonstrations, and bandwidth assignment mechanisms," *Communications Surveys & Tutorials, IEEE*, vol. 12, pp. 112-123, 2010.

[151] C. van den Bos, M. H. L. Kouwenhoven, and W. A. Serdijn, "The influence of non-linear distortion on OFDM bit error rate," in *Communications, 2000. ICC 2000. 2000 IEEE International Conference on*, 2000, pp. 1125-1129 vol.2.

[152] A. L. Billabert, F. Deshours, L. Moreno, C. Algani, and C. Rumelhard, "Modulator non linearity influence on UWB signal performance over RoF link," in *Microwave Integrated Circuits Conference (EuMIC), 2011 European*, 2011, pp. 688-691.

[153] C. Algani, A. L. Billabert, F. Deshours, H. Chettat, C. Rumelhard, F. Blache, *et al.*, "Main noise influence of the RIN laser diode of an EML transmitter used in an UWB RoF link," in *Microwave Conference (EuMC), 2010 European*, 2010, pp. 117-120.

[154] L. Wen-Yi, C. Ching-Hung, L. Chia-Hsien, T. Shah-Jye, and L. Hai-Han, "Repeaterless hybrid CATV/16-QAM OFDM transport systems," in *Lasers & Electro Optics & The Pacific Rim Conference on Lasers and Electro-Optics, 2009. CLEO/PACIFIC RIM '09. Conference on*, 2009, pp. 1-2.

[155] G. Szczepkowski and R. Farrell, "Study of Linearity and Power Consumption Requirements of CMOS Low Noise Amplifiers in Context of LTE Systems and Beyond," *ISRN Electronics*, vol. 2014, p. 11, 2014.
[156] R. W. Chang, "Orthogonal frequency multiplex data transmission system," ed: Google Patents, 1970.
[157] J. Salz and S. B. Weinstein, "Fourier transform communication system," presented at the Proceedings of the first ACM symposium on Problems in the optimization of data communications systems, Pine Mountain, Georgia, USA, 1969.
[158] A. Peled and A. Ruiz, "Frequency domain data transmission using reduced computational complexity algorithms," in *Acoustics, Speech, and Signal Processing, IEEE International Conference on ICASSP '80.*, 1980, pp. 964-967.
[159] J. S. Chow, J. C. Tu, and J. M. Cioffi, "A discrete multitone transceiver system for HDSL applications," *Selected Areas in Communications, IEEE Journal on*, vol. 9, pp. 895-908, 1991.
[160] S. Yan, M. Morant, C. Okonkwo, R. Llorente, E. Tangdiongga, and A. M. J. Koonen, "Multistandard Wireless Transmission Over SSMF and Large-Core POF for Access and In-Home Networks," *Photonics Technology Letters, IEEE*, vol. 24, pp. 736-738, 2012.
[161] C. Lin and F. Mengel, "Reduction of frequency chirping and dynamic linewidth in high-speed directly modulated semiconductor lasers by injection locking," *Electronics Letters*, vol. 20, pp. 1073-1075, 1984.
[162] T. B. Simpson, J. M. Liu, and A. Gavrielides, "Bandwidth enhancement and broadband noise reduction in injection-locked semiconductor lasers," *Photonics Technology Letters, IEEE*, vol. 7, pp. 709-711, 1995.
[163] M. Xue Jun, C. Tai, and M. C. Wu, "Improved intrinsic dynamic distortions in directly modulated semiconductor lasers by optical injection locking," *Microwave Theory and Techniques, IEEE Transactions on*, vol. 47, pp. 1172-1176, 1999.
[164] A. Murakami, K. Kawashima, and K. Atsuki, "Cavity resonance shift and bandwidth enhancement in semiconductor lasers with strong light injection," *Quantum Electronics, IEEE Journal of*, vol. 39, pp. 1196-1204, 2003.
[165] P. M. Anandarajah, S. Latkowski, C. Browning, R. Zhou, J. O'Carroll, R. Phelan, *et al.*, "Integrated Two-Section Discrete Mode Laser," *Photonics Journal, IEEE*, vol. 4, pp. 2085-2094, 2012.
[166] N. Cvijetic, A. Tanaka, H. Yue-Kai, M. Cvijetic, E. Ip, S. Yin, *et al.*, "4G mobile backhaul over OFDMA/TDMA-PON to 200 cell sites per fiber with 10Gb/s upstream burst-mode operation enabling < 1ms transmission latency," in *Optical Fiber Communication Conference and Exposition (OFC/NFOEC), 2012 and the National Fiber Optic Engineers Conference*, 2012, pp. 1-3.
[167] C. Liang, W. Jian, C. Chang Joon, and A. Nirmalathas, "Combined transmission of baseband OFDM and PON signals for integrated access networks," in *Opto-Electronics and Communications Conference, 2008 and the 2008 Australian Conference on Optical Fibre Technology. OECC/ACOFT 2008. Joint conference of the*, 2008, pp. 1-2.
[168] J. Wang, M. K. Haldar, L. Li, and F. V. C. Mendis, "Enhancement of modulation bandwidth of laser diodes by injection locking," *Photonics Technology Letters, IEEE*, vol. 8, pp. 34-36, 1996.
[169] 3GPP, "3rd Generation partnership project: Technical specification group radio access network; Evolved Universal Terrestrial Radio Access (E-UTRA); User Equipment (UE) radio transmission and reception (Release 8)," in *TS 36.101*, ed, 1999.
[170] L. Mun Seob, L. Byung-Tak, K. Hyun Seo, C. Hee Sang, and K. Jai Sang, "Self-amplified passive optical network using 8B10B line coding properties in Gigabit-Ethernet protocol," in *Optical Fiber Communication Conference. Technical Digest. OFC/NFOEC*, 2005, p. 3 pp. Vol. 3.
[171] C. Systems. (2000) Introduction to Gigabit Ethernet, Technology Brief.

[172] L. Chan Goo, L. Hyeong Ho, K. Dae Young, K. Jung Whan, and J. Hae Won, "A new line code for 10-Gigabit Ethernet: MB810," in *IEEE International Conference on Communications (ICC)*, , 2000, pp. 1774-1777 vol.3.
[173] Z. Al-Qazwini and K. Hoon, "Line coding for 10-Gb/s directly modulated lasers," in *Optical Fiber Communication (OFC), collocated National Fiber Optic Engineers Conference, 2010 Conference on (OFC/NFOEC)*, 2010, pp. 1-3.
[174] A. X. Widmer and P. A. Franaszek, "A DC-Balanced, Partitioned-Block, 8B/10B Transmission Code," *IBM Journal of Research and Development*, vol. 27, pp. 440-451, 1983.
[175] N. D. Alexandru and G. Asachi, "Power Spectral Density of MB 810 Code," presented at the Development and Application Systems, Suceava, Romania, 2012.
[176] D. Y. Kim, C. Lee, C. S. Shin, H. W. Jung, and H. H. Lee, "White Paper on the MB810 Line Code for 10GbE," 1999.
[177] J. C. Cartledge and R. C. Srinivasan, "Extraction of DFB laser rate equation parameters for system simulation purposes," *Lightwave Technology, Journal of*, vol. 15, pp. 852-860, 1997.
[178] J. Zhao, "DFT-based offset-QAM OFDM for optical communications," *Optics Express*, vol. 22, pp. 1114-1126, 2014/01/13 2014.
[179] E. Kofidis, D. Katselis, A. Rontogiannis, and S. Theodoridis, "Preamble-based channel estimation in OFDM/OQAM systems: A review," *Signal Processing*, vol. 93, pp. 2038-2054, 7// 2013.
[180] B. Saltzberg, "Performance of an Efficient Parallel Data Transmission System," *Communication Technology, IEEE Transactions on*, vol. 15, pp. 805-811, 1967.
[181] X. Zhang, Z. Li, C. Li, M. Luo, H. Li, C. Li, *et al.*, "Transmission of 100-Gb/s DDO-OFDM/OQAM over 320-km SSMF with a single photodiode," *Optics Express*, vol. 22, pp. 12079-12086, 2014/05/19 2014.
[182] L. Zhang, M. Bi, X. shilin, l. liu, and B. Hu, "A Sensitivity Improvement Channel Estimation Algorithm for Direct Detection OQAM-OFDM Systems," in *Asia Communications and Photonics Conference 2014*, Shanghai, 2014, p. ATh1E.2.
[183] J. Zhao, "DFT-based optical offset-QAM OFDM: analytical, numerical, and experimental studies," *Photonic Network Communications*, pp. 1-11, 2015/08/23 2015.
[184] Z. Li, T. Jiang, H. Li, X. Zhang, C. Li, C. Li, *et al.*, "Experimental demonstration of 110-Gb/s unsynchronized band-multiplexed superchannel coherent optical OFDM/OQAM system," *Optics Express*, vol. 21, pp. 21924-21931, 2013/09/23 2013.
[185] F. Xi, X. Yongchi, C. Zhangyuan, and Z. Fan, "Frequency-Domain Channel Estimation for Polarization-Division-Multiplexed CO-OFDM/OQAM Systems," *Lightwave Technology, Journal of*, vol. 33, pp. 2743-2750, 2015.
[186] J. Zhao, "Channel estimation in DFT-based offset-QAM OFDM systems," *Optics Express*, vol. 22, pp. 25651-25662, 2014/10/20 2014.
[187] J. Zhao and P. D. Townsend, "Dispersion tolerance enhancement using an improved offset-QAM OFDM scheme," *Optics Express*, vol. 23, pp. 17638-17652, 2015/06/29 2015.
[188] O. Xing and Z. Jian, "Performance characterization of optical offset-QAM OFDM for fiber transmission," in *Communication Systems, Networks & Digital Signal Processing (CSNDSP), 2014 9th International Symposium on*, 2014, pp. 758-762.
[189] F. A. Gutierrez, P. Perry, E. P. Martin, A. D. Ellis, F. Smyth, and L. P. Barry, "All-Analogue Real-Time Broadband Filter Bank Multicarrier Optical Communications System," *Lightwave Technology, Journal of*, vol. 33, pp. 5073-5083, 2015.
[190] S. Randel, S. Corteselli, S. Chandrasekhar, A. Sierra, X. Liu, P. J. Winzer, *et al.*, "Generation of 224-Gb/s multicarrier offset-QAM using a real-time transmitter," in *Optical Fiber Communication Conference and Exposition (OFC/NFOEC), 2012 and the National Fiber Optic Engineers Conference*, 2012, pp. 1-3.

[191] L. Yu-Min and T. Po-Lung, "Next-generation OFDMA-based passive optical network architecture supporting radio-over-fiber," *Selected Areas in Communications, IEEE Journal on*, vol. 28, pp. 791-799, 2010.

[192] J. von Hoyningen-Huene, H. Griesser, M. Eiselt, and W. Rosenkranz, "Experimental demonstration of OFDMA-PON uplink-transmission with four individual ONUs," in *Optical Fiber Communication Conference and Exposition and the National Fiber Optic Engineers Conference (OFC/NFOEC), 2013*, 2013, pp. 1-3.

[193] Q. Dayou, N. Cvijetic, H. Yue-Kai, H. Junqiang, and W. Ting, "Single-wavelength 108 Gb/s upstream OFDMA-PON transmission," in *Optical Communication, 2009. ECOC '09. 35th European Conference on*, 2009, pp. 1-2.

[194] C. Ruprecht, K. Habel, J. von Hoyningen-Huene, Y. Chen, N. Hanik, and W. Rosenkranz, "Timing Advance Tracking for Coherent OFDMA-PON Upstream System," in *Asia Communications and Photonics Conference 2013*, Beijing, 2013, p. AF1G.4.

[195] C. Ruprecht, Y. Chen, D. Fritzsche, J. von Hoyningen-Huene, N. Hanik, E. Weis, *et al.*, "37.5-km Urban Field Trial of OFDMA-PON using Colorless ONUs with Dynamic Bandwidth Allocation and TCM," in *Optical Fiber Communication Conference*, San Francisco, California, 2014, p. Th3G.5.

[196] J. P. Javaudin, D. Lacroix, and A. Rouxel, "Pilot-aided channel estimation for OFDM/OQAM," in *Vehicular Technology Conference, 2003. VTC 2003-Spring. The 57th IEEE Semiannual*, 2003, pp. 1581-1585 vol.3.

[197] Z. Jian, "Offset-QAM multicarrier technology for optical systems and networks (Invited)," in *Optical Communications and Networks (ICOCN), 2014 13th International Conference on*, 2014, pp. 1-4.

[198] C. Lélé, J. P. Javaudin, R. Legouable, A. Skrzypczak, and P. Siohan, "Channel estimation methods for preamble-based OFDM/OQAM modulations," *European Transactions on Telecommunications*, vol. 19, pp. 741-750, 2008.

[199] W. H. Chen and W. I. Way, "Multichannel single-sideband SCM/DWDM transmission systems," *Lightwave Technology, Journal of*, vol. 22, pp. 1679-1693, 2004.

[200] Q. Dayou, N. Cvijetic, H. Junqiang, and W. Ting, "A Novel OFDMA-PON Architecture With Source-Free ONUs for Next-Generation Optical Access Networks," *Photonics Technology Letters, IEEE*, vol. 21, pp. 1265-1267, 2009.

[201] A. Ben-Amram, Y. Stern, Y. London, Y. Antman, and A. Zadok, "Stable closed-loop fiber-optic delay of arbitrary radio-frequency waveforms," *Optics Express*, vol. 23, pp. 28244-28257, 2015/11/02 2015.

[202] M. Bellanger. (2010, FBMC physical layer : a primer. Available: http://www.ict-phydyas.org/

Appendix A:

List of Publications Arising From This Work

Referred Journal Papers

1. **A. Saljoghei**, C. Browning, F. Smyth, and L. P. Barry, "Investigation of the effects of laser non-linearity and RIN in direct modulation hybrid wired/wireless PON systems employing an integrated two section laser," *Optics Communications*, vol. 338, pp. 496-504, 3/1/ 2015.

2. **A. Saljoghei**, C. Browning, and L. P. Barry, "In-band insertion of RoF LTE Services in OOK based PON's using line coding techniques," Optics Communications, vol. 356, pp. 488-494, 12/1/ 2015.

Conference Papers

1. **A. Saljoghei**, C. Browning, and L. Barry, "Performance enhancement of a hybrid wired/wireless OFDM based PON infrastructure using an integrated device with optical injection," in *39th European Conference and Exhibition on Optical Communication (ECOC 2013)*, 2013, pp. 1-3.

2. **A. Saljoghei**, C. Browning, and L. Barry, "Hybrid wired/wireless OFDM-PON with direct modulation of integrated lasers employing optical injection," in *International Topical Meeting on Microwave Photonics (MWP)*, 2013, pp. 309-312.

3. **A. Saljoghei**, C. Browning, and L. Barry, "Performance Enhancement of a Hybrid Wired/Wireless OFDM Based PON Infrastructure Using an Integrated Device with Optical Injection," in *Photonics Ireland, 1-3 Nov*. 2013.

4. **A. Saljoghei**, C. Browning, and L. P. Barry, "Spectral shaping for hybrid wired/wireless PON with DC balanced encoding," in *International Topical Meeting on Microwave Photonics (MWP) and the 2014 9th Asia-Pacific Microwave Photonics Conference (APMP)*, 2014, pp. 307-310.

5. **A. Saljoghei**, C. Browning, and L. Barry, "Line Coding techniques for wired/wireless pon's," in *Photonics Ireland*, 2-4 Sep. 2015.

6. **A. Saljoghei**, F. A. Gutierrez, C. Browning, and L. P. Barry, "FBMC for directly modulated passive optical networks (PON)," in *International Topical Meeting on Microwave Photonics (MWP)*, 2015, pp. 1-4.